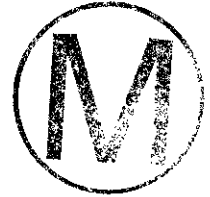

**Title 40 CFR Part 191
Compliance Certification
Application
for the
Waste Isolation Pilot Plant**



Appendix PORSURF



**United States Department of Energy
Waste Isolation Pilot Plant**

**Carlsbad Area Office
Carlsbad, New Mexico**

Porosity Surface Method



CONTENTS

1

2 ACRONYMS PORSURF-iii

3 APPENDIX PORSURF PORSURF-1

4

5 PORSURF.1 Creep Closure Method PORSURF-1

6

7 PORSURF.2 Conceptual Model for Porosity Surface Method PORSURF-2

8

9 PORSURF.3 SANTOS Numerical Analyses PORSURF-3

10

11 PORSURF.4 Dynamic Closure of the North-End and Hallways PORSURF-4

12

13 PORSURF.5 Description of Attachments PORSURF-4

14 REFERENCES PORSURF-14

15 ATTACHMENTS PORSURF-15





1

FIGURES

2 PORSURF-1. Stratigraphy for the Final Porosity Surface Calculations PORSURF-5

3 PORSURF-2. Mesh Discretization and Boundary Conditions Used for the

4 Disposal Room Analyses PORSURF-7

5 PORSURF-3. Disposal Room Porosity Curves for Various Values of the

6 Gas Generation Scale Factor (f) PORSURF-9

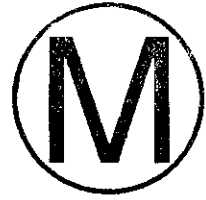
7 PORSURF-4. Disposal Room Internal Gas Pressure Generated by

8 Decomposing Waste PORSURF-11

1

ACRONYMS

2 PRP parameter record package
3 TRU transuranic
4 TWBIR Transuranic Waste Baseline Inventory Report
5 WIPP Waste Isolation Pilot Plant



THIS PAGE INTENTIONALLY LEFT BLANK





APPENDIX PORSURF

Creep closure of the excavation and the presence of either brine or gas in the waste disposal region both influence time-dependent changes in void volume in the waste disposal area. As a consequence, these processes influence two-phase fluid flow of brine and gases through the waste and its capacity for storing fluids. For the performance assessment, a porosity surface method is used to indirectly couple mechanical closure and gas generation with two-phase fluid flow calculations implemented in the BRAGFLO code. The porosity surface approach is used because current codes are not capable of fully-coupling creep closure, waste consolidation, brine availability, and gas production and migration with computational efficiency. The porosity surface method incorporates the results of closure calculations obtained from the SANTOS code, a quasistatic, large deformation finite-element structural analysis code. The adequacy of the method is documented in Freeze (1996), who concludes that the approximation is valid so long as the rate of room pressurization in final calculations is bounded by the room pressurization history that was used to develop the porosity surface.

PORSURF.1 Creep Closure Method

Creep closure is accounted for in BRAGFLO by changing the porosity of the waste disposal area according to a look-up table of porosity (porosity surface) generated using the SANTOS code. The porosity surface is constructed from a minimal set of nonlinear finite element analyses in which the gas generation potential is varied to generate porosity time history curves. Disposal room porosities and gas pressures are calculated for each of the assumed histories as a function of time. SANTOS modeling results in a three-dimensional porosity surface representing changes in gas pressure and porosity over the 10,000-year simulation period.

The completed porosity surface is compiled in tabular form and used to solve the gas and brine mass balance equations presented in Appendix BRAGFLO (p. 38). Porosity is interpolated from the porosity surface corresponding to the calculated gas pressure and fluid saturations at time level t_n . The porosity surface is then accessed iteratively for the remainder of the simulation at the end of each BRAGFLO time step t_{n+1} . The closure data provided by SANTOS can be viewed as a surface, with any gas generation history computed by BRAGFLO constrained to fall on this surface. Various techniques described in Freeze et al. (1995) were used to check the accuracy of this approach, and it was found to be a reasonable representation of the behavior observed in the complex models.

In SANTOS, gas pressure in the disposal room is computed from the ideal gas law by the following relationship:

$$p_g = f \frac{NRT}{V},$$

1 where N , R , and T are the mass of gas in g-moles at a given time, the universal gas constant,
2 and the absolute temperature in degrees kelvin, respectively. V is the current free volume of
3 the room. The gas generation variable, f , is a multiplier used in the analyses to vary the
4 amount of gas generation.

5 To simulate different gas generation potentials within the room at any given time, the baseline
6 gas production assumed for SANTOS is multiplied by a factor f that varies between 0 and
7 2.0. Values of f selected for the final compliance calculations ranged from $f = 0$ to $f = 2$ times
8 the baseline f value of $f = 1$. The condition of $f = 0$ represents the state of the repository when
9 no gas is produced; $f = 2$ represents two times the maximum expected gas generation. To
10 bound the SANTOS results within the range of the actual BRAGFLO model results, relatively
11 high gas production potentials are assumed, $f = 1$: 1050 moles/drum for corrosion and 550
12 moles/drum for microbial degradation. Values of 1 mole/year/drum are used as the gas
13 production rates for both corrosion and microbial degradation. Thirteen cases of gas
14 generation are used to define the SANTOS-generated porosity surface: $f = 0.0, 0.025, 0.05,$
15 $0.1, 0.2, 0.4, 0.5, 0.6, 0.8, 1.0, 1.2, 1.6,$ and 2.0.

16 **PORSURF.2 Conceptual Model for Porosity Surface Method**

17 The ability of salt to deform with time, eliminate voids, and create an impermeable salt barrier
18 around the waste was one of the principal reasons for locating the Waste Isolation Pilot Plant
19 (WIPP) repository in a bedded salt formation. The creep closure process is a complex and
20 interdependent series of events starting after a region within the repository is excavated.
21 Immediately upon excavation, the equilibrium state of the rock surrounding the repository is
22 disturbed, and the rock begins to deform and return to equilibrium. Eventually, at
23 equilibrium, deformation ceases, and the waste region has undergone as much compaction as
24 is possible by the weight of the rock above the repository horizon (overburden).

25 Creep closure of the excavation begins immediately and causes the volume of the cavity to
26 become smaller. If the room were empty, rather than partially filled with waste, closure would
27 proceed to the point where the void volume created by the excavation would be eliminated
28 and the surrounding halite would return to its undisturbed, uniform stress state. In a waste-
29 filled room, the waste will eventually contact the surrounding rock; the rate of closure will
30 decrease and eventually cease as the strength of the waste becomes sufficient to support the
31 rock above the room. Initially, unprocessed waste can support only small loads, but as the
32 room continues to close after contact with the waste, the waste will consolidate and support a
33 greater portion of the weight of the overburden. Consolidation will continue until it reaches
34 mechanical equilibrium.

35 The presence of either brine or gas retards the closure process. First, if brine is present and
36 immobile in the waste, closure largely ceases when the void volume decreases to the point
37 where the voids are completely filled (saturated) with brine. Consolidation continues only if
38 the brine can flow elsewhere. Second, when gas is present, closure and consolidation
39 continue until the gas (pore pressure) increases to the point where it begins to exert





1 backpressure on the surrounding rock. In this process, the waste is considered to be a skeleton
2 structure immersed in a pore fluid (the gas). As the pore pressure increases, less and less of
3 the weight of the overburden is carried by the skeleton, and more support is provided by the
4 gas. If the gas pressure increases to lithostatic pressure, the pore pressure alone is sufficient to
5 support the overburden.

6 **PORSURF.3 SANTOS Numerical Analyses**

7 Computation of repository creep closure is a particularly challenging structural engineering
8 problem, because the rock surrounding the repository continually deforms with time. Not
9 only is the deformation of the salt inelastic, but it also involves larger deformations than are
10 customarily addressed with conventional structural deformation codes. In addition, the
11 formation surrounding the repository is not homogeneous in composition, containing various
12 parting planes and interbeds with different properties than the salt.

13 Deformation of the waste is also nonlinear, with large strains, and its response is complicated
14 by the presence of gas. These complex characteristics of the materials comprising the
15 repository and its surroundings require the use of highly specialized constitutive models that
16 have been built into the SANTOS code over a number of years. Some principal aspects
17 describing the SANTOS analyses include

- 18 • **Disposal Room Configuration and Idealized Stratigraphy:** Disposal Room
19 dimensions, computational configuration, and idealized stratigraphy are defined in the
20 attached memo by Stone (1995) (Attachment 1). The idealized stratigraphy is
21 reproduced in Figure PORSURF-1.
- 22 • **Discretized Finite Element Model:** A two-dimensional plane strain model, as shown
23 in Figure PORSURF-2, is used for the SANTOS analyses. The discretized model
24 represents the room as one of an infinite number of rooms located at the repository
25 horizon. The model contains 1,680 quadrilateral uniform-strain elements and 1,805
26 nodal points. Additional detail on initial and boundary conditions is provided in
27 Attachment 1. Contact surfaces between the stored waste and the surfaces of the room
28 are addressed.
- 29 • **Geomechanical Model:** Mechanical material response models and their
30 corresponding property values are assigned to each region of the configuration. These
31 models include
 - 32 (1) a combined transient-secondary creep constitutive model for clean and
33 argillaceous halite,
 - 34 (2) an inelastic constitutive model for anhydrite, and
 - 35 (3) a volumetric plasticity model for waste.

1 Material properties are provided in Attachment 1. Appendix BACK discusses the
2 minimal effect on the analysis resulting from not incorporating backfill into the
3 SANTOS calculation (Appendix BACK, 3-4).

- 4 • **Porosity Surface:** Figures PORSURF-3 and PORSURF-4 illustrate the SANTOS
5 porosity surface results in two plots: one showing the 13 porosity curves plotted as a
6 function of time and another showing gas pressure as a function of time.

7 **PORSURF.4 Dynamic Closure of the North-End and Hallways**

8 The porosity surface method is not used to model the unfilled north end of the repository
9 occupied by the experimental and operational regions. A series of 60 BRAGFLO simulations
10 compared dynamic consolidation with a baseline case in which the porosity and permeability
11 of these regions were held constant (Vaughn et al. 1995). The study assessed the effect of
12 these two approaches on brine releases to the accessible environment (disturbed and
13 undisturbed conditions), as well as their effect on consequent brine pressures and brine
14 saturations in the modeled regions. The study concludes that assuming constant low porosity
15 and high permeability consistently leads to either similar or more conservative brine pressures
16 and brine saturations and over-predicts potential releases relative to the dynamic closure
17 model. For the performance assessment, the porosity of these regions is maintained at
18 relatively low values associated with consolidated material for the entire modeling period,
19 while the permeability of the region is fixed at a relatively high value that does not impede
20 flow.

21 **PORSURF.5 Description of Attachments**

22 The following memos and attachments are provided to document additional details of the
23 porosity surface method:

- 24 (1) **Attachment 1, Proposed Model for the Final Porosity Surface Calculations**
25 (Stone, October 27, 1995). This memo documents preliminary configuration and
26 constitutive property values for the final porosity surface calculations. Tables in the
27 memo include elastic and creep properties for clean halite and argillaceous halite,
28 volumetric strain data and material constants used in the volumetric-plasticity model
29 for waste, and elastic and Drucker-Prager constants assigned to anhydrite Marker Bed
30 139. The following relevant SAND reports, scheduled for publication in 1996, will
31 supplement and update information in this memo:

- 32 • WIPP Disposal Room Model,
- 33 • Summary of Input Data for WIPP Final Porosity Surface Calculations, and
- 34 • Final Disposal Room Structural Response Calculations.



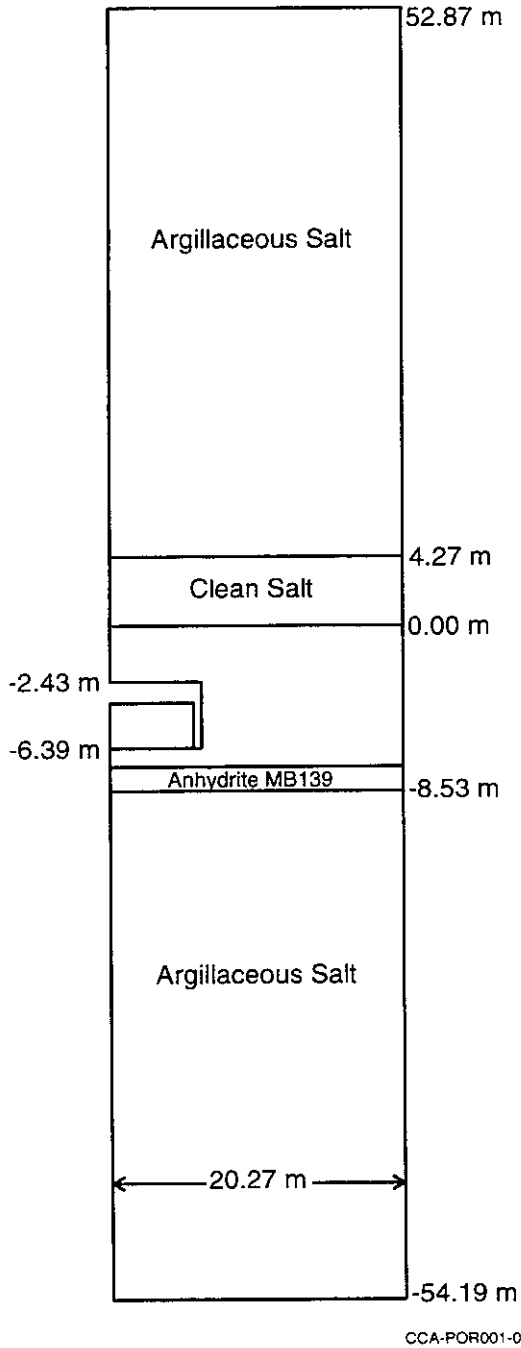
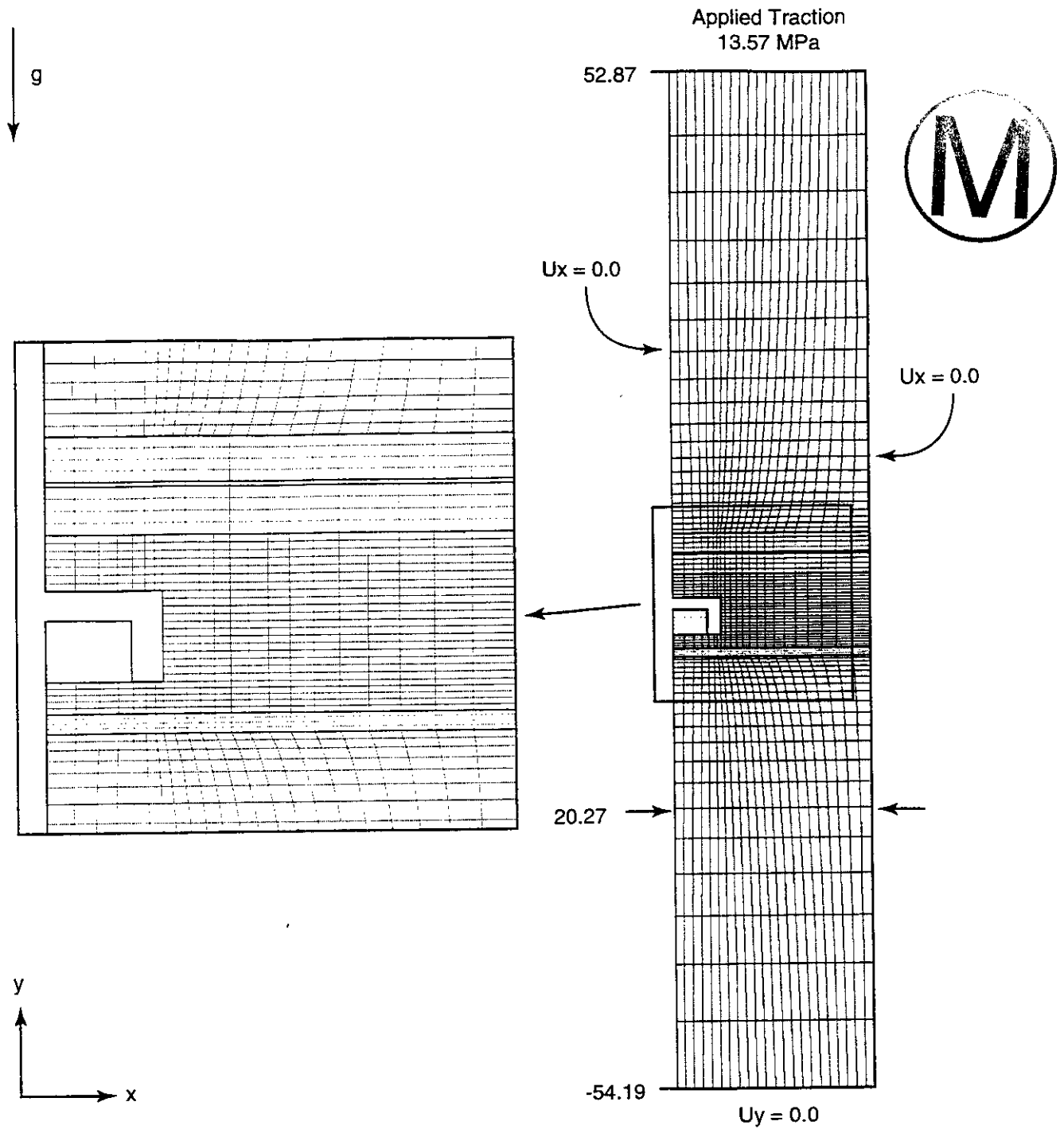


Figure PORSURF-1. Stratigraphy for the Final Porosity Surface Calculations

THIS PAGE INTENTIONALLY LEFT BLANK





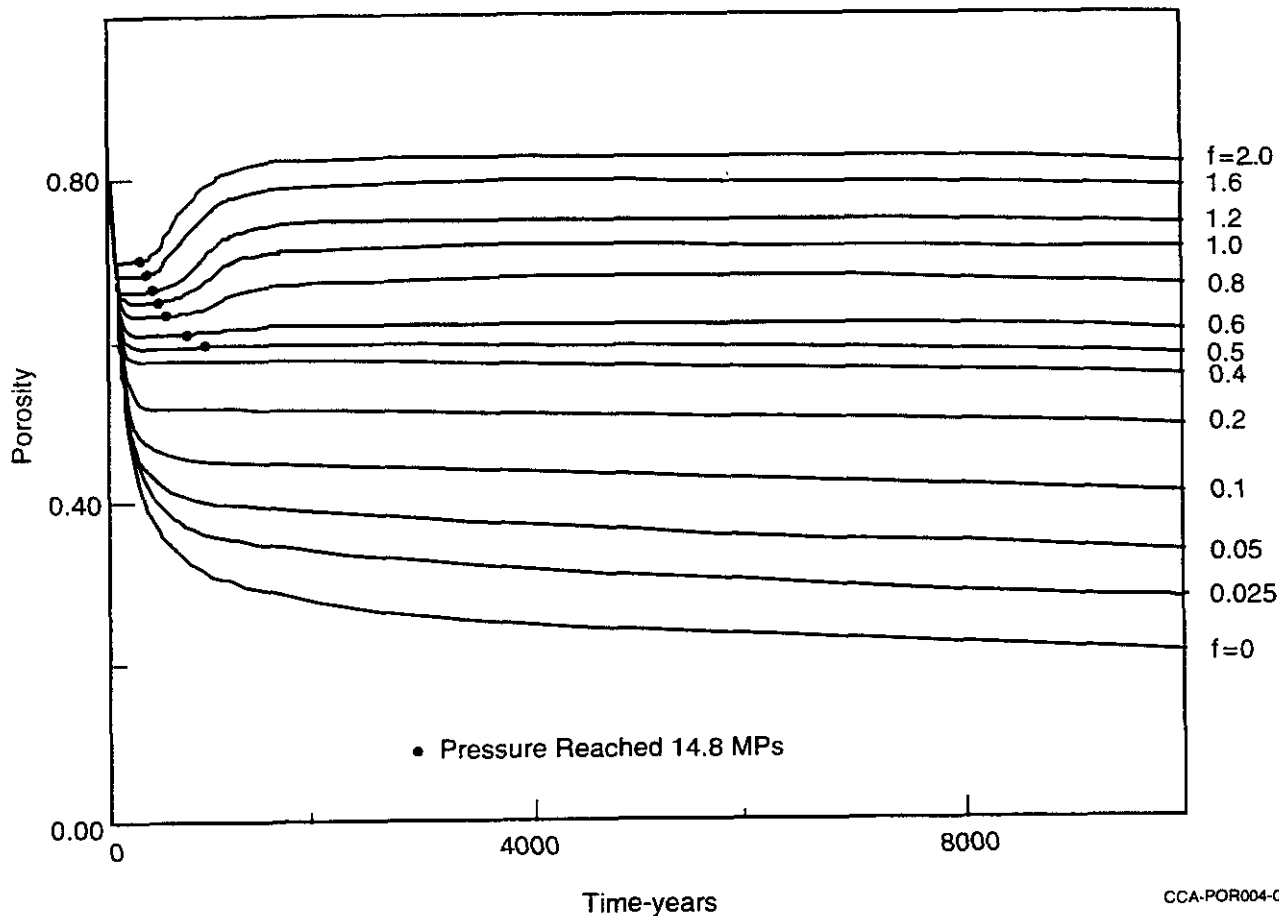
TRI-6348-44-0

1
2

Figure PORSURF-2. Mesh Discretization and Boundary Conditions Used for the Disposal Room Analyses

THIS PAGE INTENTIONALLY LEFT BLANK





CCA-POR004-0

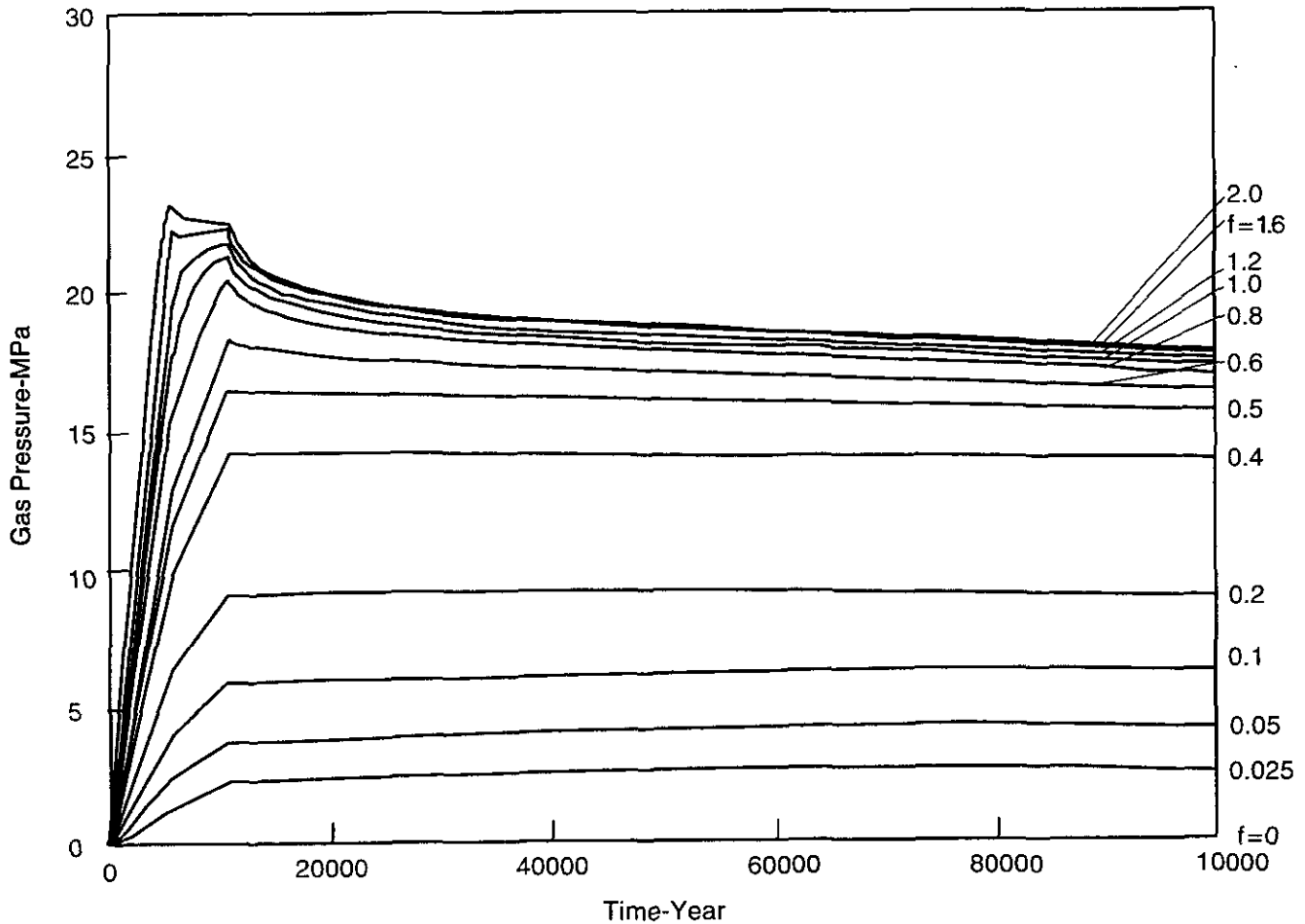


1
2
3

Figure PORSURF-3. Disposal Room Porosity Curves for Various Values of the Gas Generation Scale Factor (f). Gas Generation Values Range from 0.0 to 2.0



THIS PAGE INTENTIONALLY LEFT BLANK



CCA-POR003-0



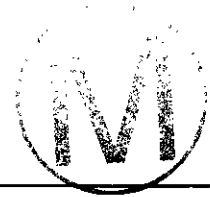
Figure PORSURF-4. Disposal Room Internal Gas Pressure Generated by Decomposing Waste. Various Gas Generation Values are Plotted with an f Ranging from 0.0 to 2.0

THIS PAGE INTENTIONALLY LEFT BLANK



- 1 (2) **Attachment 2, Baseline Inventory Assumptions for the Final Porosity Surface**
2 **Calculations** (Butcher, March 11, 1996). This memo discusses the effect of changes
3 in the Transuranic Waste Baseline Inventory Report (TWBIR) on the SANTOS
4 analyses.
- 5 (3) **Attachment 3, Corrosion and Microbial Gas Generation Potentials** (Butcher,
6 March 11, 1996). This memo discusses the rationale for using gas production
7 potentials of 1,050 moles/drum for corrosion and 550 moles/drum for microbial decay
8 in the SANTOS analyses.
- 9 (4) **Attachment 4, Resolution of Remaining Issues for the Final Disposal Room**
10 **Calculations** (Stone, April 18, 1996). This memo provides additional detail on the
11 disposal room elevation, determination of plastic constants for transuranic (TRU)
12 waste, and determination of SANTOS input constants for clean halite, argillaceous
13 halite, and anhydrite.
- 14 (5) **Attachment 5, Sample SANTOS Input File for Disposal Room Analysis.** A
15 representative sample input file is provided in this attachment. The only difference in
16 the selected set of SANTOS finite element analyses is a subroutine modifying the gas
17 generation variable.
- 18 (6) **Attachment 6, Final Porosity Surface Data.** From a parameter record package
19 (PRP), WPO 35697, final porosity surface output is provided for selected gas
20 generation scaling factors $f = 2.0$, $f = 1.0$, and $f = 0.5$. Thirteen cases of gas generation
21 are actually used in the SANTOS-generated porosity surface: $f = 0.0$, 0.025, 0.05, 0.1,
22 0.2, 0.4, 0.5, 0.6, 0.8, 1.0, 1.2, 1.6, and 2.0.
- 23 (7) **Attachment 7, SANTOS - A Two-Dimensional Finite Element Program for the**
24 **Quasistatic, Large Deformation, Inelastic Response of Solids** (Stone, March 27,
25 1996). This report provides documentation on the SANTOS code. WPO 35674.





ATTACHMENTS

1
2
3
4
5
6
7
8
9
10
11
12

- Attachment 1 Proposed Model for the Final Porosity Surface Calculations
- Attachment 2 Baseline Inventory Assumptions for the Final Porosity Surface Calculations
- Attachment 3 Corrosion and Microbial Gas Generation Potentials
- Attachment 4 Resolution of Remaining Issues for the Final Disposal Room Calculations
- Attachment 5 Sample SANTOS Input File for a Disposal Room Analysis
- Attachment 6 Sample of Selected SANTOS Final Porosity Surface Data - $f = 2.0, 1.0, 0.5$
- Attachment 7 SANTOS - A Two-Dimensional Finite Element Program for the Quasistatic, Large Deformation, Inelastic Response of Solids

THIS PAGE INTENTIONALLY LEFT BLANK





**Title 40 CFR Part 191
Compliance Certification
Application
for the
Waste Isolation Pilot Plant

PORSURF Attachment 1**

THIS PAGE INTENTIONALLY LEFT BLANK



Sandia National Laboratories

Albuquerque, New Mexico 87185

date: October 27, 1995

to: B. M. Butcher, 6748 (MS1341)

INFORMATION ONLY

Charles M. Stone

from: Charles M. Stone, 9117 (MS0443)

subject: Proposed Model for the Final Porosity Surface Calculations of Sandia M: lestone, DR 035.
Entitled Final Porosity Surface Input Parameter Values.

Introduction

Dt.
11/10/95

This memo documents our best estimate of the configuration and constitutive property values for the final porosity surface calculations. This estimate is based on information from WIPP project documents, contractor reports, scoping analyses, and from insight gained during previous disposal room analyses. The quasi-static, large deformation finite element code SANTOS [1] will be used for the analyses. It has the capability to compute an internal room pressure and to apply the resulting forces to nodes on the room boundary.

Disposal Room Model

The disposal room model consists of a rectangular room 3.96 m high by 10.06 m wide by 91.44 m in length resulting in an initial room volume of 3642.75 m³. Unlike previous calculations which included a crushed salt layer around the waste, the current analyses consider a disposal room with waste only, no backfill. The current configuration calls for 6804 drums of uniformly distributed unprocessed waste to be stored in the disposal room. The corresponding volume occupied by the waste and the drums is 1728 m³. The waste is stored in a seven-pack drum configuration with three seven-packs stacked, for a total waste height of 2.676 m, along the length of the drift. The initial porosity of the waste is 0.681 resulting in a solid volume of 551.2 m³.

Geomechanical Model

A two-dimensional plane strain disposal room model will be used for the SANTOS analyses. The model represents the room as one of an infinite number of rooms located at the repository horizon. Making use of symmetry, only half of the room needs to be modeled. The left and right boundaries are planes of symmetry with a zero-displacement boundary condition applied in the horizontal direction. The upper and lower boundaries are located approximately 50 m from the room. Previous scoping studies have shown that



locating the upper and lower boundaries at a distance of 50 m from the disposal room results in a 5 percent difference in room porosity when compared to room porosity calculated with the boundaries located at a distance of 100 m. It is felt that this small difference in room porosity is acceptable when compared to the factor of two increase in computer time associated with the larger model. A prescribed normal traction of 13.57 MPa is applied on the upper boundary and a normal traction of 14.76 MPa is applied at the lower boundary. A lithostatic stress ($\sigma_x = \sigma_y = \sigma_z$) that varies with depth is used as the initial stress on the configuration and gravity forces are included.

The stratigraphy is based on the WIPP Revised Reference Stratigraphy that is defined in [2]. Recent work by Osnes and Labreche [3] has quantified the differences in room closure obtained by assuming different stratigraphic models which incorporate different numbers of clay seams and marker beds. The full stratigraphic model consisting of 12 clay seams and 7 anhydrite layers (12-Clay) is viewed as the reference analysis. Several different models were studied including models with 7, 5, and 3 clay seams. The models also included different combinations of anhydrite layers. The only anhydrite layer in common with all the analyses is MB 139. The room closure and room porosity results reported by Osnes and Labreche showed that the simplified models reproduced the results of the 12-Clay model quite well. This suggests that a simplified model may confidently be used to capture the disposal room response. In addition, the results showed that a disposal room located in a stratigraphy composed of all salt closed considerably faster than a disposal room located in a stratigraphic model which contained anhydrite layers.

Based on these results, we feel that a simplified stratigraphic model is justified for the final porosity surface calculations. In addition, we feel that the major structural feature in the stratigraphy is the anhydrite layer at MB 139. Therefore, the proposed stratigraphic model is composed of argillaceous salt, a single clean salt layer, and MB 139. This proposed stratigraphy is shown in Figure 1. The major question regarding this stratigraphic representation is whether the clay seam at the marker bed is structurally important. In order to answer this question, several scoping analyses were run to compare room closure results for a stratigraphy with and without a clay seam beneath MB 139. A second question to be answered by the study is whether the presence of the marker bed is sufficient to reduce the rate of room closure compared to an all salt stratigraphy as found by Osnes and Labreche [3]. These questions are answered by Figure 2 which shows the disposal room volume as a function of time for the scoping analyses. The analyses showed that the presence of the clay seam beneath MB 139 did not affect the closure of the disposal room. In addition, the presence of MB 139 did slow the rate of disposal room closure when compared to an all salt stratigraphy. An additional observation from this study is the fact that the horizontal closure increased when the marker bed was included in the stratigraphy. This is due to the fact that the stiff anhydrite layer forces more salt to flow horizontally into the drift rather than flowing upward at the drift floor.

The disposal room contains material representing the stored waste. The basic half-symmetry room dimensions are 3.96 m high by 5.03 m wide. The waste and drum volume of 1728 m³ is distributed along 87.96 m of the drift at a height of 2.676 m. The assumption

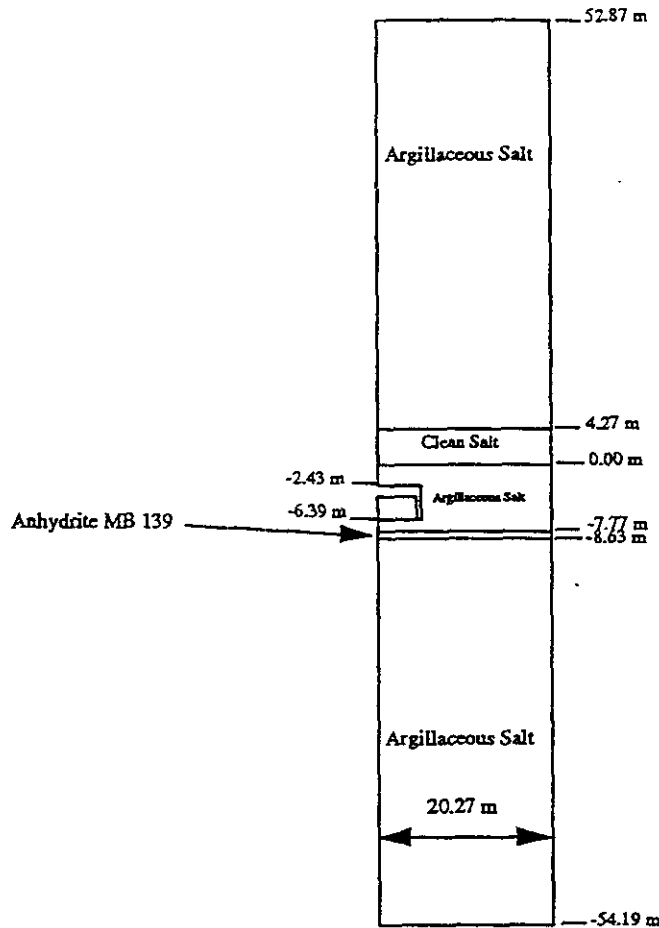


Figure 1. Proposed Stratigraphy for the Final Porosity Surface Calculations

is made that lateral deformation of a configuration of drums caused by inward movement of the walls of the disposal room is sufficient to eliminate space between the drums early in the closure process at low stress levels. Based on this assumption, the equivalent half-width of the waste is computed to be 3.735 m instead of the seven-pack width of 4.3 m. As previously described, within the room a gas pressure, p_g , will be applied around the room boundary.

Contact surfaces will be defined between the waste and room boundaries to model the contact and sliding that occurs as the room deforms and entombs the waste. Specifically, contact surfaces will be defined between the waste and floor of the room, the waste and room rib, and the waste and ceiling. All of the contacts surfaces will be allowed to separate if the forces between the surfaces reached a tensile value. This feature allows the room to reopen due to gas generation within the disposal room.

A combined transient-secondary creep constitutive model for rock salt attributed to Munson and Dawson [4] and described by Munson, et. al [5] will used for the clean and argillaceous salt. The model can be decomposed into an elastic volumetric part defined by,

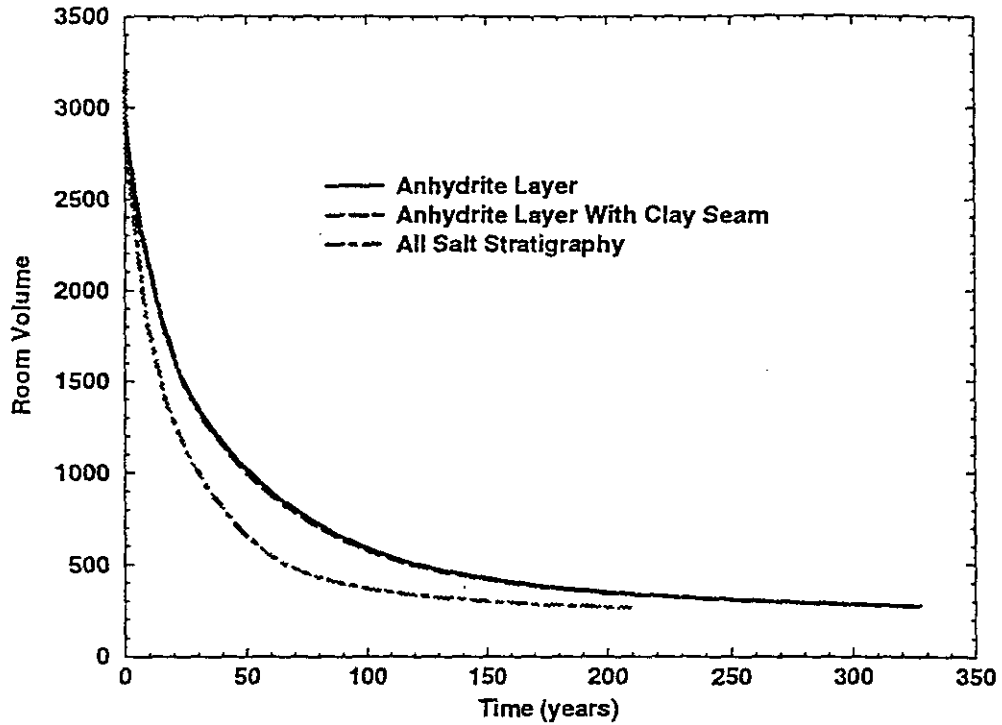


Figure 2. Disposal Room Volume History For Various Stratigraphic Assumptions.

$$\epsilon_{kk} = \frac{\sigma_{kk}}{3K} \tag{EQ 1}$$

(where the ϵ_{ij} and the σ_{ij} are the total strain and stress components, respectively, and K is the elastic bulk modulus) and a deviatoric part defined by,

$$\dot{s}_{ij} = 2G \left(\dot{e}_{ij} - F \dot{e}_s \left[\frac{\cos 2\theta}{\cos 3\theta \sqrt{J_2}} s_{ij} - \frac{\sqrt{3} \sin \theta}{\cos 3\theta J_2} \left\{ s_{ip} s_{pj} - \frac{2J_2}{3} \delta_{ij} \right\} \right] \right) \tag{EQ 2}$$

where the second term of the above equation represents the creep contribution. In the above equation, s_{ij} is the deviatoric stress defined as $s_{ij} = \sigma_{ij} - \frac{\sigma_{kk}}{3}$, G is the elastic shear modulus, and e_{ij} is the deviatoric strain defined by $e_{ij} = \epsilon_{ij} - \frac{\epsilon_{kk}}{3}$.

In the creep term of Equation 3, F is a multiplier on the steady-state creep rate to simulate the transient creep response according to the following,



$$F = \begin{cases} e^{\Delta[1-\zeta/\epsilon_t^*]^2}, & \zeta < \epsilon_t^* \\ 1, & \zeta = \epsilon_t^* \\ e^{-\delta[1-\zeta/\epsilon_t^*]^2}, & \zeta > \epsilon_t^* \end{cases} \quad \text{M} \quad (\text{EQ 3})$$

where Δ and δ are work-hardening and recovery parameters, respectively, and ϵ_t^* is the so-called transient strain limit. Finally, ζ is an internal state variable whose rate of change is determined by the following evolutionary equation,

$$\dot{\zeta} = (F - 1)\dot{\epsilon}_s. \quad (\text{EQ 4})$$

In Equation 4, the work-hardening parameter Δ is defined as $\Delta = \alpha + \beta \log(\bar{\sigma}/G)$ where α and β are constants. The variable $\bar{\sigma}$ is the equivalent Tresca stress given by

$$\bar{\sigma} = 2\sqrt{J_2} \cos \theta \quad \text{where} \quad \theta = \frac{1}{3} \arcsin \left[\frac{-3\sqrt{3}J_3}{2(J_2)^{3/2}} \right] \quad \text{is the Lode angle and is limited to the}$$

range $-\frac{\pi}{6} \leq \theta \leq \frac{\pi}{6}$. The variables J_2 and J_3 are the second and third invariants of the stress

deviator given by $J_2 = \frac{1}{2} s_{pq} s_{qp}$ and $J_3 = \frac{1}{3} s_{pq} s_{qr} s_{rp}$, respectively. The recovery

parameter δ is held constant. The transient strain limit is given by $\epsilon_t^* = K_o e^{cT} (\bar{\sigma}/G)^M$ where K_o , c , and M are constants.

The steady-state, or secondary creep, strain rate, $\dot{\epsilon}_s$, is given by

$$\dot{\epsilon}_s = A_1 e^{-Q_1/RT} \left(\frac{\bar{\sigma}}{G} \right)^{n_1} + A_2 e^{-Q_2/RT} \left(\frac{\bar{\sigma}}{G} \right)^{n_2} + |H| [B_1 e^{-Q_1/RT} + B_2 e^{-Q_2/RT}] \sinh \left[\frac{q(\bar{\sigma} - \sigma_o)}{G} \right]; \quad (\text{EQ 5})$$

where the A_i s and B_i s are constants, the Q_i s are activation energies, T is the absolute temperature, R is the universal gas constant, the n_i s are the stress exponents, q is the so-called stress constant, σ_o is the stress limit of the dislocation slip mechanism, and $|H|$ is the Heaviside step function with the argument $(\bar{\sigma} - \sigma_o)$. The material constants corresponding to the clean and argillaceous salt, used in the analyses, are given in Table 1 and Table 2.

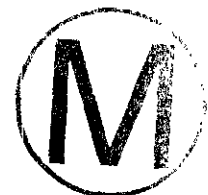
Table 1: Elastic Properties [2]

G MPa	E MPa	ν
12,400	31,000	0.25

Table 2: Creep Properties [2]

Parameters (units)	Clean Salt	Argillaceous Salt
A_1 (/sec)	8.386E22	1.407E23
Q_1 (cal/mole)	25,000	25,000
n_1	5.5	5.5
B_1 (/sec)	6.086E6	8.998E6
A_2 (/sec)	9.672E12	1.314E13
Q_2 (cal/mole)	10,000	10,000
n_2	5.0	5.0
B_2 (/sec)	3.034E-2	4.289E-2
σ_o (MPa)	20.57	20.57
q	5,335	5,335
M	3.0	3.0
K_o	6.275E5	2.470E6
c (/T)	9.198E-3	9.198E-3
α	-17.37	-14.96
β	-7.738	-7.738
δ	0.58	0.58

The stress-strain behavior of the waste was represented by a volumetric plasticity model [1] with a piecewise linear function defining the relationship between the mean stress and the volumetric strain. Compaction experiments on simulated waste were used to develop this relationship. The deviatoric response of the waste material has not been characterized. It is anticipated that when a drum filled with loosely compacted waste is compressed axially, the drum will not undergo significant lateral expansion until most of the void space inside the drum has been eliminated.



For the volumetric plasticity model, the yield surface in principal stress space is a surface of revolution with its axis centered about the hydrostat and the open end pointing into the compression direction. The open end is capped with a plane which is at right angles to the hydrostat. The deviatoric part is elastic-perfectly plastic so the surface of revolution is stationary in stress space. The volumetric part has variable strain hardening so the end plane moves outward during volumetric yielding. The volumetric hardening is defined by a set of pressure-volumetric strain relations. A flow rule is used such that deviatoric strains produce no volume change (associated flow). The model is best broken into volumetric and deviatoric parts with the deviatoric part resembling conventional plasticity. The volumetric yield function is a product of two functions, ϕ_s and ϕ_p , describing the surface of revolution and the plane normal to the pressure axis, respectively. These are given by

$$\phi_s = \frac{1}{2} s_{ij} s_{ij} - a_0 + a_1 p + a_2 p^2$$

$$\phi_p = p - g(\epsilon_v)$$

where a_0 , a_1 , a_2 are constants defining the deviatoric yield surface, p is the pressure, and ϵ_v is the volume strain. The form of g is defined in this problem by a set of piecewise linear segments relating pressure-volume strain. Table 3 lists the pressure-volumetric strain data used for the waste drum model. Note that the final point listed in the table is a linear extrapolation beyond the curve data given in [6]. The final pressure value of 12 MPa corresponds to an axial stress on a waste drum of 36 MPa. The elastic material parameters and constants defining the yield surface are given in Table 4.

Table 3: Pressure-Volumetric Strain Data Used in the Volumetric-Plasticity Model for the Waste Drums [6]

Pressure (MPa)	$\ln(\rho/\rho_0)$
1.530	0.5101
2.0307	0.6314
2.5321	0.7189
3.0312	0.7855
3.5301	0.8382
4.0258	0.8808
4.9333	0.9422
12.0	1.140

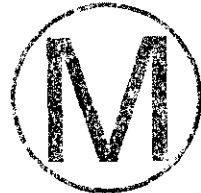


Table 4: Material Constants Used With the Volumetric Plasticity Model for the Waste

Parameter	Value
G	333. Mpa
K	222 Mpa
a ₀	1.0 Mpa
a ₁	3.0
a ₂	0.

The anhydrite layer beneath the disposal room is expected to experience inelastic material behavior. The MB 139 anhydrite layer is considered to be isotropic and elastic until yield occurs. Once the yield stress is reached plastic strain begins to accumulate. Yield is assumed to be governed by the Drucker-Prager criterion

$$\sqrt{J_2} = C - aJ_1$$



where J_2 is the second deviatoric stress invariant and J_1 is the first stress invariant (σ_{kk}). A nonassociative flow rule is used to determine the plastic strain components. The elastic properties and Drucker-Prager constants, C and a , for the anhydrite are given in Table 5.

Table 5: Elastic and Drucker-Prager Constants for Anhydrite [7]

Material	Young's Modulus (GPa)	Poisson's Ratio	C (MPa)	a
Anhydrite	75.1	0.35	1.35	0.45

Gas Generation Model

The gas generation potential and gas production rate are composed of gas from two sources: anoxic corrosion and microbial activity. Reference [8] reports that the estimated gas production potential from anoxic corrosion will be 1050 *moles/drum* with a production rate of 1 *mole/drum/year*. The gas production potential from microbial activity is estimated to be 550 *moles/drum* with a production rate of 1 *mole/drum/year*. This means that microbial activity ceases at 550 years while anoxic corrosion will continue until 1050 years after emplacement. The total amount of gas generated in a disposal room for the Baseline case was specified to be based on 6804 unprocessed waste drums per room. The total gas potential for the Baseline case is shown in Figure 3.

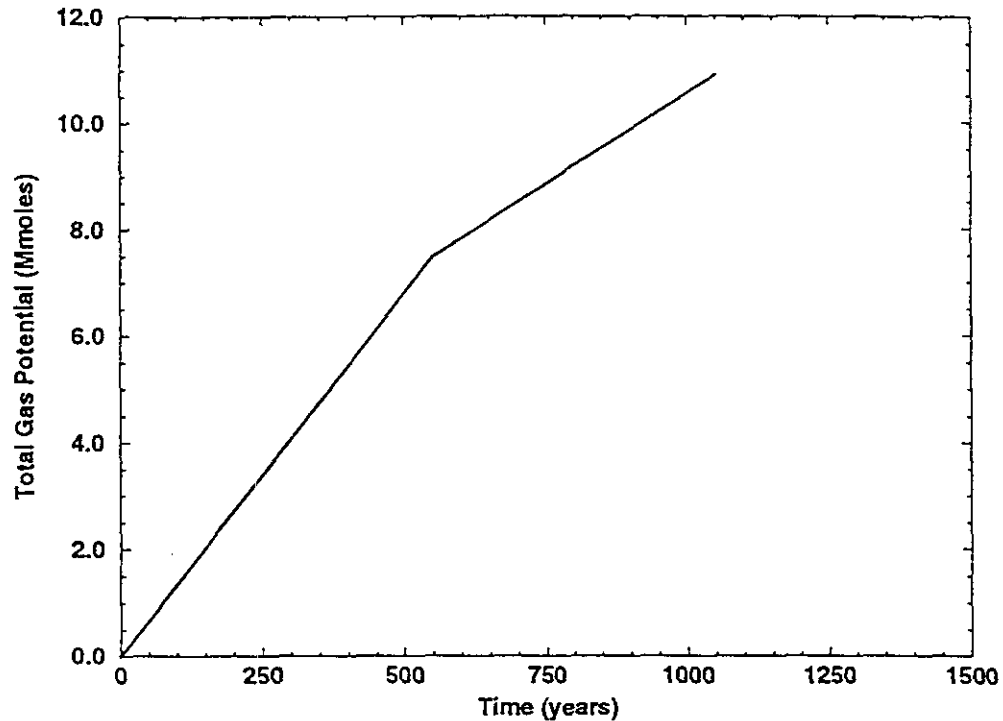


Figure 3. History of the Baseline Gas Generation Potential Used for the Disposal Room Analyses

These values for the Baseline case are considered acceptable for the calculations, even though the values for the gas generation model recommended for the final Performance Assessment BRAGFLO calculations are likely to be different. The use of the Baseline values is consistent with the porosity surface approach that compensates for the absence of detailed definition about gas generation within the repository by constructing a set of closure (void volume or porosity) curves using assumed gas generation (pressure) histories that span all of the gas generation histories that potentially might be encountered within the repository [9]. Several calculations in which the assumed rate of gas production is doubled will be made, and calculations assuming a total gas potential of 3200 moles/drum/year will also assure that the porosity surface data spans all potential gas generation histories.

The gas pressure is computed from the ideal gas law based on the current free volume in the room. Specifically, the gas pressure, p_g , is computed with the following relationship:

$$p_g = f \frac{NRT}{V}, \quad (\text{EQ } 6)$$

where N , R , and T are the mass of gas in g-moles, the universal gas constant, and the absolute temperature in degrees Kelvin. The variable V is the current free volume of the room. After each iteration in the analysis, the current room free volume is calculated based on the locations of the nodes on the boundary of the room. The variable f is a multiplier used in the study to scale the pressure by varying the amount of gas generation. A value of

$f=1$ corresponds to an analysis with full gas generation, while a value of $f=0$ corresponds to no internal pressure increase due to gas generation.

References

1. Stone, C. M., SANTOS – *A Two-Dimensional Finite Element Program for the Quasistatic, Large Deformation, Inelastic Response of Solids*, SAND90-0543, Sandia National Laboratories, Albuquerque, New Mexico, in preparation.
2. Butcher, B. M. and J. Holmes, 'Completion of milestone DR015, definition of closure analysis input parameters, due March 31, 1995,' Sandia National Laboratories, memorandum to Les Shepard and Martin Tierney, March 31, 1995.
3. Osnes, J. D. and D. A. Labreche, 'The Effect of Clay Seams and Anhydrite Layers on the Closure of Waste Isolation Pilot Plant Disposal Rooms and Guidelines for Simplifying the Modeled Stratigraphy,' RE/SPEC External Memorandum RS(RCO)-390/7-95/58, August 29, 1995.
4. Munson, D. E. and P. R. Dawson, *A Transient Creep Model for Salt During Stress Loading and Unloading*, Sandia National Laboratories, Albuquerque, New Mexico, 1982.
5. Munson, D. E., A. E. Fossum, and P. E. Senseny, *Advances in Resolution of Discrepancies Between Predicted and Measured In Situ WIPP Room Closures*, SAND88-2948, Sandia National Laboratories, Albuquerque, New Mexico, 1989.
6. Butcher, B. M., 'Waste Compressibility Curve Predictions,' Sandia National Laboratories Memorandum of Record, February 16, 1995.
7. Munson, D. E., 'Mechanical Parameters for Volume 3, SAND92-0700', Sandia Internal Memorandum, October 26, in Appendix A, pp A-107 to A-124 of Preliminary performance Assessment for the Waste Isolation Pilot Plant, December 1992, Volume 3: Model Parameters, SAND92-0700/3, prepared by Sandia National Laboratories, Albuquerque, NM.
8. Beraun, R. and P. B. Davies, 'Baseline Design Input Data Base to be Used During Calculations Effort by Division 1514 in Determining the Mechanical Creep Closure Behavior of Waste Disposal Rooms in Bedded Salt,' Memorandum to Distribution, Sandia National Laboratories, Albuquerque, NM, September 12, 1991.
9. Butcher, B. M., S. W. Webb, and J. W. Berglund, 'Disposal Room and Cuttings Models-White Paper for Systems Prioritization and Technical Baseline,' WIPP Project Document, Section 3.2.4, 1994.



Distribution:

MS-1330		SWCF-A: 1.1.1.2.3; DRM
MS-0841	9100	P. J. Hommert
MS-0835	9102	R. D. Skocypec (Route to 9111)
MS-0833	9103	J. H. Biffle (Route to 9116)
MS-0828	9104	E. D. Gorham (Route to 9114, 9115)
MS-0834	9112	A. C. Ratzel (Route to 9113)
MS-0443	9117	H. S. Morgan (Route to Staff)
MS-0437	9118	E. P. Chen (Acting) (Route to Staff)
MS-0443	9117	C. M. Stone
MS-0443	9117	J. G. Arguello
MS-0443	9117	QA File



**Title 40 CFR Part 191
Compliance Certification
Application
for the
Waste Isolation Pilot Plant

PORSURF Attachment 2**



THIS PAGE INTENTIONALLY LEFT BLANK



date: March 11, 1996; reissued July 10, 1996 after revision

to: Memorandum of Record

B. M. Butcher

from: B. M. Butcher

subject: Baseline Inventory Assumptions for the Final Porosity Surface Calculations



Final porosity surface calculations were started November 1, 1995, using waste compaction data derived from the February 1995 revision of the Baseline Inventory Report (BIR revision 1). The assumption was made, therefore, that future BIR adjustments would be small and have little effect on calculation results.

In contrast to the assumption, an updated draft revision, Draft B, November 1995, of the inventory was found to be quite different than the February version (Revision 1). These changes were qualified in the sense that reported values were not considered final until the document was approved. Revision 2 of the BIR was published on December 28, 1995, after the porosity surface calculations were completed. At that time, the consequences of the new values were reviewed in order to decide whether or not to scrap already completed calculations and start over again using the new inventory. The conclusion of the review was that Revision 2 did not contain sufficient information to assess the consequences of the revisions. It was observed that the compaction characteristics of the inventory described in Revision 1 represent an upper bound of the final porosity states (greatest porosity at any given time), because it takes more time to compact waste that has not been partially vitrified (discussed in a following paragraph). Therefore, more time is available for gas pressure to build up and stop closure. Less closure is considered conservative with regard to repository performance because the waste is more porous, and therefore would offer less resistance to the flow of radioactive brine.

Changes in Draft B are that vitrified waste is listed for the first time, the amount of iron-based metal has increased by over a factor of two and cellulosics waste has decreased in amount by a factor of three. New inventory values taken from Table ES-1 of Draft B are compared with the Revision 1 values in Table 1.

Closer examination of the differences between Revision 1 and Draft B revealed that the increase in amount of waste was because of the presence of vitrified waste. During vitrification, combustibles are burned up, causing the drop in the combustibles inventory, but the iron-based alloys remain intact. In addition, vitrification represents a 6 fold or greater reduction in waste volume, so that more of it can be used to fill the repository to capacity. In Draft B, the total amount of iron-based metal is the amount of iron in vitrified waste, augmented by the scaling process used to fill up the repository, plus the iron-based material in unprocessed waste. The procedure accounts for the increased iron content and decreased combustibles, but does not specify quantitatively how much iron is associated with the vitrified form. We need to know how much iron is associated with iron in vitrified waste and

how much is in unprocessed waste. This information is critical because the stress-strain response of iron in vitrified waste differs greatly from that of iron in unprocessed metals waste. Iron in vitrified waste is for all practical purposes locked up in it, undergoing little consolidation because the vitrification process produces a waste form that is likely to have high enough strength to resist further large scale densification. Vitrified waste thus undergoes little further consolidation during closure, whereas unprocessed metals waste undergoes a very large amount of densification during closure.

Summary: The lack of quantitative definition of the amount of iron that is associated with the vitrified waste component in Revision 2 of the BIR prevented use of this latest information in constructing the compaction curve data input for the final porosity surface calculations. Instead, final calculations were made using waste compaction data derived from the February 1995 version of the Baseline Inventory Report (BIR Revision 1). This approach is considered to provide an upper bound of the final porosity states.

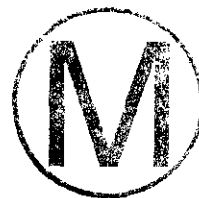
Copy to:

MS 1341 B. M. Butcher (6748) day file
MS 1330 SWCF-A: 1.1.1.2.3; DRM



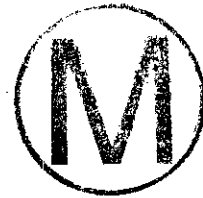
Table 1: Baseline Inventory Assumptions for Disposal Room Model Calculations

	92 PA	Rev. 1: February 1995	Rev. 2: December 1995
<u>Material</u>	kg/m ³	kg/m ³	kg/m ³
Iron Base Metals		83	170
Aluminum Base Metals		12	18
Other Metals		27	72
Total Metals	110	122	260
Other Inorganic Material	32	40	33
Vitrified	0	0	50
Cellulosics	47	170	52
Rubber		21	10
Plastics		63	33
Total Rubber and Plastics	67	84	43
Solidified Inorganic Material		130	120
Solidified Organic Material		7.8	2.6
Total Sludges	171	137.8	122.6
Cement	0	0	0
Soils	0	5.7	32
Initial Waste Density	426	560	593



**Title 40 CFR Part 191
Compliance Certification
Application
for the
Waste Isolation Pilot Plant

PORSURF Attachment 3**



THIS PAGE INTENTIONALLY LEFT BLANK



Sandia National Laboratories

Albuquerque, New Mexico 87185-1341

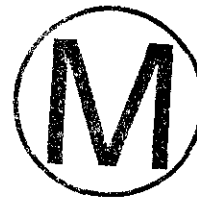
date: March 18, 1996: reissued July 10, 1996 after editorial revision

to: Memorandum of Record

INFORMATION ONLY

B. M. Butcher

from: B. M. Butcher, 6748, MS 1341



subject: Corrosion and Microbial Gas Generation Potentials

A number of values for the potential for corrosion and microbial gas generation have been used during development of the porosity surface approach (Butcher and Mendenhall, 1993, pp. 7-3 to 7-7). For example, in Lappin et. al (1989, Sec. 4.10.2) the gas generation potential was quoted as 589 moles/drum for anoxic microbial decay and 894 moles/drum for anoxic corrosion of metals.

Later, Beraún and Davies (1992) referenced Brush as recommending a gas potential of 1050 moles/drum for corrosion and 550 moles/drum for microbial decay. The source for these values was Reference 11 in Beraún and Davies (1992), which was described as "in draft," and apparently never issued. Source documentation for these values is therefore unknown, but may have been an early draft of the reference written by Brush (1991) in which the gas potential values were quoted as 900 moles/drum for corrosion and 600 moles/drum for microbial decay in the final version.

Recommended gas potentials have changed again several times since 1991. Nevertheless, use of the Beraún and Davies (1992) values of 1050 moles/drum for corrosion and 550 moles/drum for microbial decay has continued. The justification for using these values is that the porosity surface concept was adopted in order to circumvent problems related to (1) the absence of detailed definition of gas generation within the repository and (2) the realization that gas production histories typical of the repository that depend on brine inflow could not be addressed at that time as part of a mechanical closure calculation. There was no way of estimating how the brine content of the waste changes with time with structural codes such as SANTOS. To compensate for this deficiency, the porosity surface concept selects a set of gas generation histories that span all of the gas generation histories likely to be encountered within the repository. Disposal room porosities and gas pressures are calculated for each of the assumed histories as a function of time, summarized in data tables and transferred to BRAGFLO. Closure histories for specific repository conditions are then defined with the performance assessment code BRAGFLO, with which brine flow, gas generation, and gas migration are computed throughout the repository (Butcher et. al, 1994, Sections 3.2.4, 3.4.1).

In maintaining the link between SANTOS and BRAGFLO, the range of gas generation potentials for generation of the porosity surface data for the CCA exceed presently anticipated conditions for the repository. This procedure assures that BRAGFLO extrapolation outside

the data range is not needed. It also provides justification for using gas potential values that are not quite the same as values used on other performance assessment calculations. In other words, the gas model used for disposal room calculations is simply a device to enter a range of gas contents into the calculations, and should not be interpreted as having any exact significance in regard to predicted repository conditions. In other words, while it is desirable to keep these gas contents somewhat typical of parameter values used in the BRAGFLO gas model, to assist in physical intuition of the porosity surface results, the values used in SANTOS need not be exactly representative of repository conditions.

References:

- Beraún R., and P.B. Davies. 1992. "Appendix A: Baseline Design Input Data Base to be Used During Calculations Effort to be Performed by Division 1514 in Determining the Mechanical Creep Closure Behavior of Waste Disposal Rooms in Bedded Salt," *Preliminary Performance Assessment for the Waste Isolation Pilot Plant, December 1992. Volume 3: Model Parameters*. Sandia WIPP Project. SAND92-0700/3. Albuquerque, NM: Sandia National Laboratories. A-7 through A-13.
- Brush, L. H. 1991. *Current Estimates of Gas Production Rates, Gas Production Potentials, and Expected Chemical conditions Relevant to Radionuclide Chemistry for the Long-Term WIPP Performance Assessment*. Appendix A of WIPP PA (Performance Assessment) Division. 1991a. *Preliminary Comparison with 40 CFR Part 191, Subpart B for the Waste Isolation Pilot Plant, December 1991. Volume 3: Reference Data*. SAND91-0893/3. Eds. R.P. Rechar, J.D. Schreiber, H.J. Iuzzolino, M.S. Tierney, and J.S. Sandha. Albuquerque, NM: Sandia National Laboratories, Pages A-27 to A-41.
- Lappin, A.R. , R. L. Hunter, D. P. Garber, and P.B. Davies, eds. 1989. "Systems Analysis, Long-Term Radionuclide Transport, and Dose Assessments, Waste Isolation Pilot Plant (WIPP) , Southeastern New Mexico: March 1989," SAND89-0462, Sandia national Laboratories, Albuquerque, New Mexico.
- Butcher, B. M., Webb, S. W., and Berglund, J. W., 1994. "DISPOSAL ROOM AND CUTTINGS MODELS - WHITE PAPER FOR SYSTEMS PRIORITIZATION AND TECHNICAL BASELINE," WIPP Project document.
- Sandia WIPP Project. 1992. *Preliminary Performance Assessment for the Waste Isolation Pilot Plant, December 1992. Volume 3: Model Parameters*. SAND92-0700/3. Albuquerque NM: Sandia National Laboratories.



Copy to:

MS 1341 B. M. Butcher (6748) day file
MS 1330 SWCF-A: 1.1.1.2.3; DRM



**Title 40 CFR Part 191
Compliance Certification
Application
for the
Waste Isolation Pilot Plant

PORSURF Attachment 4**



THIS PAGE INTENTIONALLY LEFT BLANK



UPD 37537

Sandia National Laboratories

Albuquerque, New Mexico 87185

date: April 18, 1996

to: B. M. Butcher, 6748, MS1341

INFORMATION ONLY

Charles M. Stone

from: C. M. Stone, 9117, MS0443

subject: Resolution of remaining issues for the final disposal room calculations



Disposal Room Elevation

In Butcher and Holmes (1995), the local zero reference is defined to be Clay G which is at Elevation 387.07 m above mean sea level and the top of MB 139 is at Elevation 379.11 which results in a distance below the reference of 7.96 m. Butcher and Holmes also locates the floor of the disposal room at Elevation 380.49 m. This locates the floor 1.38 m above MB 139 and 6.58 below Clay G. The top of MB 139 is shown in Figure 2 of Butcher and Holmes (1995) and Munson (1989) to be - 7.77 m below Clay G rather than -7.96 m. It was decided to hold the top of MB 139 to be - 7.77 m as shown in the referenced figures and locate the disposal room floor 1.38 m above at -6.39 m below Clay G. It was felt that the location of the disposal room relative to MB 139 was the important dimension here. The top of the disposal room is located 3.96 m above the disposal room floor at -2.43 m relative to Clay G.

Determination of Plastic Constants for the TRU Waste

In Butcher and Holmes (1995), the inelastic deviatoric response of the TRU waste is characterized by a constitutive model of the form

$$J_2 = a_0 + a_1 p + a_2 p^2 \quad (\text{EQ 1})$$

where J_2 is the second deviatoric stress invariant, p is the pressure (positive in compression), and a_0 , a_1 , and a_2 are material constants. The material constants are defined for this particular form of deviatoric response. In SANTOS, the model for the waste is written in a different functional form

$$\bar{\sigma} = A_0 + A_1 p + A_2 p^2 \quad (\text{EQ 2})$$

where $\bar{\sigma}$ is the von Mises equivalent stress and p is the pressure (positive in compression). The material constants A_1 , A_2 , and A_3 are different from a_1 , a_2 , and a_3 .

$$K = \frac{E}{3(1-2\nu)} \quad (\text{EQ 7})$$

SANTOS requires the input to the material model which describes the anhydrite nonlinear response to be given in terms of effective stress, $\bar{\sigma} = \sqrt{3J_2}$, and pressure, $p = \frac{J_1}{3}$.

Rewriting Eq. (5) in terms of $\bar{\sigma}$ and p , we obtain the following relationship

$$\bar{\sigma} = \sqrt{3}C - 3\sqrt{3}ap. \quad (\text{EQ 8})$$

The SANTOS input constant A0 is $\sqrt{3}C$ and the input constant A1 is $3\sqrt{3}a$. The set of SANTOS input parameters for the anhydrite is given in Table 2.

Table 2: SANTOS Input Parameters for the Anhydrite Layers

Material	TWO MU (Gpa)	BULK MODULUS (Gpa)	A0 (Mpa)	A1	A2
Anhydrite	55.63	83.444	2.338	2.338	0.0

Determination of SANTOS Input Elastic Constants for Halite and Argillaceous Halite

The finite element code, SANTOS, uses TWO MU and BULK MODULUS as input for the elastic parameters in the M-D creep model. The quantity, TWO MU, is twice the shear modulus, μ . The value of the shear modulus reported by Munson for halite and argillaceous halite is 12.4 Gpa. This means that TWO MU has a value of 24.8 Gpa. The value of the BULK MODULUS is not given directly by Munson (1995) but it may be calculated from the following relation given in Fung (1965):

$$K = \frac{E}{3(1-2\nu)} \quad (\text{EQ 9})$$

where K , E and ν are the bulk modulus, Young's modulus and Poisson's ratio, respectively. The values for Young's modulus and Poisson's ratio are given by Munson (1995). The resulting value of the bulk modulus is calculated to be 20.66 Gpa.



References

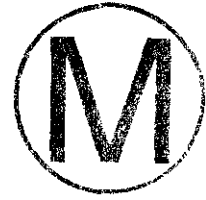
Butcher, B. M. and J. T. Holmes. 1995. "Completion of Milestone DR015, Definition of Closure Analysis Input Parameters, Due March 31, 1995," Memorandum to Les

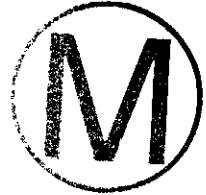
**Title 40 CFR Part 191
Compliance Certification
Application
for the
Waste Isolation Pilot Plant

PORSURF Attachment 5**



THIS PAGE INTENTIONALLY LEFT BLANK





**Sample SANTOS Input File
for a Disposal Room Analysis**



TITLE
DISPOSAL ROOM CALCULATION - FINAL - F = 2.0 - WASTE W/O BACKFILL
PLANE STRAIN
INITIAL STRESS = USER
GRAVITY = 1 = 0. = -9.79 = 0.
PLOT ELEMENT, STRESS, STRAIN, VONMISES, PRESSURE
PLOT NODAL, DISPLACEMENT, RESIDUAL
PLOT STATE, EQCS, EV
RESIDUAL TOLERANCE = 0.5
MAXIMUM ITERATIONS = 1000
MAXIMUM TOLERANCE = 100.
INTERMEDIATE PRINT = 100
ELASTIC SOLUTION
PREDICTOR SCALE FACTOR = 3
AUTO STEP .015 2.592E6 NOREDUCE 1.E-5
TIME STEP SCALE = 0.5
HOURLASS STIFFENING = .005
STEP CONTROL
500 3.1536e7
2000 3.1536e9
36000 3.1536e11
END
OUTPUT TIME
1 3.1536e7
1 3.1536e9
200 3.1536e11
END
PLOT TIME
10 3.1536e7
100 3.1536e9
120 3.1536e11
END
MATERIAL, 1, M-D CREEP MODEL, 2300. \$ ARGILLACEOUS HALITE
TWO MU = 24.8E9
BULK MODULUS = 20.66E9
A1 = 1.407E23
Q1/R = 41.94
N1 = 5.5
B1 = 8.998E6
A2 = 1.314E13
Q2/R = 16.776
N2 = 5.0
B2 = 4.289E-2
SIGO = 20.57E6
QLC = 5335.
M = 3.0
K0 = 2.47E6
C = 2.759
ALPHA = -14.96
BETA = -7.738
DELTLC = .58
RN3 = 2.
AMULT = .95
END

MATERIAL, 2, SOIL N FOAMS, 2300. \$ ANHYDRITE
TWO MU = 5.563E10
BULK MODULUS = 8.3444E10
A0 = 2.338e6
A1 = 2.338
A2 = 0.
PRESSURE CUTOFF = 0.0
FUNCTION ID = 0
END
MATERIAL, 3, M-D CREEP MODEL, 2300. \$ PURE HALITE
TWO MU = 24.8E9
BULK MODULUS = 20.66E9
A1 = 8.386E22
Q1/R = 41.94
N1 = 5.5
B1 = 6.086E6
A2 = 9.672E12
Q2/R = 16.776
N2 = 5.0
B2 = 3.034E-2
SIG0 = 20.57E6
QLC = 5335.
M = 3.0
K0 = 6.275E5
C = 2.759
ALPHA = -17.37
BETA = -7.738
DELTLC = .58
RN3 = 2.
AMULT = .95
END
MATERIAL, 4, SOIL N FOAMS, 752.
TWO MU = 3.333E8
BULK MODULUS = 2.223E8
A0 = 1.0e6
A1 = 3.
A2 = 0.
PRESSURE CUTOFF = 0.
FUNCTION ID = 2
END
NO DISPLACEMENT X = 1
NO DISPLACEMENT Y = 2
PRESSURE, 10, 1, 13.57E6
CONTACT SURFACE, 100, 400, 0., 1.E-3, 1.E40
CONTACT SURFACE, 200, 500, 0., 1.E-3, 1.E4
CONTACT SURFACE, 300, 600, 0., 1.E-3, 1.E4
CONTACT SURFACE, 300, 200, 0., 1.E-3, 1.E4
CONTACT SURFACE, 100, 200, 0., 1.E-3, 1.E4
ADAPTIVE PRESSURE, 700, 1.e-6, -6.4
FUNCTION,1 \$ FUNCTION TO DEFINE PRESCRIBED PRESSURE
0., 1.
3.1536e11, 1.
END
FUNCTION,2



0.0000, 0.0000
0.5101, 1.5300E6
0.6314, 2.0307E6
0.7189, 2.5321E6
0.7855, 3.0312E6
0.8382, 3.5301E6
0.8808, 4.0258E6
0.9422, 4.9333E6
1.1400, 12.000E6

END

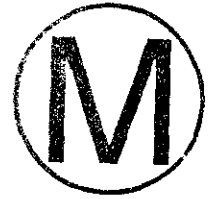
FUNCTION = 3

0. 0.5

3.1536E11 1.

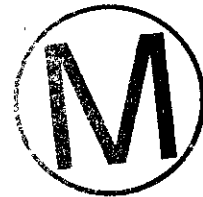
END

EXIT

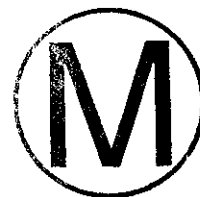


**Title 40 CFR Part 191
Compliance Certification
Application
for the
Waste Isolation Pilot Plant

PORSURF Attachment 6**



THIS PAGE INTENTIONALLY LEFT BLANK



WPO 35697
INFORMATION ONLY



Section 1

Final Porosity Surface Data

$f = 2.0$



F=2.0						
time	porosity	time	void	gas	pressure	
sec	x	years	m3/room	mols/rm	Pa	
0	0.8483495	0	3083.473	0	0	0
0.000423765	0.8483374	1.34283E-11	3083.183	3.65465E-07	2.95987E-07	3.65911E-07
0.3039016	0.8483381	9.63006E-09	3083.201	0.000262092	0.000212265	0.000262412
23.31368	0.8482744	7.38766E-07	3081.674	0.02010626	0.0162919	0.02013084
120.9136	0.8480789	3.83152E-06	3076.999	0.1042787	0.08462427	0.1044061
299.387	0.8478237	0.000009487	3070.914	0.2581982	0.2099486	0.2585141
548.8245	0.8475701	1.73912E-05	3064.889	0.4733189	0.3856271	0.473899
925.698	0.847299	2.93336E-05	3058.468	0.7983432	0.6517974	0.799319
1492.813	0.8470093	4.73044E-05	3051.633	1.287436	1.053467	1.289012
2180.684	0.8467551	6.91017E-05	3045.657	1.880672	1.541911	1.882972
3037.924	0.8465179	0.000096266	3040.099	2.619975	2.151972	2.623179
5222.593	0.8461019	0.000165494	3030.39	4.504085	3.711368	4.50958
9240.603	0.8456307	0.000292817	3019.458	7.969308	6.590497	7.979041
16740.83	0.8451068	0.000530485	3007.381	14.43768	11.98771	14.45534
30168.47	0.8445653	0.000955981	2994.983	26.01798	21.69234	26.0498
55021.53	0.8439927	0.001743527	2981.968	47.45183	39.73539	47.50989
90710.12	0.8434843	0.00287443	2970.491	78.23049	65.762	78.32616
135713.5	0.8430544	0.0043005	2960.845	117.0424	98.70861	117.1856
196221.3	0.8426387	0.006217876	2951.567	169.2257	143.1664	169.4327
263352.4	0.8423208	0.008345134	2944.505	227.1212	192.6072	227.3989
432279.8	0.84175	0.01369812	2931.897	372.808	317.5148	373.2641
758790.8	0.8410248	0.02404463	2916.008	654.3986	560.378	655.1992
1195521	0.8404011	-0.03788377	2902.458	1031.045	887.031	1032.306
1942632	0.8397102	0.06155828	2887.571	1675.37	1448.79	1677.419
3042193	0.8389793	0.09640126	2871.962	2623.657	2281.159	2626.865
4745339	0.8381719	0.1503707	2854.883	4092.489	3579.534	4097.494
6448483	0.8375347	0.2043401	2841.525	5561.32	4887.13	5568.124
8175903	0.8369728	0.2590787	2829.83	7051.086	6221.9	7059.711
10632420	0.8363128	0.3369212	2816.198	9169.647	8130.49	9180.862
13476470	0.8356398	0.4270435	2802.409	11622.42	10356	11636.63
17636660	0.8347485	0.5588721	2784.322	15210.26	13640.95	15228.87
22458370	0.8338156	0.7116627	2765.597	19368.61	17487.86	19392.29
205088000	0.8115187	6.498847	2373.229	176872.6	186100.9	177089
464465700	0.7858137	14.71803	2022.26	400565.9	494611.2	401055.5
723843000	0.7624159	22.9372	1768.82	624258.9	881268.7	625022.3
983220500	0.7417777	31.15638	1583.395	847952	1337241	848989.9
1242598000	0.727368	39.37556	1470.573	1071645	1819666	1072956
1501976000	0.7188382	47.59474	1409.237	1295339	2295232	1296923
1761353000	0.7129353	55.81392	1368.925	1519032	2770860	1520890
2020731000	0.7087163	64.0331	1341.113	1742725	3244821	1744856
2280108000	0.7057449	72.25227	1322.005	1966418	3714243	1968824
2539486000	0.7036773	80.47145	1308.934	2190111	4178069	2192789
2798863000	0.702288	88.69063	1300.254	2413804	4635550	2416757
3058241000	0.7014123	96.90981	1294.824	2637498	5086379	2640724
3465463000	0.7007026	109.8139	1290.447	2988695	5783210	2992352
3776716000	0.7004976	119.6769	1289.186	3257127	6308797	3261112
4087969000	0.7004176	129.5399	1288.694	3525558	6831331	3529870
4399224000	0.7003872	139.403	1288.508	3793992	7352527	3798633

4710477000	0.7003797	149.266	1288.462	4062424	7873010	4067392
5021729000	0.7003952	159.129	1288.557	4330855	8392617	4336153
5332982000	0.7004222	168.992	1288.723	4599287	8911654	4604914
5644234000	0.7004575	178.855	1288.94	4867718	9430184	4873673
5955487000	0.7004954	188.718	1289.172	5136149	9948421	5142432
6266740000	0.7005371	198.581	1289.429	5404581	10466280	5411197
6577992000	0.7005849	208.444	1289.722	5673012	10983600	5679949
6889248000	0.7006416	218.3071	1290.071	5941446	11500210	5948712
7200501000	0.7007089	228.1701	1290.485	6209878	12015930	6217473
7511753000	0.7007897	238.0331	1290.983	6478309	12530500	6486232
7823006000	0.700883	247.8961	1291.557	6746741	13043900	6754988
8134258000	0.7009918	257.7591	1292.228	7015172	13555840	7023752
8445511000	0.7011215	267.6221	1293.028	7283603	14065840	7292512
8756764000	0.7012783	277.4851	1293.996	7552035	14573320	7561274
9068020000	0.7014615	287.3482	1295.128	7820469	15078130	7830036
9379273000	0.7016702	297.2112	1296.42	8088901	15580130	8098794
9690525000	0.7019118	307.0742	1297.917	8357331	16078590	8367552
10001780000	0.7022331	316.9372	1299.912	8625763	16569550	8636310
10313030000	0.7025061	326.8002	1301.611	8894194	17062900	8905075
10624280000	0.702837	336.6632	1303.674	9162626	17550040	9173829
10935540000	0.7032559	346.5262	1306.293	9431057	18027990	9442597
11246790000	0.7037647	356.3893	1309.483	9699492	18495940	9711355
11558040000	0.7043823	366.2523	1313.37	9967922	18951550	9980111
11869300000	0.7051286	376.1153	1318.089	10236350	19392230	10248870
12180550000	0.7060144	385.9783	1323.722	10504790	19816080	10517640
12491800000	0.7070522	395.8413	1330.364	10773220	20220980	10786390
12803050000	0.7082474	405.7043	1338.072	11041650	20605440	11055160
13114310000	0.7096498	415.5674	1347.197	11310080	20963410	11323920
13425560000	0.7112771	425.4304	1357.897	11578510	21291840	11592670
13736810000	0.7131584	435.2934	1370.418	11846950	21586420	11861440
14048070000	0.7152778	445.1564	1384.722	12115380	21847500	12130200
14359320000	0.7176278	455.0194	1400.834	12383810	22074700	12398950
14670570000	0.7201629	464.8824	1418.518	12652240	22272050	12667720
14981830000	0.7228466	474.7454	1437.591	12920670	22442820	12936490
15293080000	0.7256501	484.6084	1457.913	13189100	22589730	13205240
15604330000	0.7285469	494.4714	1479.354	13457530	22715440	13474010
15915590000	0.7314913	504.3345	1501.62	13725970	22824980	13742760
16226840000	0.7344802	514.1975	1524.728	13994400	22918660	14011520
16538090000	0.7374783	524.0605	1548.436	14262830	23000640	14280280
16849340000	0.7404667	533.9235	1572.612	14531260	23073270	14549040
17160600000	0.7434729	543.7865	1597.501	14799690	23133370	14817800
17471850000	0.7463781	553.6495	1622.114	15018460	23092450	15019480
17783100000	0.7489718	563.5126	1644.569	15152680	22980920	15153850
18094350000	0.7513083	573.3755	1665.199	15286890	22897490	15288240
18405610000	0.7534794	583.2386	1684.719	15421110	22831120	15422620
18716860000	0.7554953	593.1016	1703.153	15555330	22780780	15557000
19028120000	0.7573975	602.9646	1720.829	15689540	22741530	15691370
19339370000	0.7592142	612.8276	1737.972	15823760	22710060	15825760
19650620000	0.7609535	622.6906	1754.627	15957970	22685490	15960130
19961870000	0.7626346	632.5536	1770.958	16092190	22665540	16094520
20273130000	0.7642738	642.4167	1787.106	16226410	22648270	16228890





20584380000	0.7658509	652.2797	1802.856	16360620	22636320	16363280
20895640000	0.7673991	662.1427	1818.524	16494840	22625580	16497660
21206890000	0.7689106	672.0057	1834.024	16629050	22617100	16632040
21518140000	0.7703854	681.8687	1849.344	16763270	22610960	16766420
21829400000	0.7718363	691.7318	1864.609	16897490	22605590	16900800
22140650000	0.7732652	701.5947	1879.834	17031700	22600790	17035180
22451900000	0.7746652	711.4578	1894.938	17165920	22597520	17169570
22763150000	0.7760349	721.3207	1909.898	17300130	22595980	17303940
23074400000	0.7774	731.1838	1924.991	17434350	22592920	17438320
23385660000	0.7787429	741.0468	1940.02	17568570	22590660	17572710
23696910000	0.7800556	750.9098	1954.888	17702780	22590280	17707080
24008170000	0.7813518	760.7728	1969.745	17837000	22590030	17841460
24319420000	0.7826373	770.6358	1984.654	17971210	22589200	17975840
24630670000	0.7839077	780.4988	1999.562	18105430	22588400	18110230
24941920000	0.7851639	790.3619	2014.477	18239640	22587520	18244600
25253180000	0.7864039	800.2249	2029.371	18373860	22586880	18378970
25564430000	0.7876278	810.0879	2044.244	18508080	22586510	18513370
25875680000	0.7888415	819.9509	2059.161	18642290	22585630	18647730
26186930000	0.7900339	829.8139	2073.985	18776510	22585790	18782110
26498190000	0.7912272	839.6769	2088.991	18910720	22583990	18916500
26809440000	0.7924027	849.5399	2103.94	19044940	22582810	19050870
27120700000	0.7935637	859.403	2118.873	19179160	22581840	19185270
27431950000	0.7947065	869.266	2133.737	19313370	22581600	19319650
27743200000	0.7958462	879.129	2148.726	19447590	22580050	19454030
28054450000	0.7969754	888.992	2163.742	19581800	22578230	19588400
28365710000	0.7980912	898.855	2178.745	19716020	22576580	19722780
28676960000	0.7992012	908.718	2193.836	19850230	22574040	19857150
28988220000	0.8002967	918.5811	2208.895	19984450	22571880	19991550
29299460000	0.8013791	928.444	2223.936	20118670	22569910	20125920
29610720000	0.8024582	938.3071	2239.096	20252880	22566780	20260300
29921970000	0.8035259	948.1701	2254.259	20387100	22563650	20394670
30233230000	0.8045833	958.0331	2269.439	20521310	22560400	20529050
30544480000	0.8056257	967.8961	2284.565	20655530	22557720	20663420
30855730000	0.8066597	977.7591	2299.732	20789750	22554700	20797820
31166980000	0.807686	987.6221	2314.946	20923960	22551240	20932200
31478240000	0.808701	997.4852	2330.153	21058180	22547890	21066570
31789490000	0.8097081	1007.348	2345.403	21192390	22544190	21200970
32100740000	0.8107073	1017.211	2360.692	21326610	22540140	21335340
32411990000	0.8116947	1027.074	2375.961	21460820	22536330	21469700
32723240000	0.8126783	1036.937	2391.331	21595040	22531640	21604090
33034500000	0.8136467	1046.8	2406.622	21729260	22527730	21738470
33345750000	0.8145774	1056.663	2421.469	21772800	22425940	21773740
33657000000	0.8154119	1066.526	2434.908	21772800	22302160	21773740
33968250000	0.8161579	1076.389	2447.025	21772800	22191720	21773730
34279500000	0.8168374	1086.252	2458.147	21772800	22091320	21773740
34590760000	0.8174528	1096.115	2468.293	21772800	22000520	21773750
34902010000	0.8180214	1105.978	2477.728	21772800	21916760	21773770
35213260000	0.8185501	1115.841	2486.553	21772800	21838950	21773740
35524520000	0.8190414	1125.704	2494.8	21772800	21766750	21773730
35835770000	0.819498	1135.567	2502.506	21772800	21699740	21773750
36147020000	0.8199269	1145.43	2509.78	21772800	21636850	21773750

36458270000	0.8203315	1155.293	2516.672	21772800	21577590	21773740
36769530000	0.8207163	1165.156	2523.257	21772800	21521280	21773750
37080780000	0.8210791	1175.019	2529.49	21772800	21468240	21773740
37392030000	0.8214247	1184.882	2535.453	21772800	21417760	21773750
37703280000	0.8217552	1194.745	2541.176	21772800	21369510	21773730
38014540000	0.8220668	1204.608	2546.592	21772800	21324080	21773750
38325820000	0.8223691	1214.472	2551.864	21772800	21280030	21773750
38637040000	0.8226575	1224.334	2556.91	21772800	21238030	21773750
38948330000	0.8229347	1234.198	2561.776	21772800	21197690	21773750
39259580000	0.8232011	1244.061	2566.467	21772800	21158940	21773750
39570800000	0.823463	1253.923	2571.092	21772800	21120890	21773760
39882050000	0.8237109	1263.786	2575.483	21772800	21084880	21773760
40193340000	0.8239498	1273.65	2579.725	21772800	21050200	21773750
40504560000	0.8241871	1283.512	2583.951	21772800	21015770	21773740
40815840000	0.8244087	1293.376	2587.908	21772800	20983640	21773750
41127100000	0.8246287	1303.239	2591.846	21772800	20951760	21773750
41438350000	0.8248404	1313.102	2595.645	21772800	20921090	21773750
41749600000	0.8250461	1322.965	2599.345	21772800	20891310	21773750
42060850000	0.8252465	1332.828	2602.957	21772800	20862320	21773750
42372110000	0.825443	1342.691	2606.508	21772800	20833910	21773760
42683360000	0.8256316	1352.554	2609.924	21772800	20806630	21773750
42994610000	0.8258139	1362.417	2613.231	21772800	20780290	21773740
43305870000	0.8259929	1372.28	2616.487	21772800	20754440	21773750
43617120000	0.8261695	1382.143	2619.705	21772800	20728950	21773750
43928370000	0.8263383	1392.006	2622.787	21772800	20704590	21773750
44239620000	0.826502	1401.869	2625.782	21772800	20680970	21773740
44550880000	0.8266633	1411.732	2628.739	21772800	20657720	21773760
44862120000	0.8268222	1421.595	2631.656	21772800	20634810	21773750
45173380000	0.8269769	1431.458	2634.502	21772800	20612520	21773750
45484630000	0.8271258	1441.321	2637.245	21772800	20591070	21773740
45795880000	0.8272752	1451.184	2640.004	21772800	20569560	21773740
46107140000	0.8274184	1461.047	2642.651	21772800	20548950	21773740
46418390000	0.8275604	1470.91	2645.282	21772800	20528530	21773760
46729640000	0.8276971	1480.773	2647.818	21772800	20508860	21773750
47040890000	0.8278323	1490.636	2650.329	21772800	20489420	21773740
47352150000	0.827964	1500.499	2652.781	21772800	20470490	21773750
47663400000	0.8280942	1510.362	2655.207	21772800	20451790	21773750
47974650000	0.8282213	1520.225	2657.58	21772800	20433530	21773750
48285900000	0.8283466	1530.088	2659.922	21772800	20415540	21773760
48597160000	0.8284681	1539.951	2662.196	21772800	20398080	21773730
48908410000	0.8285872	1549.814	2664.429	21772800	20380990	21773740
49219660000	0.8287055	1559.677	2666.65	21772800	20364010	21773730
49530920000	0.8288216	1569.54	2668.833	21772800	20347370	21773750
49842170000	0.828934	1579.403	2670.948	21772800	20331250	21773740
50153420000	0.8290455	1589.266	2673.049	21772800	20315260	21773730
50464670000	0.8291546	1599.129	2675.109	21772800	20299640	21773760
50775920000	0.8292618	1608.992	2677.134	21772800	20284280	21773750
51087180000	0.8293678	1618.855	2679.14	21772800	20269100	21773760
51398430000	0.8294716	1628.718	2681.106	21772800	20254210	21773730
51709690000	0.8295752	1638.581	2683.071	21772800	20239390	21773750
52020940000	0.8296748	1648.444	2684.962	21772800	20225120	21773730





52332190000	0.8297742	1658.307	2686.852	21772800	20210910	21773750
52643440000	0.8298711	1668.17	2688.697	21772800	20197050	21773760
52954690000	0.8299669	1678.033	2690.522	21772800	20183340	21773740
53265950000	0.8300614	1687.896	2692.324	21772800	20169830	21773740
53577200000	0.8301544	1697.759	2694.101	21772800	20156530	21773750
53888450000	0.830246	1707.622	2695.851	21772800	20143450	21773750
54199710000	0.8303366	1717.485	2697.585	21772800	20130490	21773740
54510960000	0.8304249	1727.348	2699.277	21772800	20117870	21773740
54822210000	0.8305126	1737.211	2700.959	21772800	20105350	21773750
55133460000	0.8305996	1747.074	2702.629	21772800	20092920	21773740
55444710000	0.8306851	1756.937	2704.272	21772800	20080710	21773740
55755970000	0.8307696	1766.8	2705.898	21772800	20068650	21773740
56067220000	0.8308529	1776.663	2707.502	21772800	20056750	21773730
56378470000	0.8309351	1786.526	2709.087	21772800	20045040	21773760
56689730000	0.8310156	1796.389	2710.639	21772800	20033540	21773730
57000980000	0.8310952	1806.252	2712.177	21772800	20022190	21773750
57312230000	0.8311739	1816.115	2713.698	21772800	20010970	21773750
57623480000	0.8312514	1825.978	2715.197	21772800	19999920	21773750
57934730000	0.8313285	1835.841	2716.691	21772800	19988930	21773750
58245990000	0.8314043	1845.704	2718.16	21772800	19978130	21773760
58557240000	0.8314798	1855.567	2719.624	21772800	19967370	21773750
58868490000	0.8315544	1865.43	2721.073	21772800	19956740	21773760
59179750000	0.8316272	1875.293	2722.488	21772800	19946360	21773750
59491000000	0.8316993	1885.156	2723.891	21772800	19936100	21773760
59802250000	0.831771	1895.019	2725.287	21772800	19925880	21773750
60113500000	0.8318411	1904.882	2726.652	21772800	19915890	21773740
60424760000	0.831911	1914.745	2728.016	21772800	19905950	21773760
60736010000	0.8319796	1924.608	2729.354	21772800	19896180	21773740
61047300000	0.8320476	1934.472	2730.682	21772800	19886510	21773750
61358510000	0.8321145	1944.334	2731.99	21772800	19876990	21773750
61669800000	0.8321813	1954.198	2733.296	21772800	19867470	21773730
61981050000	0.832247	1964.061	2734.584	21772800	19858130	21773750
62292270000	0.8323118	1973.923	2735.853	21772800	19848920	21773750
62603530000	0.8323762	1983.786	2737.115	21772800	19839760	21773740
62914810000	0.8324397	1993.65	2738.363	21772800	19830730	21773750
63226030000	0.8325027	2003.512	2739.6	21772800	19821770	21773750
63537310000	0.8325649	2013.376	2740.822	21772800	19812930	21773740
63848570000	0.8326268	2023.239	2742.04	21772800	19804140	21773750
64159820000	0.8326877	2033.102	2743.238	21772800	19795480	21773740
64471070000	0.8327484	2042.965	2744.434	21772800	19786870	21773760
64782320000	0.8328079	2052.828	2745.606	21772800	19778410	21773750
65093570000	0.8328671	2062.691	2746.774	21772800	19769990	21773730
65404830000	0.8329256	2072.554	2747.929	21772800	19761690	21773750
65716080000	0.8329838	2082.417	2749.079	21772800	19753430	21773750
66027340000	0.8330413	2092.28	2750.216	21772800	19745270	21773760
66338590000	0.833098	2102.143	2751.337	21772800	19737220	21773750
66649850000	0.8331543	2112.006	2752.452	21772800	19729230	21773760
66961090000	0.8332102	2121.869	2753.558	21772800	19721290	21773740
67272340000	0.8332655	2131.732	2754.654	21772800	19713450	21773750
67583600000	0.8333199	2141.595	2755.733	21772800	19705720	21773740
67894850000	0.833374	2151.458	2756.808	21772800	19698050	21773750

68206100000	0.8334275	2161.321	2757.869	21772800	19690460	21773740
68517360000	0.8334805	2171.184	2758.922	21772800	19682940	21773740
68828610000	0.8335331	2181.047	2759.969	21772800	19675490	21773750
69139860000	0.8335851	2190.91	2761.003	21772800	19668110	21773740
69451110000	0.8336369	2200.773	2762.034	21772800	19660760	21773730
69762370000	0.8336883	2210.636	2763.059	21772800	19653480	21773750
70073620000	0.8337389	2220.499	2764.068	21772800	19646310	21773750
70384880000	0.8337893	2230.362	2765.073	21772800	19639160	21773740
70696120000	0.833839	2240.225	2766.064	21772800	19632130	21773750
71007370000	0.8338883	2250.088	2767.049	21772800	19625140	21773750
71318630000	0.8339373	2259.951	2768.028	21772800	19618190	21773740
71629880000	0.8339856	2269.814	2768.994	21772800	19611360	21773750
71941140000	0.8340337	2279.677	2769.957	21772800	19604550	21773760
72252390000	0.8340813	2289.54	2770.909	21772800	19597800	21773740
72563650000	0.8341284	2299.403	2771.852	21772800	19591130	21773740
72874890000	0.8341751	2309.266	2772.788	21772800	19584520	21773750
73186140000	0.8342215	2319.129	2773.718	21772800	19577950	21773740
73497400000	0.8342674	2328.992	2774.639	21772800	19571450	21773740
73808650000	0.834313	2338.855	2775.554	21772800	19565000	21773740
74119910000	0.8343583	2348.718	2776.464	21772800	19558580	21773740
74431160000	0.8344032	2358.581	2777.367	21772800	19552230	21773740
74742420000	0.8344477	2368.444	2778.261	21772800	19545930	21773730
75053650000	0.8344919	2378.307	2779.151	21772800	19539680	21773740
75364910000	0.8345357	2388.17	2780.032	21772800	19533480	21773740
75676160000	0.8345789	2398.033	2780.902	21772800	19527370	21773740
75987420000	0.8346221	2407.896	2781.772	21772800	19521260	21773730
76298670000	0.8346649	2417.759	2782.635	21772800	19515220	21773750
76609930000	0.8347073	2427.622	2783.491	21772800	19509230	21773760
76921180000	0.8347491	2437.485	2784.334	21772800	19503310	21773750
77232420000	0.8347909	2447.348	2785.178	21772800	19497390	21773740
77543680000	0.8348323	2457.211	2786.014	21772800	19491550	21773750
77854930000	0.8348734	2467.074	2786.844	21772800	19485730	21773730
78166190000	0.834914	2476.937	2787.667	21772800	19480000	21773760
78477440000	0.8349546	2486.8	2788.488	21772800	19474260	21773750
78788700000	0.8349947	2496.663	2789.298	21772800	19468600	21773750
79099940000	0.8350345	2506.526	2790.104	21772800	19462960	21773730
79411190000	0.835074	2516.389	2790.905	21772800	19457390	21773750
79722450000	0.8351133	2526.252	2791.701	21772800	19451840	21773740
80033700000	0.8351521	2536.115	2792.488	21772800	19446350	21773740
80344960000	0.8351908	2545.978	2793.273	21772800	19440880	21773730
80656210000	0.8352293	2555.841	2794.054	21772800	19435460	21773750
80967470000	0.8352673	2565.704	2794.827	21772800	19430090	21773750
81278710000	0.8353052	2575.567	2795.597	21772800	19424740	21773750
81589960000	0.8353427	2585.43	2796.359	21772800	19419440	21773750
81901220000	0.83538	2595.293	2797.118	21772800	19414180	21773760
82212470000	0.8354171	2605.156	2797.872	21772800	19408940	21773750
82523730000	0.8354539	2615.019	2798.622	21772800	19403750	21773760
82834980000	0.8354903	2624.882	2799.362	21772800	19398600	21773740
83146240000	0.8355266	2634.745	2800.102	21772800	19393480	21773750
83457470000	0.8355626	2644.608	2800.835	21772800	19388400	21773740
83768730000	0.8355983	2654.471	2801.563	21772800	19383360	21773740





84079980000	0.8356339	2664.334	2802.289	21772800	19378340	21773740
84391270000	0.8356692	2674.198	2803.01	21772800	19373360	21773750
84702530000	0.8357042	2684.061	2803.725	21772800	19368420	21773750
85013770000	0.835739	2693.924	2804.436	21772800	19363510	21773750
85325030000	0.8357736	2703.787	2805.142	21772800	19358630	21773740
85636240000	0.835808	2713.649	2805.845	21772800	19353780	21773740
85947500000	0.8358421	2723.512	2806.542	21772800	19348970	21773740
86258750000	0.8358761	2733.375	2807.239	21772800	19344180	21773750
86570040000	0.8359098	2743.239	2807.928	21772800	19339430	21773750
86881300000	0.8359433	2753.102	2808.614	21772800	19334710	21773750
87192540000	0.8359764	2762.965	2809.292	21772800	19330030	21773740
87503790000	0.8360095	2772.828	2809.97	21772800	19325370	21773740
87815050000	0.8360423	2782.691	2810.642	21772800	19320750	21773740
88126300000	0.836075	2792.554	2811.313	21772800	19316140	21773740
88437560000	0.8361073	2802.417	2811.976	21772800	19311580	21773740
88748810000	0.8361396	2812.28	2812.639	21772800	19307040	21773750
89060070000	0.8361716	2822.143	2813.297	21772800	19302520	21773750
89371310000	0.8362033	2832.006	2813.947	21772800	19298050	21773730
89682560000	0.836235	2841.869	2814.598	21772800	19293600	21773750
89993810000	0.8362664	2851.732	2815.244	21772800	19289170	21773740
90305070000	0.8362976	2861.595	2815.885	21772800	19284770	21773730
90616320000	0.8363286	2871.458	2816.524	21772800	19280410	21773750
90927580000	0.8363595	2881.321	2817.159	21772800	19276060	21773750
91238830000	0.8363901	2891.184	2817.789	21772800	19271740	21773740
91550080000	0.8364206	2901.047	2818.417	21772800	19267450	21773740
91861330000	0.8364509	2910.91	2819.041	21772800	19263190	21773750
92172580000	0.836481	2920.773	2819.662	21772800	19258950	21773750
92483840000	0.8365109	2930.636	2820.279	21772800	19254730	21773740
92795090000	0.8365407	2940.499	2820.893	21772800	19250540	21773740
93106350000	0.8365703	2950.362	2821.504	21772800	19246370	21773740
93417600000	0.8365997	2960.225	2822.111	21772800	19242240	21773750
93728840000	0.8366289	2970.088	2822.714	21772800	19238120	21773740
94040100000	0.836658	2979.951	2823.315	21772800	19234030	21773750
94351350000	0.8366869	2989.814	2823.912	21772800	19229960	21773740
94662610000	0.8367157	2999.677	2824.507	21772800	19225910	21773740
94973860000	0.8367442	3009.54	2825.096	21772800	19221900	21773740
95285120000	0.8367726	3019.403	2825.685	21772800	19217910	21773760
95596370000	0.8368009	3029.266	2826.269	21772800	19213930	21773750
95907610000	0.8368289	3039.129	2826.849	21772800	19209980	21773740
96218870000	0.8368568	3048.992	2827.427	21772800	19206060	21773750
96530120000	0.8368846	3058.855	2828.003	21772800	19202140	21773740
96841380000	0.8369121	3068.718	2828.573	21772800	19198280	21773750
97152630000	0.8369396	3078.581	2829.142	21772800	19194420	21773750
97463890000	0.8369668	3088.444	2829.707	21772800	19190580	21773740
97775130000	0.8369941	3098.307	2830.273	21772800	19186760	21773760
98086380000	0.8370209	3108.17	2830.828	21772800	19182980	21773740
98397630000	0.8370478	3118.033	2831.387	21772800	19179200	21773750
98708890000	0.8370744	3127.896	2831.939	21772800	19175450	21773740
99020140000	0.837101	3137.759	2832.491	21772800	19171720	21773750
99331400000	0.8371273	3147.622	2833.039	21772800	19168020	21773760
99642650000	0.8371535	3157.485	2833.583	21772800	19164330	21773740

Sheet1

99953900000	0.8371796	3167.348	2834.125	21772800	19160660	21773740
1.00265E+11	0.8372055	3177.211	2834.664	21772800	19157020	21773740
1.00576E+11	0.8372313	3187.074	2835.2	21772800	19153390	21773730
1.00888E+11	0.837257	3196.937	2835.736	21772800	19149790	21773760
1.01199E+11	0.8372825	3206.8	2836.266	21772800	19146200	21773740
1.0151E+11	0.8373079	3216.663	2836.794	21772800	19142640	21773750
1.01821E+11	0.8373331	3226.526	2837.319	21772800	19139090	21773740
1.02133E+11	0.8373582	3236.389	2837.842	21772800	19135560	21773740
1.02444E+11	0.8373832	3246.252	2838.364	21772800	19132060	21773760
1.02755E+11	0.8374079	3256.115	2838.878	21772800	19128580	21773740
1.03066E+11	0.8374327	3265.978	2839.396	21772800	19125090	21773740
1.03378E+11	0.8374573	3275.841	2839.909	21772800	19121640	21773740
1.03689E+11	0.8374817	3285.704	2840.417	21772800	19118220	21773740
1.04E+11	0.837506	3295.567	2840.925	21772800	19114800	21773740
1.04311E+11	0.8375301	3305.43	2841.428	21772800	19111410	21773730
1.04623E+11	0.8375543	3315.293	2841.933	21772800	19108020	21773740
1.04934E+11	0.8375782	3325.156	2842.433	21772800	19104670	21773760
1.05245E+11	0.837602	3335.019	2842.931	21772800	19101320	21773750
1.05557E+11	0.8376256	3344.882	2843.424	21772800	19098000	21773740
1.05868E+11	0.8376492	3354.745	2843.918	21772800	19094700	21773760
1.06179E+11	0.8376725	3364.608	2844.404	21772800	19091420	21773740
1.0649E+11	0.8376959	3374.471	2844.894	21772800	19088140	21773750
1.06802E+11	0.8377191	3384.334	2845.379	21772800	19084880	21773740
1.07113E+11	0.8377421	3394.198	2845.861	21772800	19081640	21773740
1.07424E+11	0.8377651	3404.061	2846.343	21772800	19078420	21773750
1.07735E+11	0.8377879	3413.924	2846.821	21772800	19075220	21773750
1.08047E+11	0.8378106	3423.787	2847.295	21772800	19072030	21773730
1.08358E+11	0.8378333	3433.649	2847.771	21772800	19068850	21773740
1.08669E+11	0.8378558	3443.512	2848.244	21772800	19065690	21773750
1.0898E+11	0.8378782	3453.375	2848.713	21772800	19062550	21773750
1.09292E+11	0.8379003	3463.239	2849.176	21772800	19059440	21773740
1.09603E+11	0.8379225	3473.102	2849.643	21772800	19056330	21773750
1.09914E+11	0.8379446	3482.965	2850.106	21772800	19053240	21773760
1.10225E+11	0.8379665	3492.828	2850.566	21772800	19050160	21773750
1.10537E+11	0.8379883	3502.691	2851.024	21772800	19047100	21773750
1.10848E+11	0.83801	3512.554	2851.479	21772800	19044050	21773740
1.11159E+11	0.8380316	3522.417	2851.933	21772800	19041020	21773740
1.1147E+11	0.8380532	3532.28	2852.387	21772800	19038000	21773750
1.11782E+11	0.8380746	3542.143	2852.837	21772800	19034990	21773750
1.12093E+11	0.8380958	3552.006	2853.282	21772800	19032020	21773740
1.12404E+11	0.838117	3561.869	2853.728	21772800	19029040	21773740
1.12715E+11	0.8381381	3571.732	2854.172	21772800	19026080	21773740
1.13027E+11	0.8381591	3581.595	2854.614	21772800	19023140	21773750
1.13338E+11	0.8381801	3591.458	2855.056	21772800	19020200	21773750
1.13649E+11	0.8382008	3601.321	2855.492	21772800	19017290	21773740
1.1396E+11	0.8382214	3611.184	2855.925	21772800	19014400	21773740
1.14272E+11	0.8382421	3621.047	2856.362	21772800	19011510	21773760
1.14583E+11	0.8382625	3630.91	2856.791	21772800	19008640	21773740
1.14894E+11	0.8382829	3640.773	2857.221	21772800	19005780	21773740
1.15205E+11	0.8383033	3650.636	2857.652	21772800	19002930	21773760
1.15517E+11	0.8383234	3660.499	2858.075	21772800	19000100	21773740



1.15828E+11	0.8383436	3670.362	2858.501	21772800	18997280	21773750
1.16139E+11	0.8383636	3680.225	2858.923	21772800	18994470	21773750
1.1645E+11	0.8383835	3690.088	2859.343	21772800	18991680	21773750
1.16762E+11	0.8384033	3699.951	2859.76	21772800	18988900	21773740
1.17073E+11	0.8384231	3709.814	2860.178	21772800	18986130	21773740
1.17384E+11	0.8384428	3719.677	2860.595	21772800	18983370	21773750
1.17695E+11	0.8384623	3729.54	2861.006	21772800	18980640	21773750
1.18007E+11	0.8384818	3739.403	2861.418	21772800	18977900	21773740
1.18318E+11	0.8385012	3749.266	2861.829	21772800	18975180	21773750
1.18629E+11	0.8385205	3759.129	2862.237	21772800	18972480	21773750
1.1894E+11	0.8385397	3768.992	2862.643	21772800	18969780	21773740
1.19252E+11	0.8385589	3778.855	2863.049	21772800	18967110	21773760
1.19563E+11	0.8385779	3788.718	2863.451	21772800	18964440	21773750
1.19874E+11	0.8385968	3798.581	2863.85	21772800	18961790	21773750
1.20185E+11	0.8386157	3808.444	2864.25	21772800	18959150	21773760
1.20497E+11	0.8386344	3818.307	2864.645	21772800	18956510	21773730
1.20808E+11	0.8386531	3828.17	2865.042	21772800	18953900	21773740
1.21119E+11	0.8386717	3838.033	2865.435	21772800	18951300	21773740
1.2143E+11	0.8386902	3847.896	2865.828	21772800	18948700	21773740
1.21742E+11	0.8387086	3857.759	2866.217	21772800	18946120	21773730
1.22053E+11	0.838727	3867.622	2866.607	21772800	18943550	21773740
1.22364E+11	0.8387452	3877.485	2866.992	21772800	18941000	21773730
1.22675E+11	0.8387634	3887.348	2867.379	21772800	18938450	21773740
1.22987E+11	0.8387816	3897.211	2867.764	21772800	18935910	21773740
1.23298E+11	0.8387996	3907.074	2868.146	21772800	18933390	21773750
1.23609E+11	0.8388175	3916.937	2868.526	21772800	18930880	21773740
1.2392E+11	0.8388354	3926.8	2868.906	21772800	18928380	21773750
1.24232E+11	0.8388531	3936.663	2869.282	21772800	18925900	21773750
1.24543E+11	0.8388708	3946.526	2869.658	21772800	18923420	21773750
1.24854E+11	0.8388884	3956.389	2870.031	21772800	18920950	21773740
1.25165E+11	0.838906	3966.252	2870.405	21772800	18918490	21773750
1.25477E+11	0.8389235	3976.115	2870.777	21772800	18916050	21773760
1.25788E+11	0.8389408	3985.978	2871.144	21772800	18913620	21773750
1.26099E+11	0.8389581	3995.841	2871.511	21772800	18911190	21773730
1.2641E+11	0.8389754	4005.704	2871.88	21772800	18908780	21773750
1.26722E+11	0.8389925	4015.567	2872.242	21772800	18906380	21773740
1.27033E+11	0.8390096	4025.43	2872.606	21772800	18903990	21773740
1.27344E+11	0.8390266	4035.293	2872.968	21772800	18901610	21773750
1.27655E+11	0.8390436	4045.156	2873.33	21772800	18899240	21773760
1.27967E+11	0.8390604	4055.019	2873.688	21772800	18896880	21773750
1.28278E+11	0.8390772	4064.882	2874.044	21772800	18894520	21773730
1.28589E+11	0.8390939	4074.745	2874.401	21772800	18892190	21773750
1.289E+11	0.8391106	4084.608	2874.756	21772800	18889850	21773740
1.29212E+11	0.8391271	4094.471	2875.108	21772800	18887540	21773740
1.29523E+11	0.8391436	4104.334	2875.458	21772800	18885230	21773730
1.29834E+11	0.8391601	4114.197	2875.81	21772800	18882930	21773740
1.30146E+11	0.8391765	4124.061	2876.159	21772800	18880640	21773750
1.30457E+11	0.8391927	4133.923	2876.505	21772800	18878360	21773730
1.30768E+11	0.839209	4143.787	2876.853	21772800	18876090	21773750
1.31079E+11	0.8392251	4153.649	2877.196	21772800	18873830	21773740
1.31391E+11	0.8392412	4163.513	2877.539	21772800	18871580	21773740

1.31702E+11	0.8392572	4173.375	2877.88	21772800	18869340	21773730
1.32013E+11	0.8392732	4183.239	2878.222	21772800	18867110	21773750
1.32324E+11	0.8392891	4193.102	2878.562	21772800	18864890	21773760
1.32636E+11	0.8393049	4202.965	2878.899	21772800	18862670	21773750
1.32947E+11	0.8393207	4212.828	2879.236	21772800	18860470	21773760
1.33258E+11	0.8393363	4222.69	2879.568	21772800	18858270	21773730
1.33569E+11	0.8393521	4232.554	2879.906	21772800	18856070	21773740
1.33881E+11	0.8393676	4242.417	2880.238	21772800	18853900	21773740
1.34192E+11	0.8393831	4252.28	2880.569	21772800	18851730	21773740
1.34503E+11	0.8393986	4262.143	2880.9	21772800	18849580	21773760
1.34814E+11	0.8394139	4272.006	2881.226	21772800	18847420	21773730
1.35126E+11	0.8394292	4281.869	2881.554	21772800	18845290	21773740
1.35437E+11	0.8394445	4291.732	2881.881	21772800	18843160	21773760
1.35748E+11	0.8394596	4301.595	2882.204	21772800	18841040	21773750
1.36059E+11	0.8394747	4311.458	2882.526	21772800	18838920	21773730
1.36371E+11	0.8394898	4321.321	2882.85	21772800	18836820	21773750
1.36682E+11	0.8395049	4331.184	2883.173	21772800	18834710	21773750
1.36993E+11	0.8395198	4341.047	2883.492	21772800	18832630	21773750
1.37304E+11	0.8395346	4350.91	2883.808	21772800	18830560	21773750
1.37616E+11	0.8395495	4360.773	2884.127	21772800	18828480	21773750
1.37927E+11	0.8395641	4370.636	2884.44	21772800	18826420	21773730
1.38238E+11	0.8395789	4380.499	2884.758	21772800	18824370	21773760
1.38549E+11	0.8395935	4390.362	2885.07	21772800	18822330	21773750
1.38861E+11	0.839608	4400.225	2885.381	21772800	18820300	21773750
1.39172E+11	0.8396226	4410.088	2885.694	21772800	18818260	21773750
1.39483E+11	0.839637	4419.951	2886.001	21772800	18816250	21773740
1.39794E+11	0.8396513	4429.814	2886.308	21772800	18814240	21773730
1.40106E+11	0.8396657	4439.677	2886.617	21772800	18812240	21773750
1.40417E+11	0.83968	4449.54	2886.924	21772800	18810240	21773750
1.40728E+11	0.8396941	4459.403	2887.226	21772800	18808260	21773740
1.41039E+11	0.8397083	4469.266	2887.531	21772800	18806280	21773740
1.41351E+11	0.8397224	4479.129	2887.833	21772800	18804310	21773740
1.41662E+11	0.8397364	4488.992	2888.134	21772800	18802360	21773750
1.41973E+11	0.8397504	4498.855	2888.434	21772800	18800400	21773740
1.42284E+11	0.8397644	4508.718	2888.735	21772800	18798450	21773750
1.42596E+11	0.8397782	4518.581	2889.031	21772800	18796520	21773750
1.42907E+11	0.839792	4528.444	2889.328	21772800	18794590	21773750
1.43218E+11	0.8398058	4538.307	2889.623	21772800	18792670	21773750
1.43529E+11	0.8398195	4548.17	2889.918	21772800	18790750	21773750
1.43841E+11	0.8398331	4558.033	2890.21	21772800	18788840	21773730
1.44152E+11	0.8398467	4567.896	2890.502	21772800	18786940	21773730
1.44463E+11	0.8398603	4577.759	2890.795	21772800	18785050	21773750
1.44774E+11	0.8398738	4587.622	2891.085	21772800	18783160	21773740
1.45086E+11	0.8398872	4597.485	2891.373	21772800	18781290	21773740
1.45397E+11	0.8399006	4607.348	2891.661	21772800	18779420	21773740
1.45708E+11	0.839914	4617.211	2891.95	21772800	18777560	21773760
1.46019E+11	0.8399272	4627.074	2892.233	21772800	18775700	21773740
1.46331E+11	0.8399404	4636.937	2892.518	21772800	18773860	21773750
1.46642E+11	0.8399536	4646.8	2892.801	21772800	18772020	21773740
1.46953E+11	0.839967	4656.663	2893.09	21772800	18770150	21773750
1.47264E+11	0.83998	4666.526	2893.37	21772800	18768330	21773750





1.47576E+11	0.8399931	4676.389	2893.652	21772800	18766510	21773760
1.47887E+11	0.8400062	4686.252	2893.933	21772800	18764680	21773750
1.48198E+11	0.840019	4696.115	2894.209	21772800	18762880	21773740
1.48509E+11	0.8400319	4705.979	2894.488	21772800	18761080	21773750
1.48821E+11	0.8400448	4715.841	2894.765	21772800	18759290	21773750
1.49132E+11	0.8400576	4725.704	2895.041	21772800	18757500	21773750
1.49443E+11	0.8400703	4735.567	2895.314	21772800	18755730	21773750
1.49754E+11	0.8400831	4745.43	2895.591	21772800	18753940	21773750
1.50066E+11	0.8400956	4755.293	2895.859	21772800	18752190	21773740
1.50377E+11	0.8401083	4765.156	2896.133	21772800	18750420	21773740
1.50688E+11	0.8401208	4775.02	2896.403	21772800	18748680	21773750
1.50999E+11	0.8401333	4784.882	2896.673	21772800	18746930	21773750
1.51311E+11	0.8401457	4794.746	2896.94	21772800	18745200	21773740
1.51622E+11	0.8401589	4804.608	2897.224	21772800	18743360	21773740
1.51933E+11	0.8401707	4814.472	2897.479	21772800	18741700	21773730
1.52244E+11	0.8401831	4824.334	2897.746	21772800	18739980	21773740
1.52556E+11	0.8401955	4834.197	2898.014	21772800	18738250	21773740
1.52867E+11	0.8402078	4844.061	2898.28	21772800	18736530	21773740
1.53178E+11	0.84022	4853.923	2898.543	21772800	18734840	21773750
1.53489E+11	0.8402321	4863.787	2898.804	21772800	18733140	21773740
1.53801E+11	0.8402442	4873.649	2899.065	21772800	18731460	21773740
1.54112E+11	0.8402563	4883.513	2899.327	21772800	18729770	21773750
1.54423E+11	0.8402683	4893.375	2899.587	21772800	18728100	21773760
1.54734E+11	0.8402802	4903.239	2899.843	21772800	18726430	21773740
1.55046E+11	0.8402926	4913.102	2900.111	21772800	18724700	21773740
1.55357E+11	0.8403044	4922.965	2900.366	21772800	18723060	21773750
1.55668E+11	0.8403162	4932.828	2900.621	21772800	18721410	21773740
1.55979E+11	0.840328	4942.69	2900.876	21772800	18719770	21773750
1.56291E+11	0.8403397	4952.554	2901.13	21772800	18718130	21773750
1.56602E+11	0.8403513	4962.417	2901.38	21772800	18716500	21773730
1.56913E+11	0.840363	4972.28	2901.634	21772800	18714870	21773740
1.57225E+11	0.8403747	4982.143	2901.887	21772800	18713240	21773740
1.57536E+11	0.8403863	4992.006	2902.137	21772800	18711630	21773740
1.57847E+11	0.8403979	5001.869	2902.388	21772800	18710010	21773740
1.58158E+11	0.8404093	5011.732	2902.635	21772800	18708420	21773740
1.5847E+11	0.8404207	5021.595	2902.883	21772800	18706820	21773740
1.58781E+11	0.8404322	5031.458	2903.132	21772800	18705230	21773760
1.59092E+11	0.8404436	5041.321	2903.378	21772800	18703640	21773750
1.59403E+11	0.8404549	5051.184	2903.622	21772800	18702060	21773740
1.59715E+11	0.8404661	5061.047	2903.865	21772800	18700490	21773740
1.60026E+11	0.8404774	5070.91	2904.11	21772800	18698920	21773750
1.60337E+11	0.8404888	5080.773	2904.356	21772800	18697330	21773740
1.60648E+11	0.8404999	5090.636	2904.597	21772800	18695780	21773740
1.6096E+11	0.8405111	5100.499	2904.84	21772800	18694210	21773730
1.61271E+11	0.8405225	5110.362	2905.088	21772800	18692640	21773760
1.61582E+11	0.8405336	5120.225	2905.328	21772800	18691090	21773750
1.61893E+11	0.8405446	5130.088	2905.566	21772800	18689550	21773740
1.62205E+11	0.8405555	5139.951	2905.802	21772800	18688030	21773740
1.62516E+11	0.8405666	5149.814	2906.042	21772800	18686490	21773750
1.62827E+11	0.8405774	5159.677	2906.278	21772800	18684980	21773760
1.63138E+11	0.8405883	5169.54	2906.513	21772800	18683450	21773730

1.6345E+11	0.8405992	5179.403	2906.75	21772800	18681940	21773750
1.63761E+11	0.84061	5189.266	2906.985	21772800	18680440	21773760
1.64072E+11	0.8406208	5199.129	2907.219	21772800	18678930	21773750
1.64383E+11	0.8406315	5208.992	2907.45	21772800	18677440	21773750
1.64695E+11	0.8406422	5218.855	2907.683	21772800	18675940	21773740
1.65006E+11	0.8406528	5228.718	2907.914	21772800	18674460	21773750
1.65317E+11	0.8406637	5238.581	2908.149	21772800	18672940	21773730
1.65628E+11	0.8406741	5248.444	2908.376	21772800	18671490	21773740
1.6594E+11	0.8406847	5258.307	2908.606	21772800	18670010	21773740
1.66251E+11	0.8406953	5268.17	2908.836	21772800	18668540	21773750
1.66562E+11	0.8407058	5278.033	2909.064	21772800	18667080	21773750
1.66873E+11	0.8407164	5287.896	2909.295	21772800	18665600	21773750
1.67185E+11	0.8407268	5297.759	2909.52	21772800	18664150	21773740
1.67496E+11	0.8407372	5307.622	2909.747	21772800	18662690	21773740
1.67807E+11	0.8407477	5317.485	2909.975	21772800	18661240	21773750
1.68118E+11	0.840758	5327.348	2910.199	21772800	18659800	21773750
1.6843E+11	0.8407684	5337.211	2910.424	21772800	18658350	21773740
1.68741E+11	0.8407786	5347.074	2910.646	21772800	18656930	21773740
1.69052E+11	0.8407888	5356.937	2910.868	21772800	18655510	21773750
1.69363E+11	0.8407992	5366.8	2911.094	21772800	18654060	21773750
1.69675E+11	0.8408094	5376.663	2911.316	21772800	18652640	21773750
1.69986E+11	0.8408195	5386.526	2911.535	21772800	18651230	21773740
1.70297E+11	0.8408297	5396.389	2911.757	21772800	18649800	21773730
1.70608E+11	0.8408399	5406.252	2911.98	21772800	18648380	21773740
1.7092E+11	0.8408502	5416.115	2912.203	21772800	18646960	21773750
1.71231E+11	0.8408602	5425.979	2912.421	21772800	18645560	21773740
1.71542E+11	0.8408702	5435.841	2912.639	21772800	18644160	21773740
1.71853E+11	0.8408802	5445.704	2912.857	21772800	18642780	21773760
1.72165E+11	0.84089	5455.567	2913.07	21772800	18641400	21773740
1.72476E+11	0.8409	5465.43	2913.288	21772800	18640010	21773740
1.72787E+11	0.84091	5475.293	2913.506	21772800	18638630	21773760
1.73098E+11	0.8409199	5485.156	2913.721	21772800	18637250	21773760
1.7341E+11	0.8409296	5495.02	2913.933	21772800	18635890	21773750
1.73721E+11	0.8409395	5504.882	2914.149	21772800	18634510	21773750
1.74032E+11	0.8409492	5514.746	2914.359	21772800	18633160	21773740
1.74343E+11	0.840959	5524.608	2914.573	21772800	18631800	21773750
1.74655E+11	0.8409687	5534.472	2914.785	21772800	18630450	21773760
1.74966E+11	0.8409784	5544.334	2914.995	21772800	18629100	21773750
1.75277E+11	0.840988	5554.197	2915.205	21772800	18627750	21773740
1.75588E+11	0.8409976	5564.061	2915.414	21772800	18626410	21773740
1.759E+11	0.8410074	5573.923	2915.628	21772800	18625060	21773760
1.76211E+11	0.8410169	5583.787	2915.835	21772800	18623730	21773750
1.76522E+11	0.8410264	5593.649	2916.043	21772800	18622400	21773740
1.76833E+11	0.841036	5603.513	2916.252	21772800	18621060	21773740
1.77145E+11	0.8410454	5613.375	2916.456	21772800	18619750	21773730
1.77456E+11	0.841055	5623.239	2916.666	21772800	18618430	21773750
1.77767E+11	0.8410644	5633.102	2916.871	21772800	18617110	21773740
1.78078E+11	0.8410738	5642.965	2917.077	21772800	18615810	21773760
1.7839E+11	0.8410832	5652.828	2917.282	21772800	18614500	21773760
1.78701E+11	0.8410925	5662.69	2917.485	21772800	18613200	21773750
1.79012E+11	0.8411019	5672.554	2917.689	21772800	18611880	21773730





1.79323E+11	0.8411112	5682.417	2917.893	21772800	18610600	21773750
1.79635E+11	0.8411204	5692.28	2918.094	21772800	18609310	21773740
1.79946E+11	0.8411297	5702.143	2918.297	21772800	18608020	21773750
1.80257E+11	0.841139	5712.006	2918.5	21772800	18606720	21773740
1.80569E+11	0.8411483	5721.869	2918.703	21772800	18605440	21773760
1.8088E+11	0.8411574	5731.732	2918.901	21772800	18604150	21773720
1.81191E+11	0.8411667	5741.595	2919.104	21772800	18602870	21773740
1.81502E+11	0.8411757	5751.458	2919.301	21772800	18601600	21773720
1.81814E+11	0.8411849	5761.321	2919.503	21772800	18600330	21773740
1.82125E+11	0.8411939	5771.184	2919.7	21772800	18599080	21773750
1.82436E+11	0.8412033	5781.047	2919.904	21772800	18597780	21773750
1.82747E+11	0.8412122	5790.91	2920.1	21772800	18596540	21773760
1.83059E+11	0.8412212	5800.773	2920.296	21772800	18595280	21773740
1.8337E+11	0.8412302	5810.636	2920.493	21772800	18594020	21773740
1.83681E+11	0.8412393	5820.499	2920.691	21772800	18592760	21773740
1.83992E+11	0.8412483	5830.362	2920.888	21772800	18591510	21773740
1.84304E+11	0.8412572	5840.225	2921.084	21772800	18590280	21773760
1.84615E+11	0.8412662	5850.088	2921.281	21772800	18589020	21773760
1.84926E+11	0.841275	5859.951	2921.472	21772800	18587790	21773740
1.85237E+11	0.8412839	5869.814	2921.668	21772800	18586550	21773750
1.85549E+11	0.841293	5879.677	2921.866	21772800	18585280	21773740
1.8586E+11	0.8413018	5889.54	2922.059	21772800	18584060	21773750
1.86171E+11	0.8413109	5899.403	2922.259	21772800	18582790	21773750
1.86482E+11	0.8413195	5909.266	2922.447	21772800	18581600	21773750
1.86794E+11	0.8413282	5919.129	2922.637	21772800	18580380	21773740
1.87105E+11	0.8413369	5928.992	2922.828	21772800	18579170	21773740
1.87416E+11	0.8413455	5938.855	2923.016	21772800	18577970	21773740
1.87727E+11	0.8413544	5948.718	2923.211	21772800	18576730	21773740
1.88039E+11	0.841363	5958.581	2923.399	21772800	18575540	21773740
1.8835E+11	0.8413719	5968.444	2923.594	21772800	18574300	21773740
1.88661E+11	0.8413803	5978.307	2923.778	21772800	18573140	21773750
1.88972E+11	0.8413889	5988.17	2923.966	21772800	18571930	21773730
1.89284E+11	0.8413975	5998.033	2924.156	21772800	18570740	21773750
1.89595E+11	0.841406	6007.896	2924.341	21772800	18569550	21773740
1.89906E+11	0.8414146	6017.759	2924.529	21772800	18568360	21773740
1.90217E+11	0.841423	6027.622	2924.713	21772800	18567190	21773740
1.90529E+11	0.8414315	6037.485	2924.9	21772800	18566010	21773750
1.9084E+11	0.84144	6047.348	2925.087	21772800	18564820	21773740
1.91151E+11	0.8414484	6057.211	2925.271	21772800	18563660	21773750
1.91462E+11	0.8414569	6067.074	2925.457	21772800	18562480	21773750
1.91774E+11	0.8414654	6076.937	2925.644	21772800	18561300	21773760
1.92085E+11	0.8414739	6086.8	2925.83	21772800	18560110	21773750
1.92396E+11	0.8414825	6096.663	2926.019	21772800	18558910	21773750
1.92707E+11	0.8414915	6106.526	2926.217	21772800	18557660	21773750
1.93019E+11	0.8414998	6116.389	2926.398	21772800	18556510	21773750
1.9333E+11	0.8415081	6126.252	2926.58	21772800	18555350	21773740
1.93641E+11	0.8415163	6136.115	2926.76	21772800	18554210	21773740
1.93952E+11	0.8415249	6145.979	2926.949	21772800	18553010	21773740
1.94264E+11	0.8415329	6155.841	2927.124	21772800	18551890	21773730
1.94575E+11	0.8415412	6165.704	2927.306	21772800	18550740	21773730
1.94886E+11	0.8415498	6175.567	2927.496	21772800	18549550	21773750

1.95197E+11	0.8415581	6185.43	2927.678	21772800	18548400	21773750
1.95509E+11	0.841566	6195.293	2927.852	21772800	18547290	21773750
1.9582E+11	0.8415742	6205.156	2928.031	21772800	18546160	21773750
1.96131E+11	0.8415824	6215.02	2928.212	21772800	18545020	21773760
1.96442E+11	0.8415905	6224.882	2928.39	21772800	18543880	21773740
1.96754E+11	0.8415986	6234.746	2928.567	21772800	18542750	21773730
1.97065E+11	0.8416068	6244.608	2928.747	21772800	18541620	21773740
1.97376E+11	0.8416151	6254.472	2928.929	21772800	18540470	21773740
1.97687E+11	0.841623	6264.334	2929.104	21772800	18539370	21773750
1.97999E+11	0.8416319	6274.197	2929.299	21772800	18538130	21773750
1.9831E+11	0.8416402	6284.061	2929.481	21772800	18536980	21773750
1.98621E+11	0.8416482	6293.923	2929.658	21772800	18535860	21773750
1.98932E+11	0.8416564	6303.787	2929.837	21772800	18534710	21773730
1.99244E+11	0.8416647	6313.649	2930.019	21772800	18533570	21773740
1.99555E+11	0.8416728	6323.513	2930.198	21772800	18532440	21773740
1.99866E+11	0.8416817	6333.375	2930.394	21772800	18531210	21773760
2.00177E+11	0.8416913	6343.239	2930.605	21772800	18529870	21773750
2.00489E+11	0.8417006	6353.102	2930.81	21772800	18528580	21773760
2.008E+11	0.8417083	6362.965	2930.979	21772800	18527510	21773750
2.01111E+11	0.8417161	6372.828	2931.151	21772800	18526420	21773750
2.01422E+11	0.841724	6382.69	2931.324	21772800	18525320	21773740
2.01734E+11	0.8417325	6392.554	2931.511	21772800	18524140	21773740
2.02045E+11	0.8417411	6402.417	2931.7	21772800	18522940	21773740
2.02356E+11	0.841749	6412.28	2931.875	21772800	18521840	21773740
2.02667E+11	0.8417574	6422.143	2932.06	21772800	18520680	21773760
2.02979E+11	0.8417656	6432.006	2932.239	21772800	18519540	21773740
2.0329E+11	0.8417736	6441.869	2932.417	21772800	18518430	21773760
2.03601E+11	0.8417816	6451.732	2932.592	21772800	18517320	21773760
2.03912E+11	0.8417895	6461.595	2932.766	21772800	18516200	21773730
2.04224E+11	0.8417979	6471.458	2932.951	21772800	18515040	21773740
2.04535E+11	0.8418071	6481.321	2933.154	21772800	18513760	21773740
2.04846E+11	0.8418148	6491.184	2933.323	21772800	18512690	21773740
2.05157E+11	0.8418238	6501.047	2933.522	21772800	18511440	21773740
2.05469E+11	0.8418316	6510.91	2933.694	21772800	18510360	21773750
2.0578E+11	0.8418403	6520.773	2933.885	21772800	18509160	21773760
2.06091E+11	0.8418483	6530.636	2934.062	21772800	18508030	21773740
2.06403E+11	0.8418565	6540.499	2934.241	21772800	18506900	21773740
2.06714E+11	0.8418637	6550.362	2934.401	21772800	18505900	21773750
2.07025E+11	0.8418717	6560.225	2934.577	21772800	18504790	21773750
2.07336E+11	0.8418801	6570.088	2934.762	21772800	18503610	21773730
2.07648E+11	0.8418888	6579.951	2934.954	21772800	18502410	21773750
2.07959E+11	0.8418971	6589.814	2935.136	21772800	18501260	21773740
2.0827E+11	0.8419052	6599.677	2935.315	21772800	18500130	21773740
2.08581E+11	0.8419138	6609.54	2935.506	21772800	18498930	21773750
2.08893E+11	0.8419218	6619.403	2935.682	21772800	18497820	21773740
2.09204E+11	0.8419302	6629.266	2935.867	21772800	18496650	21773740
2.09515E+11	0.8419385	6639.129	2936.05	21772800	18495500	21773740
2.09826E+11	0.8419461	6648.992	2936.219	21772800	18494450	21773760
2.10138E+11	0.8419548	6658.855	2936.41	21772800	18493240	21773750
2.10449E+11	0.8419631	6668.718	2936.593	21772800	18492090	21773750
2.1076E+11	0.8419716	6678.581	2936.78	21772800	18490900	21773740





2.11071E+11	0.8419801	6688.444	2936.968	21772800	18489720	21773740
2.11383E+11	0.8419884	6698.307	2937.151	21772800	18488570	21773740
2.11694E+11	0.8419968	6708.17	2937.337	21772800	18487400	21773750
2.12005E+11	0.8420046	6718.033	2937.509	21772800	18486310	21773740
2.12316E+11	0.8420132	6727.896	2937.699	21772800	18485120	21773740
2.12628E+11	0.8420218	6737.759	2937.889	21772800	18483930	21773750
2.12939E+11	0.8420301	6747.622	2938.073	21772800	18482780	21773760
2.1325E+11	0.8420388	6757.485	2938.265	21772800	18481560	21773740
2.13561E+11	0.8420473	6767.348	2938.452	21772800	18480380	21773740
2.13873E+11	0.8420557	6777.211	2938.637	21772800	18479220	21773740
2.14184E+11	0.8420643	6787.074	2938.828	21772800	18478020	21773750
2.14495E+11	0.8420725	6796.937	2939.009	21772800	18476880	21773740
2.14806E+11	0.8420817	6806.8	2939.213	21772800	18475600	21773750
2.15118E+11	0.8420909	6816.663	2939.416	21772800	18474330	21773750
2.15429E+11	0.8420994	6826.526	2939.604	21772800	18473140	21773740
2.1574E+11	0.8421088	6836.389	2939.811	21772800	18471840	21773740
2.16051E+11	0.842117	6846.252	2939.993	21772800	18470700	21773750
2.16363E+11	0.8421264	6856.115	2940.201	21772800	18469390	21773740
2.16674E+11	0.842135	6865.979	2940.391	21772800	18468190	21773740
2.16985E+11	0.8421441	6875.841	2940.592	21772800	18466930	21773740
2.17296E+11	0.8421524	6885.704	2940.776	21772800	18465790	21773760
2.17608E+11	0.84216	6895.567	2940.944	21772800	18464730	21773750
2.17919E+11	0.8421679	6905.43	2941.119	21772800	18463630	21773750
2.1823E+11	0.8421761	6915.293	2941.3	21772800	18462500	21773760
2.18541E+11	0.8421842	6925.156	2941.479	21772800	18461360	21773740
2.18853E+11	0.8421925	6935.02	2941.663	21772800	18460200	21773730
2.19164E+11	0.8422018	6944.882	2941.87	21772800	18458920	21773760
2.19475E+11	0.8422098	6954.746	2942.046	21772800	18457800	21773730
2.19786E+11	0.8422183	6964.608	2942.234	21772800	18456620	21773730
2.20098E+11	0.842227	6974.472	2942.427	21772800	18455420	21773750
2.20409E+11	0.8422354	6984.334	2942.613	21772800	18454260	21773760
2.2072E+11	0.8422441	6994.197	2942.805	21772800	18453050	21773750
2.21031E+11	0.8422523	7004.061	2942.988	21772800	18451910	21773760
2.21343E+11	0.8422609	7013.923	2943.178	21772800	18450710	21773750
2.21654E+11	0.8422698	7023.787	2943.375	21772800	18449480	21773750
2.21965E+11	0.8422777	7033.649	2943.55	21772800	18448380	21773750
2.22276E+11	0.8422851	7043.513	2943.714	21772800	18447360	21773760
2.22588E+11	0.8422931	7053.375	2943.891	21772800	18446240	21773750
2.22899E+11	0.8423014	7063.239	2944.076	21772800	18445090	21773760
2.2321E+11	0.8423098	7073.102	2944.261	21772800	18443910	21773730
2.23521E+11	0.8423184	7082.965	2944.452	21772800	18442730	21773750
2.23833E+11	0.8423269	7092.828	2944.64	21772800	18441550	21773750
2.24144E+11	0.8423353	7102.69	2944.826	21772800	18440380	21773740
2.24455E+11	0.8423434	7112.554	2945.006	21772800	18439250	21773740
2.24766E+11	0.8423529	7122.417	2945.218	21772800	18437940	21773760
2.25078E+11	0.842361	7132.28	2945.396	21772800	18436810	21773740
2.25389E+11	0.8423697	7142.143	2945.589	21772800	18435600	21773740
2.257E+11	0.8423783	7152.006	2945.781	21772800	18434400	21773740
2.26011E+11	0.8423868	7161.869	2945.969	21772800	18433220	21773730
2.26323E+11	0.8423944	7171.732	2946.138	21772800	18432170	21773740
2.26634E+11	0.8424024	7181.595	2946.315	21772800	18431070	21773750

2.26945E+11	0.8424116	7191.458	2946.519	21772800	18429780	21773740
2.27256E+11	0.8424206	7201.321	2946.719	21772800	18428540	21773750
2.27568E+11	0.8424301	7211.184	2946.93	21772800	18427220	21773750
2.27879E+11	0.8424392	7221.047	2947.132	21772800	18425960	21773750
2.2819E+11	0.8424482	7230.91	2947.331	21772800	18424700	21773730
2.28501E+11	0.8424569	7240.773	2947.525	21772800	18423490	21773740
2.28813E+11	0.8424658	7250.636	2947.723	21772800	18422270	21773760
2.29124E+11	0.8424743	7260.499	2947.911	21772800	18421090	21773750
2.29435E+11	0.8424833	7270.362	2948.111	21772800	18419840	21773750
2.29746E+11	0.842492	7280.225	2948.304	21772800	18418630	21773740
2.30058E+11	0.8425002	7290.088	2948.487	21772800	18417480	21773740
2.30369E+11	0.84251	7299.951	2948.704	21772800	18416130	21773740
2.3068E+11	0.8425197	7309.814	2948.92	21772800	18414780	21773740
2.30991E+11	0.8425295	7319.677	2949.138	21772800	18413420	21773740
2.31303E+11	0.8425389	7329.54	2949.347	21772800	18412120	21773750
2.31614E+11	0.8425458	7339.403	2949.501	21772800	18411160	21773750
2.31925E+11	0.8425546	7349.266	2949.697	21772800	18409940	21773760
2.32236E+11	0.8425642	7359.129	2949.91	21772800	18408610	21773750
2.32548E+11	0.8425718	7368.992	2950.079	21772800	18407550	21773750
2.32859E+11	0.8425806	7378.855	2950.275	21772800	18406330	21773750
2.3317E+11	0.8425905	7388.718	2950.495	21772800	18404950	21773740
2.33482E+11	0.8425984	7398.581	2950.67	21772800	18403850	21773730
2.33793E+11	0.8426075	7408.444	2950.873	21772800	18402600	21773750
2.34104E+11	0.8426155	7418.307	2951.051	21772800	18401480	21773740
2.34415E+11	0.842625	7428.17	2951.263	21772800	18400170	21773750
2.34727E+11	0.842634	7438.033	2951.463	21772800	18398920	21773750
2.35038E+11	0.8426428	7447.896	2951.658	21772800	18397690	21773730
2.35349E+11	0.8426506	7457.759	2951.832	21772800	18396610	21773740
2.3566E+11	0.8426592	7467.622	2952.023	21772800	18395430	21773750
2.35972E+11	0.8426681	7477.485	2952.222	21772800	18394190	21773750
2.36283E+11	0.8426771	7487.348	2952.423	21772800	18392940	21773750
2.36594E+11	0.8426859	7497.211	2952.618	21772800	18391720	21773750
2.36905E+11	0.8426946	7507.074	2952.812	21772800	18390520	21773760
2.37217E+11	0.8427019	7516.937	2952.975	21772800	18389500	21773750
2.37528E+11	0.8427104	7526.8	2953.163	21772800	18388320	21773740
2.37839E+11	0.8427189	7536.663	2953.353	21772800	18387140	21773740
2.3815E+11	0.8427277	7546.526	2953.55	21772800	18385910	21773740
2.38462E+11	0.8427358	7556.389	2953.73	21772800	18384790	21773740
2.38773E+11	0.8427448	7566.252	2953.931	21772800	18383540	21773740
2.39084E+11	0.8427539	7576.115	2954.133	21772800	18382280	21773740
2.39395E+11	0.8427623	7585.979	2954.32	21772800	18381120	21773740
2.39707E+11	0.8427714	7595.841	2954.524	21772800	18379860	21773750
2.40018E+11	0.8427799	7605.704	2954.712	21772800	18378680	21773740
2.40329E+11	0.8427889	7615.567	2954.913	21772800	18377430	21773740
2.4064E+11	0.8427977	7625.43	2955.11	21772800	18376220	21773760
2.40952E+11	0.8428075	7635.293	2955.328	21772800	18374860	21773750
2.41263E+11	0.8428152	7645.156	2955.501	21772800	18373780	21773750
2.41574E+11	0.8428234	7655.02	2955.683	21772800	18372640	21773740
2.41885E+11	0.8428331	7664.882	2955.9	21772800	18371300	21773750
2.42197E+11	0.8428426	7674.746	2956.111	21772800	18369980	21773740
2.42508E+11	0.8428526	7684.608	2956.335	21772800	18368600	21773750



2.42819E+11	0.8428622	7694.472	2956.549	21772800	18367270	21773750
2.4313E+11	0.8428711	7704.334	2956.749	21772800	18366030	21773750
2.43442E+11	0.8428802	7714.197	2956.951	21772800	18364770	21773750
2.43753E+11	0.8428889	7724.061	2957.145	21772800	18363560	21773740
2.44064E+11	0.8428975	7733.923	2957.337	21772800	18362370	21773740
2.44375E+11	0.8429056	7743.787	2957.518	21772800	18361240	21773740
2.44687E+11	0.8429151	7753.649	2957.731	21772800	18359930	21773750
2.44998E+11	0.842925	7763.513	2957.952	21772800	18358550	21773740
2.45309E+11	0.8429349	7773.375	2958.173	21772800	18357190	21773760
2.4562E+11	0.842944	7783.239	2958.377	21772800	18355920	21773750
2.45932E+11	0.8429523	7793.102	2958.562	21772800	18354770	21773750
2.46243E+11	0.8429622	7802.965	2958.783	21772800	18353400	21773750
2.46554E+11	0.842971	7812.828	2958.98	21772800	18352180	21773750
2.46865E+11	0.8429799	7822.69	2959.179	21772800	18350950	21773760
2.47177E+11	0.8429883	7832.554	2959.367	21772800	18349780	21773750
2.47488E+11	0.8429976	7842.417	2959.575	21772800	18348490	21773750
2.47799E+11	0.8430063	7852.28	2959.769	21772800	18347290	21773750
2.4811E+11	0.8430151	7862.143	2959.965	21772800	18346060	21773740
2.48422E+11	0.8430244	7872.006	2960.173	21772800	18344780	21773750
2.48733E+11	0.8430333	7881.869	2960.373	21772800	18343540	21773750
2.49044E+11	0.8430429	7891.732	2960.588	21772800	18342210	21773750
2.49355E+11	0.8430513	7901.595	2960.776	21772800	18341050	21773750
2.49667E+11	0.8430601	7911.458	2960.972	21772800	18339830	21773750
2.49978E+11	0.8430698	7921.321	2961.189	21772800	18338480	21773740
2.50289E+11	0.8430786	7931.184	2961.387	21772800	18337260	21773750
2.506E+11	0.8430878	7941.047	2961.592	21772800	18335980	21773730
2.50912E+11	0.843098	7950.91	2961.821	21772800	18334580	21773750
2.51223E+11	0.843108	7960.773	2962.045	21772800	18333190	21773750
2.51534E+11	0.8431178	7970.636	2962.264	21772800	18331820	21773730
2.51845E+11	0.843128	7980.499	2962.493	21772800	18330420	21773750
2.52157E+11	0.8431376	7990.362	2962.708	21772800	18329080	21773740
2.52468E+11	0.8431466	8000.225	2962.91	21772800	18327830	21773740
2.52779E+11	0.8431564	8010.088	2963.129	21772800	18326480	21773750
2.5309E+11	0.8431664	8019.951	2963.353	21772800	18325100	21773750
2.53402E+11	0.8431768	8029.814	2963.586	21772800	18323660	21773750
2.53713E+11	0.8431867	8039.677	2963.807	21772800	18322280	21773740
2.54024E+11	0.843197	8049.54	2964.039	21772800	18320840	21773730
2.54335E+11	0.8432071	8059.403	2964.266	21772800	18319450	21773750
2.54647E+11	0.843217	8069.266	2964.488	21772800	18318090	21773760
2.54958E+11	0.8432259	8079.129	2964.687	21772800	18316850	21773750
2.55269E+11	0.8432357	8088.992	2964.906	21772800	18315490	21773740
2.5558E+11	0.843246	8098.855	2965.137	21772800	18314060	21773740
2.55892E+11	0.8432558	8108.718	2965.358	21772800	18312700	21773740
2.56203E+11	0.8432658	8118.581	2965.581	21772800	18311320	21773740
2.56514E+11	0.8432754	8128.444	2965.798	21772800	18309990	21773750
2.56825E+11	0.8432857	8138.307	2966.028	21772800	18308560	21773740
2.57137E+11	0.8432948	8148.17	2966.233	21772800	18307300	21773740
2.57448E+11	0.8433046	8158.033	2966.452	21772800	18305950	21773750
2.57759E+11	0.8433145	8167.896	2966.676	21772800	18304570	21773750
2.5807E+11	0.8433248	8177.759	2966.906	21772800	18303140	21773740
2.58382E+11	0.843335	8187.622	2967.135	21772800	18301730	21773740





2.58693E+11	0.843345	8197.485	2967.36	21772800	18300340	21773740
2.59004E+11	0.8433557	8207.349	2967.601	21772800	18298870	21773760
2.59315E+11	0.8433657	8217.211	2967.825	21772800	18297490	21773760
2.59627E+11	0.8433758	8227.074	2968.052	21772800	18296080	21773740
2.59938E+11	0.8433861	8236.938	2968.284	21772800	18294670	21773770
2.60249E+11	0.8433957	8246.8	2968.499	21772800	18293330	21773750
2.60561E+11	0.8434062	8256.663	2968.735	21772800	18291870	21773740
2.60872E+11	0.8434165	8266.526	2968.967	21772800	18290440	21773740
2.61183E+11	0.843427	8276.39	2969.203	21772800	18288990	21773750
2.61494E+11	0.8434373	8286.252	2969.435	21772800	18287570	21773760
2.61806E+11	0.8434471	8296.115	2969.654	21772800	18286210	21773740
2.62117E+11	0.8434573	8305.979	2969.884	21772800	18284790	21773740
2.62428E+11	0.8434671	8315.841	2970.105	21772800	18283440	21773750
2.62739E+11	0.8434751	8325.704	2970.284	21772800	18282330	21773740
2.63051E+11	0.8434829	8335.567	2970.46	21772800	18281250	21773750
2.63362E+11	0.8434925	8345.431	2970.676	21772800	18279920	21773750
2.63673E+11	0.8435017	8355.293	2970.883	21772800	18278650	21773750
2.63984E+11	0.843511	8365.156	2971.092	21772800	18277360	21773740
2.64296E+11	0.8435213	8375.02	2971.324	21772800	18275940	21773750
2.64607E+11	0.8435313	8384.883	2971.55	21772800	18274560	21773760
2.64918E+11	0.8435398	8394.745	2971.74	21772800	18273360	21773730
2.65229E+11	0.8435501	8404.608	2971.972	21772800	18271950	21773750
2.65541E+11	0.8435606	8414.472	2972.208	21772800	18270500	21773750
2.65852E+11	0.8435699	8424.335	2972.418	21772800	18269200	21773740
2.66163E+11	0.84358	8434.197	2972.646	21772800	18267810	21773750
2.66474E+11	0.8435889	8444.061	2972.846	21772800	18266580	21773750
2.66786E+11	0.843598	8453.924	2973.052	21772800	18265310	21773740
2.67097E+11	0.8436088	8463.786	2973.295	21772800	18263820	21773750
2.67408E+11	0.8436189	8473.649	2973.523	21772800	18262420	21773750
2.67719E+11	0.8436294	8483.513	2973.76	21772800	18260980	21773770
2.68031E+11	0.8436397	8493.376	2973.991	21772800	18259550	21773750
2.68342E+11	0.8436493	8503.238	2974.208	21772800	18258210	21773740
2.68653E+11	0.8436594	8513.102	2974.436	21772800	18256810	21773740
2.68964E+11	0.8436683	8522.965	2974.636	21772800	18255580	21773740
2.69276E+11	0.8436785	8532.827	2974.866	21772800	18254170	21773740
2.69587E+11	0.8436888	8542.69	2975.098	21772800	18252750	21773740
2.69898E+11	0.8436994	8552.554	2975.338	21772800	18251280	21773750
2.70209E+11	0.8437095	8562.417	2975.566	21772800	18249880	21773750
2.70521E+11	0.8437198	8572.279	2975.798	21772800	18248450	21773740
2.70832E+11	0.84373	8582.143	2976.028	21772800	18247040	21773740
2.71143E+11	0.8437405	8592.006	2976.266	21772800	18245590	21773750
2.71454E+11	0.8437511	8601.869	2976.504	21772800	18244120	21773730
2.71766E+11	0.8437616	8611.731	2976.742	21772800	18242670	21773750
2.72077E+11	0.8437705	8621.595	2976.943	21772800	18241440	21773750
2.72388E+11	0.8437801	8631.458	2977.16	21772800	18240110	21773750
2.72699E+11	0.8437907	8641.32	2977.399	21772800	18238640	21773740
2.73011E+11	0.8437996	8651.184	2977.6	21772800	18237410	21773740
2.73322E+11	0.8438092	8661.047	2977.817	21772800	18236080	21773740
2.73633E+11	0.8438191	8670.91	2978.04	21772800	18234720	21773750
2.73944E+11	0.8438292	8680.772	2978.269	21772800	18233320	21773750
2.74256E+11	0.8438393	8690.636	2978.497	21772800	18231920	21773750

2.74567E+11	0.8438497	8700.499	2978.733	21772800	18230490	21773760
2.74878E+11	0.8438597	8710.362	2978.958	21772800	18229100	21773750
2.75189E+11	0.8438702	8720.225	2979.196	21772800	18227640	21773740
2.75501E+11	0.8438809	8730.088	2979.438	21772800	18226160	21773740
2.75812E+11	0.843891	8739.951	2979.667	21772800	18224770	21773760
2.76123E+11	0.8439018	8749.813	2979.911	21772800	18223270	21773750
2.76434E+11	0.8439122	8759.677	2980.146	21772800	18221830	21773740
2.76746E+11	0.8439229	8769.54	2980.388	21772800	18220360	21773750
2.77057E+11	0.8439333	8779.403	2980.623	21772800	18218910	21773740
2.77368E+11	0.8439438	8789.266	2980.86	21772800	18217460	21773740
2.77679E+11	0.8439543	8799.129	2981.099	21772800	18216010	21773750
2.77991E+11	0.8439647	8808.992	2981.334	21772800	18214570	21773740
2.78302E+11	0.8439751	8818.855	2981.57	21772800	18213130	21773750
2.78613E+11	0.8439855	8828.718	2981.805	21772800	18211700	21773750
2.78924E+11	0.843996	8838.581	2982.042	21772800	18210240	21773740
2.79236E+11	0.8440065	8848.444	2982.28	21772800	18208800	21773750
2.79547E+11	0.8440162	8858.307	2982.5	21772800	18207450	21773740
2.79858E+11	0.8440258	8868.17	2982.718	21772800	18206120	21773750
2.80169E+11	0.8440366	8878.033	2982.962	21772800	18204620	21773730
2.80481E+11	0.8440471	8887.896	2983.201	21772800	18203180	21773750
2.80792E+11	0.8440573	8897.759	2983.432	21772800	18201760	21773740
2.81103E+11	0.844067	8907.622	2983.651	21772800	18200420	21773740
2.81414E+11	0.8440771	8917.485	2983.881	21772800	18199020	21773740
2.81726E+11	0.8440879	8927.349	2984.125	21772800	18197540	21773750
2.82037E+11	0.8440986	8937.211	2984.369	21772800	18196060	21773760
2.82348E+11	0.8441091	8947.074	2984.606	21772800	18194610	21773750
2.8266E+11	0.8441195	8956.938	2984.842	21772800	18193160	21773740
2.82971E+11	0.8441295	8966.8	2985.069	21772800	18191780	21773750
2.83282E+11	0.84414	8976.663	2985.307	21772800	18190330	21773740
2.83593E+11	0.8441502	8986.526	2985.538	21772800	18188920	21773740
2.83905E+11	0.8441609	8996.39	2985.782	21772800	18187440	21773750
2.84216E+11	0.8441717	9006.252	2986.027	21772800	18185940	21773740
2.84527E+11	0.8441824	9016.115	2986.269	21772800	18184470	21773740
2.84838E+11	0.8441927	9025.979	2986.503	21772800	18183050	21773750
2.8515E+11	0.8442034	9035.841	2986.747	21772800	18181560	21773750
2.85461E+11	0.8442139	9045.704	2986.985	21772800	18180110	21773740
2.85772E+11	0.8442245	9055.567	2987.226	21772800	18178640	21773740
2.86083E+11	0.8442351	9065.431	2987.467	21772800	18177190	21773760
2.86394E+11	0.8442456	9075.293	2987.705	21772800	18175740	21773760
2.86706E+11	0.844256	9085.156	2987.941	21772800	18174300	21773750
2.87017E+11	0.8442665	9095.02	2988.179	21772800	18172840	21773740
2.87328E+11	0.8442767	9104.883	2988.412	21772800	18171430	21773750
2.8764E+11	0.8442872	9114.745	2988.651	21772800	18169990	21773760
2.87951E+11	0.8442976	9124.608	2988.886	21772800	18168540	21773730
2.88262E+11	0.8443082	9134.472	2989.128	21772800	18167080	21773750
2.88573E+11	0.8443183	9144.335	2989.357	21772800	18165680	21773740
2.88885E+11	0.8443283	9154.197	2989.584	21772800	18164300	21773740
2.89196E+11	0.8443391	9164.061	2989.83	21772800	18162800	21773730
2.89507E+11	0.8443499	9173.924	2990.077	21772800	18161310	21773740
2.89818E+11	0.8443605	9183.786	2990.317	21772800	18159860	21773750
2.9013E+11	0.8443709	9193.649	2990.554	21772800	18158420	21773750



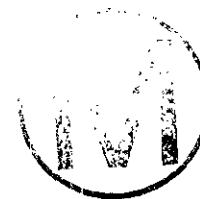


2.90441E+11	0.8443815	9203.513	2990.796	21772800	18156940	21773740
2.90752E+11	0.8443924	9213.376	2991.044	21772800	18155450	21773760
2.91063E+11	0.844403	9223.238	2991.285	21772800	18153980	21773750
2.91375E+11	0.8444135	9233.102	2991.524	21772800	18152530	21773750
2.91686E+11	0.8444241	9242.965	2991.766	21772800	18151070	21773760
2.91997E+11	0.8444347	9252.827	2992.006	21772800	18149600	21773740
2.92308E+11	0.8444452	9262.69	2992.246	21772800	18148160	21773760
2.9262E+11	0.8444557	9272.554	2992.485	21772800	18146700	21773750
2.92931E+11	0.8444663	9282.417	2992.727	21772800	18145240	21773760
2.93242E+11	0.8444769	9292.279	2992.968	21772800	18143770	21773750
2.93553E+11	0.8444875	9302.143	2993.209	21772800	18142300	21773740
2.93865E+11	0.8444982	9312.006	2993.454	21772800	18140840	21773770
2.94176E+11	0.8445088	9321.869	2993.696	21772800	18139360	21773750
2.94487E+11	0.8445183	9331.731	2993.912	21772800	18138050	21773750
2.94798E+11	0.844529	9341.595	2994.155	21772800	18136560	21773730
2.9511E+11	0.8445396	9351.458	2994.397	21772800	18135100	21773730
2.95421E+11	0.8445503	9361.32	2994.642	21772800	18133640	21773760
2.95732E+11	0.8445607	9371.184	2994.878	21772800	18132200	21773750
2.96043E+11	0.8445712	9381.047	2995.118	21772800	18130740	21773740
2.96355E+11	0.844582	9390.91	2995.365	21772800	18129250	21773750
2.96666E+11	0.8445927	9400.772	2995.609	21772800	18127780	21773750
2.96977E+11	0.8446034	9410.636	2995.854	21772800	18126290	21773740
2.97288E+11	0.8446139	9420.499	2996.093	21772800	18124850	21773750
2.976E+11	0.8446246	9430.362	2996.337	21772800	18123360	21773730
2.97911E+11	0.8446351	9440.225	2996.578	21772800	18121920	21773750
2.98222E+11	0.8446459	9450.088	2996.824	21772800	18120440	21773760
2.98533E+11	0.8446565	9459.951	2997.066	21772800	18118960	21773740
2.98845E+11	0.8446673	9469.813	2997.313	21772800	18117480	21773760
2.99156E+11	0.8446779	9479.677	2997.555	21772800	18116010	21773750
2.99467E+11	0.8446885	9489.54	2997.796	21772800	18114550	21773750
2.99778E+11	0.844699	9499.403	2998.037	21772800	18113100	21773760
3.0009E+11	0.8447089	9509.266	2998.263	21772800	18111730	21773750
3.00401E+11	0.8447196	9519.129	2998.507	21772800	18110240	21773730
3.00712E+11	0.8447297	9528.992	2998.739	21772800	18108860	21773760
3.01023E+11	0.8447404	9538.855	2998.983	21772800	18107380	21773750
3.01335E+11	0.844751	9548.718	2999.225	21772800	18105920	21773750
3.01646E+11	0.8447617	9558.581	2999.471	21772800	18104440	21773750
3.01957E+11	0.8447726	9568.444	2999.719	21772800	18102940	21773750
3.02268E+11	0.8447833	9578.307	2999.964	21772800	18101460	21773750
3.0258E+11	0.844794	9588.17	3000.208	21772800	18099980	21773740
3.02891E+11	0.8448046	9598.033	3000.451	21772800	18098510	21773730
3.03202E+11	0.8448154	9607.896	3000.698	21772800	18097020	21773730
3.03513E+11	0.8448261	9617.759	3000.944	21772800	18095550	21773750
3.03825E+11	0.8448368	9627.622	3001.188	21772800	18094070	21773740
3.04136E+11	0.8448469	9637.485	3001.42	21772800	18092670	21773740
3.04447E+11	0.844857	9647.349	3001.651	21772800	18091280	21773740
3.04758E+11	0.8448673	9657.211	3001.887	21772800	18089870	21773750
3.0507E+11	0.844878	9667.074	3002.133	21772800	18088390	21773760
3.05381E+11	0.8448888	9676.938	3002.38	21772800	18086890	21773740
3.05692E+11	0.8448995	9686.8	3002.624	21772800	18085420	21773740
3.06003E+11	0.8449101	9696.663	3002.867	21772800	18083960	21773750

3.06315E+11	0.8449208	9706.526	3003.113	21772800	18082480	21773750
3.06626E+11	0.8449314	9716.39	3003.356	21772800	18081010	21773740
3.06937E+11	0.8449421	9726.252	3003.601	21772800	18079540	21773750
3.07248E+11	0.8449527	9736.115	3003.844	21772800	18078070	21773740
3.0756E+11	0.8449634	9745.979	3004.089	21772800	18076600	21773740
3.07871E+11	0.8449741	9755.841	3004.335	21772800	18075120	21773740
3.08182E+11	0.8449843	9765.704	3004.569	21772800	18073720	21773750
3.08494E+11	0.8449944	9775.567	3004.801	21772800	18072320	21773750
3.08805E+11	0.8450052	9785.431	3005.049	21772800	18070830	21773750
3.09116E+11	0.8450161	9795.293	3005.299	21772800	18069330	21773750
3.09427E+11	0.8450267	9805.156	3005.541	21772800	18067860	21773730
3.09739E+11	0.8450376	9815.02	3005.792	21772800	18066360	21773750
3.1005E+11	0.8450483	9824.883	3006.038	21772800	18064880	21773740
3.10361E+11	0.8450585	9834.745	3006.272	21772800	18063480	21773750
3.10672E+11	0.8450689	9844.608	3006.51	21772800	18062040	21773740
3.10984E+11	0.8450798	9854.472	3006.76	21772800	18060550	21773750
3.11295E+11	0.8450905	9864.335	3007.007	21772800	18059060	21773750
3.11606E+11	0.8451015	9874.197	3007.259	21772800	18057540	21773740
3.11917E+11	0.8451124	9884.061	3007.509	21772800	18056040	21773740
3.12229E+11	0.8451233	9893.924	3007.76	21772800	18054540	21773750
3.1254E+11	0.8451341	9903.786	3008.008	21772800	18053050	21773740
3.12851E+11	0.8451449	9913.649	3008.257	21772800	18051560	21773750
3.13162E+11	0.8451557	9923.513	3008.505	21772800	18050070	21773750
3.13474E+11	0.8451665	9933.376	3008.753	21772800	18048580	21773740
3.13785E+11	0.8451774	9943.238	3009.004	21772800	18047090	21773760
3.14096E+11	0.8451881	9953.102	3009.249	21772800	18045600	21773740
3.14407E+11	0.845199	9962.965	3009.5	21772800	18044100	21773740
3.14719E+11	0.8452098	9972.827	3009.749	21772800	18042600	21773740
3.1503E+11	0.8452207	9982.69	3009.999	21772800	18041110	21773750
3.15341E+11	0.8452315	9992.554	3010.248	21772800	18039610	21773740
3.15576E+11	0.8452397	10000	3010.437	21772800	18038490	21773750







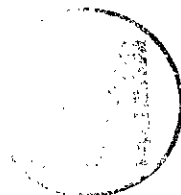
# Written	OT 12/1 :0	9:17		
# Created	NTOS 12/:5	1:12		
# Modified	GEBRA 1 :1	6:17		
@ with g0				
@ legend on				
@ legend view				
@ legend e 0.75				
@ title "DI ROOM C -		FINAL - F = 2.0 - WASTE W/O BACKFILL"		
@ subtitle vs PGAS"				
@ s0 color 1				
@ xaxis la ME"				
@ yaxis la AS"				
@ legend 0 "PGAS"				
@ s0 comment "PGAS"				
0.00E+00	0.00E+00			
1.34E-11	2.96E-07			
9.63E-09	2.12E-04			
7.39E-07	1.63E-02			
3.83E-06	8.46E-02			
9.49E-06	2.10E-01			
1.74E-05	3.86E-01			
2.93E-05	6.52E-01			
4.73E-05	1.05E+00			
6.91E-05	1.54E+00			
9.63E-05	2.15E+00			
1.65E-04	3.71E+00			
2.93E-04	6.59E+00			
5.30E-04	1.20E+01			
9.56E-04	2.17E+01			
1.74E-03	3.97E+01			
2.87E-03	6.58E+01			
4.30E-03	9.87E+01			
6.22E-03	1.43E+02			
8.35E-03	1.93E+02			
1.37E-02	3.18E+02			
2.40E-02	5.60E+02			
3.79E-02	8.87E+02			
6.16E-02	1.45E+03			
9.64E-02	2.28E+03			
1.50E-01	3.58E+03			
2.04E-01	4.89E+03			
2.59E-01	6.22E+03			
3.37E-01	8.13E+03			
4.27E-01	1.04E+04			
5.59E-01	1.36E+04			
7.12E-01	1.75E+04			
6.50E+00	1.86E+05			
1.47E+01	4.95E+05			

24



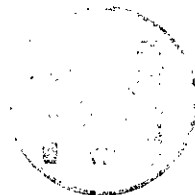


9.57E+03	18102937				
9.58E+03	18101455				
9.59E+03	18099984				
9.60E+03	18098507				
9.61E+03	18097020				
9.62E+03	18095548				
9.63E+03	18094072				
9.64E+03	18092674				
9.65E+03	18091276				
9.66E+03	18089866				
9.67E+03	18088387				
9.68E+03	18086894				
9.69E+03	18085420				
9.70E+03	18083956				
9.71E+03	18082477				
9.72E+03	18081009				
9.73E+03	18079537				
9.74E+03	18078072				
9.75E+03	18076600				
9.76E+03	18075124				
9.77E+03	18073717				
9.78E+03	18072318				
9.79E+03	18070827				
9.80E+03	18069330				
9.81E+03	18067856				
9.82E+03	18066358				
9.82E+03	18064884				
9.83E+03	18063477				
9.84E+03	18062041				
9.85E+03	18060547				
9.86E+03	18059061				
9.87E+03	18057539				
9.88E+03	18056043				
9.89E+03	18054536				
9.90E+03	18053048				
9.91E+03	18051555				
9.92E+03	18050070				
9.93E+03	18048580				
9.94E+03	18047086				
9.95E+03	18045595				
9.96E+03	18044099				
9.97E+03	18042604				
9.98E+03	18041107				
9.99E+03	18039614				
1.00E+04	18038486				
@ world x	0				
@ world x	0				
@ world y	1.33368E+12				
@ world y	0				





	9.57E+03	0.84477257					
	9.58E+03	0.84478331					
	9.59E+03	0.84479396					
	9.60E+03	0.84480466					
	9.61E+03	0.84481544					
	9.62E+03	0.8448261					
	9.63E+03	0.8448368					
	9.64E+03	0.84484692					
	9.65E+03	0.84485705					
	9.66E+03	0.84486726					
	9.67E+03	0.84487798					
	9.68E+03	0.8448888					
	9.69E+03	0.84489948					
	9.70E+03	0.84491009					
	9.71E+03	0.8449208					
	9.72E+03	0.84493145					
	9.73E+03	0.84494211					
	9.74E+03	0.84495273					
	9.75E+03	0.84496339					
	9.76E+03	0.84497409					
	9.77E+03	0.84498429					
	9.78E+03	0.84499443					
	9.79E+03	0.84500523					
	9.80E+03	0.84501608					
	9.81E+03	0.84502676					
	9.82E+03	0.84503762					
	9.82E+03	0.84504831					
	9.83E+03	0.8450585					
	9.84E+03	0.84506891					
	9.85E+03	0.84507975					
	9.86E+03	0.84509052					
	9.87E+03	0.84510155					
	9.88E+03	0.84511239					
	9.89E+03	0.84512332					
	9.90E+03	0.84513411					
	9.91E+03	0.84514493					
	9.92E+03	0.8451557					
	9.93E+03	0.8451665					
	9.94E+03	0.84517734					
	9.95E+03	0.84518815					
	9.96E+03	0.845199					
	9.97E+03	0.84520983					
	9.98E+03	0.84522069					
	9.99E+03	0.84523152					
	1.00E+04	0.84523969					
@	world	xmax	1.00E+04				
@	world	xmin	0.00E+00				
@	world	ymax	8.48E-01				
@	world	ymin	7.00E-01				



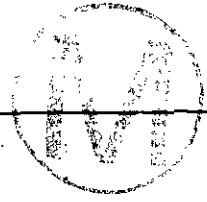
INFORMATION ONLY
WPD 35697

Section 4

Final Porosity Surface Data

$f = 1.0$





f=1.0							
time seconds	porosity x	time years	void m3/room	gas mols/rm	pressure Pa		
0	0.8483495	0	3083.473		0	0	0
0.000423702	0.8483374	1.34263E-11	3083.183	1.82705E-07	1.47972E-07	1.82929E-07	
0.296773	0.8483381	9.40417E-09	3083.201	0.000127972	0.000103643	0.000128128	
23.36187	0.8482743	7.40293E-07	3081.671	0.0100739	0.008162799	0.01008623	
127.2402	0.8480691	0.000004032	3076.764	0.05486745	0.0445295	0.05493455	
318.2111	0.8478029	1.00835E-05	3070.419	0.1372163	0.1115923	0.1373838	
648.4929	0.8474886	2.05495E-05	3062.956	0.2796376	0.227972	0.2799792	
1125.48	0.8471841	3.56643E-05	3055.755	0.4853198	0.3965851	0.4859129	
1714.348	0.8469182	5.43244E-05	3049.49	0.7392465	0.6053259	0.7401505	
2311.844	0.8467173	7.32579E-05	3044.77	0.9968935	0.8175634	0.9981125	
3076.995	0.8465121	9.75041E-05	3039.962	1.326836	1.089874	1.328459	
4706.753	0.8461837	0.000149148	3032.296	2.029606	1.671345	2.032082	
7870.086	0.8457686	0.000249388	3022.65	3.393672	2.803558	3.397825	
12501.8	0.8453746	0.000396158	3013.544	5.39092	4.466963	5.39751	
18675.95	0.8450175	0.000591805	3005.33	8.05328	6.691262	8.063131	
29664.46	0.8445905	0.00094001	2995.558	12.79165	10.66292	12.8073	
51082.95	0.8440751	0.001618721	2983.835	22.02756	18.43396	22.05449	
90492.3	0.8434966	0.002867528	2970.769	39.02132	32.79899	39.06905	
142413.1	0.843007	0.004512798	2959.785	61.41015	51.80928	61.48529	
208158.7	0.8425882	0.006596151	2950.443	89.7604	75.96695	89.87016	
356989.3	0.841984	0.01131231	2937.054	153.9379	130.8762	154.1261	
706421	0.8411067	0.02238513	2917.795	304.6169	260.6914	304.9896	
1165848	0.8404387	0.03694349	2903.272	502.727	432.3864	503.3422	
1723429	0.8398662	0.05461218	2890.922	743.1625	641.9112	744.0719	
2305388	0.8394155	0.07305332	2881.26	994.1095	861.547	995.3251	
2897987	0.8390547	0.09183167	2873.566	1249.646	1085.907	1251.173	
3616460	0.8386527	0.1145987	2865.032	1559.459	1359.163	1561.365	
4405160	0.8382877	0.1395911	2857.323	1899.556	1660.046	1901.88	
5245795	0.8379495	0.1662292	2850.209	2262.047	1981.765	2264.813	
6323490	0.8375633	0.2003793	2842.121	2726.761	2395.696	2730.095	
7694870	0.8371213	0.2438357	2832.914	3318.116	2924.729	3322.176	
9665503	0.8365571	0.3062813	2821.231	4167.876	3688.954	4172.972	
11956760	0.83597	0.3788867	2809.161	5155.89	4583.048	5162.197	
14925580	0.8353012	0.4729632	2795.516	6436.085	5748.929	6443.955	
18995150	0.8344597	0.6019199	2778.503	8190.925	7361.218	8200.948	
24423290	0.8334579	0.7739275	2758.473	10531.61	9533.517	10544.49	
31444380	0.8322798	0.9964124	2735.226	13559.18	12378.48	13575.76	
227423800	0.8085917	7.206626	2328.508	98067.75	105166.1	98187.7	
486801200	0.7811157	15.4258	1967.026	209914.3	266476.8	210171.1	
746178800	0.7538855	23.64498	1688.408	321760.9	475864.4	322154.5	
1005556000	0.7292694	31.86416	1484.772	433607.5	729229.4	434137.7	
1264934000	0.7134107	40.08334	1372.11	545454	992651.3	546121.4	
1524312000	0.7011995	48.30252	1293.509	657300.5	1268884	658104.6	
1783689000	0.6913136	56.52169	1234.431	769147	1555858	770087.9	
2043067000	0.683183	64.74088	1188.606	880994	1850812	882071.4	
2302444000	0.6766474	72.96005	1153.441	992840.5	2149371	994054.8	
2561822000	0.6714157	81.17923	1126.299	1104687	2449134	1106037	
2821199000	0.6671873	89.39841	1104.987	1216534	2749124	1218022	
3080577000	0.6637437	97.61758	1088.026	1328380	3048671	1330005	

3464456000	0.6598495	109.782	1069.259	1493914	3488749	1495740
3775709000	0.6575594	119.645	1058.422	1628129	3841114	1630120
4086961000	0.6558582	129.508	1050.465	1762345	4189251	1764499
4398214000	0.6546179	139.371	1044.714	1896561	4533116	1898881
4709467000	0.6537359	149.234	1040.648	2030776	4872877	2033260
5020720000	0.6531273	159.097	1037.856	2164992	5208909	2167641
5331975000	0.6527346	168.9601	1036.058	2299209	5541424	2302020
5643228000	0.6524982	178.8231	1034.979	2433425	5871023	2436402
5954480000	0.652365	188.6861	1034.371	2567641	6198478	2570780
6265733000	0.6522918	198.5491	1034.037	2701857	6524591	2705160
6576986000	0.6522536	208.4121	1033.863	2836072	6849857	2839541
6888238000	0.6522357	218.2751	1033.781	2970288	7174588	2973919
7199491000	0.65223	228.1381	1033.756	3104504	7498970	3108302
7510744000	0.6522328	238.0011	1033.768	3238719	7823076	3242681
7821999000	0.6522416	247.8642	1033.808	3372936	8146953	3377059
8133252000	0.6522554	257.7272	1033.871	3507152	8470625	3511441
8444505000	0.6522786	267.5902	1033.977	3641368	8793888	3645821
8755757000	0.6523026	277.4532	1034.087	3775583	9117052	3780203
9067009000	0.6523309	287.3162	1034.215	3909799	9439974	3914580
9378262000	0.6523591	297.1792	1034.344	4044015	9762816	4048962
9689515000	0.6523875	307.0422	1034.474	4178231	10085570	4183344
10000770000	0.6524194	316.9053	1034.619	4312448	10408080	4317722
10312020000	0.6524582	326.7683	1034.796	4446663	10730170	4452100
10623280000	0.6525047	336.6313	1035.008	4580879	11051780	4586480
10934530000	0.6525576	346.4943	1035.25	4715095	11372930	4720861
11245780000	0.6526151	356.3573	1035.512	4849310	11693700	4855239
11557030000	0.6526789	366.2203	1035.804	4983526	12013970	4989622
11868290000	0.6527559	-376.0833	-1036.156	5117740	12333340	5124004
12179540000	0.6528352	385.9464	1036.519	5251960	12652360	5258385
12490790000	0.6529293	395.8094	1036.949	5386175	12970310	5392763
12802050000	0.6530164	405.6724	1037.348	5520390	13288400	5527144
13113300000	0.6531334	415.5354	1037.884	5654605	13604450	5661524
13424550000	0.6533164	425.3984	1038.722	5788820	13916110	5795899
13735810000	0.6534274	435.2614	1039.232	5923040	14231790	5930286
14047060000	0.6535458	445.1244	1039.775	6057255	14546670	6064661
14358310000	0.6536756	454.9875	1040.371	6191470	14860480	6199043
14669570000	0.6538097	464.8505	1040.988	6325685	15173620	6333423
14980820000	0.6539565	474.7135	1041.663	6459900	15485520	6467800
15292070000	0.654128	484.5765	1042.453	6594115	15795280	6602180
15603320000	0.654326	494.4395	1043.366	6728335	16102680	6736563
15914580000	0.6545493	504.3025	1044.397	6862550	16407680	6870943
16225830000	0.654799	514.1655	1045.551	6996765	16710120	7005326
16537090000	0.6550739	524.0286	1046.823	7130980	17009950	7139698
16848330000	0.6553749	533.8915	1048.219	7265195	17307030	7274081
17159590000	0.6557019	543.7546	1049.738	7399415	17601250	7408461
17470840000	0.6560386	553.6176	1051.305	7509015	17814760	7509522
17782100000	0.6563558	563.4806	1052.785	7576120	17948890	7576713
18093350000	0.6566777	573.3436	1054.289	7643230	18082230	7643904
18404600000	0.657007	583.2066	1055.83	7710340	18214540	7711090
18715850000	0.6573516	593.0696	1057.446	7777445	18345180	7778283
19027110000	0.6577109	602.9327	1059.135	7844555	18474150	7845477
19338360000	0.6580895	612.7957	1060.918	7911660	18601040	7912662





19649610000	0.6584865	622.6587	1062.792	7978770	18725920	7979855
19960870000	0.6589009	632.5217	1064.753	8045880	18848810	8047044
20272120000	0.6593353	642.3847	1066.813	8112985	18969480	8114229
20583370000	0.6597925	652.2477	1068.988	8180095	19087650	8181423
20894630000	0.660269	662.1107	1071.26	8247200	19203590	8248612
21205880000	0.6607698	671.9738	1073.655	8314310	19316820	8315799
21517130000	0.6612956	681.8367	1076.178	8381415	19427260	8382995
21828390000	0.6618476	691.6998	1078.834	8448525	19534750	8450181
22139640000	0.6624261	701.5628	1081.628	8515635	19639220	8517374
22450890000	0.6630385	711.4258	1084.595	8582740	19739990	8584560
22762140000	0.6636857	721.2888	1087.743	8649850	19836910	8651749
23073400000	0.6643632	731.1519	1091.051	8716960	19930350	8718937
23384650000	0.6650808	741.0148	1094.57	8784065	20019380	8786131
23695900000	0.6658264	750.8779	1098.242	8851175	20105030	8853323
24007150000	0.666612	760.7408	1102.129	8918280	20186160	8920510
24318410000	0.6674314	770.6039	1106.203	8985390	20263320	8987709
24629660000	0.668282	780.4669	1110.452	9052495	20336670	9054890
24940910000	0.6691704	790.3299	1114.914	9119605	20405570	9122075
25252170000	0.6700824	800.1929	1119.52	9186710	20471310	9189271
25563420000	0.6710246	810.056	1124.305	9253820	20533230	9256461
25874670000	0.6719906	819.9189	1129.24	9320930	20591900	9323656
26185930000	0.6729767	829.782	1134.307	9388035	20647640	9390843
26497180000	0.673989	839.645	1139.541	9455145	20699870	9458040
26808430000	0.6750156	849.508	1144.882	9522250	20749660	9525225
27119690000	0.6760601	859.371	1150.35	9589360	20796690	9592411
27430940000	0.6771256	869.234	1155.965	9656470	20840630	9659598
27742190000	0.6782014	879.097	1161.672	9723575	20882490	9726786
28053440000	0.6792935	888.96	1167.505	9790685	20921690	9793977
28364700000	0.680393	898.8231	1173.418	9857795	20959080	9861171
28675950000	0.6815004	908.6861	1179.414	9924900	20994600	9928358
28987200000	0.6826189	918.5491	1185.513	9992010	21027940	9995547
29298460000	0.6837398	928.4121	1191.669	10059120	21059950	10062750
29609710000	0.684868	938.2751	1197.908	10126230	21090140	10129930
29920960000	0.686001	948.1381	1204.22	10193330	21118760	10197130
30232220000	0.6871359	958.0012	1210.587	10260440	21146100	10264310
30543470000	0.6882781	967.8641	1217.043	10327550	21171620	10331500
30854720000	0.6894175	977.7272	1223.53	10394660	21196330	10398700
31165980000	0.6905605	987.5902	1230.085	10461770	21219600	10465880
31477230000	0.691696	997.4532	1236.646	10528870	21242530	10533080
31788470000	0.6928368	1007.316	1243.286	10595980	21263860	10600270
32099730000	0.6939731	1017.179	1249.949	10663090	21284580	10667460
32410980000	0.6951141	1027.042	1256.689	10730200	21303750	10734640
32722230000	0.6962516	1036.905	1263.46	10797300	21322220	10801830
33033480000	0.6973876	1046.768	1270.272	10864410	21339800	10869030
33344740000	0.6984674	1056.631	1276.795	10886400	21265640	10886870
33655990000	0.6994373	1066.494	1282.694	10886400	21167850	10886880
33967250000	0.7003143	1076.357	1288.06	10886400	21079650	10886870
34278500000	0.7011116	1086.22	1292.967	10886400	20999660	10886880
34589750000	0.7018425	1096.083	1297.487	10886400	20926490	10886870
34901000000	0.7025165	1105.946	1301.676	10886400	20859160	10886880
35212250000	0.7031423	1115.809	1305.582	10886400	20796750	10886870
35523510000	0.703723	1125.672	1309.221	10886400	20738950	10886880



35834760000	0.7042652	1135.535	1312.632	10886400	20685050	10886870
36146010000	0.7047769	1145.398	1315.862	10886400	20634260	10886860
36457260000	0.7052584	1155.261	1318.913	10886400	20586550	10886880
36768520000	0.7057139	1165.124	1321.807	10886400	20541470	10886870
37079770000	0.7061473	1174.987	1324.57	10886400	20498630	10886880
37391020000	0.7065597	1184.85	1327.206	10886400	20457910	10886870
37702310000	0.7069498	1194.714	1329.706	10886400	20419440	10886870
38013560000	0.7073244	1204.577	1332.114	10886400	20382540	10886880
38324780000	0.7076829	1214.439	1334.424	10886400	20347260	10886880
38636030000	0.7080249	1224.302	1336.632	10886400	20313640	10886870
38947320000	0.7083573	1234.166	1338.784	10886400	20280990	10886880
39258540000	0.7086722	1244.028	1340.827	10886400	20250090	10886880
39569820000	0.7089795	1253.892	1342.825	10886400	20219960	10886880
39881080000	0.7092752	1263.755	1344.751	10886400	20190990	10886870
40192330000	0.7095631	1273.618	1346.63	10886400	20162810	10886870
40503580000	0.7098392	1283.481	1348.437	10886400	20135820	10886880
40814830000	0.7101073	1293.344	1350.193	10886400	20109610	10886870
41126080000	0.7103672	1303.207	1351.899	10886400	20084230	10886870
41437340000	0.7106203	1313.07	1353.564	10886400	20059540	10886880
41748590000	0.7108657	1322.933	1355.18	10886400	20035610	10886870
42059850000	0.7111037	1332.796	1356.751	10886400	20012410	10886870
42371100000	0.7113363	1342.659	1358.289	10886400	19989760	10886880
42682350000	0.7115626	1352.522	1359.786	10886400	19967740	10886870
42993600000	0.7117819	1362.385	1361.241	10886400	19946410	10886880
43304850000	0.7119977	1372.248	1362.674	10886400	19925430	10886870
43616100000	0.7122074	1382.111	1364.068	10886400	19905070	10886880
43927360000	0.7124132	1391.974	1365.439	10886400	19885080	10886870
44238610000	0.7126133	1401.837	1366.773	10886400	19865660	10886870
44549860000	0.7128092	1411.7	1368.082	10886400	19846670	10886880
44861120000	0.7130003	1421.563	1369.359	10886400	19828150	10886870
45172370000	0.7131878	1431.426	1370.615	10886400	19809980	10886870
45483620000	0.7133719	1441.289	1371.849	10886400	19792160	10886870
45794870000	0.7135503	1451.152	1373.047	10886400	19774890	10886870
46106130000	0.7137266	1461.015	1374.232	10886400	19757840	10886870
46417380000	0.7138993	1470.878	1375.395	10886400	19741140	10886880
46728630000	0.7140684	1480.741	1376.534	10886400	19724810	10886880
47039890000	0.714233	1490.604	1377.644	10886400	19708910	10886870
47351140000	0.7143956	1500.467	1378.742	10886400	19693210	10886870
47662390000	0.7145548	1510.33	1379.819	10886400	19677850	10886880
47973640000	0.7147119	1520.193	1380.882	10886400	19662700	10886880
48284900000	0.7148653	1530.056	1381.922	10886400	19647900	10886880
48596140000	0.7150159	1539.919	1382.943	10886400	19633390	10886870
48907400000	0.7151643	1549.782	1383.951	10886400	19619090	10886870
49218650000	0.7153097	1559.645	1384.939	10886400	19605100	10886880
49529910000	0.7154531	1569.508	1385.915	10886400	19591290	10886870
49841160000	0.715593	1579.371	1386.868	10886400	19577830	10886880
50152410000	0.7157313	1589.234	1387.811	10886400	19564530	10886880
50463670000	0.7158675	1599.097	1388.74	10886400	19551440	10886880
50774910000	0.7160011	1608.96	1389.653	10886400	19538600	10886880
51086170000	0.7161331	1618.823	1390.555	10886400	19525920	10886880
51397420000	0.7162624	1628.686	1391.44	10886400	19513500	10886870
51708670000	0.7163906	1638.549	1392.318	10886400	19501200	10886880



52019920000	0.7165158	1648.412	1393.176	10886400	19489170	10886870
52331180000	0.7166402	1658.275	1394.03	10886400	19477240	10886870
52642430000	0.7167621	1668.138	1394.867	10886400	19465550	10886870
52953680000	0.7168821	1678.001	1395.692	10886400	19454050	10886870
53264940000	0.7170003	1687.864	1396.505	10886400	19442720	10886870
53576190000	0.7171171	1697.727	1397.309	10886400	19431530	10886870
53887440000	0.7172319	1707.59	1398.101	10886400	19420540	10886880
54198690000	0.7173455	1717.453	1398.884	10886400	19409660	10886870
54509950000	0.7174574	1727.316	1399.656	10886400	19398950	10886870
54821200000	0.7175682	1737.179	1400.422	10886400	19388350	10886880
55132450000	0.7176768	1747.042	1401.172	10886400	19377960	10886870
55443710000	0.717784	1756.905	1401.914	10886400	19367710	10886870
55754960000	0.7178898	1766.768	1402.646	10886400	19357590	10886870
56066210000	0.7179946	1776.631	1403.372	10886400	19347580	10886870
56377460000	0.7180977	1786.494	1404.087	10886400	19337730	10886870
56688720000	0.7181998	1796.357	1404.796	10886400	19327970	10886870
56999970000	0.7183005	1806.22	1405.495	10886400	19318360	10886870
57311220000	0.7183999	1816.083	1406.186	10886400	19308870	10886870
57622470000	0.7184979	1825.946	1406.867	10886400	19299520	10886870
57933730000	0.7185949	1835.809	1407.542	10886400	19290260	10886870
58244980000	0.7186904	1845.672	1408.207	10886400	19281160	10886880
58556230000	0.7187852	1855.535	1408.868	10886400	19272120	10886880
58867480000	0.7188786	1865.398	1409.519	10886400	19263210	10886870
59178740000	0.718971	1875.261	1410.164	10886400	19254410	10886880
59489990000	0.719062	1885.124	1410.799	10886400	19245740	10886880
59801240000	0.7191522	1894.987	1411.429	10886400	19237150	10886880
60112490000	0.7192411	1904.85	1412.05	10886400	19228680	10886870
60423780000	0.7193292	1914.714	1412.666	10886400	19220280	10886860
60735030000	0.7194165	1924.577	1413.278	10886400	19211980	10886880
61046250000	0.7195025	1934.439	1413.88	10886400	19203790	10886870
61357510000	0.7195881	1944.302	1414.48	10886400	19195650	10886870
61668790000	0.7196723	1954.166	1415.07	10886400	19187640	10886870
61980010000	0.7197556	1964.028	1415.655	10886400	19179720	10886880
62291290000	0.7198378	1973.892	1416.232	10886400	19171900	10886870
62602550000	0.7199194	1983.755	1416.805	10886400	19164150	10886870
62913800000	0.7199997	1993.618	1417.369	10886400	19156510	10886870
63225050000	0.7200796	2003.481	1417.931	10886400	19148930	10886870
63536300000	0.7201586	2013.344	1418.487	10886400	19141420	10886870
63847560000	0.7202365	2023.207	1419.035	10886400	19134020	10886870
64158810000	0.7203136	2033.07	1419.579	10886400	19126700	10886870
64470060000	0.72039	2042.933	1420.117	10886400	19119450	10886870
64781310000	0.7204657	2052.796	1420.651	10886400	19112270	10886880
65092570000	0.7205408	2062.659	1421.181	10886400	19105150	10886880
65403820000	0.7206149	2072.522	1421.704	10886400	19098110	10886870
65715070000	0.7206883	2082.385	1422.222	10886400	19091140	10886870
66026330000	0.7207612	2092.248	1422.738	10886400	19084230	10886870
66337580000	0.7208331	2102.111	1423.246	10886400	19077420	10886870
66648830000	0.7209044	2111.974	1423.751	10886400	19070660	10886880
66960080000	0.7209751	2121.837	1424.251	10886400	19063960	10886870
67271340000	0.7210448	2131.7	1424.744	10886400	19057350	10886870
67582590000	0.7211141	2141.563	1425.235	10886400	19050790	10886870
67893840000	0.7211828	2151.426	1425.723	10886400	19044280	10886880



68205100000	0.7212508	2161.289	1426.205	10886400	19037840	10886870
68516350000	0.7213181	2171.152	1426.682	10886400	19031470	10886870
68827590000	0.7213848	2181.015	1427.156	10886400	19025160	10886880
69138850000	0.721451	2190.878	1427.626	10886400	19018890	10886870
69450100000	0.7215164	2200.741	1428.09	10886400	19012700	10886870
69761360000	0.7215816	2210.604	1428.554	10886400	19006540	10886880
70072610000	0.721646	2220.467	1429.012	10886400	19000440	10886870
70383860000	0.7217098	2230.33	1429.466	10886400	18994410	10886870
70695120000	0.721773	2240.193	1429.916	10886400	18988420	10886870
71006360000	0.7218358	2250.056	1430.363	10886400	18982490	10886870
71317620000	0.7218981	2259.919	1430.807	10886400	18976600	10886870
71628870000	0.7219598	2269.782	1431.247	10886400	18970770	10886870
71940130000	0.7220209	2279.645	1431.683	10886400	18965000	10886880
72251380000	0.7220814	2289.508	1432.115	10886400	18959280	10886880
72562630000	0.7221416	2299.371	1432.544	10886400	18953600	10886870
72873880000	0.7222013	2309.234	1432.97	10886400	18947960	10886870
73185130000	0.7222604	2319.097	1433.393	10886400	18942380	10886880
73496390000	0.7223189	2328.96	1433.811	10886400	18936850	10886870
73807640000	0.7223771	2338.823	1434.227	10886400	18931350	10886870
74118900000	0.7224348	2348.686	1434.64	10886400	18925910	10886880
74430140000	0.722492	2358.549	1435.049	10886400	18920510	10886870
74741400000	0.7225488	2368.412	1435.456	10886400	18915140	10886870
75052650000	0.7226052	2378.275	1435.86	10886400	18909830	10886880
75363900000	0.722661	2388.138	1436.26	10886400	18904570	10886880
75675160000	0.7227162	2398.001	1436.655	10886400	18899370	10886880
75986410000	0.7227709	2407.864	1437.047	10886400	18894200	10886870
76297670000	0.7228255	2417.727	1437.439	10886400	18889060	10886880
76608910000	0.7228796	2427.59	1437.827	10886400	18883950	10886870
76920160000	0.7229331	2437.453	1438.211	10886400	18878910	10886870
77231420000	0.7229865	2447.316	1438.595	10886400	18873880	10886880
77542670000	0.7230393	2457.179	1438.974	10886400	18868910	10886880
77853930000	0.7230918	2467.042	1439.351	10886400	18863960	10886870
78165180000	0.7231439	2476.905	1439.726	10886400	18859050	10886870
78476440000	0.7231954	2486.768	1440.096	10886400	18854200	10886870
78787680000	0.7232468	2496.631	1440.466	10886400	18849360	10886870
79098930000	0.7232977	2506.494	1440.833	10886400	18844560	10886870
79410180000	0.7233481	2516.357	1441.195	10886400	18839810	10886860
79721440000	0.7233983	2526.22	1441.557	10886400	18835090	10886870
80032690000	0.723448	2536.083	1441.915	10886400	18830410	10886870
80343950000	0.7234974	2545.946	1442.271	10886400	18825760	10886870
80655200000	0.7235464	2555.809	1442.625	10886400	18821150	10886870
80966450000	0.7235951	2565.672	1442.976	10886400	18816570	10886870
81277700000	0.7236435	2575.535	1443.325	10886400	18812020	10886870
81588950000	0.7236916	2585.398	1443.672	10886400	18807500	10886870
81900210000	0.7237391	2595.261	1444.015	10886400	18803030	10886870
82211500000	0.7237864	2605.125	1444.357	10886400	18798580	10886870
82522720000	0.7238333	2614.987	1444.696	10886400	18794170	10886870
82834000000	0.7238801	2624.851	1445.034	10886400	18789770	10886870
83145210000	0.7239263	2634.713	-1445.368	10886400	18785420	10886870
83456470000	0.7239723	2644.576	1445.701	10886400	18781100	10886870
83767720000	0.7240179	2654.439	1446.031	10886400	18776820	10886870
84078980000	0.7240633	2664.302	1446.359	10886400	18772560	10886870

84390260000	0.7241083	2674.166	1446.685	10886400	18768320	10886870
84701510000	0.724153	2684.029	1447.009	10886400	18764120	10886870
85012770000	0.7241974	2693.892	1447.331	10886400	18759960	10886880
85324010000	0.7242416	2703.755	1447.651	10886400	18755810	10886880
85635270000	0.7242852	2713.618	1447.967	10886400	18751710	10886870
85946520000	0.7243286	2723.481	1448.282	10886400	18747630	10886870
86257780000	0.7243719	2733.344	1448.596	10886400	18743570	10886870
86569030000	0.7244147	2743.207	1448.907	10886400	18739550	10886870
86880280000	0.7244572	2753.07	1449.215	10886400	18735560	10886870
87191540000	0.7244995	2762.933	1449.522	10886400	18731590	10886870
87502780000	0.7245414	2772.796	1449.827	10886400	18727660	10886880
87814040000	0.724583	2782.659	1450.129	10886400	18723750	10886870
88125290000	0.7246245	2792.522	1450.431	10886400	18719870	10886880
88436550000	0.7246655	2802.385	1450.729	10886400	18716010	10886870
88747800000	0.7247067	2812.248	1451.028	10886400	18712150	10886870
89059050000	0.7247469	2822.111	1451.32	10886400	18708380	10886870
89370300000	0.7247872	2831.974	1451.614	10886400	18704600	10886870
89681550000	0.7248271	2841.837	1451.904	10886400	18700860	10886870
89992810000	0.7248669	2851.7	1452.194	10886400	18697130	10886870
90304060000	0.7249062	2861.563	1452.48	10886400	18693450	10886870
90615320000	0.7249453	2871.426	1452.765	10886400	18689780	10886870
90926570000	0.7249842	2881.289	1453.049	10886400	18686140	10886880
91237820000	0.7250228	2891.152	1453.33	10886400	18682520	10886880
91549070000	0.7250611	2901.015	1453.609	10886400	18678930	10886870
91860320000	0.7250992	2910.878	1453.887	10886400	18675360	10886870
92171580000	0.7251369	2920.741	1454.162	10886400	18671820	10886870
92482830000	0.7251745	2930.604	1454.436	10886400	18668300	10886870
92794090000	0.7252119	2940.467	1454.709	10886400	18664810	10886880
93105340000	0.7252489	2950.33	1454.979	10886400	18661340	10886870
93416590000	0.7252857	2960.193	1455.248	10886400	18657890	10886870
93727830000	0.7253222	2970.056	1455.515	10886400	18654470	10886870
94039090000	0.7253587	2979.919	1455.782	10886400	18651060	10886880
94350340000	0.7253947	2989.782	1456.045	10886400	18647680	10886870
94661600000	0.7254305	2999.645	1456.306	10886400	18644330	10886870
94972850000	0.7254662	3009.508	1456.567	10886400	18640990	10886870
95284110000	0.7255016	3019.371	1456.826	10886400	18637680	10886870
95595350000	0.7255368	3029.234	1457.084	10886400	18634390	10886880
95906600000	0.7255717	3039.097	1457.339	10886400	18631120	10886870
96217860000	0.7256064	3048.96	1457.593	10886400	18627870	10886870
96529110000	0.725641	3058.823	1457.847	10886400	18624640	10886880
96840370000	0.7256752	3068.686	1458.097	10886400	18621430	10886870
97151620000	0.7257093	3078.549	1458.347	10886400	18618250	10886880
97462870000	0.7257431	3088.412	1458.595	10886400	18615090	10886880
97774120000	0.7257767	3098.275	1458.841	10886400	18611940	10886870
98085370000	0.7258106	3108.138	1459.089	10886400	18608780	10886880
98396630000	0.7258445	3118.001	1459.338	10886400	18605610	10886880
98707880000	0.7258773	3127.864	1459.578	10886400	18602530	10886870
99019140000	0.7259101	3137.727	1459.819	10886400	18599480	10886880
99330390000	0.7259425	3147.59	1460.057	10886400	18596440	10886870
99641640000	0.7259748	3157.453	1460.294	10886400	18593420	10886870
99952890000	0.7260069	3167.316	1460.53	10886400	18590420	10886880
1.00264E+11	0.7260389	3177.179	1460.764	10886400	18587430	10886870

1.00575E+11	0.7260706	3187.042	1460.997	10886400	18584470	10886870
1.00887E+11	0.7261021	3196.905	1461.229	10886400	18581520	10886870
1.01198E+11	0.7261334	3206.768	1461.459	10886400	18578600	10886870
1.01509E+11	0.7261646	3216.631	1461.688	10886400	18575690	10886870
1.0182E+11	0.7261954	3226.494	1461.914	10886400	18572810	10886870
1.02132E+11	0.7262262	3236.357	1462.141	10886400	18569940	10886880
1.02443E+11	0.7262566	3246.22	1462.365	10886400	18567090	10886870
1.02754E+11	0.7262869	3256.083	1462.587	10886400	18564260	10886870
1.03065E+11	0.7263173	3265.946	1462.811	10886400	18561420	10886870
1.03377E+11	0.7263472	3275.809	1463.031	10886400	18558630	10886870
1.03688E+11	0.7263769	3285.672	1463.25	10886400	18555860	10886870
1.03999E+11	0.7264065	3295.535	1463.468	10886400	18553100	10886880
1.0431E+11	0.7264358	3305.398	1463.683	10886400	18550360	10886870
1.04622E+11	0.726465	3315.261	1463.899	10886400	18547630	10886870
1.04933E+11	0.7264941	3325.125	1464.113	10886400	18544920	10886870
1.05244E+11	0.7265229	3334.987	1464.325	10886400	18542240	10886870
1.05556E+11	0.7265516	3344.851	1464.537	10886400	18539550	10886870
1.05867E+11	0.72658	3354.713	1464.746	10886400	18536900	10886870
1.06178E+11	0.7266085	3364.576	1464.956	10886400	18534250	10886870
1.06489E+11	0.7266365	3374.439	1465.163	10886400	18531630	10886870
1.068E+11	0.7266646	3384.302	1465.37	10886400	18529010	10886870
1.07112E+11	0.7266924	3394.166	1465.575	10886400	18526420	10886870
1.07423E+11	0.7267202	3404.029	1465.781	10886400	18523830	10886880
1.07734E+11	0.7267476	3413.892	1465.982	10886400	18521270	10886870
1.08046E+11	0.7267749	3423.755	1466.184	10886400	18518720	10886870
1.08357E+11	0.7268021	3433.618	1466.385	10886400	18516190	10886870
1.08668E+11	0.7268291	3443.481	1466.585	10886400	18513680	10886880
1.08979E+11	0.7268559	3453.344	1466.782	10886400	18511180	10886880
1.09291E+11	0.7268825	3463.207	1466.979	10886400	18508690	10886870
1.09602E+11	0.726909	3473.07	1467.175	10886400	18506220	10886870
1.09913E+11	0.7269354	3482.933	1467.37	10886400	18503760	10886870
1.10224E+11	0.7269618	3492.796	1467.565	10886400	18501300	10886870
1.10536E+11	0.7269878	3502.659	1467.757	10886400	18498880	10886870
1.10847E+11	0.7270137	3512.522	1467.949	10886400	18496460	10886870
1.11158E+11	0.7270394	3522.385	1468.139	10886400	18494070	10886880
1.11469E+11	0.7270653	3532.248	1468.331	10886400	18491660	10886880
1.11781E+11	0.7270907	3542.111	1468.519	10886400	18489290	10886880
1.12092E+11	0.7271159	3551.974	1468.705	10886400	18486940	10886870
1.12403E+11	0.7271411	3561.837	1468.892	10886400	18484590	10886880
1.12714E+11	0.7271661	3571.7	1469.077	10886400	18482260	10886870
1.13026E+11	0.7271913	3581.563	1469.264	10886400	18479910	10886880
1.13337E+11	0.727216	3591.426	1469.446	10886400	18477610	10886870
1.13648E+11	0.7272406	3601.289	1469.629	10886400	18475320	10886880
1.13959E+11	0.7272651	3611.152	1469.81	10886400	18473040	10886870
1.14271E+11	0.7272896	3621.015	1469.992	10886400	18470760	10886880
1.14582E+11	0.727318	3630.878	1470.202	10886400	18468110	10886870
1.14893E+11	0.7273397	3640.741	1470.363	10886400	18466090	10886870
1.15204E+11	0.7273635	3650.604	1470.54	10886400	18463870	10886870
1.15516E+11	0.7273872	3660.467	1470.715	10886400	18461670	10886870
1.15827E+11	0.7274109	3670.33	1470.891	10886400	18459470	10886880
1.16138E+11	0.7274343	3680.193	1471.065	10886400	18457280	10886870
1.16449E+11	0.7274576	3690.056	1471.237	10886400	18455110	10886870



1.16761E+11	0.7274808	3699.919	1471.41	10886400	18452960	10886880
1.17072E+11	0.727504	3709.782	1471.582	10886400	18450800	10886880
1.17383E+11	0.7275268	3719.645	1471.751	10886400	18448670	10886870
1.17694E+11	0.7275507	3729.508	1471.929	10886400	18446440	10886870
1.18006E+11	0.727573	3739.371	1472.094	10886400	18444380	10886870
1.18317E+11	0.7275956	3749.234	1472.262	10886400	18442270	10886870
1.18628E+11	0.7276183	3759.097	1472.431	10886400	18440160	10886870
1.18939E+11	0.7276406	3768.96	1472.597	10886400	18438090	10886880
1.19251E+11	0.7276627	3778.823	1472.761	10886400	18436020	10886870
1.19562E+11	0.727685	3788.686	1472.926	10886400	18433950	10886870
1.19873E+11	0.7277075	3798.549	1473.094	10886400	18431860	10886870
1.20184E+11	0.7277291	3808.412	1473.254	10886400	18429850	10886870
1.20496E+11	0.727751	3818.275	1473.417	10886400	18427820	10886870
1.20807E+11	0.7277728	3828.138	1473.579	10886400	18425790	10886870
1.21118E+11	0.7277945	3838.001	1473.741	10886400	18423770	10886870
1.21429E+11	0.727816	3847.864	1473.901	10886400	18421780	10886880
1.21741E+11	0.7278374	3857.727	1474.06	10886400	18419780	10886870
1.22052E+11	0.7278588	3867.59	1474.219	10886400	18417790	10886870
1.22363E+11	0.7278804	3877.453	1474.38	10886400	18415790	10886880
1.22674E+11	0.7279016	3887.316	1474.538	10886400	18413810	10886870
1.22986E+11	0.7279223	3897.179	1474.692	10886400	18411890	10886880
1.23297E+11	0.7279431	3907.042	1474.847	10886400	18409960	10886880
1.23608E+11	0.7279637	3916.905	1475	10886400	18408040	10886870
1.23919E+11	0.7279844	3926.768	1475.155	10886400	18406120	10886880
1.24231E+11	0.7280048	3936.631	1475.306	10886400	18404220	10886870
1.24542E+11	0.7280253	3946.494	1475.459	10886400	18402320	10886880
1.24853E+11	0.7280454	3956.357	1475.609	10886400	18400440	10886870
1.25164E+11	0.7280654	3966.22	1475.758	10886400	18398580	10886870
1.25476E+11	0.7280856	3976.083	1475.908	10886400	18396710	10886870
1.25787E+11	0.7281056	3985.946	1476.058	10886400	18394850	10886880
1.26098E+11	0.7281253	3995.809	1476.204	10886400	18393020	10886870
1.26409E+11	0.7281453	4005.672	1476.354	10886400	18391160	10886870
1.26721E+11	0.7281651	4015.535	1476.501	10886400	18389320	10886870
1.27032E+11	0.7281851	4025.398	1476.651	10886400	18387470	10886880
1.27343E+11	0.7282047	4035.261	1476.797	10886400	18385640	10886870
1.27654E+11	0.7282242	4045.125	1476.943	10886400	18383830	10886880
1.27966E+11	0.7282436	4054.987	1477.087	10886400	18382030	10886870
1.28277E+11	0.728263	4064.851	1477.232	10886400	18380230	10886870
1.28588E+11	0.728282	4074.713	1477.374	10886400	18378460	10886870
1.28899E+11	0.7283011	4084.576	1477.516	10886400	18376690	10886870
1.29211E+11	0.7283203	4094.439	1477.66	10886400	18374910	10886880
1.29522E+11	0.7283398	4104.303	1477.805	10886400	18373100	10886870
1.29833E+11	0.7283586	4114.166	1477.946	10886400	18371350	10886870
1.30144E+11	0.7283773	4124.028	1478.085	10886400	18369610	10886870
1.30456E+11	0.7283958	4133.892	1478.224	10886400	18367900	10886880
1.30767E+11	0.7284144	4143.754	1478.363	10886400	18366170	10886880
1.31078E+11	0.7284327	4153.618	1478.5	10886400	18364470	10886880
1.31389E+11	0.7284511	4163.48	1478.637	10886400	18362760	10886870
1.31701E+11	0.7284693	4173.344	1478.773	10886400	18361070	10886870
1.32012E+11	0.7284874	4183.207	1478.908	10886400	18359400	10886870
1.32323E+11	0.7285056	4193.07	1479.045	10886400	18357710	10886880
1.32635E+11	0.7285237	4202.933	1479.18	10886400	18356020	10886870



1.32946E+11	0.7285419	4212.796	1479.316	10886400	18354330	10886870
1.33257E+11	0.7285608	4222.659	1479.457	10886400	18352580	10886870
1.33568E+11	0.728579	4232.521	1479.593	10886400	18350890	10886870
1.3388E+11	0.7285963	4242.385	1479.723	10886400	18349290	10886880
1.34191E+11	0.7286136	4252.248	1479.853	10886400	18347680	10886880
1.34502E+11	0.7286311	4262.111	1479.983	10886400	18346060	10886870
1.34813E+11	0.7286483	4271.974	1480.112	10886400	18344460	10886870
1.35125E+11	0.7286655	4281.837	1480.241	10886400	18342870	10886880
1.35436E+11	0.7286827	4291.7	1480.37	10886400	18341270	10886880
1.35747E+11	0.7286999	4301.563	1480.499	10886400	18339680	10886880
1.36058E+11	0.728717	4311.426	1480.627	10886400	18338090	10886880
1.3637E+11	0.7287338	4321.289	1480.752	10886400	18336520	10886860
1.36681E+11	0.7287509	4331.152	1480.88	10886400	18334950	10886870
1.36992E+11	0.7287675	4341.015	1481.005	10886400	18333400	10886870
1.37303E+11	0.7287844	4350.878	1481.131	10886400	18331840	10886870
1.37615E+11	0.7288008	4360.741	1481.254	10886400	18330320	10886870
1.37926E+11	0.7288176	4370.604	1481.38	10886400	18328760	10886870
1.38237E+11	0.7288342	4380.467	1481.505	10886400	18327220	10886880
1.38548E+11	0.7288509	4390.33	1481.63	10886400	18325670	10886870
1.3886E+11	0.7288673	4400.193	1481.753	10886400	18324150	10886880
1.39171E+11	0.728884	4410.056	1481.878	10886400	18322600	10886870
1.39482E+11	0.7289008	4419.919	1482.004	10886400	18321040	10886870
1.39793E+11	0.7289185	4429.782	1482.137	10886400	18319400	10886870
1.40105E+11	0.7289346	4439.645	1482.257	10886400	18317900	10886860
1.40416E+11	0.7289509	4449.508	1482.38	10886400	18316400	10886880
1.40727E+11	0.7289681	4459.371	1482.509	10886400	18314810	10886880
1.41038E+11	0.7289841	4469.234	1482.629	10886400	18313320	10886870
1.4135E+11	0.7290001	4479.097	1482.749	10886400	18311840	10886870
1.41661E+11	0.7290158	4488.96	1482.867	10886400	18310380	10886870
1.41972E+11	0.7290319	4498.823	1482.988	10886400	18308890	10886870
1.42283E+11	0.7290478	4508.686	1483.107	10886400	18307420	10886870
1.42595E+11	0.7290635	4518.549	1483.225	10886400	18305960	10886870
1.42906E+11	0.7290791	4528.412	1483.342	10886400	18304510	10886870
1.43217E+11	0.7290949	4538.275	1483.461	10886400	18303050	10886870
1.43528E+11	0.7291108	4548.138	1483.58	10886400	18301580	10886870
1.4384E+11	0.7291265	4558.001	1483.698	10886400	18300130	10886880
1.44151E+11	0.7291431	4567.864	1483.823	10886400	18298590	10886880
1.44462E+11	0.7291585	4577.727	1483.939	10886400	18297160	10886880
1.44773E+11	0.7291734	4587.59	1484.051	10886400	18295780	10886880
1.45085E+11	0.7291886	4597.453	1484.165	10886400	18294370	10886870
1.45396E+11	0.7292041	4607.316	1484.281	10886400	18292940	10886870
1.45707E+11	0.7292198	4617.179	1484.399	10886400	18291480	10886870
1.46018E+11	0.7292348	4627.042	1484.512	10886400	18290100	10886880
1.4633E+11	0.7292497	4636.905	1484.624	10886400	18288720	10886880
1.46641E+11	0.7292649	4646.768	1484.739	10886400	18287300	10886880
1.46952E+11	0.7292796	4656.631	1484.849	10886400	18285940	10886870
1.47263E+11	0.7292945	4666.494	1484.961	10886400	18284560	10886870
1.47575E+11	0.7293096	4676.357	1485.075	10886400	18283160	10886870
1.47886E+11	0.7293245	4686.22	1485.187	10886400	18281780	10886870
1.48197E+11	0.7293394	4696.083	1485.299	10886400	18280410	10886880
1.48508E+11	0.7293551	4705.946	1485.417	10886400	18278950	10886870
1.4882E+11	0.7293699	4715.81	1485.528	10886400	18277580	10886870



1.49131E+11	0.7293841	4725.672	1485.635	10886400	18276260	10886870
1.49442E+11	0.7293999	4735.535	1485.754	10886400	18274800	10886870
1.49753E+11	0.7294138	4745.398	1485.859	10886400	18273510	10886870
1.50065E+11	0.7294293	4755.261	1485.976	10886400	18272080	10886880
1.50376E+11	0.729445	4765.125	1486.094	10886400	18270620	10886870
1.50687E+11	0.7294603	4774.987	1486.209	10886400	18269210	10886870
1.50998E+11	0.7294746	4784.851	1486.317	10886400	18267880	10886870
1.5131E+11	0.7294899	4794.713	1486.432	10886400	18266470	10886880
1.51621E+11	0.7295054	4804.577	1486.549	10886400	18265040	10886880
1.51932E+11	0.7295209	4814.439	1486.666	10886400	18263600	10886880
1.52243E+11	0.729535	4824.303	1486.771	10886400	18262300	10886870
1.52555E+11	0.7295505	4834.166	1486.888	10886400	18260860	10886870
1.52866E+11	0.7295641	4844.028	1486.991	10886400	18259600	10886870
1.53177E+11	0.72958	4853.892	1487.111	10886400	18258130	10886880
1.53488E+11	0.7295948	4863.754	1487.223	10886400	18256760	10886880
1.538E+11	0.729609	4873.618	1487.329	10886400	18255440	10886870
1.54111E+11	0.7296246	4883.48	1487.447	10886400	18254010	10886880
1.54422E+11	0.7296403	4893.344	1487.565	10886400	18252550	10886870
1.54733E+11	0.7296557	4903.207	1487.681	10886400	18251130	10886870
1.55045E+11	0.7296715	4913.07	1487.801	10886400	18249670	10886880
1.55356E+11	0.729687	4922.933	1487.917	10886400	18248230	10886870
1.55667E+11	0.7297025	4932.796	1488.034	10886400	18246790	10886870
1.55979E+11	0.7297166	4942.659	1488.141	10886400	18245490	10886870
1.5629E+11	0.7297315	4952.521	1488.253	10886400	18244110	10886870
1.56601E+11	0.7297464	4962.385	1488.366	10886400	18242740	10886880
1.56912E+11	0.7297606	4972.248	1488.473	10886400	18241420	10886870
1.57224E+11	0.7297747	4982.111	1488.579	10886400	18240110	10886870
1.57535E+11	0.7297892	4991.974	1488.689	10886400	18238780	10886880
1.57846E+11	0.7298025	5001.837	1488.789	10886400	18237540	10886870
1.58157E+11	0.7298176	5011.7	1488.903	10886400	18236140	10886870
1.58469E+11	0.7298331	5021.563	1489.021	10886400	18234720	10886880
1.5878E+11	0.7298478	5031.426	1489.131	10886400	18233360	10886870
1.59091E+11	0.7298623	5041.289	1489.241	10886400	18232020	10886880
1.59402E+11	0.7298775	5051.152	1489.355	10886400	18230610	10886870
1.59714E+11	0.7298922	5061.015	1489.467	10886400	18229250	10886880
1.60025E+11	0.7299076	5070.878	1489.583	10886400	18227820	10886870
1.60336E+11	0.7299221	5080.741	1489.693	10886400	18226490	10886880
1.60647E+11	0.729937	5090.604	1489.805	10886400	18225110	10886870
1.60959E+11	0.7299517	5100.467	1489.916	10886400	18223750	10886870
1.6127E+11	0.7299663	5110.33	1490.027	10886400	18222400	10886880
1.61581E+11	0.729981	5120.193	1490.138	10886400	18221040	10886870
1.61892E+11	0.7299954	5130.056	1490.247	10886400	18219710	10886880
1.62204E+11	0.7300099	5139.919	1490.356	10886400	18218370	10886870
1.62515E+11	0.7300237	5149.782	1490.461	10886400	18217090	10886870
1.62826E+11	0.7300373	5159.645	1490.563	10886400	18215840	10886870
1.63137E+11	0.7300509	5169.508	1490.667	10886400	18214580	10886880
1.63449E+11	0.730065	5179.371	1490.773	10886400	18213280	10886880
1.6376E+11	0.7300792	5189.234	1490.88	10886400	18211960	10886870
1.64071E+11	0.730094	5199.097	1490.993	10886400	18210600	10886880
1.64382E+11	0.7301094	5208.96	1491.109	10886400	18209170	10886870
1.64694E+11	0.7301213	5218.823	1491.199	10886400	18208070	10886870
1.65005E+11	0.7301353	5228.686	1491.305	10886400	18206780	10886870



1.65316E+11	0.7301494	5238.549	1491.412	10886400	18205470	10886870
1.65627E+11	0.7301641	5248.412	1491.523	10886400	18204120	10886870
1.65939E+11	0.7301785	5258.275	1491.632	10886400	18202790	10886870
1.6625E+11	0.7301922	5268.138	1491.736	10886400	18201520	10886870
1.66561E+11	0.7302063	5278.001	1491.843	10886400	18200220	10886880
1.66872E+11	0.7302195	5287.864	1491.942	10886400	18199000	10886870
1.67184E+11	0.7302329	5297.727	1492.044	10886400	18197760	10886870
1.67495E+11	0.7302475	5307.59	1492.155	10886400	18196410	10886870
1.67806E+11	0.7302614	5317.453	1492.26	10886400	18195120	10886870
1.68117E+11	0.7302766	5327.316	1492.375	10886400	18193730	10886880
1.68429E+11	0.7302909	5337.179	1492.483	10886400	18192410	10886870
1.6874E+11	0.7303046	5347.042	1492.587	10886400	18191140	10886870
1.69051E+11	0.7303167	5356.905	1492.679	10886400	18190020	10886870
1.69362E+11	0.7303289	5366.768	1492.771	10886400	18188900	10886870
1.69674E+11	0.7303414	5376.631	1492.866	10886400	18187740	10886870
1.69985E+11	0.7303543	5386.494	1492.964	10886400	18186550	10886870
1.70296E+11	0.7303673	5396.357	1493.063	10886400	18185350	10886880
1.70607E+11	0.7303814	5406.22	1493.17	10886400	18184050	10886880
1.70919E+11	0.7303947	5416.083	1493.27	10886400	18182820	10886870
1.7123E+11	0.7304093	5425.946	1493.381	10886400	18181470	10886870
1.71541E+11	0.7304219	5435.81	1493.476	10886400	18180310	10886870
1.71852E+11	0.7304348	5445.672	1493.574	10886400	18179120	10886870
1.72164E+11	0.7304496	5455.535	1493.687	10886400	18177750	10886880
1.72475E+11	0.7304636	5465.398	1493.793	10886400	18176460	10886880
1.72786E+11	0.7304758	5475.261	1493.885	10886400	18175330	10886870
1.73097E+11	0.7304889	5485.125	1493.985	10886400	18174120	10886870
1.73409E+11	0.7305029	5494.987	1494.091	10886400	18172830	10886870
1.7372E+11	0.7305177	5504.851	1494.203	10886400	18171460	10886870
1.74031E+11	0.7305315	5514.713	1494.308	10886400	18170190	10886870
1.74342E+11	0.7305447	5524.577	1494.408	10886400	18168970	10886870
1.74654E+11	0.7305601	5534.439	1494.525	10886400	18167550	10886870
1.74965E+11	0.7305747	5544.303	1494.636	10886400	18166200	10886870
1.75276E+11	0.7305896	5554.166	1494.749	10886400	18164820	10886870
1.75587E+11	0.7306026	5564.028	1494.848	10886400	18163630	10886880
1.75899E+11	0.7306162	5573.892	1494.951	10886400	18162370	10886870
1.7621E+11	0.7306306	5583.754	1495.06	10886400	18161040	10886870
1.76521E+11	0.7306444	5593.618	1495.166	10886400	18159770	10886880
1.76832E+11	0.7306591	5603.48	1495.277	10886400	18158410	10886870
1.77144E+11	0.7306713	5613.344	1495.37	10886400	18157290	10886880
1.77455E+11	0.730685	5623.207	1495.474	10886400	18156020	10886870
1.77766E+11	0.730699	5633.07	1495.58	10886400	18154730	10886870
1.78077E+11	0.7307137	5642.933	1495.692	10886400	18153380	10886880
1.78389E+11	0.7307274	5652.796	1495.796	10886400	18152120	10886880
1.787E+11	0.7307418	5662.659	1495.906	10886400	18150780	10886870
1.79011E+11	0.7307556	5672.521	1496.011	10886400	18149520	10886880
1.79322E+11	0.7307692	5682.385	1496.114	10886400	18148260	10886880
1.79634E+11	0.7307822	5692.248	1496.213	10886400	18147060	10886880
1.79945E+11	0.7307958	5702.111	1496.316	10886400	18145800	10886870
1.80256E+11	0.7308099	5711.974	1496.424	10886400	18144510	10886880
1.80567E+11	0.7308244	5721.837	1496.534	10886400	18143170	10886880
1.80879E+11	0.7308383	5731.7	1496.64	10886400	18141880	10886870
1.8119E+11	0.7308523	5741.563	1496.746	10886400	18140590	10886870



1.81501E+11	0.7308668	5751.426	1496.856	10886400	18139250	10886870
1.81813E+11	0.7308814	5761.289	1496.968	10886400	18137910	10886880
1.82124E+11	0.7308954	5771.152	1497.074	10886400	18136620	10886870
1.82435E+11	0.730909	5781.015	1497.178	10886400	18135360	10886870
1.82746E+11	0.7309227	5790.878	1497.282	10886400	18134100	10886870
1.83058E+11	0.7309356	5800.741	1497.38	10886400	18132910	10886870
1.83369E+11	0.7309502	5810.604	1497.491	10886400	18131560	10886870
1.8368E+11	0.7309629	5820.467	1497.588	10886400	18130390	10886870
1.83991E+11	0.7309761	5830.33	1497.689	10886400	18129170	10886870
1.84303E+11	0.7309898	5840.193	1497.793	10886400	18127910	10886870
1.84614E+11	0.7310027	5850.056	1497.891	10886400	18126720	10886870
1.84925E+11	0.7310165	5859.919	1497.996	10886400	18125460	10886880
1.85236E+11	0.7310304	5869.782	1498.102	10886400	18124170	10886870
1.85548E+11	0.7310444	5879.645	1498.209	10886400	18122880	10886870
1.85859E+11	0.7310578	5889.508	1498.311	10886400	18121640	10886870
1.8617E+11	0.7310718	5899.371	1498.418	10886400	18120350	10886870
1.86481E+11	0.731086	5909.234	1498.526	10886400	18119040	10886870
1.86793E+11	0.7311	5919.097	1498.633	10886400	18117760	10886880
1.87104E+11	0.7311139	5928.96	1498.739	10886400	18116480	10886880
1.87415E+11	0.7311279	5938.823	1498.845	10886400	18115180	10886870
1.87726E+11	0.7311419	5948.686	1498.952	10886400	18113890	10886870
1.88038E+11	0.7311552	5958.549	1499.054	10886400	18112670	10886880
1.88349E+11	0.7311677	5968.412	1499.149	10886400	18111510	10886870
1.8866E+11	0.7311822	5978.275	1499.26	10886400	18110180	10886880
1.88971E+11	0.7311953	5988.138	1499.359	10886400	18108970	10886870
1.89283E+11	0.7312099	5998.001	1499.471	10886400	18107630	10886880
1.89594E+11	0.7312241	6007.864	1499.579	10886400	18106320	10886870
1.89905E+11	0.7312383	6017.727	1499.688	10886400	18105010	10886880
1.90216E+11	0.7312521	6027.59	1499.793	10886400	18103750	10886880
1.90528E+11	0.7312645	6037.453	1499.887	10886400	18102600	10886870
1.90839E+11	0.7312784	6047.316	1499.994	10886400	18101320	10886880
1.9115E+11	0.7312919	6057.179	1500.096	10886400	18100080	10886870
1.91461E+11	0.7313061	6067.042	1500.205	10886400	18098770	10886870
1.91773E+11	0.7313204	6076.905	1500.314	10886400	18097450	10886870
1.92084E+11	0.7313349	6086.768	1500.425	10886400	18096120	10886880
1.92395E+11	0.731348	6096.631	1500.525	10886400	18094910	10886880
1.92706E+11	0.7313617	6106.494	1500.629	10886400	18093650	10886870
1.93018E+11	0.7313755	6116.357	1500.735	10886400	18092380	10886880
1.93329E+11	0.7313901	6126.22	1500.847	10886400	18091040	10886880
1.9364E+11	0.7314032	6136.083	1500.946	10886400	18089820	10886870
1.93951E+11	0.7314181	6145.946	1501.06	10886400	18088460	10886870
1.94263E+11	0.7314317	6155.81	1501.165	10886400	18087200	10886880
1.94574E+11	0.7314453	6165.672	1501.268	10886400	18085940	10886870
1.94885E+11	0.7314588	6175.535	1501.371	10886400	18084700	10886870
1.95196E+11	0.7314705	6185.398	1501.461	10886400	18083630	10886880
1.95508E+11	0.7314837	6195.261	1501.562	10886400	18082410	10886870
1.95819E+11	0.7314972	6205.125	1501.665	10886400	18081170	10886870
1.9613E+11	0.7315108	6214.987	1501.769	10886400	18079920	10886870
1.96441E+11	0.7315243	6224.851	1501.872	10886400	18078680	10886870
1.96753E+11	0.7315384	6234.713	1501.98	10886400	18077380	10886870
1.97064E+11	0.7315506	6244.577	1502.073	10886400	18076260	10886870
1.97375E+11	0.7315618	6254.439	1502.159	10886400	18075230	10886880



1.97686E+11	0.7315753	6264.303	1502.262	10886400	18073980	10886870
1.97998E+11	0.7315885	6274.166	1502.363	10886400	18072770	10886870
1.98309E+11	0.7316021	6284.028	1502.467	10886400	18071520	10886870
1.9862E+11	0.7316142	6293.892	1502.56	10886400	18070400	10886870
1.98931E+11	0.7316275	6303.754	1502.662	10886400	18069180	10886880
1.99243E+11	0.7316413	6313.618	1502.767	10886400	18067910	10886870
1.99554E+11	0.7316553	6323.48	1502.875	10886400	18066620	10886880
1.99865E+11	0.7316692	6333.344	1502.981	10886400	18065340	10886870
2.00176E+11	0.7316839	6343.207	1503.094	10886400	18063990	10886880
2.00488E+11	0.7316981	6353.07	1503.202	10886400	18062680	10886870
2.00799E+11	0.7317122	6362.933	1503.31	10886400	18061380	10886870
2.0111E+11	0.7317255	6372.796	1503.412	10886400	18060160	10886870
2.01421E+11	0.7317404	6382.659	1503.526	10886400	18058790	10886870
2.01733E+11	0.7317544	6392.521	1503.634	10886400	18057500	10886880
2.02044E+11	0.7317685	6402.385	1503.741	10886400	18056200	10886870
2.02355E+11	0.7317828	6412.248	1503.851	10886400	18054890	10886870
2.02666E+11	0.7317972	6422.111	1503.961	10886400	18053570	10886880
2.02978E+11	0.73181	6431.974	1504.059	10886400	18052390	10886870
2.03289E+11	0.7318239	6441.837	1504.166	10886400	18051110	10886880
2.036E+11	0.7318376	6451.7	1504.271	10886400	18049840	10886870
2.03911E+11	0.7318522	6461.563	1504.383	10886400	18048510	10886880
2.04223E+11	0.7318661	6471.426	1504.49	10886400	18047230	10886880
2.04534E+11	0.7318791	6481.289	1504.589	10886400	18046040	10886880
2.04845E+11	0.7318938	6491.152	1504.702	10886400	18044680	10886880
2.05156E+11	0.731908	6501.015	1504.811	10886400	18043380	10886880
2.05468E+11	0.7319221	6510.878	1504.919	10886400	18042080	10886880
2.05779E+11	0.731937	6520.741	1505.033	10886400	18040710	10886870
2.0609E+11	0.7319502	6530.604	1505.135	10886400	18039500	10886880
2.06401E+11	0.7319648	6540.467	1505.247	10886400	18038160	10886880
2.06713E+11	0.7319795	6550.33	1505.359	10886400	18036790	10886870
2.07024E+11	0.7319939	6560.193	1505.47	10886400	18035470	10886870
2.07335E+11	0.7320088	6570.056	1505.584	10886400	18034100	10886870
2.07647E+11	0.7320231	6579.919	1505.694	10886400	18032790	10886870
2.07958E+11	0.7320373	6589.782	1505.803	10886400	18031490	10886880
2.08269E+11	0.7320514	6599.645	1505.911	10886400	18030190	10886870
2.0858E+11	0.7320663	6609.508	1506.025	10886400	18028820	10886870
2.08892E+11	0.7320806	6619.371	1506.135	10886400	18027500	10886870
2.09203E+11	0.7320952	6629.234	1506.247	10886400	18026160	10886870
2.09514E+11	0.7321103	6639.097	1506.363	10886400	18024780	10886870
2.09825E+11	0.7321248	6648.96	1506.475	10886400	18023440	10886870
2.10137E+11	0.7321404	6658.823	1506.595	10886400	18022010	10886880
2.10448E+11	0.7321531	6668.686	1506.692	10886400	18020840	10886870
2.10759E+11	0.7321649	6678.549	1506.783	10886400	18019760	10886880
2.1107E+11	0.7321772	6688.412	1506.877	10886400	18018630	10886870
2.11382E+11	0.7321903	6698.275	1506.978	10886400	18017430	10886880
2.11693E+11	0.7322034	6708.138	1507.079	10886400	18016230	10886880
2.12004E+11	0.732217	6718.001	1507.183	10886400	18014970	10886870
2.12315E+11	0.7322301	6727.864	1507.284	10886400	18013770	10886880
2.12627E+11	0.7322428	6737.727	1507.382	10886400	18012600	10886880
2.12938E+11	0.7322565	6747.59	1507.487	10886400	18011340	10886870
2.13249E+11	0.7322709	6757.453	1507.597	10886400	18010020	10886870
2.1356E+11	0.7322848	6767.316	1507.704	10886400	18008740	10886870

2.13872E+11	0.7322981	6777.179	1507.807	10886400	18007520	10886870
2.14183E+11	0.7323112	6787.042	1507.907	10886400	18006320	10886870
2.14494E+11	0.7323254	6796.905	1508.016	10886400	18005010	10886870
2.14805E+11	0.7323391	6806.768	1508.122	10886400	18003760	10886880
2.15117E+11	0.7323526	6816.631	1508.226	10886400	18002510	10886870
2.15428E+11	0.7323667	6826.494	1508.334	10886400	18001220	10886870
2.15739E+11	0.7323803	6836.357	1508.439	10886400	17999970	10886870
2.1605E+11	0.7323927	6846.22	1508.535	10886400	17998840	10886880
2.16362E+11	0.7324073	6856.083	1508.647	10886400	17997490	10886870
2.16673E+11	0.7324212	6865.946	1508.754	10886400	17996220	10886880
2.16984E+11	0.732435	6875.81	1508.86	10886400	17994950	10886870
2.17295E+11	0.7324485	6885.672	1508.964	10886400	17993710	10886870
2.17607E+11	0.7324621	6895.535	1509.069	10886400	17992460	10886870
2.17918E+11	0.7324757	6905.398	1509.174	10886400	17991210	10886880
2.18229E+11	0.7324893	6915.261	1509.278	10886400	17989970	10886880
2.1854E+11	0.7325033	6925.125	1509.386	10886400	17988680	10886870
2.18852E+11	0.7325158	6934.987	1509.483	10886400	17987530	10886880
2.19163E+11	0.7325293	6944.851	1509.586	10886400	17986300	10886880
2.19474E+11	0.7325429	6954.713	1509.691	10886400	17985040	10886870
2.19785E+11	0.732555	6964.577	1509.784	10886400	17983930	10886870
2.20097E+11	0.7325676	6974.439	1509.882	10886400	17982770	10886870
2.20408E+11	0.7325816	6984.303	1509.99	10886400	17981490	10886880
2.20719E+11	0.7325951	6994.166	1510.094	10886400	17980240	10886870
2.2103E+11	0.7326087	7004.028	1510.198	10886400	17979000	10886870
2.21342E+11	0.7326223	7013.892	1510.303	10886400	17977760	10886870
2.21653E+11	0.7326356	7023.754	1510.406	10886400	17976540	10886880
2.21964E+11	0.7326499	7033.618	1510.516	10886400	17975220	10886870
2.22275E+11	0.7326635	7043.48	1510.621	10886400	17973980	10886880
2.22587E+11	0.732675	7053.344	1510.71	10886400	17972920	10886880
2.22898E+11	0.7326853	7063.207	1510.789	10886400	17971980	10886880
2.23209E+11	0.7326959	7073.07	1510.871	10886400	17971000	10886870
2.2352E+11	0.7327095	7082.933	1510.976	10886400	17969750	10886870
2.23832E+11	0.7327218	7092.796	1511.071	10886400	17968620	10886870
2.24143E+11	0.7327358	7102.659	1511.179	10886400	17967340	10886880
2.24454E+11	0.7327491	7112.521	1511.281	10886400	17966120	10886870
2.24765E+11	0.7327621	7122.385	1511.382	10886400	17964920	10886870
2.25077E+11	0.7327756	7132.248	1511.486	10886400	17963690	10886880
2.25388E+11	0.7327888	7142.111	1511.588	10886400	17962480	10886880
2.25699E+11	0.732802	7151.974	1511.689	10886400	17961260	10886860
2.2601E+11	0.7328144	7161.837	1511.785	10886400	17960130	10886870
2.26322E+11	0.732828	7171.7	1511.891	10886400	17958880	10886880
2.26633E+11	0.7328415	7181.563	1511.995	10886400	17957640	10886870
2.26944E+11	0.7328545	7191.426	1512.095	10886400	17956450	10886870
2.27255E+11	0.732868	7201.289	1512.199	10886400	17955220	10886880
2.27567E+11	0.7328808	7211.152	1512.298	10886400	17954030	10886870
2.27878E+11	0.7328942	7221.015	1512.402	10886400	17952810	10886880
2.28189E+11	0.7329074	7230.878	1512.504	10886400	17951600	10886880
2.285E+11	0.7329211	7240.741	1512.61	10886400	17950340	10886870
2.28812E+11	0.7329339	7250.604	1512.708	10886400	17949170	10886870
2.29123E+11	0.7329468	7260.467	1512.808	10886400	17947990	10886870
2.29434E+11	0.7329597	7270.33	1512.908	10886400	17946810	10886880
2.29745E+11	0.7329725	7280.193	1513.007	10886400	17945630	10886870

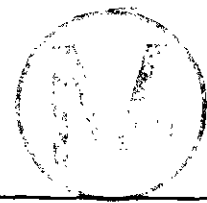




2.30057E+11	0.7329865	7290.056	1513.115	10886400	17944350	10886870
2.30368E+11	0.7329984	7299.919	1513.207	10886400	17943250	10886870
2.30679E+11	0.7330111	7309.782	1513.306	10886400	17942090	10886880
2.3099E+11	0.7330248	7319.645	1513.411	10886400	17940830	10886870
2.31302E+11	0.7330384	7329.508	1513.517	10886400	17939590	10886880
2.31613E+11	0.7330521	7339.371	1513.622	10886400	17938340	10886880
2.31924E+11	0.7330653	7349.234	1513.724	10886400	17937120	10886870
2.32236E+11	0.7330781	7359.097	1513.824	10886400	17935940	10886870
2.32547E+11	0.7330912	7368.96	1513.925	10886400	17934750	10886880
2.32858E+11	0.7331045	7378.823	1514.028	10886400	17933530	10886880
2.33169E+11	0.7331179	7388.686	1514.131	10886400	17932310	10886880
2.3348E+11	0.7331319	7398.549	1514.24	10886400	17931020	10886880
2.33792E+11	0.7331452	7408.412	1514.343	10886400	17929800	10886880
2.34103E+11	0.7331593	7418.275	1514.452	10886400	17928510	10886880
2.34414E+11	0.7331715	7428.138	1514.547	10886400	17927380	10886870
2.34726E+11	0.7331846	7438.001	1514.648	10886400	17926190	10886880
2.35037E+11	0.7331987	7447.864	1514.757	10886400	17924890	10886870
2.35348E+11	0.7332116	7457.727	1514.857	10886400	17923710	10886870
2.35659E+11	0.7332242	7467.59	1514.954	10886400	17922560	10886870
2.35971E+11	0.7332379	7477.453	1515.061	10886400	17921310	10886880
2.36282E+11	0.7332512	7487.316	1515.164	10886400	17920090	10886880
2.36593E+11	0.7332646	7497.179	1515.268	10886400	17918860	10886880
2.36904E+11	0.7332778	7507.042	1515.37	10886400	17917650	10886880
2.37216E+11	0.733292	7516.905	1515.479	10886400	17916350	10886870
2.37527E+11	0.7333052	7526.768	1515.582	10886400	17915140	10886870
2.37838E+11	0.7333191	7536.631	1515.69	10886400	17913860	10886870
2.38149E+11	0.7333335	7546.494	1515.802	10886400	17912540	10886870
2.38461E+11	0.7333479	7556.357	1515.913	10886400	17911230	10886880
2.38772E+11	0.7333612	7566.22	1516.016	10886400	17910010	10886870
2.39083E+11	0.7333735	7576.083	1516.112	10886400	17908880	10886880
2.39394E+11	0.7333877	7585.946	1516.222	10886400	17907580	10886880
2.39706E+11	0.7334016	7595.81	1516.329	10886400	17906310	10886870
2.40017E+11	0.7334158	7605.672	1516.439	10886400	17905010	10886870
2.40328E+11	0.7334293	7615.535	1516.544	10886400	17903780	10886880
2.40639E+11	0.7334438	7625.398	1516.657	10886400	17902440	10886870
2.40951E+11	0.7334567	7635.261	1516.756	10886400	17901260	10886870
2.41262E+11	0.733468	7645.125	1516.844	10886400	17900230	10886870
2.41573E+11	0.7334804	7654.987	1516.941	10886400	17899100	10886880
2.41884E+11	0.7334913	7664.851	1517.025	10886400	17898100	10886880
2.42196E+11	0.7335019	7674.713	1517.108	10886400	17897130	10886880
2.42507E+11	0.7335134	7684.577	1517.197	10886400	17896070	10886870
2.42818E+11	0.7335271	7694.439	1517.303	10886400	17894820	10886870
2.43129E+11	0.7335398	7704.303	1517.402	10886400	17893660	10886880
2.43441E+11	0.7335524	7714.166	1517.499	10886400	17892500	10886870
2.43752E+11	0.7335631	7724.028	1517.583	10886400	17891520	10886880
2.44063E+11	0.7335753	7733.892	1517.677	10886400	17890400	10886870
2.44374E+11	0.733589	7743.754	1517.784	10886400	17889150	10886880
2.44686E+11	0.7336028	7753.618	1517.891	10886400	17887880	10886870
2.44997E+11	0.7336159	7763.48	-1517.992	10886400	17886680	10886860
2.45308E+11	0.7336293	7773.344	1518.097	10886400	17885460	10886870
2.45619E+11	0.7336417	7783.207	1518.193	10886400	17884330	10886870
2.45931E+11	0.7336552	7793.07	1518.298	10886400	17883100	10886880

2.46242E+11	0.7336688	7802.933	1518.404	10886400	17881850	10886880
2.46553E+11	0.7336813	7812.796	1518.501	10886400	17880700	10886870
2.46864E+11	0.733694	7822.659	1518.599	10886400	17879540	10886870
2.47176E+11	0.7337062	7832.521	1518.694	10886400	17878430	10886870
2.47487E+11	0.7337196	7842.385	1518.798	10886400	17877200	10886870
2.47798E+11	0.7337324	7852.248	1518.898	10886400	17876030	10886880
2.48109E+11	0.7337452	7862.111	1518.998	10886400	17874860	10886880
2.48421E+11	0.7337561	7871.974	1519.082	10886400	17873860	10886870
2.48732E+11	0.7337686	7881.837	1519.179	10886400	17872720	10886870
2.49043E+11	0.7337823	7891.7	1519.286	10886400	17871460	10886870
2.49354E+11	0.7337949	7901.563	1519.384	10886400	17870310	10886870
2.49666E+11	0.7338079	7911.426	1519.485	10886400	17869120	10886870
2.49977E+11	0.7338214	7921.289	1519.59	10886400	17867880	10886870
2.50288E+11	0.7338344	7931.152	1519.691	10886400	17866690	10886870
2.50599E+11	0.7338473	7941.015	1519.792	10886400	17865510	10886870
2.50911E+11	0.7338599	7950.878	1519.89	10886400	17864370	10886880
2.51222E+11	0.7338732	7960.741	1519.993	10886400	17863150	10886870
2.51533E+11	0.7338864	7970.604	1520.096	10886400	17861940	10886870
2.51844E+11	0.7338975	7980.467	1520.182	10886400	17860920	10886870
2.52156E+11	0.7339101	7990.33	1520.28	10886400	17859770	10886870
2.52467E+11	0.7339236	8000.193	1520.386	10886400	17858540	10886880
2.52778E+11	0.7339359	8010.056	1520.481	10886400	17857420	10886880
2.53089E+11	0.7339491	8019.919	1520.584	10886400	17856210	10886880
2.53401E+11	0.7339624	8029.782	1520.688	10886400	17855000	10886880
2.53712E+11	0.733975	8039.645	1520.786	10886400	17853840	10886880
2.54023E+11	0.733987	8049.508	1520.879	10886400	17852740	10886870
2.54334E+11	0.7340001	8059.371	1520.981	10886400	17851540	10886870
2.54646E+11	0.7340136	8069.234	1521.087	10886400	17850310	10886880
2.54957E+11	0.7340271	8079.097	1521.192	10886400	17849080	10886880
2.55268E+11	0.7340398	8088.96	1521.29	10886400	17847910	10886870
2.55579E+11	0.7340528	8098.823	1521.392	10886400	17846730	10886880
2.55891E+11	0.7340657	8108.686	1521.492	10886400	17845550	10886870
2.56202E+11	0.7340791	8118.549	1521.597	10886400	17844320	10886870
2.56513E+11	0.7340918	8128.412	1521.696	10886400	17843160	10886880
2.56824E+11	0.7341055	8138.275	1521.803	10886400	17841910	10886880
2.57136E+11	0.7341183	8148.138	1521.902	10886400	17840740	10886870
2.57447E+11	0.7341316	8158.001	1522.006	10886400	17839520	10886870
2.57758E+11	0.7341427	8167.864	1522.093	10886400	17838510	10886880
2.58069E+11	0.7341533	8177.727	1522.175	10886400	17837540	10886870
2.58381E+11	0.7341645	8187.59	1522.263	10886400	17836520	10886880
2.58692E+11	0.7341771	8197.453	1522.361	10886400	17835360	10886870
2.59003E+11	0.7341884	8207.316	1522.449	10886400	17834330	10886870
2.59315E+11	0.734199	8217.18	1522.532	10886400	17833360	10886870
2.59626E+11	0.7342108	8227.042	1522.624	10886400	17832280	10886870
2.59937E+11	0.7342234	8236.905	1522.722	10886400	17831130	10886870
2.60248E+11	0.7342366	8246.769	1522.825	10886400	17829930	10886870
2.6056E+11	0.7342492	8256.631	1522.923	10886400	17828780	10886870
2.60871E+11	0.7342615	8266.494	1523.02	10886400	17827650	10886880
2.61182E+11	0.7342729	8276.357	1523.109	10886400	17826610	10886880
2.61493E+11	0.7342836	8286.221	1523.192	10886400	17825630	10886870
2.61805E+11	0.7342967	8296.083	1523.294	10886400	17824440	10886870
2.62116E+11	0.73431	8305.946	1523.398	10886400	17823220	10886870





2.62427E+11	0.7343221	8315.81	1523.492	10886400	17822120	10886870
2.62738E+11	0.7343349	8325.673	1523.593	10886400	17820950	10886880
2.6305E+11	0.734348	8335.535	1523.695	10886400	17819750	10886870
2.63361E+11	0.7343606	8345.398	1523.793	10886400	17818590	10886870
2.63672E+11	0.7343739	8355.262	1523.897	10886400	17817380	10886870
2.63983E+11	0.7343866	8365.124	1523.997	10886400	17816220	10886870
2.64295E+11	0.7343984	8374.987	1524.089	10886400	17815140	10886870
2.64606E+11	0.7344115	8384.851	1524.191	10886400	17813950	10886870
2.64917E+11	0.7344242	8394.714	1524.29	10886400	17812780	10886870
2.65228E+11	0.7344369	8404.576	1524.39	10886400	17811630	10886880
2.6554E+11	0.7344499	8414.439	1524.491	10886400	17810440	10886870
2.65851E+11	0.7344621	8424.303	1524.586	10886400	17809320	10886870
2.66162E+11	0.7344758	8434.165	1524.694	10886400	17808080	10886880
2.66473E+11	0.7344888	8444.028	1524.795	10886400	17806890	10886870
2.66785E+11	0.7345015	8453.892	1524.894	10886400	17805730	10886870
2.67096E+11	0.7345142	8463.755	1524.994	10886400	17804570	10886870
2.67407E+11	0.7345269	8473.617	1525.093	10886400	17803410	10886870
2.67718E+11	0.7345384	8483.48	1525.183	10886400	17802360	10886870
2.6803E+11	0.73455	8493.344	1525.274	10886400	17801300	10886870
2.68341E+11	0.7345632	8503.207	1525.377	10886400	17800100	10886870
2.68652E+11	0.7345753	8513.069	1525.472	10886400	17798990	10886870
2.68963E+11	0.7345887	8522.933	1525.577	10886400	17797770	10886880
2.69275E+11	0.7346002	8532.796	1525.667	10886400	17796720	10886880
2.69586E+11	0.7346133	8542.659	1525.769	10886400	17795520	10886870
2.69897E+11	0.7346264	8552.521	1525.872	10886400	17794320	10886870
2.70208E+11	0.7346383	8562.385	1525.965	10886400	17793240	10886870
2.7052E+11	0.7346512	8572.248	1526.066	10886400	17792060	10886870
2.70831E+11	0.7346642	8582.11	1526.168	10886400	17790880	10886880
2.71142E+11	0.7346761	8591.974	1526.261	10886400	17789800	10886880
2.71453E+11	0.7346877	8601.837	1526.352	10886400	17788740	10886880
2.71765E+11	0.7347001	8611.7	1526.449	10886400	17787600	10886870
2.72076E+11	0.7347124	8621.563	1526.545	10886400	17786480	10886870
2.72387E+11	0.7347258	8631.426	1526.65	10886400	17785260	10886880
2.72698E+11	0.7347383	8641.289	1526.748	10886400	17784110	10886870
2.7301E+11	0.7347505	8651.151	1526.844	10886400	17783000	10886880
2.73321E+11	0.7347636	8661.015	1526.946	10886400	17781810	10886870
2.73632E+11	0.7347758	8670.878	1527.042	10886400	17780690	10886870
2.73943E+11	0.7347881	8680.741	1527.138	10886400	17779570	10886870
2.74255E+11	0.7348013	8690.604	1527.241	10886400	17778370	10886870
2.74566E+11	0.7348135	8700.467	1527.337	10886400	17777260	10886880
2.74877E+11	0.7348258	8710.33	1527.433	10886400	17776120	10886860
2.75188E+11	0.7348379	8720.193	1527.528	10886400	17775020	10886860
2.755E+11	0.7348499	8730.056	1527.622	10886400	17773930	10886870
2.75811E+11	0.7348621	8739.919	1527.718	10886400	17772820	10886870
2.76122E+11	0.7348753	8749.782	1527.822	10886400	17771610	10886870
2.76433E+11	0.734888	8759.645	1527.921	10886400	17770460	10886870
2.76745E+11	0.7349006	8769.508	1528.02	10886400	17769310	10886870
2.77056E+11	0.7349125	8779.371	1528.114	10886400	17768230	10886880
2.77367E+11	0.7349248	8789.234	1528.21	10886400	17767100	10886870
2.77678E+11	0.7349372	8799.097	1528.307	10886400	17765970	10886870
2.7799E+11	0.7349506	8808.96	1528.412	10886400	17764750	10886870
2.78301E+11	0.7349635	8818.823	1528.513	10886400	17763570	10886870

2.78612E+11	0.7349762	8828.687	1528.613	10886400	17762410	10886870
2.78923E+11	0.7349888	8838.549	1528.712	10886400	17761260	10886870
2.79235E+11	0.7350014	8848.412	1528.811	10886400	17760110	10886870
2.79546E+11	0.7350131	8858.275	1528.903	10886400	17759050	10886870
2.79857E+11	0.7350265	8868.138	1529.008	10886400	17757830	10886880
2.80168E+11	0.735038	8878.001	1529.098	10886400	17756780	10886870
2.8048E+11	0.7350492	8887.864	1529.186	10886400	17755760	10886870
2.80791E+11	0.7350611	8897.728	1529.28	10886400	17754670	10886870
2.81102E+11	0.7350737	8907.59	1529.379	10886400	17753520	10886870
2.81413E+11	0.735085	8917.453	1529.467	10886400	17752490	10886870
2.81725E+11	0.7350963	8927.316	1529.556	10886400	17751470	10886880
2.82036E+11	0.7351067	8937.18	1529.638	10886400	17750510	10886870
2.82347E+11	0.7351179	8947.042	1529.726	10886400	17749500	10886880
2.82658E+11	0.7351298	8956.905	1529.819	10886400	17748410	10886870
2.8297E+11	0.7351418	8966.769	1529.914	10886400	17747320	10886880
2.83281E+11	0.7351547	8976.631	1530.015	10886400	17746140	10886870
2.83592E+11	0.735167	8986.494	1530.112	10886400	17745020	10886880
2.83904E+11	0.7351796	8996.357	1530.211	10886400	17743870	10886880
2.84215E+11	0.735192	9006.221	1530.308	10886400	17742740	10886870
2.84526E+11	0.7352045	9016.083	1530.406	10886400	17741600	10886870
2.84837E+11	0.7352174	9025.946	1530.508	10886400	17740430	10886880
2.85149E+11	0.7352298	9035.81	1530.605	10886400	17739300	10886870
2.8546E+11	0.7352427	9045.673	1530.707	10886400	17738120	10886880
2.85771E+11	0.7352548	9055.535	1530.802	10886400	17737020	10886880
2.86082E+11	0.7352675	9065.398	1530.902	10886400	17735860	10886870
2.86394E+11	0.7352799	9075.262	1530.999	10886400	17734730	10886870
2.86705E+11	0.7352923	9085.124	1531.097	10886400	17733600	10886870
2.87016E+11	0.7353051	9094.987	1531.197	10886400	17732440	10886870
2.87327E+11	0.7353178	9104.851	1531.298	10886400	17731280	10886880
2.87639E+11	0.7353301	9114.714	1531.394	10886400	17730160	10886870
2.8795E+11	0.7353421	9124.576	1531.489	10886400	17729060	10886870
2.88261E+11	0.7353547	9134.439	1531.588	10886400	17727920	10886880
2.88572E+11	0.7353672	9144.303	1531.686	10886400	17726780	10886870
2.88884E+11	0.7353793	9154.165	1531.781	10886400	17725680	10886870
2.89195E+11	0.7353919	9164.028	1531.881	10886400	17724530	10886880
2.89506E+11	0.7354041	9173.892	1531.976	10886400	17723420	10886870
2.89817E+11	0.735416	9183.755	1532.07	10886400	17722340	10886870
2.90129E+11	0.7354284	9193.617	1532.168	10886400	17721210	10886880
2.9044E+11	0.7354403	9203.48	1532.262	10886400	17720120	10886880
2.90751E+11	0.7354528	9213.344	1532.36	10886400	17718980	10886870
2.91062E+11	0.7354647	9223.207	1532.454	10886400	17717900	10886880
2.91374E+11	0.7354775	9233.069	1532.555	10886400	17716730	10886870
2.91685E+11	0.7354898	9242.933	1532.651	10886400	17715610	10886870
2.91996E+11	0.7355018	9252.796	1532.746	10886400	17714520	10886870
2.92307E+11	0.7355146	9262.659	1532.847	10886400	17713350	10886870
2.92619E+11	0.735527	9272.521	1532.945	10886400	17712230	10886880
2.9293E+11	0.735539	9282.385	1533.039	10886400	17711130	10886870
2.93241E+11	0.7355511	9292.248	1533.135	10886400	17710030	10886880
2.93552E+11	0.735563	9302.11	1533.228	10886400	17708940	10886870
2.93864E+11	0.7355754	9311.974	1533.326	10886400	17707810	10886870
2.94175E+11	0.7355877	9321.837	1533.423	10886400	17706700	10886870
2.94486E+11	0.7356001	9331.7	1533.521	10886400	17705570	10886870



2.94797E+11	0.7356118	9341.563	1533.613	10886400	17704510	10886880
2.95109E+11	0.7356237	9351.426	1533.707	10886400	17703420	10886870
2.9542E+11	0.7356362	9361.289	1533.805	10886400	17702280	10886870
2.95731E+11	0.7356485	9371.151	1533.903	10886400	17701160	10886870
2.96042E+11	0.7356609	9381.015	1534	10886400	17700040	10886870
2.96354E+11	0.7356727	9390.878	1534.094	10886400	17698960	10886880
2.96665E+11	0.7356846	9400.741	1534.187	10886400	17697870	10886870
2.96976E+11	0.7356971	9410.604	1534.286	10886400	17696740	10886870
2.97287E+11	0.735709	9420.467	1534.38	10886400	17695650	10886870
2.97599E+11	0.7357213	9430.33	1534.477	10886400	17694540	10886880
2.9791E+11	0.7357333	9440.193	1534.571	10886400	17693440	10886870
2.98221E+11	0.7357453	9450.056	1534.667	10886400	17692360	10886880
2.98532E+11	0.7357573	9459.919	1534.761	10886400	17691260	10886870
2.98844E+11	0.7357692	9469.782	1534.855	10886400	17690190	10886880
2.99155E+11	0.7357817	9479.645	1534.954	10886400	17689050	10886880
2.99466E+11	0.7357938	9489.508	1535.05	10886400	17687940	10886880
2.99777E+11	0.7358055	9499.371	1535.142	10886400	17686880	10886880
3.00089E+11	0.7358177	9509.234	1535.238	10886400	17685770	10886880
3.004E+11	0.7358297	9519.097	1535.333	10886400	17684680	10886880
3.00711E+11	0.7358415	9528.96	1535.426	10886400	17683600	10886870
3.01022E+11	0.7358533	9538.823	1535.519	10886400	17682530	10886870
3.01334E+11	0.7358657	9548.687	1535.617	10886400	17681400	10886870
3.01645E+11	0.7358778	9558.549	1535.713	10886400	17680300	10886880
3.01956E+11	0.7358893	9568.412	1535.804	10886400	17679260	10886880
3.02267E+11	0.7359008	9578.275	1535.895	10886400	17678200	10886870
3.02579E+11	0.7359126	9588.138	1535.988	10886400	17677130	10886870
3.0289E+11	0.7359241	9598.001	1536.079	10886400	17676080	10886870
3.03201E+11	0.7359354	9607.864	1536.168	10886400	17675050	10886870
3.03512E+11	0.735947	9617.728	1536.26	10886400	17674010	10886880
3.03824E+11	0.7359596	9627.59	1536.359	10886400	17672860	10886870
3.04135E+11	0.7359716	9637.453	1536.454	10886400	17671770	10886870
3.04446E+11	0.7359837	9647.316	1536.55	10886400	17670670	10886880
3.04757E+11	0.7359958	9657.18	1536.646	10886400	17669570	10886880
3.05069E+11	0.7360078	9667.042	1536.741	10886400	17668470	10886870
3.0538E+11	0.7360198	9676.905	1536.835	10886400	17667380	10886870
3.05691E+11	0.7360321	9686.769	1536.933	10886400	17666270	10886880
3.06002E+11	0.736044	9696.631	1537.027	10886400	17665180	10886870
3.06314E+11	0.7360559	9706.494	1537.121	10886400	17664100	10886870
3.06625E+11	0.7360681	9716.357	1537.218	10886400	17663000	10886880
3.06936E+11	0.7360799	9726.221	1537.311	10886400	17661920	10886870
3.07247E+11	0.7360918	9736.083	1537.405	10886400	17660840	10886870
3.07559E+11	0.7361038	9745.946	1537.5	10886400	17659740	10886870
3.0787E+11	0.7361153	9755.81	1537.591	10886400	17658700	10886870
3.08181E+11	0.7361271	9765.673	1537.684	10886400	17657630	10886870
3.08492E+11	0.7361392	9775.535	1537.78	10886400	17656520	10886870
3.08804E+11	0.736151	9785.398	1537.874	10886400	17655460	10886880
3.09115E+11	0.7361633	9795.262	1537.971	10886400	17654340	10886870
3.09426E+11	0.7361753	9805.124	1538.066	10886400	17653250	10886870
3.09738E+11	0.7361873	9814.987	1538.161	10886400	17652160	10886870
3.10049E+11	0.7361993	9824.851	1538.256	10886400	17651060	10886870
3.1036E+11	0.7362114	9834.714	1538.352	10886400	17649970	10886880
3.10671E+11	0.7362231	9844.576	1538.445	10886400	17648900	10886870



3.10982E+11	0.7362354	9854.439	1538.542	10886400	17647790	10886880
3.11294E+11	0.7362474	9864.303	1538.637	10886400	17646690	10886870
3.11605E+11	0.7362593	9874.165	1538.731	10886400	17645610	10886870
3.11916E+11	0.7362713	9884.028	1538.827	10886400	17644520	10886870
3.12228E+11	0.7362831	9893.892	1538.92	10886400	17643450	10886870
3.12539E+11	0.7362951	9903.755	1539.015	10886400	17642360	10886870
3.1285E+11	0.7363071	9913.617	1539.11	10886400	17641270	10886870
3.13161E+11	0.7363189	9923.48	1539.204	10886400	17640200	10886880
3.13473E+11	0.7363309	9933.344	1539.299	10886400	17639100	10886870
3.13784E+11	0.7363428	9943.207	1539.393	10886400	17638020	10886870
3.14095E+11	0.7363548	9953.069	1539.489	10886400	17636930	10886870
3.14406E+11	0.7363669	9962.933	1539.585	10886400	17635840	10886880
3.14718E+11	0.7363788	9972.796	1539.679	10886400	17634760	10886880
3.15029E+11	0.7363908	9982.659	1539.774	10886400	17633660	10886870
3.1534E+11	0.7364028	9992.521	1539.869	10886400	17632580	10886870
3.15576E+11	0.7364118	10000	1539.941	10886400	17631760	10886880



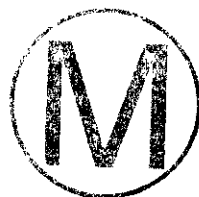


# Written	BLOT 1 :5	1:04		
# Created	SANTOS :4	8:53		
# Modified	ALGEBRA :2	9:15		
@ with g0				
@ legend on				
@ legend e view				
@ legend ize 0.75				
@ title "DI	AL ROOM -	FINAL = F = 1.0 - WASTE W/O BACKFILL"		
@ subtitle	E vs PGAS"			
@ s0	color 1			
@ xaxis la	TIME"			
@ yaxis la	PGAS"			
@ legend	0 "PGAS"			
@ s0	comment "PGAS"			
0.00E+00	0.00E+00			
1.34E-11	1.48E-07			
9.40E-09	1.04E-04			
7.40E-07	8.16E-03			
4.03E-06	4.45E-02			
1.01E-05	1.12E-01			
2.05E-05	2.28E-01			
3.57E-05	3.97E-01			
5.43E-05	6.05E-01			
7.33E-05	8.18E-01			
9.75E-05	1.09E+00			
1.49E-04	1.67E+00			
2.49E-04	2.80E+00			
3.96E-04	4.47E+00			
5.92E-04	6.69E+00			
9.40E-04	1.07E+01			
1.62E-03	1.84E+01			
2.87E-03	3.28E+01			
4.51E-03	5.18E+01			
6.60E-03	7.60E+01			
1.13E-02	1.31E+02			
2.24E-02	2.61E+02			
3.69E-02	4.32E+02			
5.46E-02	6.42E+02			
7.31E-02	8.62E+02			
9.18E-02	1.09E+03			
1.15E-01	1.36E+03			
1.40E-01	1.66E+03			
1.66E-01	1.98E+03			
2.00E-01	2.40E+03			
2.44E-01	2.92E+03			
3.06E-01	3.69E+03			
3.79E-01	4.58E+03			
4.73E-01	5.75E+03			





9519.097	17684680				
9528.9601	17683603				
9538.8231	17682527				
9548.6861	17681401				
9558.5491	17680299				
9568.4121	17679256				
9578.2751	17678204				
9588.1381	17677132				
9598.0011	17676083				
9607.8642	17675054				
9617.7272	17674008				
9627.5902	17672857				
9637.4532	17671767				
9647.3162	17670666				
9657.1792	17669567				
9667.0422	17668472				
9676.9053	17667379				
9686.7683	17666271				
9696.6313	17665184				
9706.4943	17664099				
9716.3573	17662995				
9726.2203	17661916				
9736.0833	17660837				
9745.9464	17659742				
9755.8094	17658704				
9765.6724	17657626				
9775.5354	17656524				
9785.3984	17655458				
9795.2614	17654340				
9805.1244	17653246				
9814.9874	17652161				
9824.8505	17651065				
9834.7135	17649967				
9844.5765	17648903				
9854.4395	17647789				
9864.3025	17646691				
9874.1655	17645610				
9884.0285	17644520				
9893.8916	17643452				
9903.7546	17642362				
9913.6176	17641274				
9923.4806	17640202				
9933.3436	17639103				
9943.2066	17638021				
9953.0696	17636934				
9962.9327	17635841				
9972.7957	17634758				
9982.6587	17633662				
9992.5217	17632578				
10000	17631756				
@ world xmax	0				





	9519.097	0.73582964			
	9528.9601	0.73584148			
	9538.8231	0.73585331			
	9548.6861	0.73586569			
	9558.5491	0.7358778			
	9568.4121	0.73588926			
	9578.2751	0.73590083			
	9588.1381	0.73591261			
	9598.0011	0.73592415			
	9607.8642	0.73593546			
	9617.7272	0.73594697			
	9627.5902	0.73595961			
	9637.4532	0.7359716			
	9647.3162	0.73598371			
	9657.1792	0.73599579			
	9667.0422	0.73600783			
	9676.9053	0.73601986			
	9686.7683	0.73603204			
	9696.6313	0.73604399			
	9706.4943	0.73605593			
	9716.3573	0.73606807			
	9726.2203	0.73607994			
	9736.0833	0.73609181			
	9745.9464	0.73610385			
	9755.8094	0.73611527			
	9765.6724	0.73612713			
	9775.5354	0.73613925			
	9785.3984	0.73615098			
	9795.2614	0.73616328			
	9805.1244	0.73617531			
	9814.9874	0.73618725			
	9824.8505	0.73619931			
	9834.7135	0.73621139			
	9844.5765	0.7362231			
	9854.4395	0.73623536			
	9864.3025	0.73624745			
	9874.1655	0.73625934			
	9884.0285	0.73627133			
	9893.8916	0.73628309			
	9903.7546	0.73629508			
	9913.6176	0.73630706			
	9923.4806	0.73631886			
	9933.3436	0.73633095			
	9943.2066	0.73634286			
	9953.0696	0.73635483			
	9962.9327	0.73636685			
	9972.7957	0.73637878			
	9982.6587	0.73639084			
	9992.5217	0.73640278			
	10000	0.73641182			
@	world	xmax	1.00E+04		



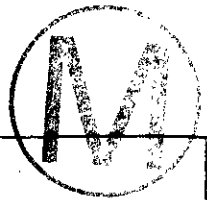
INFORMATION ONLY



Section 11

Final Porosity Surface Data

$$f = 0.05$$



f=0.05							
time	porosity	time	void	gas	pressure		
seconds	x	years	m3/room	mols/rm	Pa		
0	0.8483495	0	3083.473	0	0	0	0
0.000423992	0.8483374	1.34355E-11	3083.183	9.14152E-09	7.40366E-09	9.1527E-09	
0.3078715	0.8483381	9.75586E-09	3083.201	6.63789E-06	5.37595E-06	6.646E-06	
23.45487	0.8482741	7.4324E-07	3081.667	0.000505701	0.000409766	0.00050632	
122.553	0.8480763	3.88347E-06	3076.937	0.002642313	0.002144334	0.002645541	
304.6183	0.8478156	9.65277E-06	3070.721	0.006567745	0.00534076	0.006575775	
595.0943	0.8475312	1.88574E-05	3063.966	0.01283057	0.01045655	0.01284624	
1022.435	0.8472406	0.000032399	3057.089	0.02204428	0.01800593	0.02207126	
1559.201	0.8469802	4.94081E-05	3050.948	0.03361728	0.02751407	0.03365838	
2127.484	0.8467742	6.74159E-05	3046.106	0.04586978	0.03760183	0.04592589	
3231.056	0.8464749	0.000102386	3039.092	0.06966342	0.05723844	0.06974855	
4983.734	0.8461402	0.000157925	3031.282	0.1074522	0.08851484	0.1075836	
8103.518	0.8457437	0.000256785	3022.074	0.1747165	0.1443631	0.1749302	
14770.66	0.8452238	0.000468054	3010.071	0.318464	0.2641866	0.3188534	
26495.98	0.8446895	0.000839607	2997.819	0.5712685	0.4758411	0.5719669	
49493.74	0.8441067	0.001568362	2984.551	1.067114	0.8928094	1.068418	
92708.68	0.8434858	0.002937761	2970.525	1.998852	1.680253	2.001297	
166796.7	0.8428487	0.005285467	2956.248	3.596233	3.037624	3.600629	
240884.6	0.8424361	0.007633173	2947.063	5.19361	4.400553	5.199963	
355424.1	0.8419817	0.01126271	2937.004	7.663148	6.515235	7.672522	
646728.5	0.8412336	0.02049359	2920.568	13.94384	11.92182	13.9609	
998154.3	0.840666	0.0316296	2908.2	21.52078	18.47827	21.54711	
1444850	0.8401344	0.04578453	2896.696	31.1518	26.85391	31.1899	
2087165	0.8395799	0.06613825	2884.778	45.00048	38.9522	45.05552	
2919776	0.8390352	0.0925221	2873.151	62.95205	54.71152	63.02905	
4194413	0.8384041	0.1329129	2859.778	90.43394	78.96356	90.54461	
5512210	0.8378662	0.1746714	2848.461	118.8464	104.1845	118.9918	
6850354	0.8373946	0.2170746	2838.601	147.6975	129.9261	147.8783	
8304781	0.8369398	0.2631626	2829.147	179.0558	158.0376	179.2749	
9811738	0.836505	0.3109152	2820.157	211.5467	187.3098	211.8055	
12102360	0.8359287	0.3835007	2808.315	260.9337	232.0128	261.253	
15560210	0.8351367	0.4930733	2792.176	335.487	300.0272	335.8976	
19394220	0.8343575	0.6145657	2776.448	418.1505	376.0714	418.6619	
23385350	0.8335969	0.7410371	2761.238	504.2015	455.9609	504.8182	
29893600	0.8324711	0.947271	2738.978	644.5233	587.5937	645.3112	
34271500	0.8072757	7.423616	2308.844	5051.027	5462.763	5057.205	
493648900	0.7775997	15.64279	1927.214	10643.35	13790.37	10656.37	
753026600	0.7457311	23.86197	1616.584	16235.68	25078.39	16255.54	
1012404000	0.7182841	32.08115	1405.381	21828.02	38783.54	21854.71	
1271782000	0.6971559	40.30033	1268.878	27420.35	53961.02	27453.87	
1531159000	0.6779416	48.5195	1160.291	33012.68	71046.23	33053.05	
1790537000	0.6607512	56.73869	1073.566	38605	89792.91	38652.21	
2049914000	0.6452529	64.95786	1002.583	44197.32	110078.6	44251.38	
2309292000	0.6307496	73.17704	941.5539	49789.65	132044.8	49850.56	
2568669000	0.6172917	81.39622	889.0614	55382	155547.8	55449.7	
2828047000	0.6053513	89.61539	845.4853	60974.3	180081.2	61048.92	
3087424000	0.5943223	97.83457	807.5142	66566.65	205841.9	66648.06	
3466116000	0.5795724	109.8346	759.8461	74731.48	245586.8	74822.84	
3777369000	0.568379	119.6976	725.8463	81442.25	280176.9	81541.85	

4088621000	0.5578557	129.5606	695.4519	88153.02	316517.4	88260.88
4399874000	0.5480298	139.4236	668.3494	94863.83	354425.1	94979.88
4711127000	0.5387371	149.2866	643.7802	101574.6	393980.8	101698.9
5022380000	0.5301546	159.1496	621.9518	108285.4	434750.8	108417.8
5333635000	0.522201	169.0127	602.4232	114996.3	476660.5	115136.9
5644888000	0.514859	178.8757	584.9646	121707	519533.2	121855.9
5956140000	0.5080373	188.7387	569.2102	128417.8	563352.3	128574.9
6267393000	0.5016382	198.6017	554.8237	135128.6	608162.2	135293.8
6578646000	0.4957653	208.4647	541.9418	141839.4	653539.2	142012.9
6889898000	0.4904456	218.3277	530.5295	148550.2	699183.2	148731.9
7201151000	0.4854691	228.1907	520.0671	155261	745470.3	155450.9
7512407000	0.4808434	238.0538	510.522	161971.8	792231.7	162169.9
7823659000	0.4765531	247.9168	501.8199	168682.6	839362.6	168888.9
8134911000	0.4725541	257.7798	493.8361	175393.4	886865.3	175607.9
8446164000	0.468761	267.6428	486.3744	182104.2	934924.4	182326.9
8757417000	0.4652254	277.5058	479.5146	188815	983245.3	189045.9
9068670000	0.4619312	287.3688	473.2043	195525.8	1031769	195764.9
9379923000	0.4588327	297.2318	467.339	202236.5	1080575	202483.9
9691175000	0.4559083	307.0948	461.8645	208947.3	1129665	209203
10002430000	0.453173	316.9579	456.7971	215658.2	1178881	215922
10313680000	0.4505996	326.8209	452.0756	222368.9	1228260	222640.9
10624940000	0.4481796	336.6839	447.6757	229079.7	1277763	229359.8
10936190000	0.4459159	346.5469	443.5948	235790.5	1327294	236078.9
11247440000	0.443771	356.4099	439.7588	242501.3	1376978	242798
11558690000	0.4417841	366.2729	436.2316	249212.1	1426525	249517
11869950000	0.4398825	376.1359	432.8792	255923	1476284	256236
12181200000	0.4380837	385.999	429.729	262633.8	1526100	262954.9
12492450000	0.4364117	395.862	426.8189	269344.5	1575766	269673.9
12803710000	0.4348132	405.725	424.0528	276055.3	1625562	276393
13114960000	0.4332954	415.588	421.4408	282766	1675399	283112.1
13426210000	0.431864	425.451	418.9902	289476.8	1725192	289831
13737460000	0.4305224	435.314	416.7047	296187.8	1774868	296550.1
14048720000	0.429254	445.177	414.5536	302898.5	1824499	303268.9
14359970000	0.4280546	455.04	412.5284	309609.3	1874077	309988
14671230000	0.4269254	464.9031	410.6294	316320	1923553	316707.1
14982480000	0.425856	474.7661	408.8379	323031	1972968	323425.8
15293730000	0.4248612	484.6291	407.1773	329741.8	2022169	330144.9
15604980000	0.4239121	494.4921	405.5984	336452.5	2071356	336863.9
15916240000	0.4230223	504.3551	404.1229	343163.3	2120385	343583.1
16227490000	0.4221819	514.2181	402.7334	349874	2169309	350302
16538740000	0.4213875	524.0812	401.4237	356584.8	2218131	357021
16850000000	0.4206397	533.9442	400.1942	363295.8	2266819	363740.1
17161250000	0.4199354	543.8072	399.039	370006.5	2315375	370459.1
17472500000	0.4192626	553.6702	397.9381	375468.5	2353336	375494
17783750000	0.4186074	563.5332	396.8685	378824	2380790	378853.5
18095010000	0.4179685	573.3962	395.8278	382179.5	2408217	382213
18406260000	0.4173439	583.2592	394.8126	385534.8	2435631	385572.5
18717520000	0.4167428	593.1223	393.8376	388890.3	2462935	388932
19028770000	0.416158	602.9852	392.891	392245.5	2490194	392291.4
19340020000	0.4155935	612.8483	391.9791	395601	2517363	395651
19651270000	0.4150462	622.7113	391.0966	398956.5	2544466	399010.4
19962530000	0.4145152	632.5743	390.242	402311.8	2571509	402370





20273780000	0.413999	642.4373	389.4127	405667.3	2598502	405729.6
20585040000	0.4134986	652.3004	388.6102	409022.5	2625427	409088.9
20896280000	0.4130121	662.1633	387.8313	412378	2652304	412448.5
21207540000	0.4125196	672.0264	387.0441	415733.5	2679346	415808
21518790000	0.4120611	681.8893	386.3124	419088.8	2706110	419167.6
21830050000	0.4116129	691.7524	385.5982	422444.3	2732851	422527
22141300000	0.4111827	701.6154	384.9138	425799.5	2759478	425886.6
22452550000	0.4107707	711.4784	384.2593	429155	2785983	429246.2
22763800000	0.4103692	721.3414	383.6223	432510.3	2812449	432605.5
23075060000	0.4099827	731.2045	383.0099	435865.8	2838822	435965.1
23386310000	0.4096067	741.0674	382.4149	439221	2865148	439324.5
23697560000	0.409245	750.9305	381.8433	442576.5	2891379	442683.9
24008820000	0.4088955	760.7935	381.2916	445932	2917537	446043.4
24320070000	0.4085549	770.6565	380.7546	449287.3	2943657	449403
24631320000	0.408227	780.5195	380.2382	452642.8	2969690	452762.4
24942580000	0.4079095	790.3825	379.7388	455998.3	2995660	456122
25253830000	0.4076037	800.2455	379.2582	459353.5	3021548	459481.5
25565080000	0.4073066	810.1085	378.7918	462709	3047388	462841.1
25876340000	0.4070166	819.9716	378.337	466064.3	3073197	466200.5
26187590000	0.4067398	829.8346	377.9033	469419.8	3098896	469560.2
26498840000	0.4064715	839.6976	377.4833	472775	3124539	472919.5
26810090000	0.4062116	849.5606	377.0768	476130.5	3150127	476279
27121350000	0.4059601	859.4236	376.6838	479486	3175657	479638.6
27432600000	0.4057162	869.2866	376.303	482841.3	3201136	482998
27743850000	0.4054797	879.1497	375.934	486196.8	3226565	486357.4
28055100000	0.4052527	889.0126	375.5802	489552	3251914	489717.1
28366360000	0.4050321	898.8757	375.2365	492907.5	3277221	493076.6
28677610000	0.4048184	908.7387	374.9039	496263	3302477	496436.1
28988860000	0.4046129	918.6017	374.5843	499618.3	3327663	499795.6
29300120000	0.4044133	928.4647	374.274	502973.8	3352807	503154.9
29611370000	0.4042206	938.3278	373.9747	506329	3377896	506514.7
29922620000	0.4040349	948.1907	373.6864	509684.5	3402922	509874
30233880000	0.4038543	958.0538	373.4062	513040	3427914	513233.5
30545130000	0.4036802	967.9167	373.1362	516395.3	3452849	516593
30856380000	0.4035111	977.7798	372.8742	519750.8	3477745	519952.4
31167640000	0.403349	987.6428	372.6232	523106	3502575	523312.2
31478890000	0.4031919	997.5058	372.3799	526461.5	3527362	526671.5
31790150000	0.4030402	1007.369	372.1453	529817	3552101	530031.1
32101400000	0.4028934	1017.232	371.9182	533172.3	3576797	533390.5
32412650000	0.4027517	1027.095	371.6992	536527.8	3601446	536750
32723910000	0.4026152	1036.958	371.4883	539883	3626045	540109.6
33035160000	0.4024831	1046.821	371.2844	543238.5	3650603	543469.1
33346410000	0.4023517	1056.684	371.0816	544320	3658476	544343.7
33657660000	0.4022168	1066.547	370.8734	544320	3660530	544343.8
33968920000	0.4020801	1076.41	370.6626	544320	3662611	544343.6
34280170000	0.401943	1086.273	370.4513	544320	3664701	544343.7
34591420000	0.4018048	1096.136	370.2384	544320	3666808	544343.7
34902680000	0.4016658	1105.999	370.0243	544320	3668930	544343.7
35213930000	0.401527	1115.862	369.8106	544320	3671049	544343.6
35525180000	0.4013876	1125.725	369.5962	544320	3673179	544343.6
35836430000	0.4012485	1135.588	369.3823	544320	3675307	544343.8
36147690000	0.4011095	1145.451	369.1685	544320	3677434	544343.5



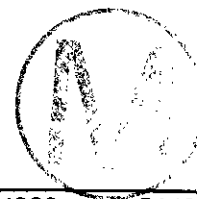
36458930000	0.4009696	1155.314	368.9536	544320	3679577	544343.7
36770190000	0.4008305	1165.177	368.74	544320	3681708	544343.6
37081440000	0.4006913	1175.04	368.5263	544320	3683842	544343.5
37392700000	0.4005525	1184.903	368.3134	544320	3685972	544343.6
37703950000	0.4004138	1194.766	368.1007	544320	3688103	544343.8
38015200000	0.4002752	1204.629	367.8882	544320	3690232	544343.6
38326450000	0.4001372	1214.492	367.6768	544320	3692355	544343.7
38637700000	0.3999988	1224.355	367.4648	544320	3694485	544343.8
38948960000	0.3998617	1234.218	367.2549	544320	3696596	544343.6
39260210000	0.3997246	1244.081	367.0452	544320	3698709	544343.8
39571460000	0.3995879	1253.944	366.8361	544320	3700816	544343.6
39882720000	0.3994511	1263.807	366.627	544320	3702926	544343.5
40193970000	0.3993156	1273.67	366.42	544320	3705019	544343.7
40505220000	0.3991804	1283.533	366.2135	544320	3707109	544343.8
40816470000	0.3990456	1293.396	366.0077	544320	3709193	544343.7
41127730000	0.3989109	1303.259	365.8022	544320	3711278	544343.9
41438980000	0.3987771	1313.122	365.5981	544320	3713348	544343.6
41750230000	0.3986438	1322.985	365.3948	544320	3715415	544343.8
42061480000	0.3985104	1332.848	365.1916	544320	3717483	544343.8
42372740000	0.3983785	1342.711	364.9907	544320	3719528	544343.7
42683990000	0.3982467	1352.574	364.79	544320	3721574	544343.6
42995240000	0.3981152	1362.437	364.5898	544320	3723616	544343.4
43306500000	0.3979853	1372.3	364.3923	544320	3725636	544343.7
43617750000	0.3978555	1382.163	364.1949	544320	3727655	544343.6
43929000000	0.3977267	1392.026	363.9991	544320	3729661	544343.8
44240250000	0.3975981	1401.889	363.8037	544320	3731664	544343.7
44551500000	0.3974699	1411.752	363.6091	544320	3733662	544343.8
44862760000	0.3973429	1421.615	363.4163	544320	3735642	544343.7
45174010000	0.3972161	1431.478	363.2239	544320	3737621	544343.8
45485260000	0.3970902	1441.341	363.0329	544320	3739586	544343.5
45796520000	0.3969654	1451.204	362.8438	544320	3741537	544343.8
46107800000	0.3968407	1461.068	362.6548	544320	3743487	544343.8
46419050000	0.3967165	1470.931	362.4666	544320	3745429	544343.6
46730270000	0.3965932	1480.793	362.2799	544320	3747360	544343.7
47041530000	0.3964708	1490.656	362.0946	544320	3749276	544343.4
47352810000	0.3963487	1500.52	361.91	544320	3751190	544343.7
47664030000	0.3962276	1510.382	361.7268	544320	3753089	544343.6
47975280000	0.3961065	1520.245	361.5437	544320	3754991	544343.8
48286570000	0.3959866	1530.109	361.3625	544320	3756872	544343.5
48597820000	0.3958677	1539.972	361.183	544320	3758741	544343.8
48909070000	0.3957488	1549.835	361.0034	544320	3760610	544343.6
49220330000	0.395631	1559.698	360.8256	544320	3762464	544343.8
49531580000	0.3955136	1569.561	360.6485	544320	3764311	544343.7
49842830000	0.3953965	1579.424	360.4719	544320	3766155	544343.6
50154080000	0.3952807	1589.287	360.2973	544320	3767981	544343.8
50465340000	0.3951651	1599.15	360.123	544320	3769803	544343.5
50776590000	0.3950503	1609.013	359.9501	544320	3771615	544343.7
51087840000	0.3949361	1618.876	359.7782	544320	3773418	544343.8
51399090000	0.3948223	1628.739	359.6069	544320	3775215	544343.8
51710350000	0.3947094	1638.602	359.437	544320	3776999	544343.7
52021600000	0.3945971	1648.465	359.2681	544320	3778775	544343.8
52332850000	0.3944855	1658.328	359.1003	544320	3780541	544343.8



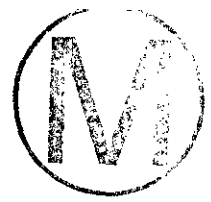
52644110000	0.3943744	1668.191	358.9333	544320	3782300	544343.8
52955360000	0.3942641	1678.054	358.7675	544320	3784047	544343.6
53266610000	0.3941543	1687.917	358.6026	544320	3785787	544343.6
53577860000	0.394045	1697.78	358.4385	544320	3787521	544343.8
53889110000	0.3939363	1707.643	358.2754	544320	3789244	544343.6
54200370000	0.3938283	1717.506	358.1133	544320	3790960	544343.8
54511620000	0.393721	1727.369	357.9524	544320	3792665	544343.8
54822880000	0.3936142	1737.232	357.7923	544320	3794362	544343.8
55134130000	0.3935076	1747.095	357.6325	544320	3796056	544343.6
55445380000	0.3934022	1756.958	357.4745	544320	3797732	544343.4
55756630000	0.393297	1766.821	357.317	544320	3799407	544343.5
56067880000	0.3931923	1776.684	357.1602	544320	3801075	544343.5
56379130000	0.3930886	1786.547	357.0051	544320	3802727	544343.6
56690390000	0.392985	1796.41	356.85	544320	3804381	544343.8
57001640000	0.3928826	1806.273	356.6969	544320	3806013	544343.6
57312890000	0.3927799	1816.136	356.5433	544320	3807652	544343.6
57624150000	0.3926786	1825.999	356.3919	544320	3809269	544343.5
57935400000	0.3925776	1835.862	356.241	544320	3810884	544343.7
58246650000	0.3924772	1845.725	356.0911	544320	3812489	544343.8
58557900000	0.3923771	1855.588	355.9416	544320	3814090	544343.8
58869160000	0.3922776	1865.451	355.7931	544320	3815682	544343.8
59180410000	0.3921788	1875.314	355.6456	544320	3817264	544343.7
59491660000	0.3920804	1885.177	355.4988	544320	3818839	544343.5
59802910000	0.3919824	1895.04	355.3527	544320	3820409	544343.5
60114170000	0.3918854	1904.903	355.2081	544320	3821965	544343.6
60425420000	0.3917887	1914.766	355.064	544320	3823517	544343.7
60736670000	0.3916924	1924.629	354.9205	544320	3825062	544343.6
61047920000	0.3915967	1934.492	354.778	544320	3826599	544343.7
61359180000	0.3915017	1944.355	354.6365	544320	3828125	544343.6
61670430000	0.391407	1954.218	354.4956	544320	3829648	544343.8
61981680000	0.3913129	1964.081	354.3556	544320	3831161	544343.8
62292930000	0.3912191	1973.944	354.2161	544320	3832669	544343.6
62604190000	0.3911264	1983.807	354.0782	544320	3834163	544343.8
62915440000	0.3910337	1993.67	353.9404	544320	3835654	544343.6
63226690000	0.3909419	2003.533	353.804	544320	3837133	544343.6
63537950000	0.3908502	2013.396	353.6677	544320	3838612	544343.6
63849200000	0.3907593	2023.259	353.5327	544320	3840077	544343.6
64160450000	0.3906686	2033.122	353.3981	544320	3841541	544343.8
64471700000	0.3905787	2042.985	353.2646	544320	3842992	544343.6
64782950000	0.3904891	2052.848	353.1317	544320	3844439	544343.8
65094210000	0.3904001	2062.711	352.9996	544320	3845877	544343.6
65405460000	0.3903114	2072.574	352.8681	544320	3847311	544343.8
65716720000	0.3902234	2082.437	352.7376	544320	3848733	544343.6
66027970000	0.3901357	2092.3	352.6076	544320	3850152	544343.6
66339220000	0.3900484	2102.163	352.4783	544320	3851566	544343.8
66650470000	0.3899621	2112.026	352.3504	544320	3852963	544343.6
66961720000	0.3898759	2121.889	352.2227	544320	3854360	544343.6
67272970000	0.3897904	2131.752	352.0962	544320	3855744	544343.6
67584230000	0.389705	2141.615	351.9698	544320	3857130	544343.7
67895510000	0.3896204	2151.479	351.8446	544320	3858503	544343.8
68206740000	0.3895359	2161.341	351.7196	544320	3859874	544343.8
68517990000	0.389452	2171.204	351.5956	544320	3861235	544343.8

68829230000	0.3893687	2181.067	351.4724	544320	3862588	544343.7
69140490000	0.389286	2190.93	351.3502	544320	3863933	544343.9
69451740000	0.3892033	2200.793	351.2279	544320	3865276	544343.6
69763000000	0.3891212	2210.656	351.1067	544320	3866612	544343.8
70074290000	0.3890399	2220.52	350.9866	544320	3867935	544343.8
70385530000	0.3889588	2230.383	350.8669	544320	3869255	544343.9
70696790000	0.3888779	2240.246	350.7474	544320	3870571	544343.5
71008000000	0.3887976	2250.108	350.6289	544320	3871880	544343.6
71319290000	0.3887177	2259.972	350.511	544320	3873182	544343.6
71630540000	0.3886382	2269.835	350.3938	544320	3874478	544343.6
71941800000	0.3885594	2279.698	350.2776	544320	3875763	544343.6
72253050000	0.3884808	2289.561	350.1617	544320	3877046	544343.6
72564300000	0.3884026	2299.424	350.0465	544320	3878322	544343.6
72875560000	0.3883247	2309.287	349.9317	544320	3879595	544343.8
73186800000	0.3882474	2319.15	349.8178	544320	3880858	544343.8
73498060000	0.3881703	2329.013	349.7043	544320	3882117	544343.6
73809310000	0.3880938	2338.876	349.5916	544320	3883368	544343.6
74120570000	0.3880175	2348.739	349.4794	544320	3884616	544343.8
74431820000	0.3879417	2358.602	349.3678	544320	3885856	544343.6
74743070000	0.3878663	2368.465	349.2569	544320	3887091	544343.8
75054320000	0.3877914	2378.328	349.1467	544320	3888318	544343.8
75365570000	0.3877167	2388.191	349.0369	544320	3889540	544343.6
75676830000	0.3876422	2398.054	348.9273	544320	3890761	544343.5
75988080000	0.3875685	2407.917	348.819	544320	3891970	544343.7
76299340000	0.3874949	2417.78	348.7109	544320	3893177	544343.8
76610590000	0.3874217	2427.643	348.6033	544320	3894377	544343.5
76921840000	0.3873489	2437.506	348.4964	544320	3895572	544343.6
77233090000	0.3872763	2447.369	348.3898	544320	3896765	544343.7
77544340000	0.3872042	2457.232	348.284	544320	3897949	544343.8
77855600000	0.3871326	2467.095	348.1789	544320	3899126	544343.8
78166850000	0.3870612	2476.958	348.0741	544320	3900299	544343.6
78478110000	0.38699	2486.821	347.9697	544320	3901470	544343.8
78789360000	0.3869194	2496.684	347.8661	544320	3902631	544343.6
79100610000	0.3868486	2506.547	347.7623	544320	3903796	544343.6
79411860000	0.3867787	2516.41	347.6599	544320	3904948	544344
79723110000	0.3867091	2526.273	347.5578	544320	3906093	544343.7
80034370000	0.3866397	2536.136	347.4561	544320	3907236	544343.6
80345620000	0.3865706	2545.999	347.3549	544320	3908375	544343.7
80656880000	0.3865018	2555.862	347.2541	544320	3909509	544343.6
80968120000	0.3864334	2565.725	347.154	544320	3910638	544343.9
81279370000	0.3863651	2575.588	347.054	544320	3911763	544343.6
81590620000	0.3862973	2585.451	346.9547	544320	3912882	544343.6
81901880000	0.3862297	2595.314	346.8558	544320	3913998	544343.6
82213130000	0.3861626	2605.177	346.7577	544320	3915107	544343.8
82524390000	0.3860957	2615.04	346.6598	544320	3916212	544343.7
82835640000	0.3860292	2624.903	346.5626	544320	3917310	544343.7
83146890000	0.3859631	2634.766	346.4659	544320	3918403	544343.6
83458140000	0.3858972	2644.629	346.3696	544320	3919494	544343.9
83769390000	0.3858315	2654.492	346.2736	544320	3920580	544343.8
84080650000	0.3857656	2664.355	346.1773	544320	3921670	544343.7
84391900000	0.3857008	2674.218	346.0826	544320	3922743	544343.7
84703160000	0.3856362	2684.081	345.9883	544320	3923813	544343.8

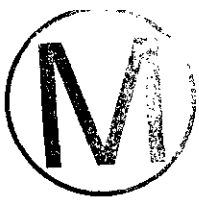




85014410000	0.3855716	2693.944	345.894	544320	3924882	544343.7
85325660000	0.3855074	2703.807	345.8002	544320	3925947	544343.8
85636910000	0.3854435	2713.67	345.707	544320	3927006	544343.8
85948160000	0.3853799	2723.533	345.6142	544320	3928060	544343.8
86259420000	0.3853166	2733.396	345.5218	544320	3929111	544343.8
86570670000	0.3852535	2743.259	345.4297	544320	3930156	544343.4
86881930000	0.3851906	2753.122	345.338	544320	3931200	544343.6
87193180000	0.3851281	2762.985	345.2469	544320	3932239	544343.8
87504420000	0.3850657	2772.848	345.1559	544320	3933275	544343.7
87815680000	0.3850039	2782.711	345.0658	544320	3934302	544343.6
88126930000	0.3849421	2792.574	344.9758	544320	3935328	544343.6
88438190000	0.3848806	2802.437	344.8862	544320	3936351	544343.7
88749440000	0.3848194	2812.3	344.797	544320	3937369	544343.6
89060700000	0.3847584	2822.163	344.7082	544320	3938384	544343.7
89371940000	0.3846978	2832.026	344.62	544320	3939392	544343.8
89683190000	0.384637	2841.889	344.5315	544320	3940404	544343.8
89994440000	0.384577	2851.752	344.4442	544320	3941403	544343.8
90305700000	0.3845169	2861.615	344.3567	544320	3942404	544343.7
90616990000	0.3844573	2871.479	344.27	544320	3943396	544343.6
90928210000	0.3843975	2881.341	344.183	544320	3944393	544343.6
91239460000	0.3843386	2891.204	344.0973	544320	3945376	544343.7
91550710000	0.3842798	2901.067	344.0118	544320	3946356	544343.6
91861960000	0.384221	2910.93	343.9263	544320	3947337	544343.6
92173210000	0.3841626	2920.793	343.8415	544320	3948311	544343.7
92484470000	0.3841042	2930.656	343.7566	544320	3949286	544343.7
92795760000	0.3840463	2940.52	343.6724	544320	3950253	544343.6
93107010000	0.3839885	2950.383	343.5885	544320	3951218	544343.6
93418260000	0.3839308	2960.246	343.5047	544320	3952183	544343.8
93729480000	0.3838732	2970.108	343.421	544320	3953144	544343.5
94040760000	0.3838165	2979.972	343.3387	544320	3954093	544343.7
94352020000	0.3837596	2989.835	343.2561	544320	3955045	544343.8
94663270000	0.3837031	2999.698	343.1741	544320	3955990	544343.8
94974530000	0.3836465	3009.561	343.092	544320	3956936	544343.7
95285780000	0.3835902	3019.424	343.0103	544320	3957878	544343.6
95597030000	0.3835344	3029.287	342.9294	544320	3958813	544343.8
95908270000	0.3834786	3039.15	342.8484	544320	3959747	544343.6
96219530000	0.3834231	3049.013	342.7679	544320	3960678	544343.8
96530780000	0.3833674	3058.876	342.6872	544320	3961610	544343.6
96842040000	0.3833122	3068.739	342.6072	544320	3962535	544343.6
97153290000	0.383257	3078.602	342.5272	544320	3963461	544343.7
97464550000	0.383202	3088.465	342.4475	544320	3964383	544343.7
97775790000	0.3831477	3098.328	342.3688	544320	3965294	544343.6
98087040000	0.3830933	3108.191	342.29	544320	3966207	544343.6
98398300000	0.3830391	3118.054	342.2115	544320	3967117	544343.6
98709550000	0.3829847	3127.917	342.1328	544320	3968030	544343.8
99020810000	0.3829309	3137.78	342.0549	544320	3968934	544343.8
99332060000	0.3828769	3147.643	341.9767	544320	3969840	544343.6
99643320000	0.3828235	3157.506	341.8994	544320	3970738	544343.6
99954560000	0.3827706	3167.369	341.8229	544320	3971627	544343.7
1.00266E+11	0.3827175	3177.232	341.7461	544320	3972519	544343.6
1.00577E+11	0.3826645	3187.095	341.6694	544320	3973411	544343.6
1.00888E+11	0.3826123	3196.958	341.5939	544320	3974290	544343.7



1.012E+11	0.3825589	3206.821	341.5168	544320	3975187	544343.7
1.01511E+11	0.3825074	3216.684	341.4423	544320	3976055	544343.8
1.01822E+11	0.3824552	3226.547	341.3668	544320	3976933	544343.6
1.02133E+11	0.3824034	3236.41	341.292	544320	3977806	544343.8
1.02445E+11	0.3823519	3246.273	341.2176	544320	3978673	544343.7
1.02756E+11	0.3823004	3256.136	341.1432	544320	3979541	544343.8
1.03067E+11	0.3822486	3265.999	341.0683	544320	3980414	544343.6
1.03378E+11	0.3821968	3275.862	340.9935	544320	3981287	544343.6
1.0369E+11	0.3821459	3285.725	340.92	544320	3982146	544343.8
1.04001E+11	0.3820948	3295.588	340.8462	544320	3983008	544343.7
1.04312E+11	0.3820441	3305.451	340.773	544320	3983863	544343.6
1.04623E+11	0.3819933	3315.314	340.6997	544320	3984721	544343.8
1.04935E+11	0.3819419	3325.177	340.6255	544320	3985587	544343.4
1.05246E+11	0.3818896	3335.04	340.5501	544320	3986470	544343.6
1.05557E+11	0.3818405	3344.903	340.4792	544320	3987300	544343.5
1.05868E+11	0.3817913	3354.766	340.4083	544320	3988133	544343.9
1.0618E+11	0.3817415	3364.629	340.3365	544320	3988974	544343.8
1.06491E+11	0.3816923	3374.492	340.2655	544320	3989805	544343.6
1.06802E+11	0.3816396	3384.355	340.1895	544320	3990696	544343.6
1.07113E+11	0.3815881	3394.218	340.1153	544320	3991566	544343.5
1.07425E+11	0.3815379	3404.081	340.043	544320	3992416	544343.7
1.07736E+11	0.3814872	3413.944	339.9699	544320	3993275	544343.8
1.08047E+11	0.3814377	3423.807	339.8986	544320	3994113	544343.8
1.08358E+11	0.3813864	3433.67	339.8247	544320	3994980	544343.6
1.0867E+11	0.3813349	3443.533	339.7505	544320	3995853	544343.6
1.08981E+11	0.3812847	3453.396	339.6783	544320	3996703	544343.8
1.09292E+11	0.3812326	3463.259	339.6032	544320	3997586	544343.6
1.09603E+11	0.381184	3473.122	339.5333	544320	3998410	544343.8
1.09915E+11	0.3811333	3482.985	339.4603	544320	3999269	544343.6
1.10226E+11	0.3810807	3492.848	339.3846	544320	4000161	544343.7
1.10537E+11	0.3810283	3502.711	339.3092	544320	4001050	544343.7
1.10848E+11	0.3809764	3512.574	339.2346	544320	4001930	544343.6
1.1116E+11	0.3809246	3522.437	339.1601	544320	4002810	544343.8
1.11471E+11	0.3808717	3532.3	339.084	544320	4003708	544343.8
1.11782E+11	0.3808228	3542.163	339.0137	544320	4004538	544343.8
1.12093E+11	0.3807735	3552.026	338.9428	544320	4005376	544343.8
1.12405E+11	0.3807226	3561.889	338.8696	544320	4006241	544343.8
1.12716E+11	0.3806714	3571.752	338.7961	544320	4007111	544343.9
1.13027E+11	0.3806212	3581.615	338.7239	544320	4007963	544343.6
1.13339E+11	0.3805708	3591.479	338.6515	544320	4008820	544343.6
1.1365E+11	0.380522	3601.341	338.5814	544320	4009651	544343.7
1.13961E+11	0.3804705	3611.204	338.5074	544320	4010527	544343.6
1.14272E+11	0.3804201	3621.067	338.435	544320	4011385	544343.6
1.14583E+11	0.3803717	3630.93	338.3655	544320	4012208	544343.6
1.14895E+11	0.3803218	3640.793	338.2939	544320	4013057	544343.5
1.15206E+11	0.3802761	3650.656	338.2284	544320	4013837	544343.9
1.15517E+11	0.3802333	3660.52	338.1669	544320	4014566	544343.8
1.15829E+11	0.3801882	3670.383	338.1022	544320	4015333	544343.6
1.1614E+11	0.3801453	3680.246	338.0407	544320	4016064	544343.7
1.16451E+11	0.3801017	3690.108	337.9781	544320	4016808	544343.7
1.16762E+11	0.380057	3699.972	337.914	544320	4017570	544343.7
1.17074E+11	0.3800128	3709.835	337.8506	544320	4018324	544343.7



1.17385E+11	0.3799708	3719.698	337.7904	544320	4019040	544343.7
1.17696E+11	0.3799274	3729.561	337.7281	544320	4019781	544343.6
1.18007E+11	0.3798843	3739.424	337.6664	544320	4020516	544343.7
1.18319E+11	0.3798409	3749.287	337.6042	544320	4021257	544343.7
1.1863E+11	0.3797987	3759.15	337.5437	544320	4021976	544343.5
1.18941E+11	0.3797545	3769.013	337.4804	544320	4022732	544343.8
1.19252E+11	0.3797118	3778.876	337.4192	544320	4023461	544343.6
1.19564E+11	0.3796669	3788.739	337.3549	544320	4024228	544343.6
1.19875E+11	0.3796235	3798.602	337.2927	544320	4024970	544343.6
1.20186E+11	0.3795809	3808.465	337.2317	544320	4025698	544343.6
1.20497E+11	0.3795366	3818.328	337.1683	544320	4026456	544343.8
1.20809E+11	0.3794963	3828.191	337.1106	544320	4027145	544343.8
1.2112E+11	0.3794548	3838.054	337.0511	544320	4027855	544343.6
1.21431E+11	0.3794134	3847.917	336.9919	544320	4028564	544343.8
1.21742E+11	0.3793718	3857.78	336.9324	544320	4029275	544343.8
1.22054E+11	0.3793306	3867.643	336.8734	544320	4029979	544343.6
1.22365E+11	0.3792884	3877.506	336.813	544320	4030702	544343.6
1.22676E+11	0.3792434	3887.369	336.7487	544320	4031473	544343.8
1.22987E+11	0.3792034	3897.232	336.6915	544320	4032158	544343.8
1.23299E+11	0.3791627	3907.095	336.6332	544320	4032854	544343.4
1.2361E+11	0.3791223	3916.958	336.5755	544320	4033548	544343.8
1.23921E+11	0.3790813	3926.821	336.5169	544320	4034250	544343.8
1.24232E+11	0.3790394	3936.684	336.457	544320	4034968	544343.7
1.24544E+11	0.3789987	3946.547	336.3988	544320	4035666	544343.7
1.24855E+11	0.3789589	3956.41	336.3419	544320	4036348	544343.6
1.25166E+11	0.3789192	3966.273	336.2852	544320	4037030	544343.8
1.25477E+11	0.3788785	3976.136	336.227	544320	4037727	544343.6
1.25789E+11	0.3788393	3985.999	336.171	544320	4038401	544343.8
1.261E+11	0.3787981	3995.862	336.1122	544320	4039107	544343.7
1.26411E+11	0.3787594	4005.725	336.0569	544320	4039772	544343.7
1.26722E+11	0.3787086	4015.588	335.9843	544320	4040644	544343.6
1.27034E+11	0.3786689	4025.451	335.9277	544320	4041326	544343.8
1.27345E+11	0.3786307	4035.314	335.8731	544320	4041982	544343.6
1.27656E+11	0.3785924	4045.177	335.8185	544320	4042641	544343.9
1.27967E+11	0.3785524	4055.04	335.7614	544320	4043328	544343.8
1.28279E+11	0.3785146	4064.903	335.7074	544320	4043978	544343.8
1.2859E+11	0.3784733	4074.766	335.6485	544320	4044688	544343.8
1.28901E+11	0.3784346	4084.629	335.5932	544320	4045353	544343.6
1.29212E+11	0.3783953	4094.492	335.5372	544320	4046028	544343.6
1.29524E+11	0.3783565	4104.355	335.4818	544320	4046696	544343.6
1.29835E+11	0.3783171	4114.218	335.4256	544320	4047375	544343.7
1.30146E+11	0.3782796	4124.081	335.3722	544320	4048020	544343.8
1.30457E+11	0.3782419	4133.944	335.3184	544320	4048669	544343.7
1.30769E+11	0.378199	4143.807	335.2573	544320	4049407	544343.7
1.3108E+11	0.3781587	4153.67	335.1998	544320	4050101	544343.6
1.31391E+11	0.3781155	4163.533	335.1382	544320	4050845	544343.6
1.31702E+11	0.3780772	4173.396	335.0836	544320	4051506	544343.7
1.32014E+11	0.3780406	4183.259	335.0315	544320	4052136	544343.7
1.32325E+11	0.3780041	4193.122	334.9795	544320	4052765	544343.7
1.32636E+11	0.3779671	4202.985	334.9268	544320	4053403	544343.8
1.32947E+11	0.3779292	4212.848	334.8728	544320	4054056	544343.7
1.33259E+11	0.3778901	4222.711	334.8171	544320	4054731	544343.8



1.3357E+11	0.3778544	4232.574	334.7663	544320	4055346	544343.7
1.33881E+11	0.3778176	4242.438	334.7138	544320	4055982	544343.7
1.34192E+11	0.3777806	4252.3	334.6611	544320	4056619	544343.4
1.34504E+11	0.3777442	4262.163	334.6093	544320	4057248	544343.6
1.34815E+11	0.3777075	4272.026	334.5571	544320	4057882	544343.7
1.35126E+11	0.3776709	4281.889	334.505	544320	4058513	544343.6
1.35437E+11	0.3776347	4291.752	334.4535	544320	4059139	544343.7
1.35749E+11	0.3775987	4301.615	334.4023	544320	4059761	544343.8
1.3606E+11	0.3775619	4311.479	334.3499	544320	4060396	544343.6
1.36371E+11	0.3775248	4321.341	334.2971	544320	4061038	544343.7
1.36682E+11	0.3774894	4331.205	334.2468	544320	4061649	544343.7
1.36994E+11	0.3774539	4341.067	334.1963	544320	4062263	544343.7
1.37305E+11	0.377417	4350.931	334.1438	544320	4062901	544343.7
1.37616E+11	0.3773809	4360.793	334.0925	544320	4063525	544343.7
1.37928E+11	0.3773459	4370.657	334.0427	544320	4064130	544343.6
1.38239E+11	0.3773067	4380.52	333.987	544320	4064809	544343.8
1.3855E+11	0.3772711	4390.382	333.9363	544320	4065425	544343.6
1.38861E+11	0.3772374	4400.246	333.8885	544320	4066007	544343.6
1.39172E+11	0.3771998	4410.108	333.8351	544320	4066659	544343.9
1.39484E+11	0.3771668	4419.972	333.7881	544320	4067230	544343.6
1.39795E+11	0.3771313	4429.834	333.7377	544320	4067845	544343.8
1.40106E+11	0.3770966	4439.698	333.6884	544320	4068446	544343.7
1.40418E+11	0.3770614	4449.561	333.6384	544320	4069055	544343.6
1.40729E+11	0.3770265	4459.424	333.5888	544320	4069660	544343.6
1.4104E+11	0.3769919	4469.287	333.5397	544320	4070259	544343.6
1.41351E+11	0.3769573	4479.149	333.4906	544320	4070858	544343.6
1.41663E+11	0.3769223	4489.013	333.4409	544320	4071466	544343.8
1.41974E+11	0.3768872	4498.875	333.3911	544320	4072075	544343.9
1.42285E+11	0.3768525	4508.739	333.3418	544320	4072676	544343.7
1.42596E+11	0.3768189	4518.602	333.2941	544320	4073258	544343.6
1.42908E+11	0.3767826	4528.465	333.2426	544320	4073889	544343.8
1.43219E+11	0.3767484	4538.328	333.1941	544320	4074481	544343.6
1.4353E+11	0.3767143	4548.191	333.1456	544320	4075074	544343.6
1.43841E+11	0.3766809	4558.054	333.0983	544320	4075653	544343.6
1.44153E+11	0.3766471	4567.917	333.0504	544320	4076240	544343.8
1.44464E+11	0.3766131	4577.78	333.0021	544320	4076830	544343.6
1.44775E+11	0.3765795	4587.643	332.9544	544320	4077414	544343.6
1.45086E+11	0.376544	4597.506	332.9041	544320	4078030	544343.6
1.45398E+11	0.3765105	4607.369	332.8566	544320	4078613	544343.8
1.45709E+11	0.376474	4617.232	332.8048	544320	4079247	544343.6
1.4602E+11	0.3764433	4627.095	332.7613	544320	4079780	544343.6
1.46331E+11	0.3764099	4636.958	332.714	544320	4080361	544343.7
1.46643E+11	0.3763764	4646.821	332.6665	544320	4080943	544343.6
1.46954E+11	0.3763416	4656.684	332.6172	544320	4081548	544343.6
1.47265E+11	0.3763098	4666.547	332.5721	544320	4082101	544343.6
1.47576E+11	0.376277	4676.41	332.5256	544320	4082673	544343.8
1.47888E+11	0.376243	4686.273	332.4774	544320	4083264	544343.6
1.48199E+11	0.3762104	4696.136	332.4313	544320	4083831	544343.8
1.4851E+11	0.3761785	4705.999	332.3861	544320	4084386	544343.7
1.48821E+11	0.3761465	4715.862	332.3408	544320	4084943	544343.7
1.49133E+11	0.376112	4725.725	332.2919	544320	4085544	544343.7
1.49444E+11	0.3760802	4735.588	332.2469	544320	4086097	544343.6

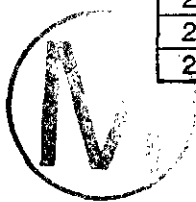
1.49755E+11	0.3760459	4745.451	332.1983	544320	4086695	544343.7
1.50066E+11	0.3760148	4755.314	332.1543	544320	4087237	544343.8
1.50378E+11	0.3759792	4765.177	332.1039	544320	4087857	544343.8
1.50689E+11	0.3759498	4775.04	332.0623	544320	4088369	544343.7
1.51E+11	0.3759172	4784.903	332.0161	544320	4088937	544343.6
1.51311E+11	0.3758852	4794.766	331.9708	544320	4089494	544343.4
1.51623E+11	0.3758525	4804.629	331.9246	544320	4090065	544343.7
1.51934E+11	0.3758202	4814.492	331.8789	544320	4090628	544343.7
1.52245E+11	0.3757879	4824.355	331.8332	544320	4091191	544343.6
1.52556E+11	0.3757566	4834.218	331.7889	544320	4091738	544343.8
1.52868E+11	0.3757253	4844.081	331.7446	544320	4092283	544343.6
1.53179E+11	0.3756931	4853.944	331.6991	544320	4092844	544343.5
1.5349E+11	0.3756624	4863.807	331.6557	544320	4093381	544343.7
1.53801E+11	0.3756305	4873.67	331.6106	544320	4093937	544343.6
1.54113E+11	0.3755985	4883.533	331.5653	544320	4094495	544343.4
1.54424E+11	0.3755661	4893.396	331.5195	544320	4095063	544343.8
1.54735E+11	0.3755335	4903.259	331.4734	544320	4095632	544343.6
1.55046E+11	0.3754997	4913.122	331.4257	544320	4096223	544343.8
1.55358E+11	0.3754698	4922.985	331.3834	544320	4096744	544343.6
1.55669E+11	0.3754367	4932.848	331.3366	544320	4097322	544343.6
1.5598E+11	0.3754047	4942.711	331.2914	544320	4097882	544343.7
1.56291E+11	0.3753703	4952.574	331.2428	544320	4098484	544343.8
1.56603E+11	0.3753364	4962.438	331.1949	544320	4099076	544343.6
1.56914E+11	0.3753081	4972.3	331.155	544320	4099570	544343.7
1.57225E+11	0.3752761	4982.163	331.1097	544320	4100131	544343.7
1.57536E+11	0.375245	4992.026	331.0659	544320	4100674	544343.8
1.57848E+11	0.3752142	5001.889	331.0223	544320	4101213	544343.6
1.58159E+11	0.3751814	5011.752	330.976	544320	4101787	544343.7
1.5847E+11	0.3751509	5021.615	330.933	544320	4102320	544343.7
1.58781E+11	0.3751153	5031.479	330.8827	544320	4102944	544343.7
1.59093E+11	0.3750839	5041.341	330.8384	544320	4103492	544343.5
1.59404E+11	0.3750544	5051.205	330.7968	544320	4104009	544343.7
1.59715E+11	0.3750244	5061.067	330.7545	544320	4104535	544343.8
1.60026E+11	0.3749922	5070.931	330.709	544320	4105099	544343.8
1.60338E+11	0.374962	5080.793	330.6664	544320	4105627	544343.6
1.60649E+11	0.3749304	5090.657	330.6218	544320	4106183	544343.9
1.6096E+11	0.374897	5100.52	330.5747	544320	4106766	544343.6
1.61271E+11	0.374867	5110.382	330.5323	544320	4107293	544343.6
1.61583E+11	0.3748364	5120.246	330.4892	544320	4107829	544343.7
1.61894E+11	0.3748028	5130.108	330.4418	544320	4108417	544343.5
1.62205E+11	0.3747749	5139.972	330.4025	544320	4108907	544343.7
1.62516E+11	0.374742	5149.834	330.3561	544320	4109484	544343.7
1.62828E+11	0.3747091	5159.698	330.3097	544320	4110061	544343.6
1.63139E+11	0.3746786	5169.561	330.2667	544320	4110597	544343.8
1.6345E+11	0.3746504	5179.424	330.227	544320	4111091	544343.7
1.63761E+11	0.3746187	5189.287	330.1823	544320	4111647	544343.7
1.64073E+11	0.3745868	5199.149	330.1373	544320	4112208	544343.8
1.64384E+11	0.3745546	5209.013	330.0919	544320	4112773	544343.6
1.64695E+11	0.3745228	5218.875	330.0471	544320	4113331	544343.6
1.65006E+11	0.3744887	5228.739	329.9991	544320	4113929	544343.6
1.65318E+11	0.3744577	5238.602	329.9554	544320	4114474	544343.6
1.65629E+11	0.3744272	5248.465	329.9125	544320	4115009	544343.6

1.6594E+11	0.3743984	5258.328	329.8719	544320	4115515	544343.5
1.66252E+11	0.3743654	5268.191	329.8254	544320	4116095	544343.5
1.66563E+11	0.3743316	5278.054	329.7778	544320	4116690	544343.6
1.66874E+11	0.374299	5287.917	329.7319	544320	4117263	544343.6
1.67185E+11	0.3742674	5297.78	329.6875	544320	4117818	544343.7
1.67497E+11	0.3742401	5307.643	329.649	544320	4118298	544343.5
1.67808E+11	0.3742086	5317.506	329.6047	544320	4118852	544343.6
1.68119E+11	0.374178	5327.369	329.5616	544320	4119390	544343.6
1.6843E+11	0.3741481	5337.232	329.5195	544320	4119917	544343.6
1.68742E+11	0.3741158	5347.095	329.4741	544320	4120485	544343.6
1.69053E+11	0.3740856	5356.958	329.4316	544320	4121016	544343.6
1.69364E+11	0.3740543	5366.821	329.3876	544320	4121567	544343.6
1.69675E+11	0.3740228	5376.684	329.3433	544320	4122122	544343.7
1.69987E+11	0.3739919	5386.547	329.2998	544320	4122666	544343.7
1.70298E+11	0.3739584	5396.41	329.2527	544320	4123256	544343.7
1.70609E+11	0.3739304	5406.273	329.2133	544320	4123750	544343.8
1.7092E+11	0.3739011	5416.136	329.1721	544320	4124266	544343.8
1.71232E+11	0.3738711	5425.999	329.1299	544320	4124793	544343.5
1.71543E+11	0.3738391	5435.862	329.0849	544320	4125359	544343.8
1.71854E+11	0.3738095	5445.725	329.0433	544320	4125879	544343.6
1.72165E+11	0.3737771	5455.588	328.9978	544320	4126452	544343.9
1.72477E+11	0.3737479	5465.451	328.9567	544320	4126966	544343.7
1.72788E+11	0.3737155	5475.314	328.9112	544320	4127537	544343.7
1.73099E+11	0.3736848	5485.177	328.868	544320	4128078	544343.6
1.7341E+11	0.3736539	5495.04	328.8246	544320	4128624	544343.6
1.73722E+11	0.373621	5504.903	328.7784	544320	4129203	544343.6
1.74033E+11	0.3735918	5514.766	328.7374	544320	4129720	544343.8
1.74344E+11	0.3735612	5524.629	328.6944	544320	4130260	544343.8
1.74655E+11	0.3735317	5534.492	328.653	544320	4130779	544343.6
1.74967E+11	0.3735023	5544.355	328.6117	544320	4131300	544343.8
1.75278E+11	0.3734719	5554.218	328.569	544320	4131836	544343.7
1.75589E+11	0.3734407	5564.081	328.5252	544320	4132388	544343.9
1.759E+11	0.3734078	5573.944	328.479	544320	4132967	544343.6
1.76212E+11	0.3733801	5583.807	328.4401	544320	4133458	544343.8
1.76523E+11	0.3733479	5593.67	328.3949	544320	4134026	544343.6
1.76834E+11	0.3733181	5603.533	328.3531	544320	4134552	544343.6
1.77145E+11	0.3732878	5613.396	328.3105	544320	4135088	544343.5
1.77457E+11	0.3732546	5623.259	328.264	544320	4135676	544343.9
1.77768E+11	0.3732246	5633.122	328.2219	544320	4136205	544343.6
1.78079E+11	0.3731907	5642.985	328.1743	544320	4136806	544343.8
1.7839E+11	0.3731597	5652.848	328.1308	544320	4137353	544343.6
1.78702E+11	0.3731294	5662.711	328.0883	544320	4137890	544343.8
1.79013E+11	0.3731008	5672.574	328.0482	544320	4138394	544343.5
1.79324E+11	0.3730715	5682.438	328.0071	544320	4138914	544343.7
1.79635E+11	0.3730412	5692.3	327.9646	544320	4139450	544343.6
1.79947E+11	0.3730097	5702.163	327.9205	544320	4140007	544343.7
1.80258E+11	0.372977	5712.026	327.8746	544320	4140586	544343.6
1.80569E+11	0.372949	5721.889	327.8354	544320	4141082	544343.7
1.8088E+11	0.372918	5731.752	327.7919	544320	4141632	544343.8
1.81192E+11	0.372884	5741.615	327.7443	544320	4142233	544343.7
1.81503E+11	0.3728538	5751.479	327.7019	544320	4142767	544343.5
1.81814E+11	0.372827	5761.341	327.6644	544320	4143244	544343.9



1.82125E+11	0.3727939	5771.205	327.618	544320	4143829	544343.6
1.82437E+11	0.3727613	5781.067	327.5723	544320	4144407	544343.6
1.82748E+11	0.372731	5790.931	327.5298	544320	4144945	544343.6
1.83059E+11	0.3727039	5800.793	327.4919	544320	4145425	544343.7
1.8337E+11	0.3726747	5810.657	327.451	544320	4145943	544343.7
1.83682E+11	0.3726425	5820.52	327.4059	544320	4146513	544343.6
1.83993E+11	0.3726133	5830.382	327.365	544320	4147032	544343.7
1.84304E+11	0.3725793	5840.246	327.3174	544320	4147635	544343.7
1.84615E+11	0.3725513	5850.108	327.2782	544320	4148132	544343.7
1.84927E+11	0.3725208	5859.972	327.2355	544320	4148673	544343.7
1.85238E+11	0.3724906	5869.834	327.1932	544320	4149208	544343.5
1.85549E+11	0.3724597	5879.698	327.15	544320	4149757	544343.6
1.8586E+11	0.3724284	5889.561	327.1061	544320	4150314	544343.6
1.86172E+11	0.3723961	5899.424	327.061	544320	4150886	544343.6
1.86483E+11	0.3723662	5909.287	327.0191	544320	4151418	544343.6
1.86794E+11	0.3723365	5919.149	326.9776	544320	4151946	544343.8
1.87105E+11	0.3723054	5929.013	326.9341	544320	4152498	544343.8
1.87417E+11	0.3722779	5938.875	326.8956	544320	4152986	544343.6
1.87728E+11	0.3722465	5948.739	326.8517	544320	4153545	544343.8
1.88039E+11	0.3722168	5958.602	326.8101	544320	4154074	544343.8
1.8835E+11	0.372188	5968.465	326.7698	544320	4154585	544343.6
1.88662E+11	0.3721562	5978.328	326.7254	544320	4155151	544343.8
1.88973E+11	0.3721271	5988.191	326.6847	544320	4155668	544343.7
1.89284E+11	0.3720959	5998.054	326.6411	544320	4156223	544343.8
1.89595E+11	0.3720688	6007.917	326.6031	544320	4156706	544343.6
1.89907E+11	0.3720371	6017.78	326.5589	544320	4157268	544343.6
1.90218E+11	0.3720055	6027.643	326.5147	544320	4157832	544343.8
1.90529E+11	0.3719782	6037.506	326.4765	544320	4158318	544343.7
1.90841E+11	0.371949	6047.369	326.4357	544320	4158836	544343.4
1.91152E+11	0.3719196	6057.232	326.3947	544320	4159361	544343.8
1.91463E+11	0.3718885	6067.095	326.3512	544320	4159915	544343.8
1.91774E+11	0.3718568	6076.958	326.3069	544320	4160480	544343.8
1.92086E+11	0.3718253	6086.821	326.2629	544320	4161040	544343.6
1.92397E+11	0.3717966	6096.684	326.2228	544320	4161552	544343.7
1.92708E+11	0.3717684	6106.547	326.1834	544320	4162053	544343.5
1.93019E+11	0.3717357	6116.41	326.1378	544320	4162637	544343.7
1.93331E+11	0.3717043	6126.273	326.0939	544320	4163197	544343.7
1.93642E+11	0.3716718	6136.136	326.0486	544320	4163775	544343.6
1.93953E+11	0.3716433	6145.999	326.0088	544320	4164284	544343.7
1.94264E+11	0.3716149	6155.862	325.9691	544320	4164790	544343.6
1.94576E+11	0.3715851	6165.725	325.9275	544320	4165322	544343.6
1.94887E+11	0.3715545	6175.588	325.8848	544320	4165868	544343.6
1.95198E+11	0.3715234	6185.451	325.8414	544320	4166423	544343.7
1.95509E+11	0.3714907	6195.314	325.7957	544320	4167007	544343.6
1.95821E+11	0.371462	6205.177	325.7557	544320	4167519	544343.7
1.96132E+11	0.3714328	6215.04	325.715	544320	4168040	544343.7
1.96443E+11	0.3714019	6224.903	325.6719	544320	4168591	544343.6
1.96754E+11	0.3713726	6234.766	325.631	544320	4169115	544343.7
1.97066E+11	0.3713429	6244.629	325.5896	544320	4169645	544343.6
1.97377E+11	0.3713132	6254.492	325.5482	544320	4170175	544343.6
1.97688E+11	0.3712834	6264.355	325.5066	544320	4170709	544343.8
1.97999E+11	0.3712522	6274.218	325.4631	544320	4171266	544343.7

1.98311E+11	0.3712234	6284.081	325.4229	544320	4171780	544343.6
1.98622E+11	0.3711938	6293.944	325.3817	544320	4172309	544343.6
1.98933E+11	0.3711636	6303.807	325.3396	544320	4172849	544343.6
1.99244E+11	0.3711352	6313.67	325.3	544320	4173357	544343.6
1.99556E+11	0.3711061	6323.533	325.2594	544320	4173878	544343.6
1.99867E+11	0.3710745	6333.396	325.2154	544320	4174443	544343.7
2.00178E+11	0.3710445	6343.259	325.1736	544320	4174979	544343.6
2.00489E+11	0.3710168	6353.122	325.135	544320	4175476	544343.8
2.00801E+11	0.3709854	6362.985	325.0912	544320	4176037	544343.6
2.01112E+11	0.3709573	6372.848	325.0521	544320	4176539	544343.5
2.01423E+11	0.3709269	6382.711	325.0098	544320	4177085	544343.8
2.01734E+11	0.3708966	6392.574	324.9676	544320	4177627	544343.8
2.02046E+11	0.3708648	6402.438	324.9233	544320	4178196	544343.8
2.02357E+11	0.370837	6412.3	324.8846	544320	4178694	544343.8
2.02668E+11	0.3708073	6422.163	324.8432	544320	4179225	544343.6
2.02979E+11	0.3707778	6432.026	324.8021	544320	4179755	544343.7
2.03291E+11	0.3707467	6441.889	324.7589	544320	4180311	544343.8
2.03602E+11	0.3707181	6451.752	324.719	544320	4180825	544343.8
2.03913E+11	0.3706855	6461.615	324.6736	544320	4181409	544343.7
2.04224E+11	0.3706559	6471.479	324.6325	544320	4181938	544343.6
2.04536E+11	0.370627	6481.341	324.5922	544320	4182457	544343.6
2.04847E+11	0.3705964	6491.205	324.5497	544320	4183006	544343.8
2.05158E+11	0.3705669	6501.067	324.5086	544320	4183535	544343.7
2.05469E+11	0.370539	6510.931	324.4698	544320	4184035	544343.6
2.05781E+11	0.3705049	6520.793	324.4224	544320	4184646	544343.6
2.06092E+11	0.3704773	6530.657	324.384	544320	4185141	544343.6
2.06403E+11	0.3704495	6540.52	324.3453	544320	4185640	544343.5
2.06714E+11	0.370419	6550.382	324.3029	544320	4186189	544343.7
2.07026E+11	0.3703857	6560.246	324.2566	544320	4186786	544343.6
2.07337E+11	0.3703576	6570.108	324.2175	544320	4187292	544343.8
2.07648E+11	0.3703243	6579.972	324.1713	544320	4187889	544343.8
2.07959E+11	0.3702972	6589.834	324.1336	544320	4188375	544343.7
2.08271E+11	0.3702673	6599.698	324.092	544320	4188913	544343.8
2.08582E+11	0.3702378	6609.561	324.051	544320	4189442	544343.6
2.08893E+11	0.3702108	6619.424	324.0135	544320	4189928	544343.7
2.09204E+11	0.37018	6629.287	323.9707	544320	4190481	544343.6
2.09516E+11	0.3701519	6639.149	323.9316	544320	4190986	544343.6
2.09827E+11	0.3701223	6649.013	323.8905	544320	4191518	544343.6
2.10138E+11	0.3700927	6658.875	323.8494	544320	4192051	544343.7
2.10449E+11	0.3700633	6668.739	323.8086	544320	4192579	544343.7
2.10761E+11	0.3700363	6678.602	323.7711	544320	4193066	544343.8
2.11072E+11	0.3700043	6688.465	323.7266	544320	4193642	544343.8
2.11383E+11	0.3699741	6698.328	323.6847	544320	4194184	544343.7
2.11694E+11	0.3699453	6708.191	323.6447	544320	4194703	544343.8
2.12006E+11	0.3699145	6718.054	323.6019	544320	4195256	544343.6
2.12317E+11	0.3698853	6727.917	323.5614	544320	4195782	544343.7
2.12628E+11	0.369855	6737.78	323.5193	544320	4196329	544343.8
2.12939E+11	0.3698257	6747.643	323.4786	544320	4196856	544343.7
2.13251E+11	0.3697962	6757.506	323.4377	544320	4197388	544343.9
2.13562E+11	0.3697663	6767.369	323.3962	544320	4197925	544343.6
2.13873E+11	0.3697378	6777.232	323.3567	544320	4198439	544343.8
2.14184E+11	0.3697094	6787.095	323.3173	544320	4198950	544343.7





2.14496E+11	0.3696766	6796.958	323.2717	544320	4199541	544343.5
2.14807E+11	0.3696505	6806.821	323.2355	544320	4200013	544343.8
2.15118E+11	0.3696217	6816.684	323.1956	544320	4200531	544343.7
2.15429E+11	0.3695895	6826.547	323.1509	544320	4201112	544343.7
2.15741E+11	0.3695622	6836.41	323.1131	544320	4201604	544343.8
2.16052E+11	0.3695291	6846.273	323.0671	544320	4202201	544343.6
2.16363E+11	0.3695005	6856.136	323.0275	544320	4202716	544343.6
2.16675E+11	0.3694734	6865.999	322.9899	544320	4203206	544343.7
2.16986E+11	0.3694452	6875.862	322.9508	544320	4203715	544343.7
2.17297E+11	0.3694151	6885.725	322.9091	544320	4204257	544343.6
2.17608E+11	0.3693854	6895.588	322.8679	544320	4204794	544343.6
2.1792E+11	0.3693557	6905.451	322.8268	544320	4205330	544343.8
2.18231E+11	0.3693254	6915.314	322.7848	544320	4205877	544343.7
2.18542E+11	0.3692968	6925.177	322.7451	544320	4206394	544343.6
2.18853E+11	0.3692677	6935.04	322.7048	544320	4206920	544343.8
2.19165E+11	0.3692377	6944.903	322.6632	544320	4207462	544343.7
2.19476E+11	0.3692072	6954.766	322.621	544320	4208012	544343.6
2.19787E+11	0.3691807	6964.629	322.5843	544320	4208491	544343.7
2.20098E+11	0.3691496	6974.492	322.5412	544320	4209053	544343.6
2.2041E+11	0.3691226	6984.355	322.5038	544320	4209541	544343.6
2.20721E+11	0.3690934	6994.218	322.4634	544320	4210070	544343.8
2.21032E+11	0.3690626	7004.081	322.4207	544320	4210627	544343.8
2.21343E+11	0.3690359	7013.944	322.3838	544320	4211109	544343.8
2.21655E+11	0.369005	7023.807	322.341	544320	4211668	544343.8
2.21966E+11	0.3689752	7033.67	322.2997	544320	4212207	544343.7
2.22277E+11	0.3689446	7043.533	322.2574	544320	4212761	544343.8
2.22588E+11	0.3689138	7053.396	322.2148	544320	4213318	544343.8
2.229E+11	0.3688856	7063.259	322.1758	544320	4213829	544343.9
2.23211E+11	0.3688588	7073.122	322.1387	544320	4214313	544343.8
2.23522E+11	0.36883	7082.985	322.0988	544320	4214834	544343.6
2.23833E+11	0.3687979	7092.848	322.0544	544320	4215417	544343.9
2.24145E+11	0.3687701	7102.711	322.0159	544320	4215920	544343.8
2.24456E+11	0.36874	7112.574	321.9743	544320	4216465	544343.8
2.24767E+11	0.3687112	7122.438	321.9344	544320	4216986	544343.6
2.25078E+11	0.368685	7132.3	321.8982	544320	4217461	544343.6
2.2539E+11	0.3686558	7142.163	321.8578	544320	4217990	544343.6
2.25701E+11	0.3686263	7152.026	321.817	544320	4218525	544343.6
2.26012E+11	0.3685971	7161.889	321.7766	544320	4219054	544343.6
2.26323E+11	0.368567	7171.752	321.735	544320	4219599	544343.5
2.26635E+11	0.3685375	7181.615	321.6942	544320	4220135	544343.6
2.26946E+11	0.3685058	7191.479	321.6505	544320	4220709	544343.7
2.27257E+11	0.3684762	7201.341	321.6096	544320	4221247	544343.8
2.27568E+11	0.3684485	7211.205	321.5713	544320	4221750	544343.9
2.2788E+11	0.3684186	7221.067	321.5299	544320	4222292	544343.7
2.28191E+11	0.3683893	7230.931	321.4895	544320	4222823	544343.8
2.28502E+11	0.3683609	7240.793	321.4502	544320	4223338	544343.6
2.28813E+11	0.3683328	7250.657	321.4114	544320	4223849	544343.8
2.29125E+11	0.3683036	7260.52	321.3711	544320	4224379	544343.8
2.29436E+11	0.3682744	7270.382	321.3307	544320	4224910	544343.8
2.29747E+11	0.3682435	7280.246	321.288	544320	4225470	544343.6
2.30058E+11	0.3682155	7290.108	321.2494	544320	4225979	544343.7
2.3037E+11	0.368186	7299.972	321.2086	544320	4226515	544343.6



2.30681E+11	0.3681559	7309.834	321.1671	544320	4227062	544343.8
2.30992E+11	0.3681261	7319.698	321.1259	544320	4227603	544343.5
2.31303E+11	0.3680966	7329.561	321.0852	544320	4228139	544343.6
2.31615E+11	0.368069	7339.424	321.0471	544320	4228641	544343.6
2.31926E+11	0.3680389	7349.287	321.0056	544320	4229189	544343.8
2.32237E+11	0.368009	7359.149	320.9643	544320	4229733	544343.8
2.32548E+11	0.3679829	7369.013	320.9283	544320	4230207	544343.7
2.3286E+11	0.3679524	7378.875	320.8862	544320	4230761	544343.6
2.33171E+11	0.3679242	7388.739	320.8473	544320	4231276	544343.8
2.33482E+11	0.3678963	7398.602	320.8088	544320	4231783	544343.8
2.33793E+11	0.3678671	7408.465	320.7686	544320	4232314	544343.8
2.34105E+11	0.3678371	7418.328	320.7272	544320	4232860	544343.8
2.34416E+11	0.3678091	7428.191	320.6885	544320	4233369	544343.6
2.34727E+11	0.3677806	7438.054	320.6492	544320	4233889	544343.7
2.35038E+11	0.367753	7447.917	320.6112	544320	4234392	544343.8
2.3535E+11	0.3677247	7457.78	320.5721	544320	4234906	544343.5
2.35661E+11	0.367695	7467.643	320.5312	544320	4235448	544343.7
2.35972E+11	0.3676654	7477.506	320.4904	544320	4235987	544343.7
2.36283E+11	0.3676369	7487.369	320.4511	544320	4236507	544343.8
2.36595E+11	0.3676078	7497.232	320.411	544320	4237036	544343.6
2.36906E+11	0.3675792	7507.095	320.3716	544320	4237558	544343.8
2.37217E+11	0.3675493	7516.958	320.3304	544320	4238103	544343.8
2.37528E+11	0.367521	7526.821	320.2914	544320	4238619	544343.8
2.3784E+11	0.3674909	7536.684	320.2499	544320	4239167	544343.6
2.38151E+11	0.3674612	7546.547	320.209	544320	4239709	544343.6
2.38462E+11	0.3674339	7556.41	320.1714	544320	4240208	544343.8
2.38773E+11	0.3674032	7566.273	320.1291	544320	4240767	544343.6
2.39085E+11	0.3673741	7576.136	320.089	544320	4241298	544343.6
2.39396E+11	0.3673481	7585.999	320.0532	544320	4241773	544343.6
2.39707E+11	0.3673195	7595.862	320.0138	544320	4242295	544343.6
2.40018E+11	0.3672904	7605.725	319.9738	544320	4242826	544343.7
2.4033E+11	0.3672616	7615.588	319.9341	544320	4243352	544343.6
2.40641E+11	0.367233	7625.451	319.8947	544320	4243874	544343.6
2.40952E+11	0.3672048	7635.314	319.8559	544320	4244389	544343.6
2.41263E+11	0.3671755	7645.177	319.8156	544320	4244924	544343.6
2.41575E+11	0.367145	7655.04	319.7736	544320	4245482	544343.6
2.41886E+11	0.3671175	7664.903	319.7357	544320	4245986	544343.8
2.42197E+11	0.3670884	7674.766	319.6957	544320	4246516	544343.6
2.42508E+11	0.3670591	7684.629	319.6554	544320	4247051	544343.6
2.4282E+11	0.3670322	7694.492	319.6184	544320	4247544	544343.8
2.43131E+11	0.3670029	7704.355	319.5781	544320	4248079	544343.6
2.43442E+11	0.3669733	7714.218	319.5374	544320	4248622	544343.9
2.43754E+11	0.3669452	7724.081	319.4987	544320	4249134	544343.5
2.44065E+11	0.3669159	7733.944	319.4584	544320	4249672	544343.8
2.44376E+11	0.3668866	7743.807	319.4181	544320	4250207	544343.6
2.44687E+11	0.3668577	7753.67	319.3784	544320	4250736	544343.7
2.44999E+11	0.3668277	7763.533	319.3371	544320	4251285	544343.6
2.4531E+11	0.3667975	7773.396	319.2956	544320	4251837	544343.6
2.45621E+11	0.3667683	7783.259	319.2555	544320	4252372	544343.7
2.45932E+11	0.3667419	7793.122	319.2192	544320	4252855	544343.6
2.46244E+11	0.366715	7802.985	319.1822	544320	4253348	544343.6
2.46555E+11	0.3666855	7812.848	319.1417	544320	4253890	544343.9



2.46866E+11	0.3666568	7822.711	319.1022	544320	4254414	544343.6
2.47177E+11	0.3666282	7832.574	319.0629	544320	4254938	544343.6
2.47489E+11	0.3665972	7842.438	319.0204	544320	4255506	544343.7
2.478E+11	0.3665712	7852.3	318.9846	544320	4255983	544343.6
2.48111E+11	0.3665411	7862.163	318.9433	544320	4256534	544343.6
2.48422E+11	0.3665133	7872.026	318.9051	544320	4257045	544343.8
2.48734E+11	0.3664844	7881.889	318.8654	544320	4257575	544343.8
2.49045E+11	0.366456	7891.752	318.8264	544320	4258095	544343.6
2.49356E+11	0.3664275	7901.615	318.7873	544320	4258618	544343.8
2.49667E+11	0.3663979	7911.479	318.7466	544320	4259161	544343.7
2.49979E+11	0.3663689	7921.341	318.7068	544320	4259693	544343.6
2.5029E+11	0.3663428	7931.205	318.671	544320	4260171	544343.6
2.50601E+11	0.366315	7941.067	318.6328	544320	4260683	544343.8
2.50912E+11	0.3662867	7950.931	318.594	544320	4261202	544343.8
2.51224E+11	0.3662576	7960.793	318.554	544320	4261735	544343.5
2.51535E+11	0.3662294	7970.657	318.5153	544320	4262253	544343.5
2.51846E+11	0.3662009	7980.52	318.4762	544320	4262777	544343.6
2.52157E+11	0.3661712	7990.382	318.4355	544320	4263324	544343.9
2.52469E+11	0.3661437	8000.246	318.3977	544320	4263828	544343.6
2.5278E+11	0.3661142	8010.108	318.3573	544320	4264370	544343.8
2.53091E+11	0.3660864	8019.972	318.3191	544320	4264881	544343.6
2.53402E+11	0.3660571	8029.834	318.2789	544320	4265420	544343.7
2.53714E+11	0.366028	8039.698	318.239	544320	4265955	544343.8
2.54025E+11	0.3659994	8049.561	318.1998	544320	4266480	544343.6
2.54336E+11	0.3659709	8059.424	318.1607	544320	4267003	544343.5
2.54647E+11	0.3659447	8069.287	318.1248	544320	4267486	544343.6
2.54959E+11	0.3659164	8079.149	318.086	544320	4268007	544343.8
2.5527E+11	0.3658877	8089.013	318.0467	544320	4268535	544343.8
2.55581E+11	0.3658603	8098.875	318.0091	544320	4269039	544343.7
2.55892E+11	0.3658312	8108.739	317.9692	544320	4269574	544343.6
2.56204E+11	0.3658034	8118.602	317.9311	544320	4270086	544343.7
2.56515E+11	0.3657744	8128.465	317.8914	544320	4270620	544343.8
2.56826E+11	0.3657462	8138.328	317.8527	544320	4271139	544343.6
2.57137E+11	0.3657177	8148.191	317.8137	544320	4271663	544343.6
2.57449E+11	0.3656893	8158.054	317.7748	544320	4272186	544343.7
2.5776E+11	0.3656609	8167.917	317.7359	544320	4272710	544343.8
2.58071E+11	0.3656321	8177.78	317.6964	544320	4273240	544343.6
2.58382E+11	0.3656025	8187.643	317.6559	544320	4273786	544343.8
2.58694E+11	0.3655742	8197.506	317.6171	544320	4274306	544343.5
2.59005E+11	0.3655477	8207.369	317.5808	544320	4274796	544343.7
2.59316E+11	0.3655188	8217.231	317.5413	544320	4275329	544343.8
2.59627E+11	0.3654886	8227.095	317.4999	544320	4275884	544343.6
2.59939E+11	0.365459	8236.958	317.4594	544320	4276431	544343.8
2.6025E+11	0.3654298	8246.821	317.4194	544320	4276970	544343.8
2.60561E+11	0.3654015	8256.684	317.3807	544320	4277491	544343.7
2.60872E+11	0.3653745	8266.547	317.3438	544320	4277990	544343.9
2.61184E+11	0.3653453	8276.41	317.3038	544320	4278528	544343.7
2.61495E+11	0.3653148	8286.272	317.2621	544320	4279091	544343.8
2.61806E+11	0.3652851	8296.136	317.2214	544320	4279639	544343.7
2.62117E+11	0.3652591	8305.999	317.1859	544320	4280119	544343.8
2.62429E+11	0.3652302	8315.862	317.1463	544320	4280652	544343.6
2.6274E+11	0.365201	8325.725	317.1064	544320	4281191	544343.7



2.63051E+11	0.3651724	8335.588	317.0672	544320	4281720	544343.6
2.63362E+11	0.3651433	8345.451	317.0274	544320	4282258	544343.7
2.63674E+11	0.3651166	8355.314	316.9909	544320	4282751	544343.7
2.63985E+11	0.3650884	8365.177	316.9524	544320	4283272	544343.8
2.64296E+11	0.3650597	8375.04	316.9131	544320	4283803	544343.7
2.64607E+11	0.365032	8384.903	316.8752	544320	4284314	544343.6
2.64919E+11	0.3650029	8394.766	316.8354	544320	4284852	544343.5
2.6523E+11	0.3649749	8404.629	316.7972	544320	4285369	544343.6
2.65541E+11	0.3649451	8414.492	316.7565	544320	4285922	544343.9
2.65852E+11	0.364918	8424.355	316.7194	544320	4286423	544343.8
2.66164E+11	0.3648891	8434.218	316.6799	544320	4286957	544343.7
2.66475E+11	0.3648604	8444.081	316.6407	544320	4287487	544343.6
2.66786E+11	0.3648327	8453.944	316.6029	544320	4288001	544343.9
2.67098E+11	0.3648031	8463.808	316.5624	544320	4288547	544343.6
2.67409E+11	0.3647745	8473.67	316.5233	544320	4289077	544343.5
2.6772E+11	0.3647471	8483.533	316.4859	544320	4289584	544343.6
2.68031E+11	0.3647198	8493.396	316.4486	544320	4290090	544343.6
2.68342E+11	0.3646903	8503.259	316.4084	544320	4290637	544343.8
2.68654E+11	0.3646614	8513.122	316.3689	544320	4291172	544343.8
2.68965E+11	0.3646341	8522.985	316.3316	544320	4291678	544343.8
2.69276E+11	0.3646045	8532.849	316.2912	544320	4292225	544343.6
2.69587E+11	0.3645773	8542.711	316.2541	544320	4292730	544343.8
2.69899E+11	0.3645481	8552.574	316.2142	544320	4293270	544343.6
2.7021E+11	0.3645214	8562.438	316.1778	544320	4293765	544343.7
2.70521E+11	0.364491	8572.301	316.1362	544320	4294330	544343.7
2.70833E+11	0.364462	8582.163	316.0967	544320	4294866	544343.6
2.71144E+11	0.3644345	8592.026	316.0592	544320	4295377	544343.8
2.71455E+11	0.3644049	8601.89	316.0187	544320	4295926	544343.6
2.71766E+11	0.3643782	8611.752	315.9824	544320	4296421	544343.8
2.72078E+11	0.3643498	8621.615	315.9436	544320	4296948	544343.8
2.72389E+11	0.3643203	8631.479	315.9034	544320	4297495	544343.8
2.727E+11	0.3642924	8641.342	315.8653	544320	4298012	544343.6
2.73011E+11	0.3642642	8651.204	315.8268	544320	4298535	544343.4
2.73323E+11	0.3642361	8661.067	315.7885	544320	4299058	544343.7
2.73634E+11	0.364208	8670.931	315.7502	544320	4299581	544343.9
2.73945E+11	0.3641788	8680.794	315.7104	544320	4300121	544343.6
2.74256E+11	0.3641516	8690.656	315.6733	544320	4300627	544343.7
2.74568E+11	0.3641236	8700.52	315.6351	544320	4301148	544343.8
2.74879E+11	0.364096	8710.383	315.5975	544320	4301661	544343.8
2.7519E+11	0.3640691	8720.245	315.5609	544320	4302159	544343.7
2.75501E+11	0.3640416	8730.108	315.5233	544320	4302670	544343.4
2.75813E+11	0.364014	8739.972	315.4857	544320	4303183	544343.5
2.76124E+11	0.3639854	8749.835	315.4467	544320	4303715	544343.5
2.76435E+11	0.3639585	8759.697	315.4101	544320	4304215	544343.6
2.76746E+11	0.3639282	8769.561	315.3688	544320	4304778	544343.5
2.77058E+11	0.3639004	8779.424	315.331	544320	4305296	544343.8
2.77369E+11	0.3638718	8789.286	315.292	544320	4305829	544343.8
2.7768E+11	0.3638451	8799.149	315.2556	544320	4306324	544343.6
2.77991E+11	0.3638157	8809.013	315.2156	544320	4306871	544343.6
2.78303E+11	0.3637876	8818.876	315.1773	544320	4307395	544343.7
2.78614E+11	0.3637579	8828.738	315.1369	544320	4307947	544343.6
2.78925E+11	0.3637311	8838.602	315.1004	544320	4308446	544343.6



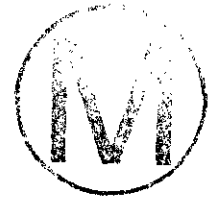
2.79236E+11	0.3637036	8848.465	315.063	544320	4308958	544343.7
2.79548E+11	0.3636759	8858.328	315.0252	544320	4309474	544343.6
2.79859E+11	0.3636476	8868.19	314.9867	544320	4310002	544343.8
2.8017E+11	0.3636201	8878.054	314.9493	544320	4310514	544343.8
2.80481E+11	0.3635928	8887.917	314.9121	544320	4311022	544343.6
2.80793E+11	0.3635644	8897.78	314.8735	544320	4311551	544343.7
2.81104E+11	0.3635355	8907.643	314.8342	544320	4312091	544343.9
2.81415E+11	0.3635067	8917.506	314.795	544320	4312626	544343.7
2.81726E+11	0.3634787	8927.369	314.7569	544320	4313148	544343.7
2.82038E+11	0.363451	8937.231	314.7192	544320	4313665	544343.7
2.82349E+11	0.3634242	8947.095	314.6828	544320	4314164	544343.7
2.8266E+11	0.3633961	8956.958	314.6445	544320	4314688	544343.6
2.82971E+11	0.363369	8966.821	314.6076	544320	4315195	544343.7
2.83283E+11	0.3633392	8976.684	314.5671	544320	4315750	544343.6
2.83594E+11	0.3633109	8986.547	314.5287	544320	4316279	544343.9
2.83905E+11	0.3632828	8996.41	314.4904	544320	4316802	544343.5
2.84216E+11	0.3632541	9006.272	314.4514	544320	4317339	544343.7
2.84528E+11	0.3632277	9016.136	314.4155	544320	4317831	544343.6
2.84839E+11	0.3631986	9025.999	314.376	544320	4318373	544343.6
2.8515E+11	0.3631695	9035.862	314.3364	544320	4318917	544343.6
2.85461E+11	0.3631425	9045.725	314.2997	544320	4319422	544343.7
2.85773E+11	0.363115	9055.588	314.2624	544320	4319936	544343.8
2.86084E+11	0.363087	9065.451	314.2243	544320	4320458	544343.6
2.86395E+11	0.3630581	9075.314	314.185	544320	4320998	544343.5
2.86706E+11	0.3630302	9085.177	314.1472	544320	4321520	544343.8
2.87018E+11	0.3630018	9095.04	314.1086	544320	4322050	544343.7
2.87329E+11	0.3629754	9104.903	314.0727	544320	4322543	544343.5
2.8764E+11	0.3629457	9114.766	314.0324	544320	4323099	544343.7
2.87951E+11	0.3629172	9124.629	313.9937	544320	4323633	544343.9
2.88263E+11	0.3628906	9134.492	313.9576	544320	4324129	544343.7
2.88574E+11	0.362862	9144.355	313.9187	544320	4324666	544343.8
2.88885E+11	0.3628322	9154.218	313.8782	544320	4325221	544343.4
2.89196E+11	0.362806	9164.081	313.8427	544320	4325712	544343.7
2.89508E+11	0.3627784	9173.944	313.8052	544320	4326230	544343.8
2.89819E+11	0.362748	9183.808	313.7639	544320	4326798	544343.6
2.9013E+11	0.3627192	9193.67	313.7249	544320	4327337	544343.8
2.90441E+11	0.3626918	9203.533	313.6877	544320	4327850	544343.8
2.90753E+11	0.3626636	9213.396	313.6494	544320	4328378	544343.7
2.91064E+11	0.3626361	9223.259	313.6121	544320	4328894	544343.8
2.91375E+11	0.362608	9233.122	313.5739	544320	4329420	544343.7
2.91686E+11	0.3625814	9242.985	313.5379	544320	4329917	544343.7
2.91998E+11	0.3625534	9252.849	313.4999	544320	4330442	544343.7
2.92309E+11	0.3625229	9262.711	313.4585	544320	4331013	544343.6
2.9262E+11	0.3624956	9272.574	313.4215	544320	4331525	544343.7
2.92932E+11	0.3624682	9282.438	313.3843	544320	4332039	544343.6
2.93243E+11	0.3624395	9292.301	313.3454	544320	4332578	544343.8
2.93554E+11	0.362411	9302.163	313.3068	544320	4333111	544343.7
2.93865E+11	0.3623825	9312.026	313.2681	544320	4333646	544343.6
2.94177E+11	0.3623556	9321.89	313.2316	544320	4334150	544343.5
2.94488E+11	0.3623261	9331.752	313.1917	544320	4334705	544343.9
2.94799E+11	0.3622986	9341.615	313.1544	544320	4335221	544343.8
2.9511E+11	0.3622707	9351.479	313.1166	544320	4335744	544343.8

2.95422E+11	0.3622421	9361.342	313.0778	544320	4336280	544343.6
2.95733E+11	0.3622145	9371.204	313.0404	544320	4336799	544343.8
2.96044E+11	0.3621863	9381.067	313.0022	544320	4337328	544343.7
2.96355E+11	0.3621584	9390.931	312.9644	544320	4337852	544343.7
2.96667E+11	0.3621315	9400.794	312.9279	544320	4338357	544343.6
2.96978E+11	0.3621028	9410.656	312.8891	544320	4338897	544343.9
2.97289E+11	0.3620743	9420.52	312.8505	544320	4339431	544343.7
2.976E+11	0.3620459	9430.383	312.812	544320	4339966	544343.8
2.97912E+11	0.3620191	9440.245	312.7757	544320	4340468	544343.6
2.98223E+11	0.3619887	9450.108	312.7345	544320	4341040	544343.6
2.98534E+11	0.3619621	9459.972	312.6985	544320	4341541	544343.8
2.98845E+11	0.3619327	9469.835	312.6587	544320	4342093	544343.7
2.99157E+11	0.3619045	9479.697	312.6205	544320	4342623	544343.6
2.99468E+11	0.3618768	9489.561	312.583	544320	4343143	544343.5
2.99779E+11	0.3618478	9499.424	312.5438	544320	4343690	544343.8
3.0009E+11	0.36182	9509.286	312.5062	544320	4344212	544343.7
3.00402E+11	0.361791	9519.149	312.4669	544320	4344759	544343.8
3.00713E+11	0.3617643	9529.013	312.4308	544320	4345261	544343.8
3.01024E+11	0.3617341	9538.876	312.3899	544320	4345830	544343.8
3.01335E+11	0.3617073	9548.738	312.3537	544320	4346334	544343.8
3.01647E+11	0.3616789	9558.602	312.3152	544320	4346868	544343.6
3.01958E+11	0.3616503	9568.465	312.2766	544320	4347407	544343.8
3.02269E+11	0.3616222	9578.328	312.2386	544320	4347937	544343.9
3.0258E+11	0.3615936	9588.19	312.1999	544320	4348474	544343.7
3.02892E+11	0.3615668	9598.054	312.1636	544320	4348979	544343.6
3.03203E+11	0.3615377	9607.917	312.1243	544320	4349527	544343.6
3.03514E+11	0.3615106	9617.78	312.0876	544320	4350039	544343.7
3.03825E+11	0.3614819	9627.643	312.0488	544320	4350579	544343.6
3.04137E+11	0.3614538	9637.506	312.0108	544320	4351109	544343.6
3.04448E+11	0.361426	9647.369	311.9733	544320	4351634	544343.9
3.04759E+11	0.3613977	9657.231	311.935	544320	4352168	544343.8
3.0507E+11	0.3613701	9667.095	311.8977	544320	4352687	544343.7
3.05382E+11	0.3613408	9676.958	311.8581	544320	4353240	544343.7
3.05693E+11	0.3613137	9686.821	311.8215	544320	4353752	544343.8
3.06004E+11	0.3612849	9696.684	311.7826	544320	4354295	544343.8
3.06315E+11	0.361255	9706.547	311.7422	544320	4354858	544343.6
3.06627E+11	0.3612259	9716.41	311.7029	544320	4355407	544343.6
3.06938E+11	0.3611967	9726.272	311.6634	544320	4355959	544343.6
3.07249E+11	0.3611693	9736.136	311.6264	544320	4356477	544343.8
3.0756E+11	0.3611405	9745.999	311.5875	544320	4357020	544343.6
3.07872E+11	0.3611132	9755.862	311.5506	544320	4357535	544343.5
3.08183E+11	0.3610835	9765.725	311.5106	544320	4358097	544343.8
3.08494E+11	0.361056	9775.588	311.4734	544320	4358617	544343.7
3.08805E+11	0.3610273	9785.451	311.4347	544320	4359159	544343.8
3.09117E+11	0.3609998	9795.314	311.3975	544320	4359678	544343.6
3.09428E+11	0.3609714	9805.177	311.3592	544320	4360215	544343.6
3.09739E+11	0.360944	9815.04	311.3222	544320	4360733	544343.6
3.1005E+11	0.3609151	9824.903	311.2832	544320	4361279	544343.6
3.10362E+11	0.3608879	9834.766	311.2465	544320	4361795	544343.8
3.10673E+11	0.3608586	9844.629	311.207	544320	4362347	544343.6
3.10984E+11	0.3608309	9854.492	311.1696	544320	4362872	544343.6
3.11295E+11	0.3608017	9864.355	311.1302	544320	4363424	544343.6



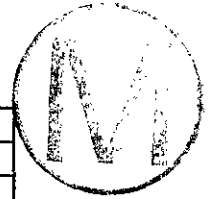
3.11607E+11	0.360774	9874.218	311.0928	544320	4363949	544343.7
3.11918E+11	0.360745	9884.081	311.0537	544320	4364498	544343.8
3.12229E+11	0.3607168	9893.944	311.0157	544320	4365030	544343.6
3.1254E+11	0.3606893	9903.808	310.9786	544320	4365552	544343.8
3.12852E+11	0.3606603	9913.67	310.9395	544320	4366100	544343.6
3.13163E+11	0.3606321	9923.533	310.9015	544320	4366635	544343.8
3.13474E+11	0.3606042	9933.396	310.8638	544320	4367162	544343.4
3.13785E+11	0.3605756	9943.259	310.8253	544320	4367705	544343.7
3.14097E+11	0.3605473	9953.122	310.7871	544320	4368241	544343.6
3.14408E+11	0.3605191	9962.985	310.7491	544320	4368776	544343.8
3.14719E+11	0.3604903	9972.849	310.7103	544320	4369321	544343.6
3.1503E+11	0.3604622	9982.711	310.6724	544320	4369854	544343.6
3.15342E+11	0.3604341	9992.574	310.6346	544320	4370387	544343.8
3.15576E+11	0.3604126	10000	310.6056	544320	4370795	544343.8





# Written	LOT 12/	:0	9:30		
# Created	ANTOS 1	:1	4:55		
# Modified	LGBRA	:5	0:59		
@ with g0					
@ legend on					
@ legend view					
@ legend ze 0.75					
@ title "Di	L ROOM	-	FINAL - F = 0.05 - WASTE W/O BACKFILL"		
@ subtitle	vs PGAS"				
@ s0	color	1			
@ xaxis la	IME"				
@ yaxis la	GAS"				
@ legend	0 "PGAS"				
@ s0	comment "PGAS"				
0.00E+00	0.00E+00				
1.34E-11	7.40E-09				
9.76E-09	5.38E-06				
7.43E-07	4.10E-04				
3.88E-06	2.14E-03				
9.65E-06	5.34E-03				
1.89E-05	1.05E-02				
3.24E-05	1.80E-02				
4.94E-05	2.75E-02				
6.74E-05	3.76E-02				
1.02E-04	5.72E-02				
1.58E-04	8.85E-02				
2.57E-04	1.44E-01				
4.68E-04	2.64E-01				
8.40E-04	4.76E-01				
1.57E-03	8.93E-01				
2.94E-03	1.68E+00				
5.29E-03	3.04E+00				
7.63E-03	4.40E+00				
1.13E-02	6.52E+00				
2.05E-02	1.19E+01				
3.16E-02	1.85E+01				
4.58E-02	2.69E+01				
6.61E-02	3.90E+01				
9.25E-02	5.47E+01				
1.33E-01	7.90E+01				
1.75E-01	1.04E+02				
2.17E-01	1.30E+02				
2.63E-01	1.58E+02				
3.11E-01	1.87E+02				
3.84E-01	2.32E+02				
4.93E-01	3.00E+02				
6.15E-01	3.76E+02				
7.41E-01	4.56E+02				





9538.8757	4345829.3				
9548.7387	4346333.5				
9558.6017	4346867.9				
9568.4647	4347406.4				
9578.3277	4347936.3				
9588.1907	4348473.5				
9598.0538	4348979.1				
9607.9168	4349526.8				
9617.7798	4350038.4				
9627.6428	4350578.7				
9637.5058	4351109.1				
9647.3688	4351633.6				
9657.2318	4352167.4				
9667.0948	4352686.9				
9676.9579	4353240.1				
9686.8209	4353751.4				
9696.6839	4354294.3				
9706.5469	4354858.1				
9716.4099	4355407				
9726.2729	4355958.7				
9736.1359	4356476.4				
9745.999	4357020				
9755.862	4357535.2				
9765.725	4358097.1				
9775.588	4358616.7				
9785.451	4359158.7				
9795.314	4359677.8				
9805.177	4360214.7				
9815.0401	4360733.2				
9824.9031	4361278.7				
9834.7661	4361794.7				
9844.6291	4362347				
9854.4921	4362871.9				
9864.3551	4363423.6				
9874.2181	4363948.5				
9884.0812	4364497.6				
9893.9442	4365029.8				
9903.8072	4365551.8				
9913.6702	4366099.7				
9923.5332	4366635				
9933.3962	4367162.1				
9943.2592	4367704.6				
9953.1222	4368240.7				
9962.9853	4368775.5				
9972.8483	4369320.9				
9982.7113	4369853.4				
9992.5743	4370386.9				
10000	4370794.3				
@ world xmax	0				
@ world xmin	0				
@ world ymax	3.70794E+12				



	9538.8757	0.36173406			
	9548.7387	0.36170728			
	9558.6017	0.36167889			
	9568.4647	0.36165029			
	9578.3277	0.36162216			
	9588.1907	0.36159364			
	9598.0538	0.36156668			
	9607.9168	0.36153773			
	9617.7798	0.36151058			
	9627.6428	0.36148192			
	9637.5058	0.36145378			
	9647.3688	0.36142596			
	9657.2318	0.36139765			
	9667.0948	0.3613701			
	9676.9579	0.36134077			
	9686.8209	0.36131367			
	9696.6839	0.3612849			
	9706.5469	0.36125502			
	9716.4099	0.36122594			
	9726.2729	0.36119671			
	9736.1359	0.36116929			
	9745.999	0.36114051			
	9755.862	0.36111323			
	9765.725	0.36108348			
	9775.588	0.36105597			
	9785.451	0.36102729			
	9795.314	0.36099982			
	9805.177	0.36097142			
	9815.0401	0.36094399			
	9824.9031	0.36091513			
	9834.7661	0.36088785			
	9844.6291	0.36085864			
	9854.4921	0.36083089			
	9864.3551	0.36080173			
	9874.2181	0.36077399			
	9884.0812	0.36074497			
	9893.9442	0.36071686			
	9903.8072	0.36068929			
	9913.6702	0.36066034			
	9923.5332	0.36063208			
	9933.3962	0.36060424			
	9943.2592	0.36057561			
	9953.1222	0.36054731			
	9962.9853	0.36051909			
	9972.8483	0.36049031			
	9982.7113	0.36046221			
	9992.5743	0.36043407			
	10000	0.36041258			
@	world	xmax	1.00E+04		
@	world	xmin	0.00E+00		
@	world	ymax	8.48E-01		





**Title 40 CFR Part 191
Compliance Certification
Application
for the
Waste Isolation Pilot Plant

PORSURF Attachment 7**



THIS PAGE INTENTIONALLY LEFT BLANK





SANTOS—A Two-Dimensional Finite Element Program for the Quasistatic, Large Deformation, Inelastic Response of Solids

Charles M. Stone
Engineering and Manufacturing Mechanics Department

Sandia National Laboratories
Albuquerque, NM 87185

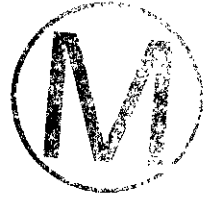
ABSTRACT

SANTOS is a finite element program designed to compute the quasistatic, large deformation, inelastic response of two-dimensional planar or axisymmetric solids. The code is derived from the transient dynamic code PRONTO 2D. The solution strategy used to compute the equilibrium states is based on a self-adaptive dynamic relaxation solution scheme, which is based on explicit central difference pseudo-time integration and artificial mass proportional damping. The element used in SANTOS is a uniform strain 4-node quadrilateral element with an hourglass control scheme to control the spurious deformation modes. Finite strain constitutive models for many common engineering materials are included. A robust master-slave contact algorithm for modeling sliding contact is implemented. An interface for coupling to an external code is also provided.

ACKNOWLEDGMENTS

The author acknowledges the technical contributions of L.M. Taylor and D.P. Flanagan, who developed the PRONTO architecture and provided the framework from which SANTOS is derived. Much of this manual is derived from their original PRONTO manual. Significant contributions to the development of SANTOS were made by several of the early users. J.G. Argüello and G.W. Wellman ran the various versions of the code and provided constructive feedback about its performance and capabilities. Greg Sjaardema produced the early scripts and system procedures that provided the users with an easy way to run the code. Martin Heinstein took a new look at the contact surface problem and significantly improved both the location and application phases of the contact surface algorithm. H.S. Morgan's early work in integration of unified-creep-plasticity models provided the basis for integrating the time-dependent constitutive models. The efforts of the many other individuals who ran early versions of the code and provided helpful comments are gratefully acknowledged.

This report was prepared with the support of the Waste Isolation Pilot Plant (WIPP) Project. The support of WIPP Principal Investigator B.M. Butcher is acknowledged.



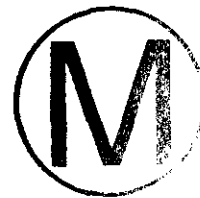


CONTENTS

1.0	INTRODUCTION.....	1
2.0	GOVERNING EQUATIONS.....	3
2.1	Kinematics.....	3
2.2	Stress and Strain Rates.....	5
2.3	Fundamental Equations.....	8
3.0	NUMERICAL FORMULATION.....	9
3.1	Four-Node Uniform Strain Element.....	9
3.1.1	Plane Strain Case.....	11
3.1.2	Axisymmetric Case.....	14
3.1.3	Lumped Mass Matrix.....	17
3.2	Explicit Time Integration.....	18
3.3	Finite Rotation Algorithm.....	18
3.4	Determination of Effective Moduli.....	20
3.5	Determination of the Stable Time Increment.....	21
3.6	Hourglass Control Algorithm.....	22
3.7	Dynamic Relaxation.....	25
3.8	Convergence Measures.....	29
4.0	CONSTITUTIVE MODELS.....	31
4.1	Integration of the Rate Equations.....	31
4.2	Adaptive Time Stepping.....	33
4.3	Basic Definitions and Assumptions.....	34
4.4	Elastic Material, Hooke's Law.....	36
4.5	Elastic Plastic Material with Combined Kinematic and Isotropic Hardening.....	36
4.5.1	Isotropic Hardening.....	38
4.5.2	Kinematic Hardening.....	40
4.5.3	Combined Isotropic and Kinematic Hardening.....	42
4.5.4	Numerical Implementation.....	44
4.6	Soils and Crushable Foams Model.....	47
4.7	Low Density Foams.....	53
4.8	Elastic-Plastic Power Law Hardening Material.....	56
4.9	Power Law Creep Material Model.....	60
4.10	Thermoelastic Material Model.....	61
4.11	Thermoelastic-Plastic Power Law Hardening Material Model.....	63
4.12	Multi-mechanism Deformation (M-D) Creep Model.....	65
4.13	Volumetric Creep Model.....	70
4.14	Viscoelastic Material Model.....	72
5.0	CONTACT SURFACES.....	79
5.1	Location Phase.....	79
5.2	Application Phase.....	81
6.0	LOADS AND BOUNDARY CONDITIONS.....	83
6.1	Kinematic Boundary Conditions.....	83
6.1.1	No Displacement Boundary Conditions.....	83
6.1.2	Prescribed Displacement Boundary Conditions.....	83

CONTENTS (Continued)

6.1.3 Sloping Roller Boundary Conditions.....	83	
6.2 Traction Boundary Conditions and Distributed Loads.....	84 83	8/27/96
6.2.1 Pressure.....	84	
6.2.2 Adaptive Pressure.....	86	
6.2.3 Nodal Forces.....	86	
6.2.4 Gravity Forces, Body Forces, and Distributed Loads.....	86	
6.2.5 Thermal Forces.....	87	
7.0 REFERENCES.....	89	
APPENDIX A: SANTOS Users Manual.....	A-1	
APPENDIX B: User Subroutines.....	B-1	
APPENDIX C: Printed Output Description.....	C-1	
APPENDIX D: Adding a New Constitutive Model to SANTOS.....	D-1	
APPENDIX E: Verification and Sample Problems.....	E-1	





Figures

2.1.1	Original, deformed, and intermediate configurations of a body.....	4
2.2.1	Computed stress-strain curves for a body undergoing simple shear using the Jaumann rate	7
2.2.2	Computed stress-strain curves for a body undergoing simple shear using the Green-Naghdi rate.....	7
3.1.1	Mode shapes for the four-node constant strain quadrilateral element.....	11
3.7.1	A model equilibrium iteration sequence in a multi-dimensional configuration space of nodal point positions developed with dynamic relaxation showing convergence at load step $n + 1$	27
4.5.1	Yield surface in deviatoric stress space.....	37
4.5.2	Conversion of data from a uniaxial tension test to equivalent plastic strain versus von Mises stress.....	39
4.5.3	Geometric interpretation of the consistency condition for kinematic hardening	41
4.5.4	Effect of the choice of the hardening parameter, β , on the computed uniaxial response	43
4.5.5	Geometric interpretation of the incremental form of the consistency condition for combined hardening	45
4.5.6	Geometric interpretation of the radial return correction.....	46
4.6.1	Pressure-dependent yield surface for the soils and crushable foams material model	48
4.6.2	Forms of valid yield surface which can be defined for the soils and crushable foams material model.....	49
4.6.3	Pressure versus volumetric strain curve in terms of a user-defined curve, $F(\epsilon_v)$, for the soils and crushable foams material model	50
4.6.4	Possible loading cases for the pressure versus volumetric strain response using the soils and crushable foams material mode.....	52
4.7.1	Foam volume strain versus mean stress for 6602 foam at various confining pressures	54
4.7.2	Foam volume strain versus mean stress for 9505 foam at various confining pressures	54
4.8.1	Stress versus strain curve for a typical ferritic steel exhibiting Lüders strain.....	58
4.14.1	Mechanical analogy of the standard linear solid.....	73
5.1	Schematic showing the effect of changing the master-slave designation between two surfaces.....	80
5.2.1	Schematic showing the penetration of the master surface by slave node I	81
6.2.1	Definition of a pressure boundary condition along an element side.....	85



1.0 INTRODUCTION

SANTOS is a finite element program developed for quasistatic, large deformation, inelastic analysis of two-dimensional solids. It is a powerful analysis tool that allows the user to address the solution of complex problems that include both material and geometric nonlinearities. The wide variety of constitutive models in the code allows SANTOS to be used for a wide class of problems from geomechanics to metal forming.

In 1986, Taylor and Flanagan at Sandia National Laboratories/New Mexico developed a new transient dynamics finite element code, which they named PRONTO (Taylor and Flanagan, 1987), that replaced the widely used HONDO II (Key et al., 1978) code. PRONTO employed the same explicit central difference time integration operator as HONDO II in addition to some new state-of-the-art features such as a uniform strain quadrilateral element with single point integration, improved critical time step estimates, and more robust contact surfaces. The code was written in a modular fashion with an easy-to-use interface for adding new constitutive models. The code architecture and storage schemes in PRONTO were also developed to take advantage of vector processing on the CRAY computer and to allow for the solution of extremely large problems. It seemed only natural, therefore, to take advantage of the development work of Taylor and Flanagan and adapt PRONTO for the solution of quasistatic problems by adding a self-adaptive dynamic relaxation scheme. A similar procedure was employed when adapting HONDO II to produce the SANCHO (Stone et al., 1985) quasistatic finite element code. The development and use of SANCHO showed that the same excellent results obtained for highly nonlinear transient dynamics problems using explicit methods could be achieved for quasistatic problems using an explicit method such as dynamic relaxation.

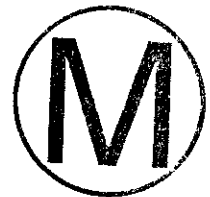
SANTOS belongs to a small but growing class of special purpose finite element codes which use iterative or indirect solution methods to achieve quasistatic solutions. A companion code to SANTOS is JAC (Biffle and Blanford, 1994) which utilizes a nonlinear conjugate gradient iterative scheme for obtaining quasistatic solutions. The solution algorithm in SANTOS is based on a self-adaptive dynamic relaxation scheme with uniform mesh homogenization which is identical to the method used in SANCHO. Because SANTOS is explicit in nature, there is no stiffness matrix to form or to factorize which reduces the amount of computer storage necessary for execution. Dynamic relaxation is not a new quasistatic solution technique with some of the early introductory papers on dynamic relaxation appearing in the mid-1960s. Dynamic relaxation is attractive for three reasons: 1) it is vectorizable, 2) it is versatile, and 3) it is reliable. Because it can be made explicit, it is highly vectorizable for modern digital calculations. In an explicit form, it is ideal for dealing with large deformations, finite strains, inelastic material behavior and contact surfaces. It is reliable in that if the algorithm converges and equilibrium is achieved, then the solution obtained will be good. An early introduction of the idea is given by Otter et al. (1966), but a more recent work which summarizes all of the significant contributions on the topic since Otter et al. can be found in Underwood (1983). Additional information on dynamic relaxation can be found in the paper by Papadarakakis (1974).

There are many features and capabilities in SANTOS that make it a very versatile and user-friendly computer program. The code has a user-oriented data input scheme based on a free-field reader with keyword descriptors that allow the user to define a complex problem with very few commands. The material library in SANTOS contains several nonlinear constitutive models that can be used to model many different engineering materials from

metals to foams. The material model interface is also well documented so that new materials may be easily added. SANTOS has the capability to accept temperature history data from an external source for solving thermal stress problems. If the temperature history changes only in time and is uniform throughout the structure, it can be generated within SANTOS itself. The contact or sliding of two surfaces with friction can also be modeled using SANTOS. Surfaces can open or close as the solution dictates, which allows many physical processes to be realistically modeled. Fixed contact surfaces may be used to join two regions with different mesh discretizations. A code interface (Taylor and Flanagan, 1988) is provided which allows an external, user-generated code to pass data to SANTOS and to access internally computed SANTOS variables. An example of such coupling would be a porous flow code providing a pore pressure field to SANTOS and SANTOS providing updated nodal coordinates and stress components to the external code.

SANTOS resides and is maintained in the Sandia National Laboratories Engineering Analysis Code Access System (SEACAS) (Sjaardema, 1993). The program is designed to work with a separate mesh generation program that produces geometry and connectivity information in the SEACO format (Taylor and Flanagan, 1987). The results from a SANTOS calculation are written in the SEACO format to a separate file for processing by separate graphical post-processing and visualization software. SANTOS is written in standard FORTRAN with any system-dependent coding contained in the SUPES (Red-Horse et al., 1990) utilities package.

In the following sections of this report, a description of the theory and the computational models used in SANTOS are given. A description of the available constitutive models is also provided. Because SANTOS is derived directly from PRONTO, many of the theoretical sections are taken directly from the PRONTO theoretical report. An input guide for use of the program is included along with several sample problems and their solutions.





2.0 GOVERNING EQUATIONS

In this chapter, we present the underlying continuum mechanics concepts necessary to follow the development of the numerical algorithms in the following chapters. Bold face characters denote tensors. The order of the tensor is implied by the context of the equation.

2.1 Kinematics

A material point in the reference configuration B_0 with position vector \mathbf{X} occupies position \mathbf{x} at time t in the deformed configuration B . Hence we write $\mathbf{x} = \chi(\mathbf{X}, t)$. The motion from the original configuration to the deformed configuration shown in Figure 2.1.1 has a deformation gradient \mathbf{F} given by

$$\mathbf{F} = \frac{\partial \mathbf{x}}{\partial \mathbf{X}}, \quad \det(\mathbf{F}) > 0 \quad (2.1.1)$$

Applying the polar decomposition theorem to \mathbf{F} :

$$\mathbf{F} = \mathbf{V} \mathbf{R} = \mathbf{R} \mathbf{U} \quad (2.1.2)$$

where \mathbf{V} and \mathbf{U} are the symmetric, positive definite left and right stretch tensors, respectively, and \mathbf{R} is a proper orthogonal rotation tensor. Figure 2.1.1 illustrates the intermediate orientations defined by the two alternate decompositions of \mathbf{F} defined by Equation (2.1.2). The determination of \mathbf{R} as defined by Equation (2.1.2) presents a significant numerical challenge. In Section 3.3, we describe the incremental algebraic algorithm that we use to determine \mathbf{R} .

The velocity of the material point \mathbf{X} is written as $\mathbf{v} = \dot{\mathbf{x}}$ where the superposed dot indicates time differentiation holding the material point fixed. The velocity gradient is denoted by \mathbf{L} and may be expressed as

$$\mathbf{L} = \frac{\partial \mathbf{v}}{\partial \mathbf{x}} = \frac{\partial \mathbf{v}}{\partial \mathbf{X}} \frac{\partial \mathbf{X}}{\partial \mathbf{x}} = \dot{\mathbf{F}} \mathbf{F}^{-1} \quad (2.1.3)$$

The velocity gradient can be written in terms of the symmetric (\mathbf{D}) and antisymmetric (\mathbf{W}) parts, respectively,

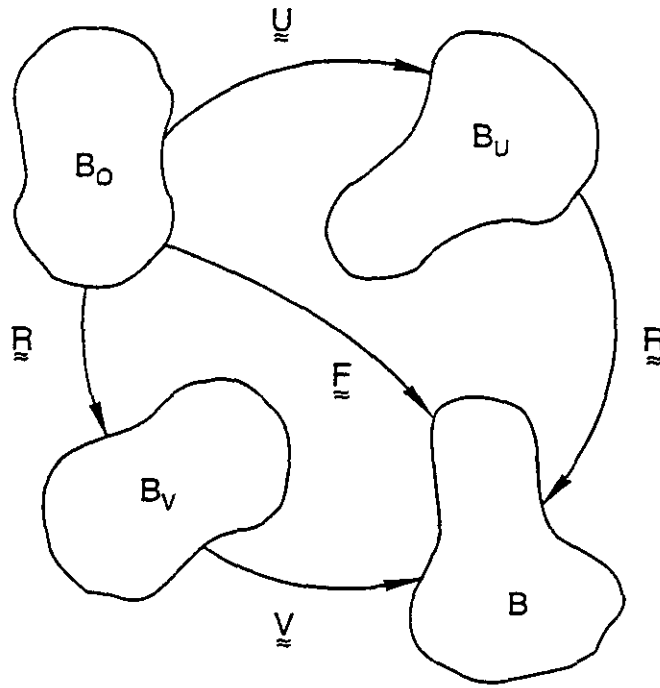
$$\mathbf{L} = \mathbf{D} + \mathbf{W} \quad (2.1.4)$$

Using the right decomposition from Equation (2.1.2) in Equation (2.1.3) gives

$$\mathbf{L} = \dot{\mathbf{R}} \mathbf{R}^T + \mathbf{R} \dot{\mathbf{U}} \mathbf{U}^{-1} \mathbf{R}^T \quad (2.1.5)$$

Dienes [13] denoted the first term on the right-hand side of Equation (2.1.5) by Ω :

$$\Omega = \dot{\mathbf{R}} \mathbf{R}^T \quad (2.1.6)$$



TRI-6348-2-0

Figure 2.1.1. Original, deformed, and intermediate configurations of a body.

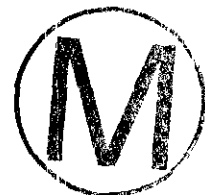
Both \mathbf{W} and $\mathbf{\Omega}$ are antisymmetric and represent a rate of rotation (or angular velocity) about some axes. In general, $\mathbf{\Omega} \neq \mathbf{W}$. The difference arises when the last term of Equation (2.1.5) is not symmetric. The symmetric part of $\dot{\mathbf{U}} \mathbf{U}^{-1}$ is the unrotated deformation rate tensor \mathbf{d} as defined below (note that both $\dot{\mathbf{U}}$ and \mathbf{U}^{-1} are symmetric).

$$\mathbf{d} = \frac{1}{2} (\dot{\mathbf{U}} \mathbf{U}^{-1} + \mathbf{U}^{-1} \dot{\mathbf{U}}) = \mathbf{R}^T \mathbf{D} \mathbf{R} \quad . \quad (2.1.7)$$

There are two possible cases which can cause rotation of a material line element: rigid body rotation and shear. Because total shear vanishes along the axes of principal stretch, the rotation of these axes defines the total rigid body rotation of a material point.

It is a simple exercise in vector analysis to show that Equation (2.1.6) represents the rate of rigid body rotation at a material point as shown by Dienes (1979). It is equally simple to show that \mathbf{W} represents the rate of rotation of the principal axes of the rate of deformation \mathbf{D} . Since \mathbf{D} and \mathbf{W} have no sense of the history of deformation, they are not sufficient to define the rate of rotation in a finite deformation context.

Line elements where the rate of shear vanishes rotate solely due to rigid body rotations. These line elements are along the principal axes of $\dot{\mathbf{U}}$. We will apply a similar observation below as we derive Dienes' (1979) expression for calculating $\mathbf{\Omega}$:





Using the left decomposition of Equation (2.1.2) in Equation (2.1.3) gives

$$\mathbf{L} = \dot{\mathbf{V}} \mathbf{V}^{-1} + \mathbf{V} \boldsymbol{\Omega} \mathbf{V}^{-1} \quad (2.1.8)$$

Postmultiplying by \mathbf{V} yields an expression which defines the decomposition of \mathbf{L} into \mathbf{V} and $\boldsymbol{\Omega}$:

$$\mathbf{L} \mathbf{V} = \dot{\mathbf{V}} + \mathbf{V} \boldsymbol{\Omega} \quad (2.1.9)$$

When the dual vector of the above expression is taken, the symmetric $\dot{\mathbf{V}}$ vanishes to yield a set of three linear equations for the three independent components of $\boldsymbol{\Omega}$.

The antisymmetric part of a tensor may be expressed in terms of its dual vector and the permutation tensor ϵ_{ijk} . Define the following dual vectors;

$$\omega_i = \epsilon_{ijk} \Omega_{jk} \quad (2.1.10)$$

$$w_i = \epsilon_{ijk} W_{jk} \quad (2.1.11)$$

Using Equations (2.1.4), (2.1.10), and (2.1.11) in Equation (2.1.9) results in the expression that Dienes (1979) gave for determining $\boldsymbol{\Omega}$ from \mathbf{W} and \mathbf{V} ;

$$\boldsymbol{\omega} = \mathbf{w} - 2[\mathbf{V} - \mathbf{I} \operatorname{tr}(\mathbf{V})]^{-1} \mathbf{z} \quad (2.1.12)$$

where

$$z_i = \epsilon_{ijk} V_{jm} D_{mk} \quad (2.1.13)$$

We observe from the above expressions that $\boldsymbol{\Omega} = \mathbf{W}$ if and only if the product $\mathbf{V} \mathbf{D}$ is symmetric. This condition requires that the principal axes of the deformation rate \mathbf{D} coincide with the principal axes of the current stretch \mathbf{V} . Clearly, a pure rotation is a special case of this condition since \mathbf{D} , and consequently Equation (2.1.13), vanish.

2.2 Stress and Strain Rates

Our constitutive model architecture is posed in terms of the conventional Cauchy stress, but we adopt the approach of Johnson and Bammann (1984) and define a Cauchy stress in the unrotated configuration. The reader seeking more detail than is presented here should see Flanagan and Taylor (1987). The "true" stress in the deformed configuration is denoted by \mathbf{T} . The Cauchy stress in the unrotated configuration is denoted by $\boldsymbol{\sigma}$. These two stress measures are related by

$$\boldsymbol{\sigma} = \mathbf{R}^T \mathbf{T} \mathbf{R} \quad (2.2.1)$$

Each material point in the unrotated configuration has its own reference frame which rotates such that the deformation in this frame is a pure stretch. Then \mathbf{T} is simply the tensor $\boldsymbol{\sigma}$ in the fixed global reference frame. The conjugate strain rate measures to \mathbf{T} and $\boldsymbol{\sigma}$ are \mathbf{D} and \mathbf{d} , respectively. These strain rates were defined by Equations (2.1.4) and (2.1.7), respectively.

conjugate strain rate measures to T and σ are D and d , respectively. These strain rates were defined by Equations (2.1.4) and (2.1.7), respectively.

The Principal of Material Frame Indifference (or objectivity) stipulates that a constitutive law must be insensitive to a change of reference frame (Truesdell, 1966). This requires that only objective quantities may be used in a constitutive law. An objective quantity is one which transforms in the same manner as the energy conjugate stress and strain rate pair under a superposed rigid body motion. The fundamental advantage of the unrotated stress over the true stress is that the material derivative of σ is objective, whereas the material derivative of T is not.

The Jaumann rate defined below is frequently used in constitutive relationships to resolve the need for an objective rate of Cauchy stress.

$$\hat{T} = \dot{T} - W T + T W \quad (2.2.2)$$

A similar stress rate, called the Green-Naghdi rate by Johnson and Bammann (1984) can be derived by transforming the rate of the unrotated Cauchy stress to the fixed global frame as follows:

$$\hat{\sigma} = R \dot{\sigma} R^T = \dot{T} - \Omega T + T \Omega \quad (2.2.3)$$

The Jaumann rate and the Green-Naghdi rate are very similar in form. The important difference between the two is that the Green-Naghdi rate is kinematically consistent with the rate of Cauchy stress, while the Jaumann rate is not. By this statement we mean that $\hat{\sigma}$ is identical to \dot{T} in the absence of rigid body rotations. It is clear that \hat{T} need not equal \dot{T} under the same conditions since W need not vanish with rigid body rotations.

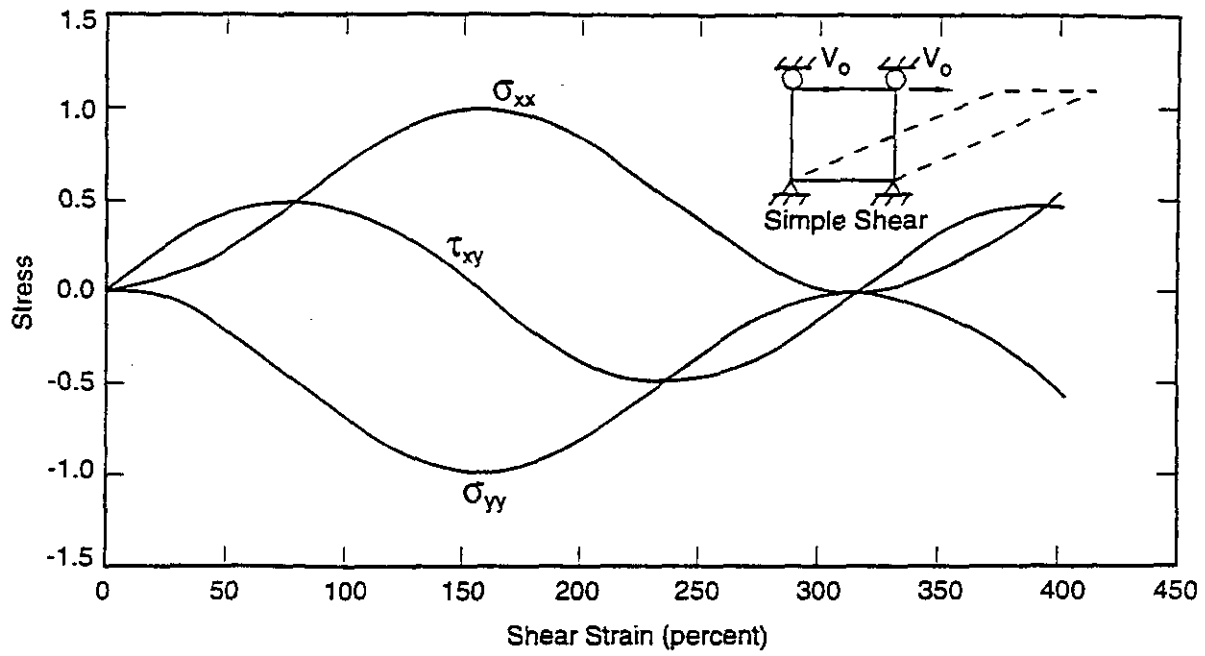
The simple shear problem presented by Dienes (1979) serves as an excellent demonstration of the symptoms which can occur due to the deficiency of the Jaumann rate. Figure 2.2.1 shows a body which undergoes the following motion:

$$x(t) = X + k t Y, \quad y(t) = Y, \quad z(t) = Z \quad (2.2.4)$$

Dienes applied a simple linear isotropic hypoelastic material law to both the Jaumann rate (2.2.2) and the Green-Naghdi rate (2.2.3). The analytic solution for the true stresses as a function of time using the Jaumann rate is shown in Figure 2.2.1. The Green-Naghdi rate solution is shown in Figure 2.2.2 and demonstrates a monotonic increase in stress with increasing shear strain, while the Jaumann rate results in a harmonic oscillation of the stress. The reason that the Jaumann rate produces this oscillation in stress is that W gives a constant rate of rotation for the motion defined by Equation (2.2.4), while Ω vanishes with time. Clearly, the body experiences rotations which diminish over time, but the Jaumann rate continues to drive the stress convection terms at a constant rate. This leads to the oscillatory behavior of the stresses shown in Figure 2.2.1.

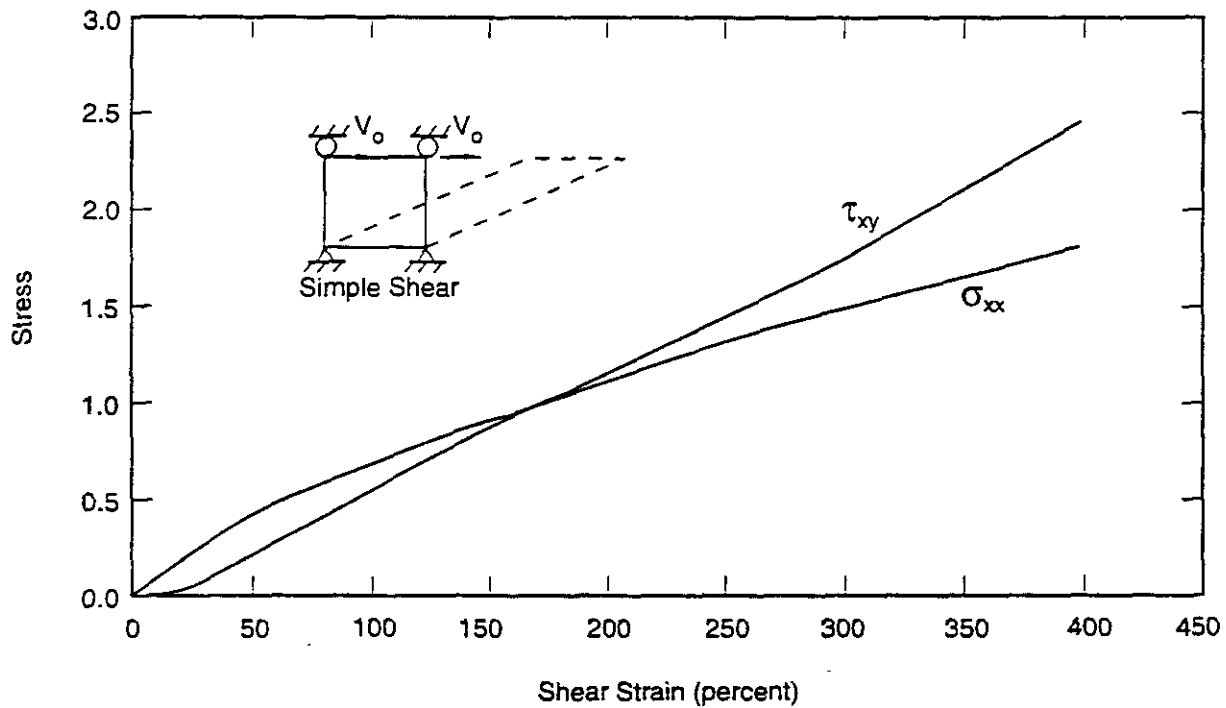
A distinct advantage of the unrotated reference frame is that all constitutive models are cast without regard to finite rotations. This greatly simplifies the numerical implementation of new constitutive models. The rotations of





TRI-6348-3-0

Figure 2.2.1. Computed stress-strain curves for a body undergoing simple shear using the Jaumann rate.



TRI-6348-4-0

Figure 2.2.2. Computed stress-strain curves for a body undergoing simple shear using the Green-Naghdi rate.

global state variables (e.g., stress and strain) are dealt with on a global level which ensures that all constitutive models are consistent. Internal state variables (e.g., backstress) see no rotations whatsoever.

The drawback to working in the unrotated reference frame is that we must accurately determine the rotation tensor, \mathbf{R} , which is not a straightforward numerical calculation. We present an incremental, algebraic algorithm to accomplish this task in Section 3.4.

2.3 Fundamental Equations

The equilibrium equation for the body is

$$\text{div } \mathbf{T} + \rho \mathbf{b} = 0 \quad (2.3.1)$$

where ρ is the mass density per unit volume and \mathbf{b} is a specific body force vector.

We seek the solution to Equation (2.3.1) subject to the boundary conditions

$$\mathbf{u} = \mathbf{f}(t) \text{ on } S_u \quad (2.3.2)$$

where S_u represents the portion of the boundary on which kinematic quantities are specified (displacement). In addition to satisfying the kinematic boundary conditions given by Equation (2.3.2), we must satisfy the traction boundary conditions

$$\mathbf{T} \cdot \mathbf{n} = \mathbf{s}(t) \text{ on } S_T \quad (2.3.3)$$

where S_T represents the portion of the boundary on which tractions are specified. The boundary of the body is given by the union of S_u and S_T , and we note that for a valid mechanics problem S_u and S_T have a null intersection.

The jump conditions at all contact discontinuities must satisfy the relation

$$(\mathbf{T}^+ - \mathbf{T}^-) \cdot \mathbf{n} = 0 \text{ on } S_c \quad (2.3.4)$$

where S_c represents the contact surface intersection and the subscripts "+" and "-" denote different sides of the contact surface.

To utilize dynamic relaxation as a solution strategy for quasistatics problems, we must first convert the equilibrium equations into equations of motion by adding an acceleration term. Thus,

$$\text{div } \mathbf{T} + \rho \mathbf{b} = \rho \ddot{\mathbf{u}} \quad (2.3.5)$$

where $\ddot{\mathbf{u}}$ is the acceleration of the material point. Now, all that remains is to introduce the concept of mesh homogenization and artificial damping as well as integrate forward in time from initial conditions until the transient dynamic response has damped out to the static result with equilibrium satisfied. Further description of the implementation of the dynamic relaxation method will be discussed in a later section (Section 3.7).





3.0 NUMERICAL FORMULATION

In this chapter, we describe the finite element formulation of the problem and the numerical algorithms required to perform the spatial and temporal integration of the equations of motion.

3.1 Four-Node Uniform Strain Element

The four-node two-dimensional isoparametric element is widely used in computational mechanics. Optimal integration schemes for these elements, however, present a dilemma. A one-point integration of the element under-integrates the element, resulting in a rank deficiency for the element which manifests itself in spurious zero energy modes, commonly referred to as hourglass modes. A two-by-two integration of the element over-integrates the element and can lead to serious problems of element locking in fully plastic and incompressible problems. The four-point integration also carries a tremendous computational penalty compared to the one-point rule. We use the one-point integration of the element and implement an hourglass control scheme to eliminate the spurious modes. The development presented below follows directly from Flanagan and Belytschko (1981). We assume that the reader is somewhat familiar with the finite element method and will not go into a complete description of the method. The reader can consult numerous texts on the method (Hughes, 1987).

The quadrilateral element relates the spatial coordinates x_i to the nodal coordinates x_{iI} through the isoparametric shape functions ϕ_I as follows:

$$x_i = x_{iI} \phi_I(\xi, \eta) . \quad (3.1.1)$$

In accordance with indicial notation convention, repeated subscripts imply summation over the range of that subscript. The lowercase subscripts have a range of two, corresponding to the two-dimensional spatial coordinate directions. Uppercase subscripts have a range of four, corresponding to the element nodes.

The same shape functions are used to define the element displacement field in terms of the nodal displacements u_{iI}

$$u_i = u_{iI} \phi_I . \quad (3.1.2)$$

Since the same shape functions apply to both spatial coordinates and displacements, their material derivative (represented by a superposed dot) must vanish. Hence, the velocity field may be given by

$$\dot{u}_i = \dot{u}_{iI} \phi_I \quad (3.1.3)$$

and likewise for the acceleration field

$$\ddot{u}_i = \ddot{u}_{iI} \phi_I . \quad (3.1.4)$$

The velocity gradient tensor, L , is defined in terms of nodal velocities as

$$L_{ij} = \dot{u}_{i,j} = \dot{u}_{iI} \phi_{I,j} . \quad (3.1.5)$$

By convention, a comma preceding a lowercase subscript denotes differentiation with respect to the spatial coordinates (e.g., $\dot{u}_{i,j}$ denotes $\partial \dot{u}_i / \partial x_j$).

The two-dimensional isoparametric-shape functions map the unit square in ξ - η to an arbitrary quadrilateral in x - y , as shown in Figure 3.1.1. We choose to center the unit square at the origin in ξ - η space so that the shape functions may be conveniently expanded in terms of an orthogonal set of base vectors, given in Table 3.1, as follows:

$$\phi_I = \frac{1}{4} \Sigma_I + \frac{1}{2} \xi \Lambda_{1I} + \frac{1}{2} \eta \Lambda_{2I} + \xi \eta \Gamma_I \quad (3.1.6)$$

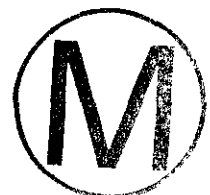
Table 3.1

node	ξ	η	Σ_I	Λ_{1I}	Λ_{2I}	Γ_I
1	-.5	-.5	1	-1	-1	1
2	.5	-.5	1	1	-1	-1
3	.5	.5	1	1	1	1
4	-.5	.5	1	-1	1	-1

The above vectors represent the displacement modes of a unit square. The first vector, Σ_I , accounts for rigid body translation. We call Σ the summation vector since it may be employed in indicial notation to represent the algebraic sum of a vector.

The linear base vectors Λ_{iI} may be readily combined to define the uniform normal strains and shear strain in the element. We refer to Λ_{iI} as the volumetric base vectors since, as we will illustrate below, they are the only base vectors that appear in the element area expression.

The last vector, Γ_I , gives rise to linear strain modes that are neglected in the uniform strain integration. This vector defines the hourglass patterns for a unit cube. The displacement modes represented by the vectors in Table 3.1 are also shown in Figure 3.1.1.



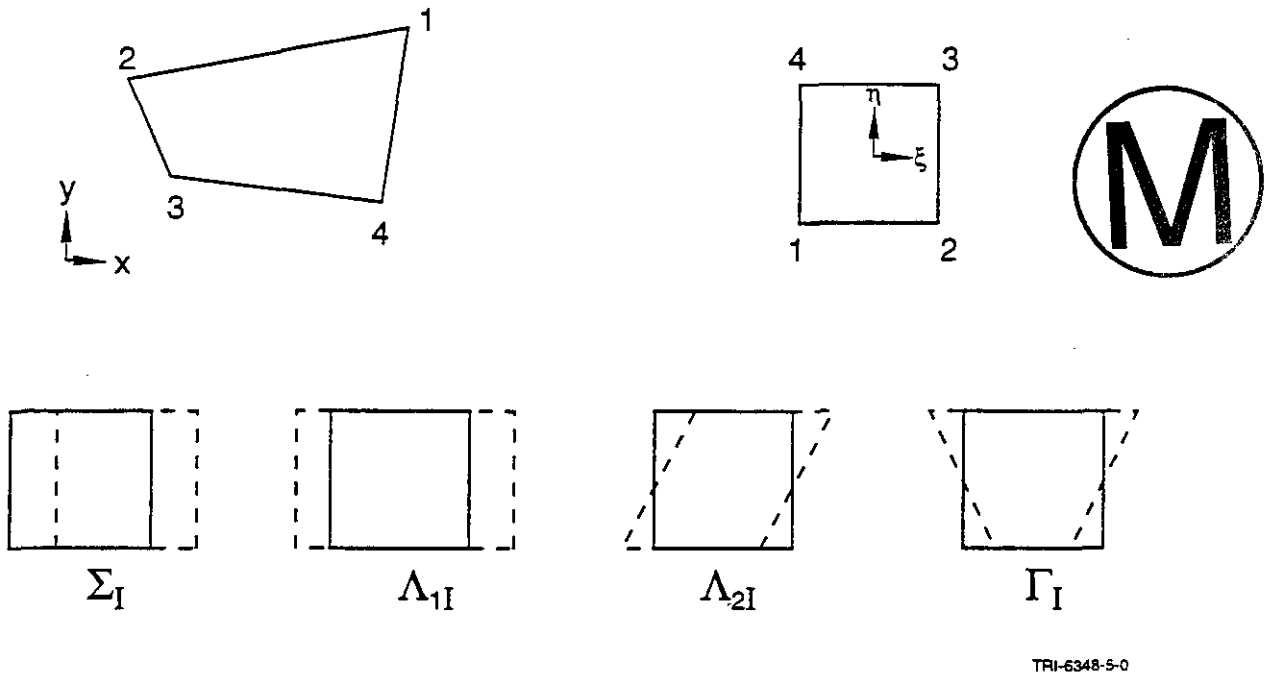


Figure 3.1.1. Mode shapes for the four-node constant strain quadrilateral element.

3.1.1 Plane Strain Case

In the finite element method, we replace the momentum Equation (2.3.5) with a weak form of the equation. Using the principle of virtual work, we write the weak form of the equation as

$$\sum_e \int_{V_e} (\mathbf{T}_{ij,j} + \rho b_i - \rho \ddot{u}_i) \delta u_i \, dV = 0 \quad (3.1.7)$$

where δu_i represents an arbitrary virtual displacement field, with the same interpolation as Equation (3.1.2), which satisfies the kinematic constraints. In plane strain, the thickness of the body is considered uniform and arbitrary and therefore can be eliminated from the preceding expression. Integrating by parts and applying Gauss' divergence theorem to Equation (3.1.7) then gives

$$\sum_e \left[\int_{S_e} \mathbf{T}_{ij} n_j \delta u_i \, d\ell - \int_{A_e} \mathbf{T}_{ij} \delta u_{i,j} \, dA + \int_{A_e} \rho b_i \delta u_i \, dA - \int_{A_e} \rho \ddot{u}_i \delta u_i \, dA \right] = 0 \quad (3.1.8)$$

The summation symbol represents the assembly of element force vectors into a global nodal force array. We assume that the reader understands the details of this assembly; we will not discuss it further in this document.

The second integral in the preceding equation is used to define the element internal force vector f_{iI} as

$$\delta u_{iI} f_{iI} = \int_{A_e} T_{ij} \delta u_{i,j} dA \quad (3.1.9)$$

The first and third integrals define the external force vector, and the fourth integral defines the inertial response.

We perform one-point integration by neglecting the nonlinear portion of the element displacement field, thereby considering a state of uniform strain and stress. The preceding expression is approximated by

$$f_{iI} = \bar{T}_{ij} \int_{A_e} \phi_{I,j} dA \quad (3.1.10)$$

where we have eliminated the arbitrary virtual displacements, and \bar{T}_{ij} represents the assumed uniform stress tensor. By neglecting the nonlinear displacements, we have assumed that the mean stresses depend only on the mean strains. Mean kinematic quantities are defined by integrating over the element as follows:

$$\bar{u}_{i,j} = \frac{1}{A} \int_V \dot{u}_{i,j} dA \quad (3.1.11)$$

We now define the discrete gradient operator as

$$B_{iI} = \int_A \phi_{I,i} dA \quad (3.1.12)$$

The mean velocity gradient, applying Equation (3.1.5), is given by

$$\dot{\bar{u}}_{i,j} = \frac{1}{A} \dot{u}_{iI} B_{jI} \quad (3.1.13)$$

Combining Equations (3.1.10) and (3.1.12), we may express the nodal forces by

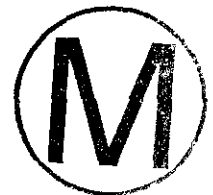
$$f_{iI} = \bar{T}_{ij} B_{jI} \quad (3.1.14)$$

Computing nodal forces with this integration scheme requires evaluation of the gradient operator and the element area. These two tasks are linked since

$$x_{i,j} = \delta_{ij} \quad (3.1.15)$$

where δ_{ij} is the Kroneker delta. Equations (3.1.1), (3.1.12), and (3.1.15) yield

$$x_{iI} B_{jI} = \int_V (x_{iI} \phi_{I,j}) dA = A \delta_{ij} \quad (3.1.16)$$





Consequently, the gradient operator may be expressed by

$$B_{II} = \frac{\partial A}{\partial x_{II}} \quad (3.1.17)$$

To integrate the element area in closed form, we use the Jacobian of the isoparametric transformation to transform the integral in x-y space to an integral over the unit square:

$$A = \int_{-1/2}^{+1/2} \int_{-1/2}^{+1/2} J \, d\eta \, d\xi \quad (3.1.18)$$

where

$$J = \frac{\partial x}{\partial \xi} \frac{\partial y}{\partial \eta} - \frac{\partial x}{\partial \eta} \frac{\partial y}{\partial \xi} \quad (3.1.19)$$

Therefore, Equation (3.1.18) can be written as

$$A = x_I y_J C_{IJ} \quad (3.1.20)$$

where

$$C_{IJ} = \int_{-1/2}^{1/2} \int_{-1/2}^{1/2} \left(\frac{\partial \phi_I}{\partial \xi} \frac{\partial \phi_J}{\partial \eta} - \frac{\partial \phi_I}{\partial \eta} \frac{\partial \phi_J}{\partial \xi} \right) d\eta \, d\xi \quad (3.1.21)$$

In light of Equation (3.1.6), the above integration involves at most bilinear functions. Therefore, only the constant term does not vanish and the integration yields

$$C_{IJ} = \frac{1}{4} (\Lambda_{II} \Lambda_{2J} - \Lambda_{2I} \Lambda_{IJ}) \quad (3.1.22)$$

Note that C_{IJ} is antisymmetric:

$$C_{IJ} = -C_{JI} \quad (3.1.23)$$

Evaluating Equation (3.1.22), we obtain the following explicit representation for C_{IJ} :

$$C_{IJ} = \frac{1}{2} \begin{bmatrix} 0 & 1 & 0 & -1 \\ -1 & 0 & 1 & 0 \\ 0 & -1 & 0 & 1 \\ 1 & 0 & -1 & 0 \end{bmatrix} \quad (3.1.24)$$

Substituting the above expression into Equation (3.1.20), we obtain the familiar expression for the area of a quadrilateral:

$$A = \frac{1}{2}[(x_3 - x_1)(y_4 - y_2) + (x_2 - x_4)(y_3 - y_1)] \quad (3.1.25)$$

Using this result in Equation (3.1.17), the B matrix may be expressed as

$$B_{IJ} = C_{IJ} \begin{Bmatrix} y_j \\ -x_j \end{Bmatrix} = \frac{1}{2} \begin{bmatrix} (y_2 - y_4)(y_3 - y_1)(y_4 - y_2)(y_1 - y_3) \\ (x_4 - x_2)(x_1 - x_3)(x_2 - x_4)(x_3 - x_1) \end{bmatrix} \quad (3.1.26)$$

The mean stress approach used here gives the same result in two dimensions as the one-point quadrature rule for the quadrilateral because the Jacobian is at most bilinear.

3.1.2 Axisymmetric Case

The axisymmetric quadrilateral poses a special problem for the finite element method in that we must reduce a three-dimensional variational Equation (3.1.7) to a two-dimensional element domain. The formulation is complicated by the fact that the variational principle is cast in cylindrical, rather than Cartesian coordinates.

We will start by defining the cylindrical coordinate system as follows:

$$r^\alpha = (r, z, \theta) \quad (3.1.27)$$

While the above ordering of the coordinates is unconventional (and not right-handed), it degrades cleanly to the axisymmetric case. Note that Greek indices have a range of three and that superscripts and subscripts indicate contravariant and covariant tensor components, respectively.

The shape functions of the axisymmetric uniform strain quadrilateral are the same as those for the plane strain case (Table 3.1) and are defined implicitly in terms of the nodal coordinates

$$r_i = r_{iI} \phi_I \quad (3.1.28)$$

Note that lowercase English indices have a range of two and that, since the two-dimensional coordinate system is Cartesian, there is no distinction between covariant and contravariant tensor components.

In our Lagrangian formulation, the same shape functions are applied to the displacement fields. This implies that the material derivatives of the shape functions vanish. As a result, these shape functions also apply to the velocity field, just as in the plane strain case:

$$\dot{r}_i = \dot{r}_{iI} \phi_I \quad (3.1.29)$$

The weak form given by Equation (3.1.7) is expressed in cylindrical coordinates as

$$\int_{V_e} \left(T^{\alpha\beta} |_{,\beta} + \rho b^\alpha - \rho \ddot{u}^\alpha \right) \delta u_\alpha dV = 0 \quad (3.1.30)$$



We are now faced with a three-dimensional variational principle, but only a two-dimensional element. Because the differential of volume imposes a factor of r on the differential of area ($dV = 2\pi r dA$), there is an implicit r weighting on the integrand of the weak form in Equation (3.1.30). This means that the integrand vanishes near the axis of symmetry ($r = 0$) regardless of the variations! This also means that the discretized equations generated by the finite element method become ill-conditioned near the axis.

This difficulty is resolved by dividing the integrand of Equation (3.1.30) by r to reduce the integration to the element domain. However, we must carry this weighting factor in order to apply Gauss' theorem in three dimensions. This technique was referred to as a Petrov-Galerkin, or area-weighted finite element, formulation by Goudreau and Hallquist (1982).

$$\sum_e \left[\frac{1}{2\pi} \int_{V_e} \Gamma^{\alpha\beta} \left| \left(\frac{1}{r} \delta u_\alpha \right) \right|_\beta dV + \int_{A_e} \rho b^\alpha \delta u_\alpha dA - \int_{A_e} \rho \ddot{u}^\alpha \delta u_\alpha dA \right] = 0 \quad (3.1.31)$$

Integrating by parts and applying Gauss' theorem yields the following:

$$\sum_e \left[\int_{S_e} \Gamma^{\alpha\beta} \delta u_\alpha n_\beta ds - \int_{A_e} \Gamma^{\alpha\beta} \left(\frac{1}{r} \delta u_\alpha \right) \right|_\beta r dA + \int_{A_e} \rho b^\alpha \delta u_\alpha dA - \int_{A_e} \rho \ddot{u}^\alpha \delta u_\alpha dA \right] = 0 \quad (3.1.32)$$

Evaluating the covariant derivative in the preceding equation yields

$$\begin{aligned} \left(\frac{1}{r} \delta u_\alpha \right) \right|_\beta &= \left(\frac{1}{r} \delta u_\alpha \right)_{,\beta} - \Gamma_{\alpha\beta}^\gamma \left(\frac{1}{r} \delta u_\gamma \right) \\ &= \frac{1}{r} \delta u_{\alpha,\beta} - \frac{1}{r} \Gamma_{\alpha\beta}^\gamma \delta u_\gamma - \frac{1}{r^2} \delta_{1\beta} \delta u_\alpha \end{aligned} \quad (3.1.33)$$

where $\Gamma_{\alpha\beta}^\gamma$ are the Euclidian Christoffel symbols associated with the cylindrical coordinate system. The only nonzero components are

$$\Gamma_{33}^1 = -r \quad (3.1.34)$$

$$\Gamma_{13}^3 = \Gamma_{31}^3 = \frac{1}{r}$$

We are now in a position to degenerate the variational equations to the axisymmetric case. The axisymmetry conditions require that variations and derivatives in θ vanish. Combining Equations (3.1.32) to (3.1.34) and enforcing axisymmetry gives





$$\sum_e \left[\int_{S_e} T_{ij} n_j \delta u_i dS - \int_{A_e} \left(T_{ij} \delta u_{i,j} + r T^{33} \delta u_1 - \frac{1}{r} T_{ij} \delta u_i \right) dA \right. \\ \left. + \int_{A_e} \rho b_i \delta u_i dA - \int_{A_e} \rho \ddot{u}_i \delta u_i dA \right] = 0 \quad (3.1.35)$$

Note that we have dropped the contravariant superscript notation for English indices in going from Equations (3.1.32) to (3.1.35) because as we stated previously, there is no distinction between contravariant and covariant components in our two-dimensional coordinate system.

A byproduct of the Petrov-Galerkin formulation is that the resulting weak form for the axisymmetric case, Equation (3.1.35), is nearly identical to that of the plane strain case, Equation (3.1.8). The only difference is the addition of the last two terms to the internal force expression, which is the second integral above. This is clearly a major architectural advantage to SANTOS.

Note that the last term of the axisymmetric internal force expression is not associated with strain. These forces are analogous to the convected force term which appears in the stress divergence as shown below.

$$T^{\alpha\beta} \Big|_{\beta} = T^{\alpha\beta}{}_{,\beta} + \Gamma_{\gamma\beta}^{\alpha} T^{\gamma\beta} + \Gamma_{\gamma\beta}^{\beta} T^{\alpha\gamma} \\ = T^{\alpha\beta}{}_{,\beta} + \Gamma_{\gamma\beta}^{\alpha} T^{\gamma\beta} + \frac{1}{r} T^{\alpha 1} \quad (3.1.36)$$

If the $1/r$ correction is omitted in Equation (3.1.31), the final term in the axisymmetric internal force disappears.

It is convenient for a finite element program to work with physical, rather than tensoral, stress components. In our formulation, the hoop stress is the only component which requires such a distinction. The physical hoop stress T_{33} is given by

$$T_{33} = r^2 T_{33} \quad (3.1.37)$$

The internal forces are then given by

$$f_{iI} = \int_A T_{ij} \phi_{I,j} dA + \int_A (T_{33} \delta_{i1} - T_{i1}) \frac{1}{r} \phi_I dA \quad (3.1.38)$$

Evaluating all these integrals with single-point integration yields

$$f_{iI} = \bar{T}_{ij} B_{jI} + (T_{33} \delta_{i1} - T_{i1}) \frac{A}{4\bar{r}} \Sigma_I \quad (3.1.39)$$

where

$$\bar{r} = \frac{1}{4} \Sigma_I r_I \quad (3.1.40)$$

We now see that the internal force vector for the axisymmetric case, Equation (3.1.39), is the same as that for the plane strain case, Equation (3.1.14), with the addition of the hoop stress and covected forces.

The velocity gradient in cylindrical coordinates is

$$\dot{u}_\alpha|_\beta = \dot{u}_{\alpha,\beta} - \Gamma_{\alpha\beta}^\gamma \dot{u}_\gamma \quad (3.1.41)$$

Substituting Equation (3.1.34) into the above equation and enforcing axisymmetry leaves only five nonzero components: the four in-plane components, and the physical hoop strain rate D_{33} . This additional strain rate component is defined conjugate to Equation (3.1.37) as

$$D_{33} = \frac{1}{2} \dot{u}_{33} = \frac{\dot{u}_1}{r} \quad (3.1.42)$$

We evaluate this quantity with one-point integration as follows:

$$\bar{D}_{33} = \frac{\dot{\bar{u}}_1}{\bar{r}} \quad (3.1.43)$$

where \bar{r} is given by Equation (3.1.40) and

$$\dot{\bar{u}}_1 = \frac{1}{4} \sum_I \dot{u}_{II} \quad (3.1.44)$$

3.1.3 Lumped Mass Matrix

One of the aforementioned advantages of using the Petrov-Galerkin method for the axisymmetric case is that the inertial terms in the variational statement of the boundary value problem are identical for both the plane strain, Equation (3.1.8), and axisymmetric, Equation (3.1.35), cases. Therefore, we can treat both cases at one time.

To reap the benefits of an explicit architecture, we must diagonalize the mass matrix. We do this by integrating the inertial energy variation as follows:

$$\int_A \rho u_i \delta u_i dA = \ddot{u}_{II} m_{IJ} \delta u_{IJ} \quad (3.1.45)$$

where

$$m_{IJ} = \rho A \delta_{IJ} \quad (3.1.46)$$

and δ_{IJ} is the Kroneker delta. Clearly, the assembly process for the global mass matrix from the individual element matrices results in a global mass matrix which is diagonal and can be expressed as a vector, M_I .



3.2 Explicit Time Integration

SANTOS uses a modified central difference scheme to integrate the equations of motion through time. By this we mean that the velocities are integrated with a forward difference, while the displacements are integrated with a backward difference. The integration scheme for a node is expressed as

$$\ddot{u}_t = (f_t^{\text{EXT}} - f_t^{\text{INT}}) / M \quad (3.2.1)$$



$$\dot{u}_{t+\Delta t} = \dot{u}_t + \Delta t \ddot{u}_t \quad (3.2.2)$$

and

$$u_{t+\Delta t} = u_t + \Delta t \dot{u}_{t+\Delta t} \quad (3.2.3)$$

where f_t^{EXT} and f_t^{INT} are the external and internal nodal forces, respectively, M is the nodal point lumped mass, and Δt is the time increment.

The central difference operator is conditionally stable. It can be shown that the Courant stability limit for the operator is given in terms of the highest eigenvalue in the system (ω_{max}):

$$\Delta t \leq \frac{2}{\omega_{\text{max}}} \quad (3.2.4)$$

In Section 3.5, we discuss how the highest eigenvalue is approximated and how we determine a stable time increment.

3.3 Finite Rotation Algorithm

We stated in Section 2.2 that one of our fundamental numerical challenges in the development of an accurate algorithm for finite rotations was the determination of \mathbf{R} , the rotation tensor defined by the polar decomposition of the deformation gradient \mathbf{F} . We developed an incremental algorithm for reasons of computational efficiency and numerical accuracy. The validity of the unrotated reference frame is based on the orthogonal transformation given by Equation (2.2.1). Therefore, the crux of integrating Equation (2.1.6) for \mathbf{R} is to maintain the orthogonality of \mathbf{R} . If one integrates $\dot{\mathbf{R}} = \boldsymbol{\Omega}\mathbf{R}$ via a forward difference scheme, the orthogonality of \mathbf{R} degenerates rapidly no matter how fine the time increments. We instead adapted the algorithm of Hughes and Winget (1980) for integrating incremental rotations as follows.

A rigid body rotation over a time increment Δt may be represented by

$$\mathbf{x}_{t+\Delta t} = \mathbf{Q}_{\Delta t} \mathbf{x}_t \quad (3.3.1)$$

where $\mathbf{Q}_{\Delta t}$ is a proper orthogonal tensor with the same rate of rotation as \mathbf{R} given by Equation (2.1.6). The total rotation \mathbf{R} is updated via the highly accurate expression below.

$$\mathbf{R}_{t+\Delta t} = \mathbf{Q}_{\Delta t} \mathbf{R}_t . \quad (3.3.2)$$

For a constant rate of rotation, the midpoint velocity and the midpoint coordinates are related by

$$\frac{1}{\Delta t} (\mathbf{x}_{t+\Delta t} - \mathbf{x}_t) = \frac{1}{2} \Omega (\mathbf{x}_{t+\Delta t} + \mathbf{x}_t) . \quad (3.3.3)$$

Combining Equations (3.3.1) and (3.3.3) yields

$$(\mathbf{Q}_{\Delta t} - \mathbf{I}) \mathbf{x}_t = \frac{\Delta t}{2} \Omega (\mathbf{Q}_{\Delta t} + \mathbf{I}) \mathbf{x}_t . \quad (3.3.4)$$

Since \mathbf{x}_t is arbitrary in Equation (3.3.4), it may be eliminated. We then solve for $\mathbf{Q}_{\Delta t}$. The result is

$$\mathbf{Q}_{\Delta t} = \left(\mathbf{I} - \frac{\Delta t}{2} \Omega \right)^{-1} \left(\mathbf{I} + \frac{\Delta t}{2} \Omega \right) . \quad (3.3.5)$$

The accuracy of this integration scheme is dependent on the accuracy of the midpoint relationship of Equation (3.3.3). The rate of rotation must not vary significantly over the time increment. Furthermore, Hughes and Winget (1980) showed that the conditioning of Equation (3.3.5) degenerates as $\Delta t \Omega$ grows.

Our complete numerical algorithm for a single time step is as follows:

1. Calculate \mathbf{D} and \mathbf{W} .
2. Compute $\mathbf{z}_i = \mathbf{e}_{ijk} \mathbf{V}_{jm} \mathbf{D}_{mk}$,
 $\boldsymbol{\omega} = \mathbf{w} - 2[\mathbf{V} - \mathbf{I} \text{tr}(\mathbf{V})]^{-1} \mathbf{z}$, and
 $\Omega_{ij} = \frac{1}{2} \mathbf{e}_{ijk} \omega_k$.
3. Solve $\left(\mathbf{I} - \frac{\Delta t}{2} \Omega \right) \mathbf{R}_{t+\Delta t} = \left(\mathbf{I} + \frac{\Delta t}{2} \Omega \right) \mathbf{R}_t$.
4. Calculate $\dot{\mathbf{V}} = (\mathbf{D} + \mathbf{W}) \mathbf{V} - \mathbf{V} \Omega$.
5. Update $\mathbf{V}_{t+\Delta t} = \mathbf{V}_t + \Delta t \dot{\mathbf{V}}_{\Delta t}$.
6. Compute $\mathbf{d} = \mathbf{R}^T \mathbf{D} \mathbf{R}$.
7. Integrate $\dot{\boldsymbol{\sigma}} = \mathbf{f}(\mathbf{d}, \boldsymbol{\sigma})$.
8. Compute $\mathbf{T} = \mathbf{R} \boldsymbol{\sigma} \mathbf{R}^T$.

This algorithm requires that the tensors \mathbf{V} and \mathbf{R} be stored in memory for each element.





3.4 Determination of Effective Moduli

Algorithms for calculating the stable time increment and hourglass control require dilatational and shear moduli. In SANTOS, we use an algorithm for adaptively determining the effective dilatational and shear moduli of the material.

Because SANTOS uses an explicit integration algorithm, the constitutive response over a time step can be recast *a posteriori* as a hypoelastic relationship. We approximate this relationship as isotropic. This defines effective moduli, $\hat{\lambda}$ and $\hat{\mu}$ in terms of the hypoelastic stress increment and strain increment as follows:

$$\Delta\sigma_{ij} = \Delta t(\hat{\lambda}d_{kk} \delta_{ij} + 2\hat{\mu} d_{ij}) \quad (3.4.1)$$

Equation (3.4.1) can be rewritten in terms of volumetric and deviatoric parts as

$$\Delta\sigma_{kk} = \Delta t(3\hat{\lambda} + 2\hat{\mu}) d_{kk} \quad (3.4.2)$$

and

$$s_{ij} = \Delta t 2\hat{\mu} \varepsilon_{ij} \quad (3.4.3)$$

where

$$s_{ij} = \Delta\sigma_{ij} - \frac{1}{3}\Delta\sigma_{kk} \delta_{ij} \quad (3.4.4)$$

and

$$\varepsilon_{ij} = d_{ij} - \frac{1}{3}d_{kk} \delta_{ij} \quad (3.4.5)$$

The effective bulk modulus follows directly from Equation (3.4.2) as

$$3\hat{K} = 3\hat{\lambda} + 2\hat{\mu} = \frac{\Delta\sigma_{kk}}{\Delta t d_{mm}} \quad (3.4.6)$$

Taking the inner product of Equation (3.4.3) with itself and solving for the effective shear modulus $2\hat{\mu}$ gives

$$2\hat{\mu} = \sqrt{\frac{S_{ij} S_{ij}}{\Delta t^2 \varepsilon_{mn} \varepsilon_{mn}}} \quad (3.4.7)$$

Using the result of Equation (3.4.6) with Equation (3.4.7), we can calculate the effective dilatational modulus $\hat{\lambda} + 2\hat{\mu}$:

$$\hat{\lambda} + 2\hat{\mu} = \frac{1}{3}(3\hat{K} + 2 \cdot (2\hat{\mu})) \quad (3.4.8)$$

If the strain increments are insignificant, Equations (3.4.6) and (3.4.7) will not yield numerically meaningful results. In this circumstance, SANTOS sets the dilatational modulus to an initial estimate, $\lambda_o + 2\mu_o$. An initial estimate for the dilatational modulus is, therefore, the only parameter which every constitutive model is required to provide to the time step control algorithm.

In a case where the volumetric strain increment is significant but the deviatoric increment is not, the effective shear modulus can be estimated by rearranging Equation (3.4.8) as follows:

$$2\hat{\mu} = \frac{1}{2}(3(\lambda_o + 2\mu_o) - 3\hat{K}) \quad (3.4.9)$$

If neither strain increment is significant, SANTOS sets the effective shear modulus to the initial dilatational modulus. The algorithm that SANTOS follows to estimate the effective dilatational and shear moduli is summarized in Table 3.2.

Table 3.2

$\Delta t d_{kk} > 10^{-6}$	$\Delta t^2 \epsilon_{ij} \epsilon_{ij} > 10^{-12}$	$\hat{\lambda} + 2\hat{\mu}$	$2\hat{\mu}$
Yes	Yes	(3.4.8)	(3.4.7)
Yes	No	$\lambda_o + 2\mu_o$	(3.4.9)
No	Yes	$\lambda_o + 2\mu_o$	(3.4.7)
No	No	$\lambda_o + 2\mu_o$	$\lambda_o + 2\mu_o$

3.5 Determination of the Stable Time Increment

Flanagan and Belytschko (1984) provided eigenvalue estimates for the uniform strain quadrilateral described in Section 3.1. They showed that the maximum eigenvalue was bounded by

$$4 \frac{\lambda + 2\mu}{\rho} \frac{B_{iI} B_{iI}}{A^2} \geq \omega_{\max}^2 \geq 2 \frac{\lambda + 2\mu}{\rho} \frac{B_{iI} B_{iI}}{A^2} \quad (3.5.1)$$

Using the effective dilatational modulus from Section 3.4 with the eigenvalue estimates of Equation (3.5.1) allows us to write the stability criteria of Equation (3.2.4) as

$$\Delta t^2 \leq \frac{(\rho_o A_o) A}{(\lambda + 2\mu) B_{iI} B_{iI}} \quad (3.5.2)$$





The stable time increment is determined from Equation (3.5.2) as the minimum over all elements.

The estimate of the critical time increment given in the preceding equation is for the case where there is no damping present in the system. If we define ε as the fraction of critical damping in the highest element mode, the stability criterion of Equation (3.5.2) becomes

$$\Delta t \leq \Delta \hat{t} \left(\sqrt{1 + \varepsilon^2} - \varepsilon \right) . \quad (3.5.3)$$

Conventional estimates of the critical time increment size have been based on the transit time of the dilatational wave over the shortest dimension of an element or zone. For the undamped case, this gives

$$\Delta t = \ell / c \quad (3.5.4)$$

where c is the dilatational wave speed and ℓ is the shortest element dimension.

There are two fundamental and important differences between the time increment limits given by Equations (3.5.2) and (3.5.4). First, our time increment limit is dependent on a characteristic element dimension, which is based on the finite element gradient operator and does not require an ad hoc guess of this dimension. This characteristic element dimension, ℓ , is defined by inspection of Equation (3.5.2) as

$$\ell = A / \sqrt{B_{iI} B_{iI}} . \quad (3.5.5)$$

Second, the sound speed used in the estimate is based on the current response of the material and not on the original elastic sound speed. For materials that experience a reduction in stiffness due to plastic flow, this can result in significant increases in the critical time increment.

It should be noted that the stability analysis performed at each time step predicts the critical time increment for the next step. Our assumption is that the conservativeness of this estimate compensates for any reduction in the stable time increment over a single time step.

3.6 Hourglass Control Algorithm

The mean stress-strain formulation of the uniform strain element considers only a fully linear velocity field. The remaining portion of the nodal velocity field is the so-called hourglass field. Excitation of these modes may lead to severe, unresisted mesh distortion. The hourglass control algorithm described here is taken directly from Flanagan and Belytschko (1981). The method isolates the hourglass modes so that they may be treated independently of the rigid body and uniform strain modes.

A fully linear velocity field for the quadrilateral can be described by

$$\dot{u}_i^{lin} = \dot{\bar{u}}_i + \dot{\bar{u}}_{i,j} (x_j - \bar{x}_j) . \quad (3.6.1)$$



The mean coordinates \bar{x}_i correspond to the center of the element and are defined as

$$\bar{x}_i = \frac{1}{4} x_{iI} \sum_I \quad (3.6.2)$$

The mean translational velocity is similarly defined by

$$\dot{\bar{u}}_i = \frac{1}{4} \dot{u}_{iI} \sum_I \quad (3.6.3)$$

The linear portion of the nodal velocity field may be expressed by specializing Equation (3.6.1) to the nodes as follows:

$$\dot{u}_{iI}^{lin} = \dot{\bar{u}}_i \sum_I + \dot{\bar{u}}_{i,j} (x_{jI} - \bar{x}_j \sum_I) \quad (3.6.4)$$

where \sum_I is used to maintain consistent index notation and indicates that $\dot{\bar{u}}_i$ and \bar{x}_j are independent of position within the element. From Equations (3.1.16) and (3.6.4) and the orthogonality of the base vectors, it follows that

$$\dot{u}_{iI} \sum_I = \dot{u}_{iI}^{lin} \sum_I = 4\dot{\bar{u}}_i \quad (3.6.5)$$

and

$$\dot{u}_{iI} B_{jI} = \dot{u}_{iI}^{lin} B_{jI} = A\dot{\bar{u}}_{i,j} \quad (3.6.6)$$

The hourglass field \dot{u}_{iI}^{hg} may now be defined by removing the linear portion of the nodal velocity field:

$$\dot{u}_{iI}^{hg} = \dot{u}_{iI} - \dot{u}_{iI}^{lin} \quad (3.6.7)$$

Equations (3.6.5) through (3.6.7) prove that \sum_I and B_{jI} are orthogonal to the hourglass field:

$$\dot{u}_{iI}^{hg} \sum_I = 0 \quad (3.6.8)$$

$$\dot{u}_{iI}^{hg} B_{jI} = 0 \quad (3.6.9)$$

Furthermore, it can be shown that the B matrix is a linear combination of the volumetric base vectors, Λ_I , so Equation (3.6.9) can be written as

$$\dot{u}_{iI}^{hg} \Lambda_I = 0 \quad (3.6.10)$$

Equations (3.6.8) and (3.6.10) show that the hourglass field is orthogonal to all the base vectors in Table 3.1 except the hourglass base vectors. Therefore, \dot{u}_{iI}^{hg} may be expanded as a linear combination of the hourglass base vectors as follows:

$$\dot{u}_{iI}^{hg} = \frac{1}{2} \dot{q}_i \Gamma_I \quad (3.6.11)$$

The hourglass nodal velocities are represented by \dot{q}_i above (the leading constant is added to normalize Γ_I). We now define the hourglass-shape vector γ_I such that

$$\dot{q}_i = \frac{1}{2} \dot{u}_{iI} \gamma_I \quad (3.6.12)$$

By substituting Equations (3.6.4), (3.6.7), and (3.6.12) into (3.6.11), then multiplying by Γ_I and using the orthogonality of the base vectors, we obtain the following:

$$\dot{u}_{iI} \Gamma_I - \dot{u}_{i,j} x_{jI} \Gamma_I = \dot{u}_{iI} \gamma_I \quad (3.6.13)$$

With the definition of the mean velocity gradient, Equation (3.1.13), we can eliminate the nodal velocities above. As a result, we can compute γ_I from the following expression:

$$\gamma_I = \Gamma_I - \frac{1}{A} B_{iI} x_{iJ} \Gamma_J \quad (3.6.14)$$

The difference between the hourglass-base vectors Γ_I and the hourglass-shape vectors γ_I is very important. They are identical if and only if the quadrilateral is a parallelogram. For a general shape, Γ_I is orthogonal to B_{jI} while γ_I is orthogonal to the linear velocity field \dot{u}_{iI}^{lin} . While Γ_I defines the hourglass pattern, γ_I is necessary to accurately detect hourglassing. Equation (3.6.14) is simple enough for the quadrilateral that it can be written explicitly as

$$\gamma_I = \frac{1}{A} \begin{bmatrix} x_2(y_3 - y_4) + x_3(y_4 - y_2) + x_4(y_2 - y_3) \\ x_3(y_1 - y_4) + x_4(y_3 - y_1) + x_1(y_4 - y_3) \\ x_4(y_1 - y_2) + x_1(y_2 - y_4) + x_2(y_4 - y_1) \\ x_1(y_3 - y_2) + x_2(y_1 - y_3) + x_3(y_2 - y_1) \end{bmatrix} \quad (3.6.15)$$

For the purpose of controlling the hourglass modes, we define generalized forces Q_i , which are conjugate to \dot{q}_i so that the rate of work is

$$\dot{u}_{iI} f_{iI}^{hg} = Q_i \dot{q}_i \quad (3.6.16)$$



for arbitrary \dot{u}_{ij} . Using Equation (3.6.12), it follows that the contribution of the hourglass resistance to the nodal forces is given by

$$f_{ij}^{hg} = \frac{1}{2} Q_i \gamma_I \quad (3.6.17)$$

Two types of hourglass resistance are used in SANTOS: artificial stiffness and artificial damping. We express this combination as

$$Q_i = Q_i^K + Q_i^V \quad (3.6.18)$$

In terms of the tunable stiffness (κ) and viscosity (ϵ) factors, these resistances are given by

$$\dot{Q}_i^K = \frac{\kappa}{2} 2\hat{\mu} \frac{B_{ij} B_{ji}}{A} \dot{q}_i \quad (3.6.19)$$

$$Q_i^V = \epsilon \sqrt{\max(0, 2\hat{\mu})} m \dot{q}_i \quad (3.6.20)$$

Note that the stiffness expression must be integrated, which further requires that this resistance be stored in a global array.

Observe that the nodal antihourglass forces of Equation (3.6.17) have the shape of γ_I rather than Γ_I . This fact is essential since the antihourglass forces should be orthogonal to the linear velocity field, so that no energy is transferred to or from the rigid body and uniform strain modes by the antihourglassing scheme.

We would prefer to use only hourglass stiffness and, in fact, this is what is used for the plane strain case ($\kappa = .05$ and $\epsilon = 0.0$). Unfortunately, the nonstrain terms in the Petrov-Galerkin formulation give rise to an instability which is best stabilized using hourglass viscosity. For the axisymmetric case, values of $\kappa = .01$ and $\epsilon = .03$ are used.

3.7 Dynamic Relaxation

As a solution strategy for quasistatic mechanics problems, dynamic relaxation involves first converting the equilibrium equations into equations of motion by adding an acceleration term, secondly, introducing an artificial damping, and finally, integrating forward in time from initial conditions until the transient dynamic response has damped out to the static result with equilibrium satisfied. To produce the transient dynamic problem, an acceleration term is added to the equilibrium Equation (2.3.1), thus becoming

$$\text{div } \mathbf{T} + \rho \mathbf{f}_b - r \frac{\partial^2 \mathbf{u}}{\partial \tau^2} = 0 \quad (3.7.1)$$

where \mathbf{u} is the displacement of the material point and r is a spatially varying density selected to minimize the number of iteration steps needed to reach equilibrium. The temporal quantity τ is a pseudo-time scale connected with the dynamic relaxation process but distinct from real time t . The acceleration term is discretized the same way that it would be in a true dynamics calculation. This leads us to write the discrete dynamic system as

$$M(r) \ddot{q} = f^{EXT} - f^{INT} \tag{3.7.2}$$

where $M(r)$ is the mass matrix, $\ddot{q} = \ddot{u}(t)$, f^{INT} is the divergence of the stress field, and f^{EXT} is the vector of prescribed body forces and surface tractions. The mass matrix is computed using the fictitious density, r . This density is different for each element, and it is selected such that the element has the same transit time for a dilatational wave as every other element in the mesh. This process is called mesh homogenization, and it is effective in minimizing the number of iterations for convergence.

At time t_n , equilibrium is satisfied such that $f_n^{INT} = f_n^{EXT}$. A new solution is initiated by incrementing the load to its value at time t_{n+1} . In general, equilibrium will not initially be satisfied so that the force imbalance will be represented by the acceleration term:

$$M(r) \ddot{q} = f_{n+1}^{EXT} - f_{n+1}^{INT} \tag{3.7.3}$$

Central difference expressions are introduced first for the acceleration in terms of the velocity, \dot{u} and then for the velocity in terms of the displacement, u . The resulting equations are

$$\begin{aligned} \dot{u}_{\tau+\Delta\tau} &= \dot{u}_{\tau} + \Delta\tau M(r)^{-1} \left(f_{\tau}^{EXT} - f_{\tau}^{INT} \right) \\ u_{\tau+\Delta\tau} &= u_{\tau} + \Delta\tau \dot{u}_{\tau+\Delta\tau} \end{aligned} \tag{3.7.4}$$

The dynamic relaxation algorithm is based on these two expressions (Equation (3.7.4)). It is a convenient time to introduce the concept of the equilibrium iteration. As the load is incremented to a new value at t_{n+1} , the iteration process begins with calculation of the internal forces f^{INT} and the calculation of the force imbalance. If the force imbalance is greater than a user-specified tolerance, then another iteration through the solution sequence is required. When equilibrium is reached the iteration process stops and new loads are calculated for the next time increment. The central difference expressions above must be solved at each iteration with the appropriate amount of damping to reach the quasistatic solution. These equations take the following form for iteration, i , with the self-adaptive damping parameter, δ .

$$\begin{aligned} \dot{u}^{i+1}_{\tau+\Delta\tau} &= \delta \dot{u}^i_{\tau} + \Delta\tau \delta M(r)^{-1} \left(f_{\tau}^{EXT} - f_{\tau}^{INT^i} \right) \\ u^{i+1}_{\tau+\Delta\tau} &= u^i_{\tau} + \Delta\tau \dot{u}^i_{\tau+\Delta\tau} \end{aligned} \tag{3.7.5}$$

Every iteration i leads to a new trial configuration and trial stress state. The path in solution space traced out by the steps is artificial; it is a by-product of the dynamic relaxation, as is the advance in time τ . The trial states i represent equilibrium iterations. Figure 3.7.1 depicts the process in a multidimensional solution space of the nodal point coordinates. The point n is an equilibrium solution and the point $n+1$ is the equilibrium state being sought.



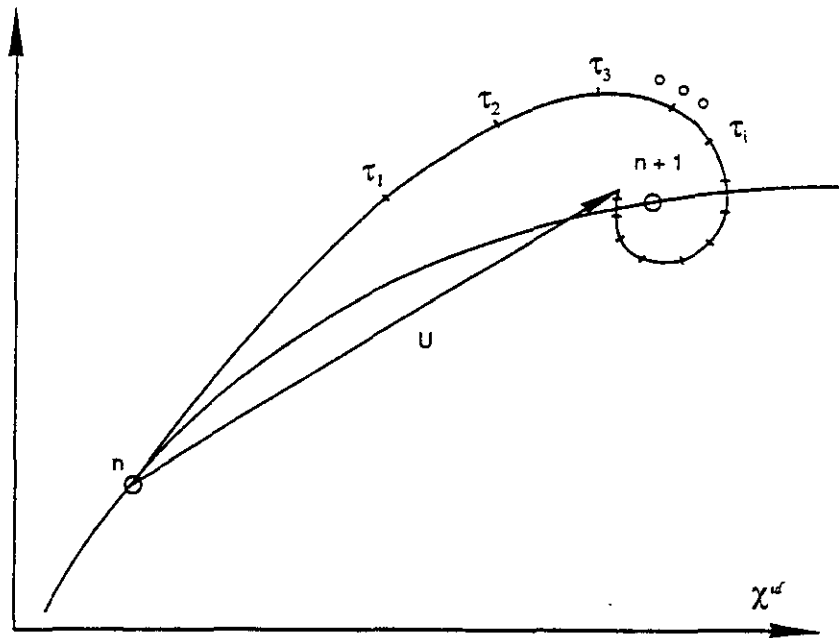


Figure 3.7.1. A model equilibrium iteration sequence in a multi-dimensional configuration space of nodal point positions developed with dynamic relaxation showing convergence at load step $n+1$. The straight line path from n to the last step calculated from dynamic relaxation is the interval over which the stress is evaluated using the real time step Δt .

The curved path between n and $n+1$ traces out the true solution. The spiral path marked with the tics and parameterized by steps in τ is the sequence of trial states generated by the dynamic relaxation method. The straight line from n to the last step calculated from dynamic relaxation is the interval over which the stress is evaluated using the real time step Δt . This is an important point in the implementation of the dynamic relaxation scheme. The internal forces f^{INT} are re-evaluated at each step i using the trial geometry and when equilibrium is achieved; a straight line approximation to the true path between n and $n+1$ is used for the constitutive model calculations. This scheme uncouples the path dependence and real-time dependence of the constitutive behavior from the arbitrary sequence of trial states generated by the dynamic relaxation method.

Convergence is based on achieving an acceptably small equilibrium imbalance. Because the converged solution is a straight line approximation, the true state at $n+1$ will not be found, but a nearby equilibrium state will be found nonetheless. This truncation error is common to the more conventional finite element methods and can be reduced by decreasing the time step size. The only questions remaining are how to select the variable density r , the pseudo-time step $\Delta\tau$, and the damping parameter δ to find a converged solution in the minimum number of steps.

The performance of dynamic relaxation is tied to the minimum natural frequency ω_0 and the maximum natural frequency ω_1 of the discrete equations. The damping per cycle is frequency dependent. For a given damping factor δ , the decrease in amplitude per cycle is greatest for the lowest frequency component. The damping is then chosen to provide critical damping for the lowest frequency. By looking at the characteristic equation associated with the

iteration matrix which relates the velocities and displacements at step n+1 to those at step n, the expression for the damping parameter, δ , is found to be

$$\delta = 1 - (4\omega_0\omega_1) / (\omega_0\omega_1)^2 . \quad (3.7.6)$$

The allowable range on δ is (0,1). A stability analysis on this set of explicit equations produces a critical pseudo-time step given by

$$\Delta\tau_c = 2 / ((\omega_0 + \omega_1)\sqrt{\delta}) . \quad (3.7.7)$$

If the problem is linear so ω_0 and ω_1 are fixed, then the number of time steps, N, required to reduce the vibration amplitude by a factor of ten is

$$N = 1.15 (\omega_1/\omega_0) . \quad (3.7.8)$$

From this equation, it is seen that any effort to reduce the ratio ω_1/ω_0 speeds convergence.

From the linear problem and a uniform mesh of dimension Δx , the maximum frequency ω_1 is given by

$$\omega_1 = 2c / \Delta x = 2 / \Delta\tau . \quad (3.7.9)$$

In this expression, c is the dilatational wave speed given by

$$c = (\lambda + 2\mu) / r \quad (3.7.10)$$

and r is the pseudo-density used for the computation of the fictitious mass. If we substitute the quantity $2/\Delta\tau$ for ω_1 and remember that $\omega_1 \gg \omega_0$, then the expression for the damping parameter becomes

$$\delta = 1 - 2\omega_0\Delta\tau . \quad (3.7.11)$$

The fundamental frequency ω_0 is continuously estimated using an approximate value found using the Rayleigh Quotient. At each iteration i in the dynamic relaxation scheme, a new estimate $(\omega_0)_i$ is computed as

$$\omega_{0_i} = \sqrt{(\mathbf{u}_i^T \mathbf{K} \mathbf{u}_i) / \mathbf{u}_i^T \mathbf{M} \mathbf{u}_i} \quad (3.7.12)$$

where \mathbf{K} is a diagonal stiffness matrix whose j^{th} component is computed from

$$K^j = \frac{f_i^{j\text{INT}} - f_{i-1}^{j\text{INT}}}{\Delta\tau u_{i-1}^j} . \quad (3.7.13)$$

With each estimate of the fundamental frequency, a new value of the damping is computed. This has the virtue that the lowest active mode will be found in the event that the fundamental mode is not participating (Underwood, 1983).





3.8 Convergence Measures

When an iterative method, such as dynamic relaxation, is used to solve for static equilibrium, some criterion must be used to determine when the estimated solution is sufficiently close to the actual solution. Convergence of the equilibrium iteration process is achieved when a measure of the problem force imbalance reaches a value less than or equal to a user-supplied error tolerance. The force imbalance is the sum of the external and internal nodal forces which at equilibrium should sum to zero.

In SANTOS, two different convergence error measures are available to the analyst. The first error measure is based on satisfying the following inequality:

$$\frac{\|R_j\|}{\|F_n\|} \leq \text{TOL} \quad (3.8.1)$$

where $\|\cdot\|$ denotes the L_2 norm of a vector, R_j is the residual or imbalance force vector at iteration j , and F_n is the external force vector at step n which is composed of applied tractions, body forces (gravity forces), thermal forces, and the reactions at nodes where zero displacement boundary conditions are applied. Equation 3.8.1 is a measure of how close the problem is to a state of equilibrium. The quantity TOL is input by the analyst as a means of identifying the relative imbalance the analyst is willing to accept in the solution. In SANTOS, TOL is set by default to a value of 0.5 percent. This error is called the GLOBAL CONVERGENCE measure and is the default error measure.

The second error measure implemented in SANTOS is based on satisfying the error tolerance on a node-by-node basis. This error measure is called the LOCAL CONVERGENCE measure. The rationale for this criterion is that what is an acceptable force imbalance in one portion of the problem may be unacceptable at another location. For example, further reduction of a set of force residuals acting in a region of the problem where the elements are large and stiff may produce only a small change in the element stresses in this region. If, however, the same set of force residuals was present at a different location where the element sizes were much smaller and the material was much more flexible, further reduction of the residuals could produce a large change in the element stresses. To address these concerns, the LOCAL CONVERGENCE error measure is included as an option.

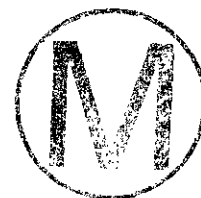
The error measure for each component i and iteration j of the residual force vector is defined as:

$$\frac{|R_j^i|}{|F_n^i| + \sum_e \max(|f_j^i|^e, f_{\min}^e)} \leq \text{TOL} \quad (3.8.2)$$

where R_j^i is the residual or imbalance force, F_n^i is the external force, f_j^i is the internal force, and f_{\min} is the minimum internal force in an element produced by a reference hydrostatic stress state specified by the analyst. The minimum internal force is introduced to ensure that the denominator is never zero and to prevent elements with negligible stresses from controlling the convergence of the problem. The internal force contribution is summed over

all the elements, e , connected to node i . This error measure is satisfied when each component of the force vector satisfies the criterion.





4.0 CONSTITUTIVE MODELS

One of the primary reasons for developing SANTOS was to take advantage of the many state-of-the-art features available in PRONTO and adapt them to quasistatic mechanics problems. One of those features is the flexible material model interface which allows a constitutive model to be added to the code with minimal effort. The constitutive developer does not have to be familiar with the internal workings of SANTOS but only needs to modify a few well documented subroutines to add a new material model. The material model implementation requires the user to provide entries in a few data statements to define the limits of the internal data structure. The code also requires the constitutive developer to provide estimates of the initial dilatational and shear moduli so that the program can compute an initial stable time step. The material model may contain internal state variables that define the state or evolution of the material. The implementation requires that the developer provide names and any required initialization for the internal state variables. The internal state variable names for each material currently implemented are provided in the User Guide section. These quantities may be individually selected for output to the plotting data base. The final changes to the material model subroutines require the developer to provide names for any necessary input quantities such as Young's modulus or Poisson's ratio. The input names for the material models currently implemented are given in the User Guide section. The code currently contains twelve continuum material models with more models being developed as our applications require them. The models range from purely elastic behavior to time-dependent viscoplastic response.

SANTOS utilizes an indirect solution technique which can require hundreds of thousands of calls to the constitutive model during a complex analysis. Thus, efficient implementation of the constitutive model is a primary concern. Considerable effort has gone into writing each material model subroutine such that the routine vectorizes on a vector supercomputer. The material model routine is written in terms of the unrotated Cauchy stress, σ , and the deformation rate in the unrotated configuration, d . The basic assumption is that the deformation or strain rate is constant over the step. The deformation rate that is available to the constitutive subroutine is the mechanical strain rate, i.e., any thermal strain rate contribution to the total strain rate has already been removed. During each iteration, the latest kinematic quantities are used to update the stress. Stresses written to the plotting data base are rotated to the current configuration.

4.1 Integration of the Rate Equations

The constitutive models are written in a rate form and must be integrated forward at each time step. In SANTOS, a forward Euler or a backward Euler integration of the rate equations is used for many of the constitutive models. The forward Euler integration assumes that

$$f^{n+1} = f^n + \dot{f}(f^n)\Delta t \quad (4.1.1)$$

where f is the quantity to be integrated, n refers to the current step for which values of f are available and $n+1$ refers to the next step for which values of f are being sought. The quantity \dot{f} is defined using the known quantities at step n , and Δt is the time step increment. The forward Euler scheme is simple and computationally efficient but is conditionally stable. The time step size allowed is controlled by a stability criterion that varies with each material model.

The backward Euler integrator has the following form

$$f^{n+1} = f^n + \dot{f}(f^{n+1})\Delta t \tag{4.1.2}$$

where the term \dot{f} is evaluated at step $n+1$. This solution method is implicit and therefore requires some type of iterative method such as Newton-Raphson to solve for f^{n+1} . The method is computationally more demanding than forward Euler, but the scheme is unconditionally stable. The only restriction on the time step size is accuracy of the solution.

The time-dependent material models implemented in SANTOS, such as the creep and viscoplastic models, use the forward Euler operator even though the method is conditionally stable. The implementations rely on subincrementation within the global time step, Δt , to maintain numerical stability. In most instances, the user-specified global solution step, Δt , is larger than the time step needed for accuracy and stability. Economic considerations do not allow the user to take the number of global solution time steps needed to ensure an accurate and stable solution; therefore, the global solution time step is broken into subincrements for integrating the constitutive model. The size of each subincrement adapts to the change in stress occurring within the global solution step. So although this subincrementation process maintains the direction and magnitude of the total strain increments as constant for the global step, it allows the stress components to change over the step. That is, after each subincremental time step, the stresses and inelastic strain rates as well as the critical time step are updated before computing the solution for the next subincrement.

The implementation of this algorithm is designed to take advantage of the vector architecture of the Cray computer. The constitutive model is called with the total strain rates for the step and the stress from the previous step. Processing is done on a block of 64 elements, one block at a time. There are two FORTRAN loops involved in this approach. The outer loop is an implicit loop that adapts the size of the subincrement as the stresses change within the global solution step. This loop is not vectorizable. The inner loop computes the stresses for a block of NE elements, with NE having a maximum of 64. This loop is vectorizable. An additional feature of this approach, which is unique to indirect solution schemes, is that each element block may have its own unique number of subincrements. Thus, the amount of computation is minimal for elements in regions where the stress is small and the computational effort is concentrated where the stress is largest.

The key to the scheme is the accurate determination of the stable time step which is accomplished using the work of Corneau (1975) who developed a method for analytically determining the stable time step for a particular constitutive model. To determine the analytical expression for the stable time step size, we introduce the following linearized differential equation

$$\dot{s} = \dot{\sigma}_t + \frac{\partial}{\partial \sigma} \dot{\sigma}_t (s - \sigma_t) \tag{4.1.3}$$

where the quantity, σ_t , represents the deviatoric stress at time t . This equation represents a first-order Taylor series expansion about the stress state at time t . This equation can be rewritten as

$$\dot{y} + Ay = f \tag{4.1.4}$$



where y is a column vector containing the stress components and A is a square matrix defined by

$$A = \left[\frac{\partial}{\partial \sigma} (\dot{\sigma}) \right]_t .$$

A stability analysis of the forward Euler integrator shows that the time interval is stable if $\Delta t < \frac{2}{|\lambda_{\max}|}$ where λ_{\max} is the largest eigenvalue of the square matrix A . Once we have the analytic expression for the stable time step, we can write an efficient, vectorized material model subroutine for implementation into SANTOS.

4.2 Adaptive Time Stepping

One important feature available for the time-dependent material models in SANTOS is the capability to do adaptable time stepping. This feature is desirable when the mechanics of the problem dictate small time steps during the early stress transient, but the stress reaches a steady state at later times and the analyst desires to use larger time steps. If we consider a function $f(t)$ which is analytic in the neighborhood of a point t :

$$f(t+h) = f(t) + hf'(t) + \frac{h^2}{2} f''(t) + \frac{h^3}{3!} f'''(t) + \dots \quad (4.2.1)$$

The forward Euler method is obtained by taking the first two terms of the series:

$$f(t+h) = f(t) + hf'(t) + O(h^2) \quad (4.2.2)$$

where $O(h^2)$ is the error associated with the truncation. The above equation can be rewritten in a slightly different form:

$$f(t+h) = f(t) + hf'(t) + \frac{h^2}{2} f''(\xi) \quad (4.2.3)$$

where $t_i < \xi < t+h$ or

$$f_{i+1} = f_i + hf'_i + \frac{h^2}{2} f''(\xi) \quad (4.2.4)$$

and $t_i < \xi < t_{i+1}$ where the last term is the truncation error per step.

If it is assumed that f'' is fairly constant over the i^{th} step interval, an estimate of the truncation error E_T at the i^{th} step can be obtained from

$$E_{T_i} \cong \frac{h^2}{2} f''_i \quad (4.2.5)$$

where f'' is evaluated at $\xi = t_i$.

The criterion for the time step control is

$$|E_{T_i}| < \epsilon |f_i| \tag{4.2.6}$$

where ϵ is some small number. Replacing E_{T_i} in the above expression with $\frac{h^2}{2} f_i''$ and solving for the time step, h , gives the following expression

$$h < \sqrt{\frac{2\epsilon |f_i|}{|f_i''|}} \tag{4.2.7}$$

In SANTOS, we choose to control the time step with the effective stress so that the above equation becomes

$$h < \sqrt{\frac{2\epsilon \bar{\sigma}_i}{\bar{\sigma}_i''}} \tag{4.2.8}$$

The accuracy of the method depends on the value of ϵ chosen. For example, we might restrict the error to 1 percent of $\bar{\sigma}_i$ at the beginning of the step so ϵ would be selected as 0.01. Experience has shown that values of ϵ in the range .01 - .02 produce acceptable results.

4.3 Basic Definitions and Assumptions

The constitutive models implemented in SANTOS are described in the following sections. The fundamental assumptions used in developing the models are presented along with some details of their implementation. The nomenclature used for the descriptions will be presented first. Several of the models have their descriptions taken from other sources, and we will follow the nomenclature of those sources where appropriate. Throughout the report, components of tensors will appear using indicial notation, σ_{ij} , while equivalent scalar quantities appear with a bar, $\bar{\sigma}$.

The material model development makes the fundamental assumption of an additive strain rate decomposition of the total strain rate components, d_{ij} , into elastic and inelastic parts.

$$d_{ij} = d_{ij}^{el} + d_{ij}^{in} \tag{4.3.1}$$

The resulting stress rate, $\dot{\sigma}_{ij}$, is determined from the elastic part of the strain rate using Hooke's law

$$\dot{\sigma}_{ij} = C_{ijkl} d_{kl}^{el} = C_{ijkl} (d_{kl} - d_{kl}^{in}) \tag{4.3.2}$$

where C is a 4th order tensor of Hookean elastic constants. The stress rate can be broken into two independent parts representing volumetric and deviatoric behavior. The volumetric behavior is assumed for most material models to be purely elastic with the volumetric strain rate, d_{kk} , linearly related to the pressure, \dot{p} , through the relation





$$\dot{p} = \frac{\dot{\sigma}_{kk}}{3} = Kd_{kk} \quad (4.3.3)$$

where K is the bulk modulus of the material. Because the strain rates are assumed constant over the step, the pressure at the end of the step can be easily found from the expression

$$p_{n+1} = p_n + Kd_{kk}\Delta t \quad (4.3.4)$$

where Δt is the time step size and p_n is the pressure at the beginning of the step. There are material models in SANTOS that do not have a linear bulk response. These exceptions include the volumetric creep model, soil and crushable foam model, and low density foam model. The particular volumetric response for each of these models will be discussed in each individual section.

The deviatoric stress rate, \dot{S}_{ij} , is computed from the relation

$$\dot{S}_{ij} = \dot{\sigma}_{ij} - \dot{p}\delta_{ij} \quad (4.3.5)$$

where δ_{ij} is the Kronecker delta. If we rewrite the equation for the stress rate in terms of the deviatoric stress part, we have

$$\dot{S}_{ij} = 2\mu(\dot{\epsilon}_{ij} - \dot{\epsilon}_{ij}^{in}) \quad (4.3.6)$$

where $\dot{\epsilon}_{ij}$ is the deviatoric component of the strain rate, d_{ij} . The deviatoric strain rate components are similarly calculated.

$$\dot{\epsilon}_{ij} = d_{ij} - \frac{1}{3}d_{kk}\delta_{ij} \quad (4.3.7)$$

In most of the material models currently implemented in SANTOS, we assume von Mises flow, and we can define the equivalent von Mises stress, $\bar{\sigma} = \sqrt{\frac{3}{2}S_{ij}S_{ij}}$, and the equivalent deviatoric strain rate, $\bar{\dot{\epsilon}} = \sqrt{\frac{2}{3}\dot{\epsilon}_{ij}\dot{\epsilon}_{ij}}$. It is convenient to introduce the idea of an elastic "trial" stress state for the end of the time step. This stress state is used in the plasticity models to determine if yielding will occur during the step, and it is also used for the time-dependent models. Given the deviatoric stress state at the beginning of the step, S_{ij}^n , the elastic "trial" stress state for the end of the step is

$$S_{ij}^T = S_{ij}^n + 2\mu\dot{\epsilon}_{ij}\Delta t \quad (4.3.8)$$

where μ is the shear modulus, Δt is the time step increment, and $\dot{\epsilon}_{ij}$ is the deviatoric strain rate. If yielding does not occur during the time step, then the trial stress becomes the final stress state at S_{ij}^{n+1} .

4.4 Elastic Material, Hooke's Law

A linear elastic material is defined using Hooke's Law. In a rate form, this is written as

$$\dot{\sigma}_{ij} = \lambda(d_{kk})\delta_{ij} + 2\mu d_{ij} \tag{4.4.1}$$

where λ and μ are the elastic Lamé material constants. The stress rate equation is integrated forward using the backward Euler integrator. The model has no internal state variables.

The PROP array for this material contains the following entries:

PROP(1) - Young's modulus, E

PROP(2) - Poisson's ratio, ν

PROP(3) - λ

PROP(4) - 2μ

4.5 Elastic Plastic Material with Combined Kinematic and Isotropic Hardening

The elastic plastic model is based on a standard von Mises yield condition and uses combined kinematic and isotropic hardening. Isotropic hardening is the behavior where the radius of the yield surface grows equally in all directions due to plastic straining. Kinematic hardening is the behavior where the radius of the yield surface remains constant, but the center of the yield surface translates in the direction of the plastic strain rate. In this discussion of the elastic plastic material model, we assume that the material is yielding and that plastic straining will occur. In the event that yielding does not occur, the material behavior is elastic and the stress is computed using Hooke's Law as described in Section 4.4. This model is widely used in many finite element computer programs, and the current derivation is taken from Taylor and Flanagan (1987).

Some definitions and assumptions are outlined here. Referring to Figure 4.5.1, which shows the yield surface in deviatoric stress space, we define the backstress (the center of the yield surface) by the tensor, α .

If σ is the current value of the stress, we define the deviatoric part of the current stress by

$$S = \sigma - \frac{1}{3} \text{tr}\sigma \delta \tag{4.5.1}$$

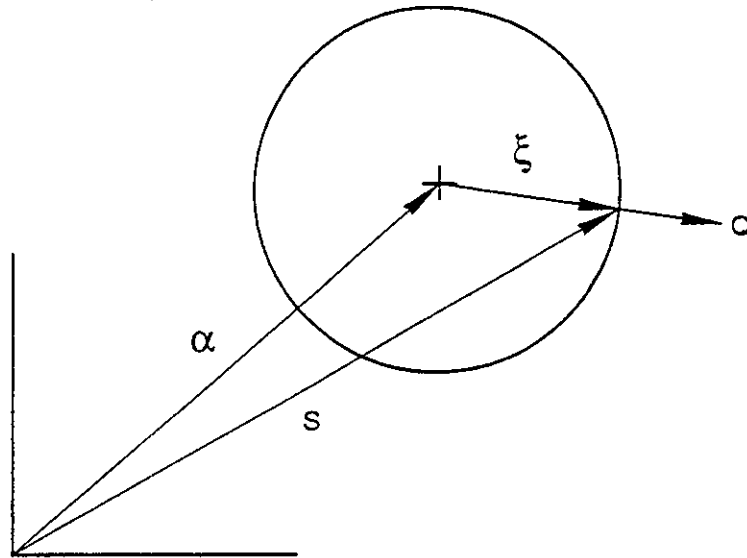
We define the stress difference measured by subtracting the backstress from the deviatoric stress by

$$\xi = \sigma - \alpha \tag{4.5.2}$$

The magnitude of the stress difference, R, is defined by

$$R = |\xi| = \sqrt{\xi:\xi} \tag{4.5.3}$$





TRI-6348-7-0

Figure 4.5.1. Yield surface in deviatoric stress space.

where we denote the inner product of second order tensors by $S:S = S_{ij} S_{ij}$. Note that if the backstress is zero (isotropic hardening case), the stress difference is equal to the deviatoric part of the current stress, S .

The von Mises yield surface is defined as

$$f(\sigma) = \frac{1}{2} \xi:\xi = \kappa^2 \quad (4.5.4)$$

The von Mises effective stress, $\bar{\sigma}$, is defined by

$$\bar{\sigma} = \sqrt{\frac{3}{2} \xi:\xi} \quad (4.5.5)$$

Since R is the magnitude of the deviatoric stress tensor when $\alpha = 0$, it follows that

$$R = \sqrt{2} \kappa = \sqrt{\frac{2}{3}} \bar{\sigma} \quad (4.5.6)$$

The normal to the yield surface can be determined from Equation (4.5.4)

$$Q = \frac{\partial f}{\partial \sigma} \bigg/ \left| \frac{\partial f}{\partial \sigma} \right| = \xi / R \quad (4.5.7)$$

We assume that the strain rate can be decomposed into elastic and plastic parts by an additive decomposition

$$d = d^{el} + d^{pl} \quad (4.5.8)$$

and assume that the plastic part of the strain rate is given by a normality condition

$$\mathbf{d}^{pl} = \gamma \mathbf{Q} \quad (4.5.9)$$

when the scalar multiplier, γ , must be determined.

A scalar measure of equivalent plastic strain rate is defined by

$$\bar{d}^{pl} = \sqrt{\frac{2}{3} \mathbf{d}^{pl} : \mathbf{d}^{pl}} \quad (4.5.10)$$

which is chosen such that

$$\bar{\sigma} \bar{d}^{pl} = \boldsymbol{\sigma} : \mathbf{d}^{pl} \quad (4.5.11)$$

The stress rate is assumed to be purely due to the elastic part of the strain rate and is expressed in terms of Hooke's law by

$$\dot{\boldsymbol{\sigma}} = \lambda \text{tr} \mathbf{d}^{el} \boldsymbol{\delta} + 2\mu \mathbf{d}^{el} \quad (4.5.12)$$

where λ and μ are the Lamé constants for the material.

Below, we develop the theory for the cases of isotropic hardening, kinematic hardening, and combined hardening separately so that the reader can see the details for each case.

4.5.1 Isotropic Hardening

In the isotropic hardening case, the backstress is zero and the stress difference is equal to the deviatoric stress, S . We write a consistency condition by taking the rate of Equation (4.5.4)

$$\dot{f}(\boldsymbol{\sigma}) = 2 \kappa \dot{\kappa} \quad (4.5.13)$$

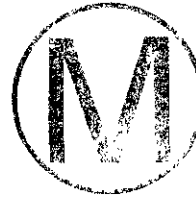
By consistency we mean that the state of stress must remain on the yield surface at all times. We use the chain rule and the definition of the normal to the yield surface given by Equation (4.5.7) to obtain

$$\dot{f}(\boldsymbol{\sigma}) = \frac{\partial f}{\partial \boldsymbol{\sigma}} : \dot{\boldsymbol{\sigma}} = \left| \frac{\partial f}{\partial \boldsymbol{\sigma}} \right| \mathbf{Q} : \dot{\boldsymbol{\sigma}} \quad (4.5.14)$$

and from Equations (4.5.3) and (4.5.4)

$$\left| \frac{\partial f}{\partial \boldsymbol{\sigma}} \right| = |S| = R \quad (4.5.15)$$

Combining Equations (4.5.13), (4.5.14), and (4.5.15)



$$\frac{1}{R} S : \dot{\sigma} = \dot{R} \quad (4.5.16)$$

Because S is deviatoric, $S : \dot{\sigma} = S : \dot{S}$ and

$$S : \dot{S} = \frac{d}{dt} \left(\frac{1}{2} S : S \right) = \frac{d}{dt} \left(\frac{\bar{\sigma}^2}{3} \right) = \frac{2}{3} \bar{\sigma} \dot{\sigma} \quad (4.5.17)$$

Then Equation (4.5.16) can be written as

$$\dot{R} = \sqrt{\frac{2}{3}} \dot{\bar{\sigma}} = \sqrt{\frac{2}{3}} H' \bar{d}^{pl} \quad (4.5.18)$$

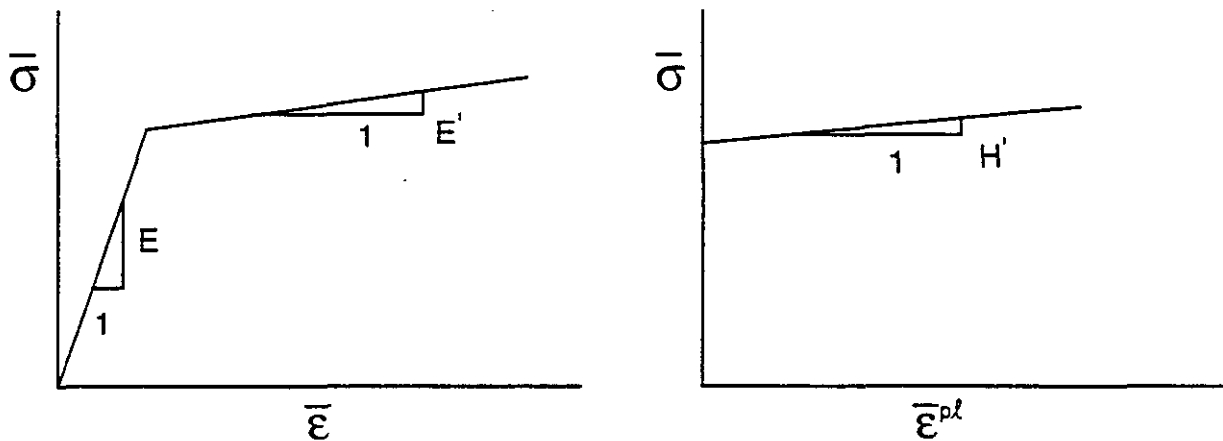
where H' is the slope of the yield stress versus equivalent plastic strain ($\bar{\sigma}$ versus $\bar{\epsilon}^{pl}$). This is derivable from the data from a uniaxial tension test as shown in Figure 4.5.2.

The consistency condition, Equation (4.5.16) and Equation (4.5.18), result in

$$\sqrt{\frac{2}{3}} H' \bar{d}^{pl} = Q : \dot{\sigma} \quad (4.5.19)$$

We define the trial elastic stress rate $\dot{\sigma}^tr$ by

$$\dot{\sigma}^tr = C : \dot{d} \quad (4.5.20)$$



$$H' = \frac{E E'}{E - E'}$$

TRI-6348-B-0

Figure 4.5.2. Conversion of data from a uniaxial tension test to equivalent plastic strain versus von Mises stress.

where C is the fourth order tensor of elastic coefficients defined by Equation (4.5.12). Combining the strain rate decomposition defined in Equation (4.5.8) with Equations (4.5.19) and (4.5.20) yields

$$\sqrt{\frac{2}{3}} H' \bar{d}^{pl} = Q : \dot{\sigma}^T - Q : C : d^{pl} \quad (4.5.21)$$

We note that because Q is deviatoric, $C:Q = 2\mu Q$ and $Q:C:Q = 2\mu$. Then using the normality condition, Equation (4.5.9), the definition of equivalent plastic strain, Equation (4.5.10), and Equation (4.5.21)

$$\frac{2}{3} H' \gamma = Q : \dot{\sigma}^T - \gamma 2\mu \quad (4.5.22)$$

and since Q is deviatoric ($Q : \dot{\sigma}^T = 2\mu Q : d$), we can determine γ from Equation (4.5.22) as

$$\gamma = \frac{1}{(1 + H'/3\mu)} Q : d \quad (4.5.23)$$

The current normal to the yield surface, Q , and the total strain rate, d , are known quantities. Hence, from Equation (4.5.23), γ can be determined which can be used in Equation (4.5.9) to determine the plastic part of the strain rate which, with the additive strain rate decomposition and the elastic stress rate of Equations (4.5.8) and (4.5.12), completes the definition of the rate equations.

We still must explain how to integrate the rate equations subject to the constraint that the stress must remain on the yield surface. We will show how that is accomplished in Section 4.5.4.

4.5.2 Kinematic Hardening

Just as before with the isotropic hardening case, we write a von Mises yield condition but now in terms of the stress difference

$$f(\xi) = \frac{1}{2} \xi : \xi = \kappa^2 \quad (4.5.24)$$

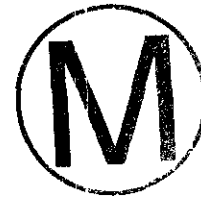
It is important to remember that α and ξ are deviatoric tensors. The consistency condition is written for kinematic hardening as

$$\dot{f}(\xi) = 0 \quad (4.5.25)$$

because the size of the yield surface does not grow with kinematic hardening; therefore, $\dot{\kappa} = 0$. Using the chain rule on Equation (4.5.25)

$$\frac{\partial f}{\partial \xi} : \dot{\xi} = 0 \quad (4.5.26)$$





and

$$\frac{\partial f}{\partial \xi} = \left| \frac{\partial f}{\partial \xi} \right| Q = R Q \quad (4.5.27)$$

Combining Equations (4.5.26) and (4.5.27) and assuming that $R \neq 0$

$$Q : \dot{\xi} = 0 \quad (4.5.28)$$

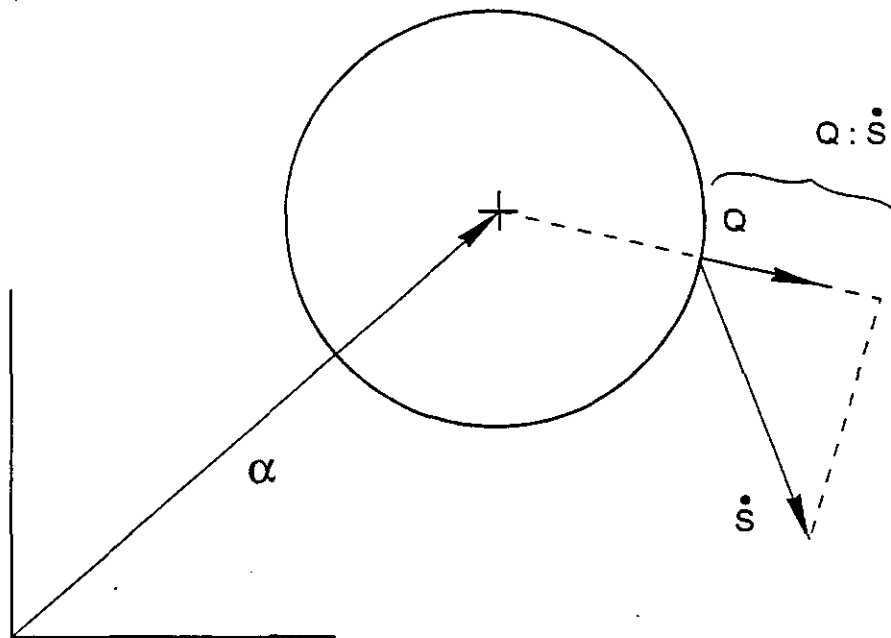
or

$$Q : (\dot{S} - \dot{\alpha}) = 0 \quad (4.5.29)$$

A geometric interpretation of Equation (4.5.29) is shown in Figure 4.5.3, where it can be seen that the backstress moves in a direction parallel to the normal to the yield surface.

We must now decide how $\dot{\alpha}$ is defined. Recall that for the isotropic hardening case, Equation (4.5.29),

$$Q : \dot{\sigma} = \sqrt{\frac{2}{3}} H' \bar{d}^{Pl} = \frac{2}{3} H' \gamma \quad (4.5.30)$$



TRI-6348-9-0

Figure 4.5.3. Geometric interpretation of the consistency condition for kinematic hardening.



The kinematic hardening condition assumes that

$$\dot{\alpha} = \phi \mathbf{d}^{Pl} = \phi \gamma \mathbf{Q} \quad (4.5.31)$$

where ϕ is a material parameter. Equation (4.5.31) combined with Equation (4.5.29) gives a result identical to the isotropic hardening case, Equation (4.5.30), if ϕ is chosen to be $\frac{2}{3}H'$. Hence, either Equation (4.5.30) or (4.5.31) gives us a scalar condition on $\dot{\alpha}$. Note that both of these are assumptions and must be shown to be reasonable. Of course, experience with material models based on these assumptions has proven them to be reasonable representations of material behavior.

Using Equation (4.5.30), the strain rate decomposition, Equation (4.5.8), and the elastic strain rate, Equation (4.5.12), in the consistency condition for kinematic hardening, Equation (4.5.29) gives

$$\frac{2}{3}H' \gamma \mathbf{Q} = \dot{\sigma}^{tr} - \mathbf{C}:\mathbf{d}^{Pl} \quad (4.5.32)$$

Taking the tensor inner product of both sides of Equation (4.5.32) with \mathbf{Q} gives

$$\mathbf{Q}:\frac{2}{3}H' \gamma \mathbf{Q} = \mathbf{Q}:(\dot{\sigma}^{tr} - 2\mu\gamma \mathbf{Q}) \quad (4.5.33)$$

Again, because \mathbf{Q} is deviatoric; $\mathbf{C}:\mathbf{Q} = 2\mu \mathbf{Q}$ and $\mathbf{Q}:\mathbf{C}:\mathbf{Q} = 2\mu$.

Solving Equation (4.5.33) for γ gives

$$\gamma = \frac{1}{(1 + H'/3\mu)} \mathbf{Q}:\dot{\sigma} \quad (4.5.34)$$

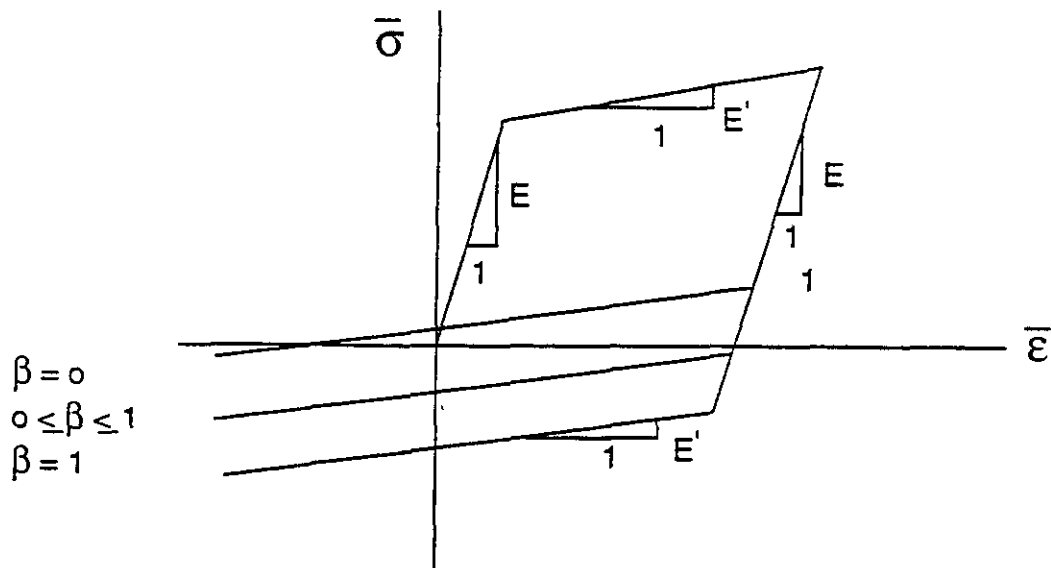
which is the same result as was obtained for the isotropic hardening case.

4.5.3 Combined Isotropic and Kinematic Hardening

For the combined hardening case, we define a scalar parameter, β , which determines the amount of each type of hardening. We require that

$$0 \leq \beta \leq 1 \quad (4.5.35)$$

Figure 4.5.4 illustrates the uniaxial response which will be computed for $\bar{\sigma}$ for different choices of β . When $\beta = 0$ we have only kinematic hardening, and when $\beta = 1$ we have only isotropic hardening.



TRI-6348-10-0

Figure 4.5.4. Effect of the choice of the hardening parameter, β , on the computed uniaxial response.

$$\dot{R} = \sqrt{\frac{2}{3}} H' \bar{d}^{Pl} \beta \quad (4.5.36)$$

and

$$\dot{\alpha} = \frac{2}{3} H' \bar{d}^{Pl} (1-\beta) = \frac{2}{3} H' \gamma Q (1-\beta) \quad (4.5.37)$$

As before, we write a consistency condition

$$Q : \dot{\xi} = \dot{R} \quad (4.5.38)$$

or

$$Q : (\dot{S} - \dot{\alpha}) = \sqrt{\frac{2}{3}} H' \bar{d}^{Pl} \beta \quad (4.5.39)$$

Using the elastic stress rate and the additive strain rate decomposition with Equation (4.2.56) and taking the tensor product with the normal, Q

$$Q : \dot{\sigma}^T - \gamma Q : C : Q - Q : \left[\frac{2}{3} H' \gamma (1-\beta) \right] Q = Q : \left[\sqrt{\frac{2}{3}} H' \sqrt{\frac{2}{3}} \beta \gamma \right] Q \quad (4.5.40)$$

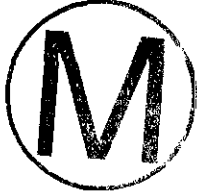


Solving for γ

$$\gamma = \frac{1}{(1 + H'/3\mu)} \mathbf{Q} : \mathbf{d} \quad (4.5.41)$$

which is the same result obtained for each of the independent cases.

We summarize the governing equations for the combined theory:



$$\dot{\sigma} = \mathbf{C} : (\mathbf{d} - \mathbf{d}^{pl}) = \dot{\sigma}^{tr} \quad (4.5.42)$$

$$\dot{R} = \beta \sqrt{\frac{2}{3}} H' \bar{d}^{pl} = \beta \frac{2}{3} H' \gamma \quad (4.5.43)$$

$$\dot{\alpha} = (1 - \beta) \frac{2}{3} H' \mathbf{d}^{pl} \quad (4.5.44)$$

$$\mathbf{d}^{pl} = \begin{cases} 0, & \text{elastic; } f(\xi) < \kappa^2 \\ \gamma \mathbf{Q}, & \text{plastic; } f(\xi) \geq \kappa^2 \end{cases} \quad (4.5.45)$$

$$\gamma = \frac{1}{(1 + H'/3\mu)} \mathbf{Q} : \mathbf{d} \quad (4.5.46)$$

$$\mathbf{Q} = \frac{\partial f}{\partial \xi} / \left| \frac{\partial f}{\partial \xi} \right| = \xi / R \quad (4.5.47)$$

4.5.4 Numerical Implementation

Our finite element algorithm requires an incremental form of Equations (4.5.41) through (4.5.43). Additionally, we must have an algorithm which integrates the incremental equations subject to the constraint that the stress remains on the yield surface.

The incremental analogs of Equations (4.5.42) through (4.5.44) are

$$\sigma_{n+1} = \sigma_{n+1}^{tr} - \Delta\gamma 2\mu \mathbf{Q} \quad (4.5.48)$$

$$R_{n+1} = R_n + \frac{2}{3} \beta H' \Delta\gamma \quad (4.5.49)$$

and

$$\alpha_{n+1} = \alpha_n + (1 - \beta) \frac{2}{3} H' \Delta\gamma \mathbf{Q} \quad (4.5.50)$$

where $\Delta\gamma$ represents the product of the time increment and the equivalent plastic strain rate ($\Delta\gamma = \Delta t \dot{\gamma}$).

The subscripts n and $n+1$ refer to the beginning and end of a time step, respectively.

We also need an incremental analog to the rate forms of the consistency condition given by Equations (4.5.13), (4.5.25), and (4.5.39). At the end of the time step, we insist that the stress state must be on the yield surface. Hence, the incremental consistency condition is

$$\alpha_{n+1} + R_{n+1} \mathbf{Q} = \mathbf{S}_{n+1} \quad (4.5.51)$$

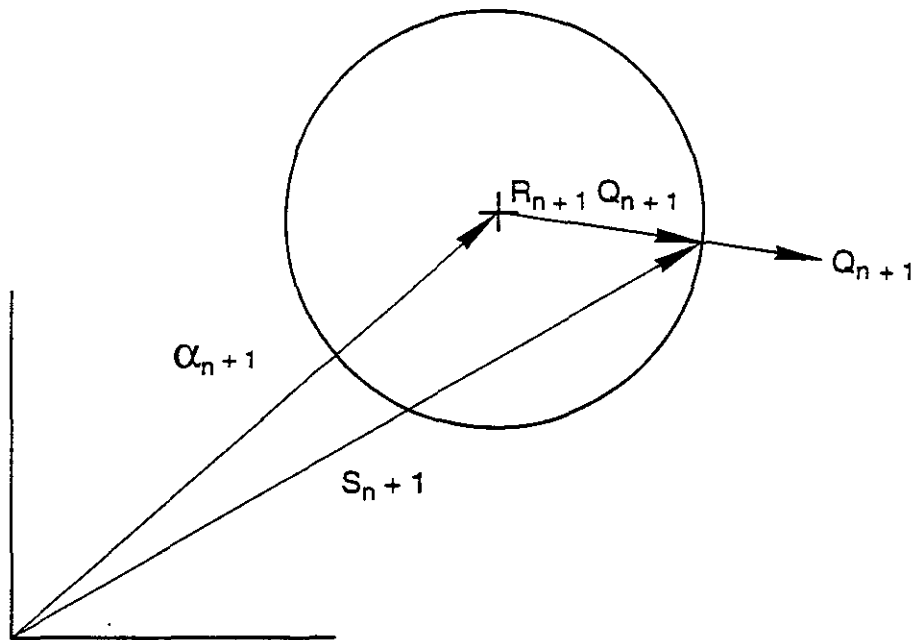
Equation (4.5.51) is shown graphically in Figure 4.5.5.

Substituting the definitions given by Equations (4.5.48) through (4.5.50) into the consistency condition of Equation (4.5.51)

$$\left[\alpha_n + (1-\beta) \frac{2}{3} H' \Delta\gamma \mathbf{Q} \right] + \left[R_n + \frac{2}{3} \beta H' \Delta\gamma \right] \mathbf{Q} = \left[\mathbf{S}_{n+1}^r - \Delta\gamma 2\mu \mathbf{Q} \right] \quad (4.5.52)$$

Taking the tensor product of both sides of Equation (4.5.52) with \mathbf{Q} and solving for $\Delta\gamma$

$$\Delta\gamma = \frac{1}{2\mu} \frac{1}{(1+H'/3\mu)} \left(\left| \xi_{n+1}^r \right| - R_n \right) \quad (4.5.53)$$



TRI-6348-11-0

Figure 4.5.5. Geometric interpretation of the incremental form of the consistency condition for combined hardening.



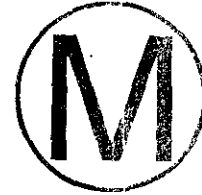
It follows from Equation (4.5.53) that the plastic strain increment is proportional to the magnitude of the excursion of the elastic trial stress past the yield surface (see Figure 4.5.6).

Using the result of Equation (4.5.53) in Equations (4.5.48) through (4.5.50) completes the algorithm. In addition we can compute

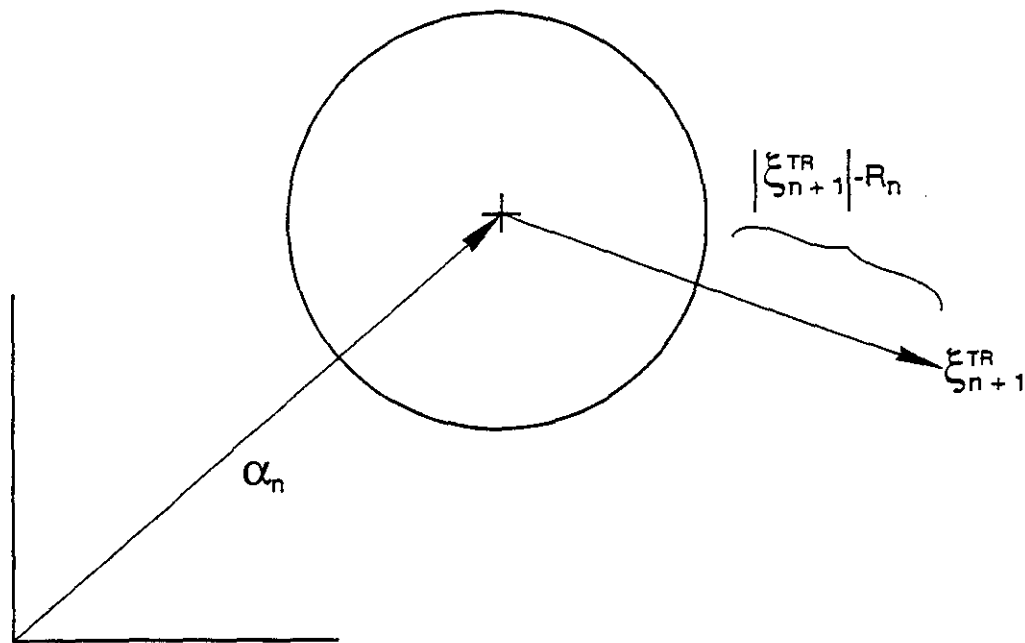
$$\Delta d^{pl} = Q \Delta \gamma \tag{4.5.54}$$

and

$$\Delta \vec{d}^{pl} = \sqrt{\frac{2}{3}} \Delta \gamma \cdot \tag{4.5.55}$$



The results of Equation (4.5.53) applied to Equation (4.5.48) show that the final stress is calculated by returning the elastic trial stress radially to the final yield surface at the end of the time step (hence the derivation of the name Radial Return Method). Estimates of the accuracy of this method and other methods for similarly integrating the rate equations are available in Krieg and Krieg (1977) and Schreyer et al. (1979) Note that the last term in Equation (4.5.48) (the radial return correction) is purely deviatoric.



TRI-6348-12-0

Figure 4.5.6. Geometric interpretation of the radial return correction.

The elastic plastic material model uses six internal state variables:

- EQPS - equivalent plastic strain
- RADIUS - current radius of yield surface
- ALPHA11 - 1,1 component of backstress in unrotated configuration
- ALPHA22 - 2,2 component of backstress in unrotated configuration
- ALPHA33 - 3,3 component of backstress in unrotated configuration
- ALPHA12 - 1,2 component of backstress in unrotated configuration.

The PROP array for this material contains the following entries:

- PROP(1) - Young's modulus, E
- PROP(2) - Poisson's ratio, ν
- PROP(3) - Yield Stress, σ_{yd}
- PROP(4) - Hardening Modulus, H
- PROP(5) - β
- *PROP(6) - 2μ
- *PROP(7) - 3μ
- *PROP(8) - $1/(2\mu(1 + H/3\mu))$ (Note: $H' = H/(1 - E/H)$)
- *PROP(9) - λ
- *PROP(10) - $2\beta H/3$
- *PROP(11) - $2(1 - \beta)H/3$

4.6 Soils and Crushable Foams Model

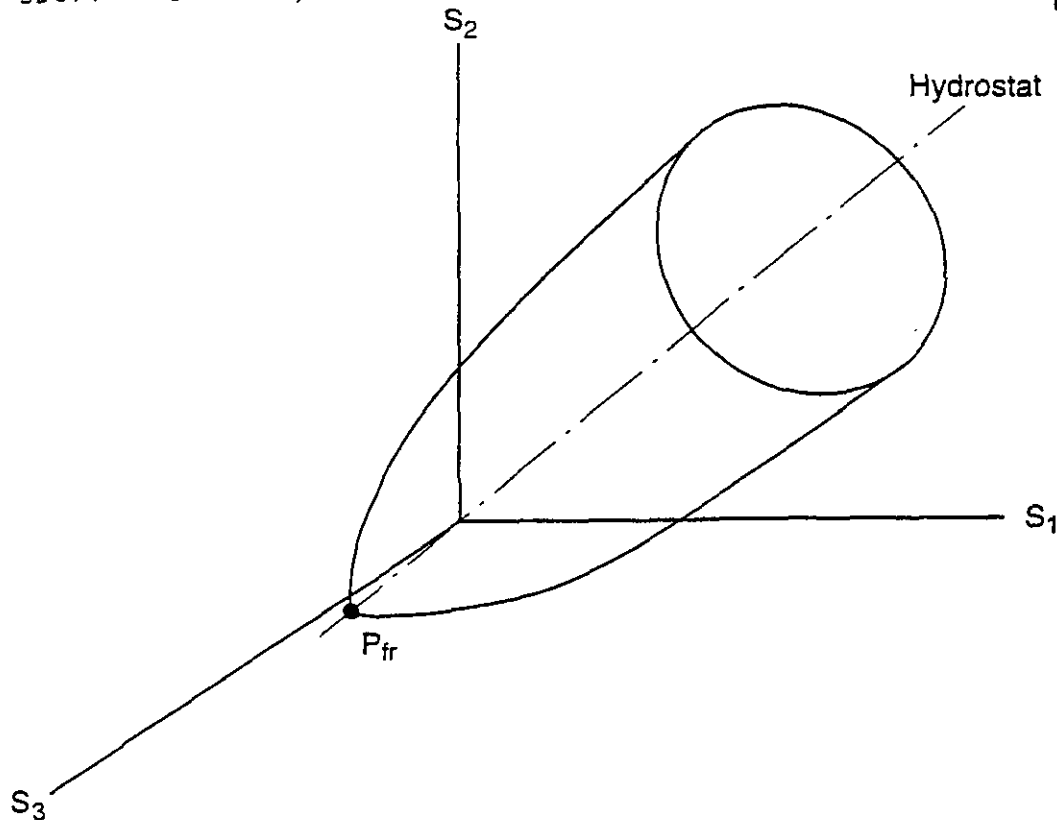
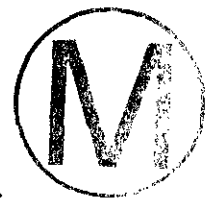
The soils and crushable foams model in SANTOS is a direct descendant of the model developed by Krieg (1972). One major difficulty with the original version of this material model which has confounded users is that the pressure dependence of the yield stress is expressed in terms of J_2 , the second invariant of the stress tensor. We have reformulated the model so that the yield stress is written directly in terms of the pressure. NOTE: this means that old data must be converted.

The yield surface assumed is a surface of revolution about the hydrostat in principal stress space as shown in Figure 4.6.1. In addition, a planar end cap on the normally open end is assumed. The yield stress is specified as a polynomial in pressure, p (positive in compression)

$$\sigma_{yd} = a_0 + a_1 p + a_2 p^2 \quad (4.6.1)$$

The determination of the yield stress from Equation (4.3.1) places severe restrictions on the admissible values of a_0 , a_1 , and a_2 . There are three valid cases as shown in Figure 4.6.2. First, the user may specify a positive a_0 , and a_1 and a_2 equal to zero as shown in Figure 4.6.2a. This gives an elastic-perfectly plastic deviatoric response, and the yield surface is a cylinder oriented along the hydrostat in principal stress space. Second, a conical yield surface





TRI-6348-13-0

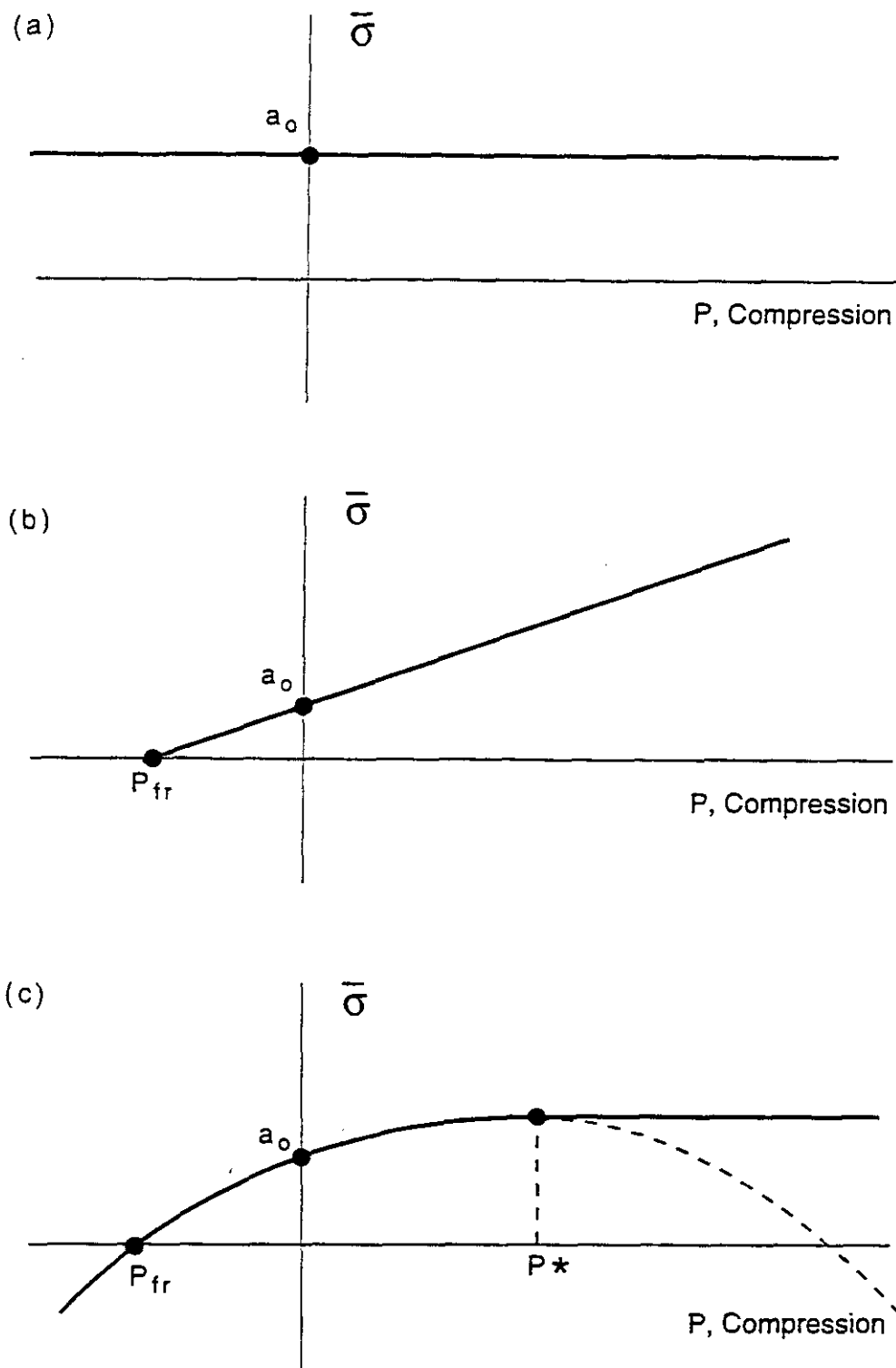
Figure 4.6.1. Pressure-dependent yield surface for the soils and crushable foams material model.

(Figure 4.6.2b) is given by setting a_2 to zero and entering appropriate values of a_0 and a_1 . The program checks the user's input to determine whether a valid (negative) tensile fracture pressure, P_{fr} , results from the input data. The third case results when all three constants are nonzero and the program detects that a valid negative tensile failure pressure can be derived from the data. This case is shown in Figure 4.6.2c. A valid set of constants for the third case results in a parabola as shown in Figure 4.6.2c. We have drawn the descending portion of the curve with a dashed line, indicating that the program does not use that portion of the curve. Instead, when the pressure exceeds P^* , the yield stress is held constant as shown at the maximum value.

The plasticity theories for the volumetric and deviatoric parts of the material response are completely uncoupled. The volumetric response is computed first. The mean pressure, p , is assumed to be positive in compression, and a yield function is written for the volumetric response as

$$\phi_p = p - f_p(\epsilon_v) \quad (4.6.2)$$

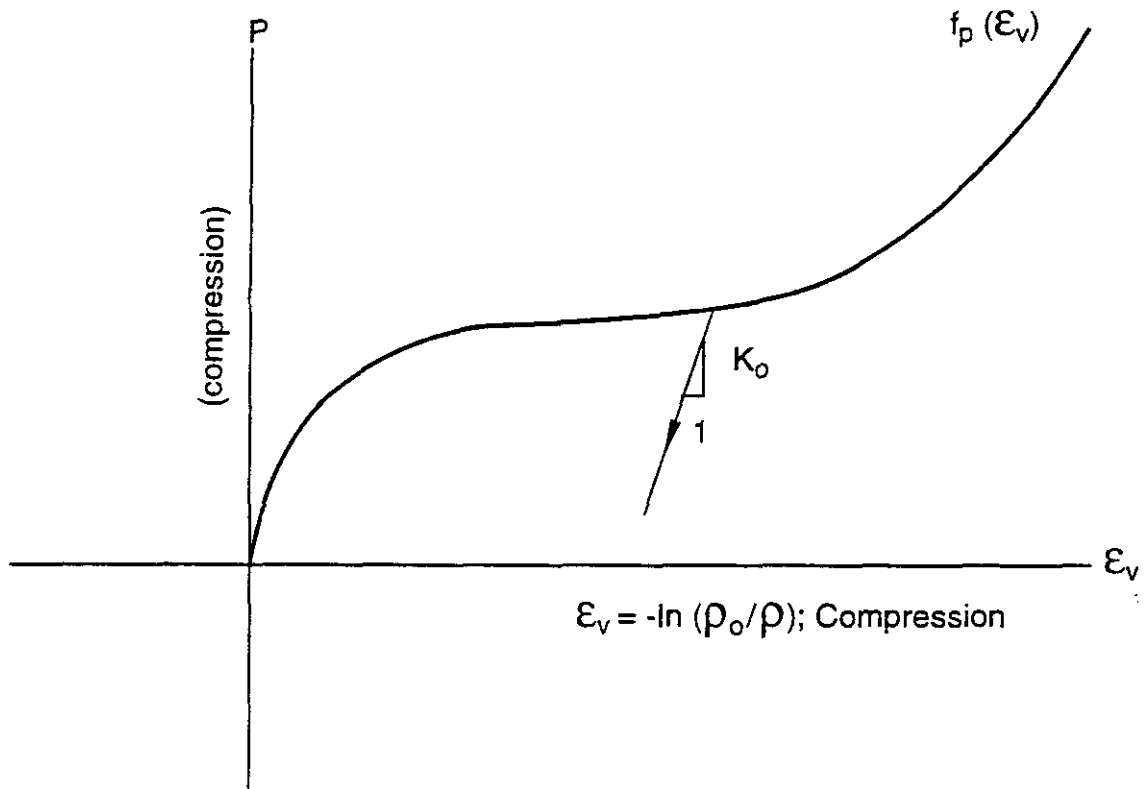
where $f_p(\epsilon_v)$ defines the volumetric stress-strain curve for the pressure as shown in Figure 4.6.3. This function is defined by the user with the restriction that the slope of the function must be less than or equal to the unloading bulk modulus, K_0 , everywhere. If the user wishes the volumetric response to be purely elastic, he simply specifies no function identification (e.g., FUNCTION ID = 0). The yield function, ϕ_p , determines the motion of the end cap along the hydrostat.



TRI-6348-14-0

Figure 4.6.2. Forms of valid yield surface which can be defined for the soils and crushable foams material model.





TRI-6348-15-0

Figure 4.6.3. Pressure versus volumetric strain curve in terms of a user-defined curve, $F(\epsilon_v)$, for the soils and crushable foams material model.

The mean volumetric strain is updated as

$$\epsilon_v^{n+1} = \epsilon_v^n + \Delta t \dot{\epsilon}_v \quad (4.6.3)$$

where $\dot{\epsilon}_v$ is the volumetric part of the strain rate ($\dot{\epsilon}_v = \frac{1}{3} \text{tr } \mathbf{d}$).

There are three possible regimes of the pressure-volumetric strain response. Tensile failure is assumed to occur if the pressure becomes smaller (more negative) than P_{ff} . The quantity ϵ_{ff} is initialized to $-P_{ff}/K_0$ by the program. If tensile failure is detected, the pressure is set to $-P_{ff}$. Remember, pressure is negative in tension! Failure by monotonic tensile loading is shown in Figure 4.6.4a. As long as $\epsilon_v < \epsilon_{ff}$, the pressure will remain equal to $-P_{ff}$.

If the volumetric strain exceeds ϵ_{ff} , a check is then made to see if

$$\epsilon_v < \epsilon_u \quad (4.6.4)$$

where ϵ_u is the most positive (compressive) volumetric strain previously experienced by the material, set initially to zero by the program. If Equation (4.6.4) is satisfied, the step is elastic and

$$p^{n+1} = p^n - K_0 \Delta \epsilon_v \quad (4.6.5)$$

This elastic response is shown in Figure 4.6.4b.

If Equation (4.6.4) is not satisfied, the volumetric response is along the curve defined by $f_p(\epsilon_v)$ and

$$p^{n+1} = f_p(\epsilon_v^{n+1}) \quad (4.6.6)$$

and we set

$$\epsilon_u = \epsilon_v^{n+1} \quad (4.6.7)$$

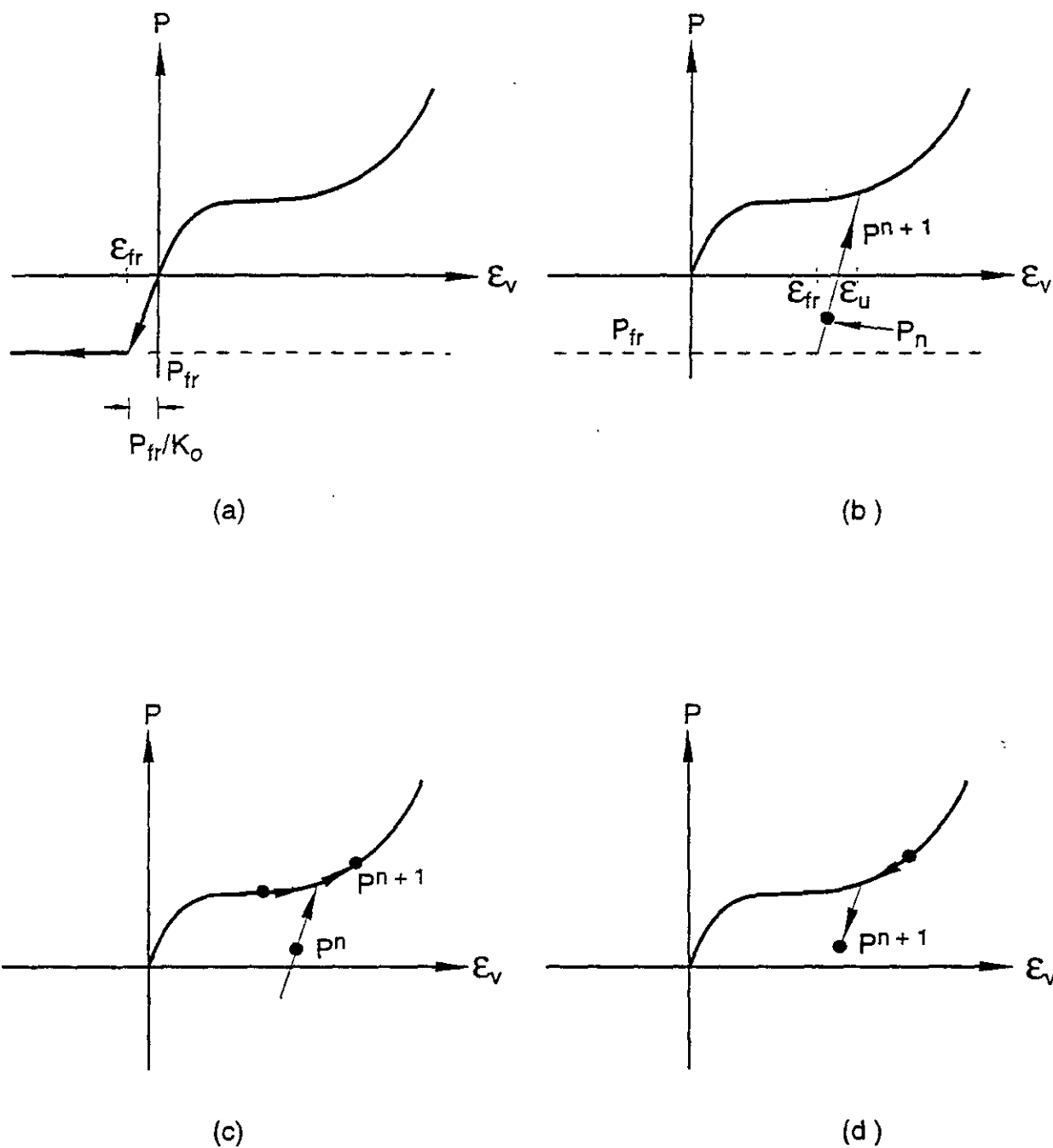
This response is shown in Figure 4.6.4c. Note, that if Equation (4.6.5) is used to determine p , we also drag ϵ_{ff} along so that if we unload from the curve, $f_p(\epsilon_v)$, we will fracture at the appropriate strain level as shown in Figure 4.6.4d.

The deviatoric part of the response is computed next and uses a conventional plasticity theory with radial return. See Krieg and Krieg (1977). The trial elastic deviatoric stresses are computed as

$$\mathbf{S}^{\text{tr}} = \mathbf{S}_n + 2\mu \Delta t \dot{\epsilon} \quad (4.6.8)$$

where $\dot{\epsilon}$ is the deviatoric part of the strain rate. The current value of yield stress is calculated using Equation (4.6.1), and the von Mises effective stress, $\bar{\sigma}$, is computed as





TRI-6348-16-0

Figure 4.6.4. Possible loading cases for the pressure versus volumetric strain response using the soils and crushable foams material mode.



$$\bar{\sigma} = \sqrt{\frac{3}{2} S:S} \quad (4.6.9)$$

The yield condition is checked to determine whether $\bar{\sigma} < \sigma_{yd}$. If this is the case, the trial stress is the correct deviatoric stress at the end of the time step, $S_{n+1} = S^tr$. If yield is exceeded, a simple radial return is performed to calculate the deviatoric stress at the end of the time step

$$S_{n+1} = \frac{\sigma_{yd}}{\bar{\sigma}} S^tr \quad (4.6.10)$$

Finally, the total stress is determined by

$$\sigma_{n+1} = S^{n+1} + p^{n+1} \delta \quad (4.6.11)$$

The Soils and Crushable Foams model uses four internal state variables:

- EVMAX - maximum compressive volumetric strain experienced (always positive),
- EVFRAC - current value of volumetric fracture strain (positive in compression),
- EV - current value of volumetric strain (positive in compression),
- NUM - integer pointing to the last increment in the pressure function where the interpolate was found.

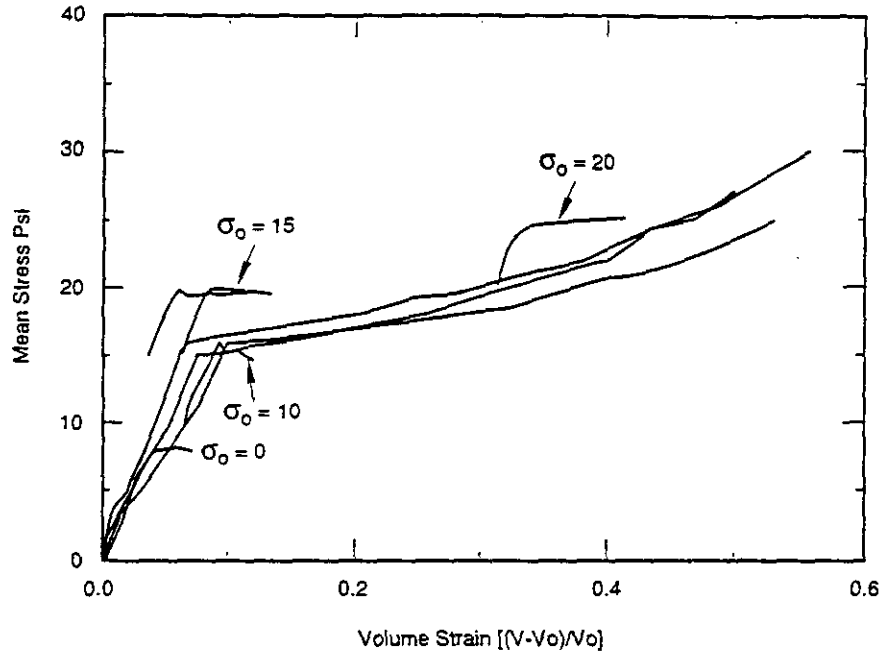
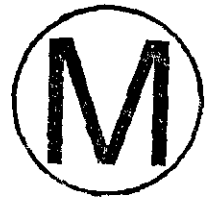
The PROP array contains the following entries for this material:

- PROP(1) - 2μ
- PROP(2) - Bulk Modulus, K
- PROP(3) - a_0
- PROP(4) - a_1
- PROP(5) - a_2
- PROP(6) - Function ID number.

4.7 Low Density Foams

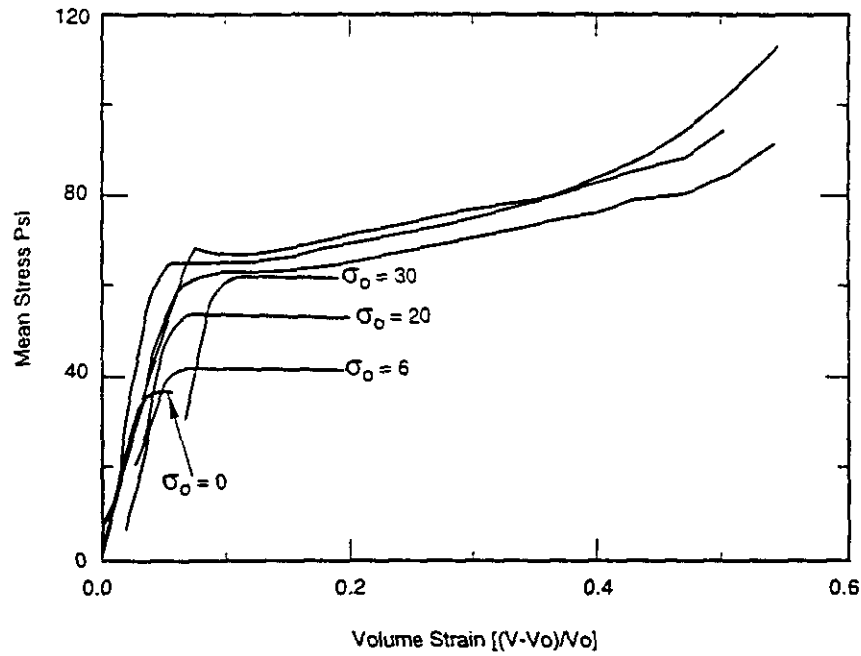
The low density foams model presented here was developed by Neilsen, Morgan, and Krieg (1987) and is based on results from experimental tests on low density, closed-cell polyurethane foams. These foams having densities ranging from 2 to 10 pounds per cubic foot have been proposed for use as energy absorbers in nuclear waste shipping containers. Representative responses of closed-cell polyurethane foams for various hydrostatic, uniaxial, and triaxial laboratory test conditions are shown in Figures 4.7.1 and 4.7.2. These results indicate that the volumetric response of the foam is highly dependent on load history. This implies that typical decompositions of total foam response into an independent volumetric part and a mean stress (pressure) dependent deviatoric part are not valid for this class of foam. Many "soil and crushable foam" models, including the other foam model described





TRI-6348-18-0

Figure 4.7.1. Foam volume strain versus mean stress for 6602 foam at various confining pressures.



TRI-6348-17-0

Figure 4.7.2. Foam volume strain versus mean stress for 9505 foam at various confining pressures.

in Section 4.6, use such decompositions and hence are not valid for low-density, closed-cell polyurethane foams. The model presented here reproduces experimental test responses more accurately for this class of foams than the model in Section 4.6.

The experimental tests on which this model is based were performed by the Civil Engineering Research Facility of the University of New Mexico with the results reported in (Nielsen et al., 1987). Foam samples were subjected to static, compressive stresses during these tests. In most of the tests, air was trapped in the closed cells of the foams and could not escape because the samples were jacketed with an impervious material. In this constitutive model, the total foam response is decomposed into contributions from the skeleton and from air trapped in the closed cells of the foam. The contribution of the air to the total foam response is dependent on the application. If the foam is used in a vented application where the air can escape, the contribution of the air is zero and the foam and skeleton responses are identical. If the foam is used in an application where the air cannot escape (such as a sealed shipping container) the foam pressure is considered to be the sum of pressure carried by the skeleton and the air pressure. That is,

$$P_f = P_{sk} + P_{air} \quad (4.7.1)$$

where p_f and p_{sk} are the mean stresses (first invariants of the stress tensor divided by three) of the foam and skeleton, respectively. The mean stresses and air pressure are assumed positive in tension. The air pressure is determined from

$$P_{air} = \frac{p_0 \gamma}{1 + \gamma - \phi} \quad (4.7.2)$$

where γ is the engineering volume strain (first invariant of the total strains), which is positive in tension and p_0 and ϕ are model parameters. The parameter p_0 is the initial foam pressure (usually atmospheric pressure of 14.7 psi), and ϕ is the ratio of the foam density to the polymer density from which the foam is produced.

Test data indicate that the skeleton response in any principal stress direction is independent of loading in any other principal stress direction. Thus, Poisson's ratio for the skeleton is equal to zero. Test data also indicate that the yield strength of the skeleton in any principal stress direction can be expressed in terms of the engineering volume strain and the second invariant of the deviatoric strains with the following relationship

$$\hat{f}_i = \begin{cases} A + B(1 + C\gamma); & \Pi'_e > 0 \\ B(1 + C\gamma); & \Pi'_e = 0 \end{cases} \quad (4.7.3)$$

where Π'_e is the second invariant of the deviatoric strain tensor; γ is the engineering volume strain as in Equation (4.7.2); A, B, and C are constants determined from fitting Equation (4.7.3) to the laboratory data. Constants B and C are determined from hydrostatic test data where Π'_e is zero, and A is determined from any test where the loading is deviatoric.

Numerical implementation of the model is as follows. Foam stresses and strains from the previous time increment are saved. At the beginning of the next time increment, the old skeleton stresses are computed from the old foam



stresses and the old air pressure. The strain rates for the new time increment are used to determine new strain increments and trial elastic stress increments for the skeleton. These stress increments are added to the old skeleton stresses to produce new trial stresses for the skeleton. The trial skeleton stresses are then rotated to principal stress directions and compared with the yield stress determined from Equation (4.7.3). If yield occurs, the skeleton stresses are set to the yield stress. If yield does not occur, the trial skeleton principal stresses become the final skeleton principal stresses. The final skeleton stresses are obtained by rotating the final skeleton principal stresses back to the unrotated configuration. Then, the final foam stresses are obtained by adding the air pressure contribution for the new strain state to the new skeleton stresses.

Input parameters for the model are the constants E , p_0 , ϕ , A , B , and C , which are defined above. If the foam is used in an application where the air can escape, p_0 should be input as zero. Otherwise, p_0 is the atmospheric pressure at the beginning of the simulation.

There are no internal state variables for this model.

The PROP array contains the following entries for this material type:

- PROP(1) - Young's modulus, E
- PROP(2) - A
- PROP(3) - B
- PROP(4) - C
- PROP(5) - NAIR
- PROP(6) - p_0
- PROP(7) - ϕ .



4.8 Elastic-Plastic Power Law Hardening Material

One of the more commonly used models in the SANTOS material library is the elastic-plastic combined isotropic/kinematic hardening model. This model considers the hardening modulus to be a constant, which means that the post-yield effective stress, $\bar{\sigma}$, versus effective plastic strain, $\bar{\epsilon}_p$, relationship is linear. For a large class of important problems, a linear $\bar{\sigma}$ versus $\bar{\epsilon}_p$ relationship may be adequate for the post-yield behavior over the range of interest. This, however, places a severe restriction on the materials to be modeled or requires *a priori* information about the expected strain levels in the problem so that an approximate hardening modulus may be selected to produce a good approximation to the correct stress state based on the expected strain values. In addition, the strain range of interest must be small (no large strain gradients) so that the linear hardening relationship is applicable. However, there are classes of problems in which the linear approximation for plastic hardening is inadequate. A constant hardening modulus cannot adequately describe the post-yield behavior to predict structural behavior in the detail required. Determination of limit load response is an example of a class of problems for which linear hardening is inappropriate.

To overcome these restrictions, a variable hardening plasticity model (Stone et al., 1990) has been included in SANTOS. The use of piecewise linear segments to represent the hardening curve was an initial consideration based on the capability to match any material hardening behavior, but the resulting material model subroutine was not

amenable to vectorization. Vectorization requirements limit the form of the model to a functional relationship between effective stress and effective plastic strain. The form of the current implementation considers the post-yield stress to be described by a power law involving the equivalent plastic strain with the option to include a Lüders strain segment. The form of the hardening model was selected for its simplicity and ability to match the post-yield behavior of many engineering materials. The model has the form during a plastic loading process

$$\bar{\sigma} - \sigma_{ys} = A(\bar{\epsilon}_p - \epsilon_L)^m \quad (4.8.1)$$

where A and m are material constants, $\bar{\epsilon}_p$ is the equivalent plastic strain, $\bar{\sigma}$ is the effective stress, σ_{ys} is the initial yield stress, and ϵ_L is the Lüders strain or yield plateau strain. The use of brackets in the above equation denotes the use of a Heaviside function. The function is zero until the arithmetic expression within the brackets becomes positive. The material constants for this model can be determined from the measured stress versus strain data through simple curve fitting techniques. By suitably choosing the material constants A and m , the form of the model can represent either elastic/perfectly plastic or linear hardening material behavior in addition to the power law hardening response. The proposed material model is strictly valid for isotropic hardening behavior where the radius of the yield surface grows equally in all directions due to plastic straining.

Many engineering materials exhibit the phenomenon of Lüders straining. A typical stress versus strain curve for such a material is shown in Figure 4.8.1. In reality, Lüders strain does not occur at constant stress but rather in a serrated fashion. Each serration corresponds to the formation of a new Lüders band. The serrations are small enough that a constant stress representation is adequate. In common ferrous alloys, Lüders strain as well as other yield point phenomena are generally associated with the interaction between solute atoms and dislocations.

The constitutive routine is entered with the stress state at the beginning of the step, S_{ij}^n , the strain-rate over the step, $\dot{\epsilon}_{ij}$, and the time step, Δt . An elastic trial stress, S_{ij}^{tr} , is computed and a von Mises yield criterion is used to compute a trial effective stress, $\bar{\sigma}^{tr}$, which is compared to the current radius of the yield surface. If the trial effective stress is less than the radius of the yield surface, then the load step is elastic and the trial stress becomes the final stress, S_{ij}^{n+1} . If the effective stress is greater than the radius of the yield surface, then plastic straining will occur over the step and the final stress state and plastic strain increment remain to be computed.

The expression for the stress at the end of the step is

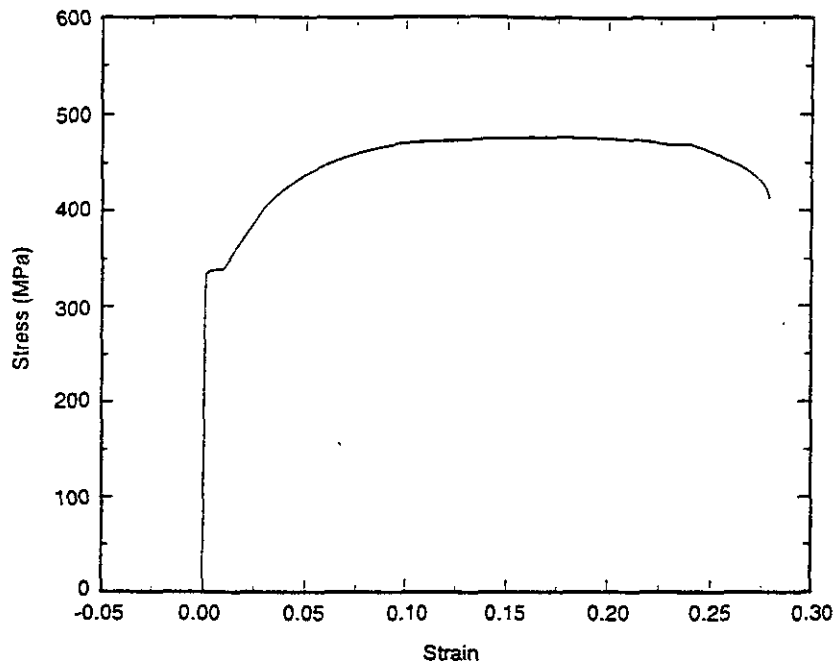
$$S_{ij}^{n+1} = S_{ij}^n + \dot{S}_{ij} \left(S_{ij}^{n+1} \right) \Delta t \quad (4.8.2)$$

where we have used a backward Euler integration for the stress. The stress rate at the end of the step, \dot{S}_{ij}^{n+1} , is computed as follows

$$\dot{S}_{ij}^{n+1} = 2\mu(\dot{\epsilon}_{ij} - \dot{\epsilon}_{p_{ij}}) \quad (4.8.3)$$

where $\dot{\epsilon}_{p_{ij}}$ are the components of plastic strain.





TRI-6348-19-0

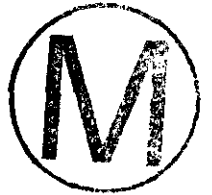


Figure 4.8.1. Stress versus strain curve for a typical ferritic steel exhibiting Lüders strain.

For von Mises flow, we can write the above as

$$\dot{S}_{ij}^{n+1} = 2\mu\dot{\epsilon}_{ij} - 2\mu\left(\frac{3\gamma}{2}\frac{S_{ij}^{n+1}}{\bar{\sigma}^{n+1}}\right) \quad (4.8.4)$$

where γ is a scalar quantity.

Substituting the above expression for \dot{S}_{ij}^{n+1} into the expression for S_{ij}^{n+1} results in

$$S_{ij}^{n+1} = S_{ij}^n + 2\mu\dot{\epsilon}_{ij}\Delta t - 3\mu\frac{S_{ij}^{n+1}}{\bar{\sigma}^{n+1}}\Delta\gamma \quad (4.8.5)$$

where $\Delta\gamma = \gamma\Delta t$. The first two expressions on the right-hand-side of the equation define the trial stress S_{ij}^{tr} so that the final expression becomes

$$S_{ij}^{n+1} = S_{ij}^{tr} - \left(3\mu\frac{S_{ij}^{n+1}}{\bar{\sigma}^{n+1}}\Delta\gamma\right) \quad (4.8.6)$$

We make use of the following identity

$$\frac{S_{ij}^{n+1}}{\bar{\sigma}^{n+1}} = \frac{S_{ij}^{\text{tr}}}{\bar{\sigma}^{\text{tr}}} \quad (4.8.7)$$

to get the final expression for the stress at the end of the step

$$S_{ij}^{n+1} = S_{ij}^{\text{tr}} \left(1 - \frac{3\mu\Delta\gamma}{\bar{\sigma}^{\text{tr}}} \right) \quad (4.8.8)$$

The plastic strain increment $\Delta\gamma$, is the only unknown in the equation. To solve for the plastic strain increment, we must go back to our expression for the yield function. Combining the yield function with the expression for S_{ij}^{n+1} and making use of the identity, we get

$$\bar{\sigma}^{\text{tr}} - 3\mu\Delta\gamma = \sigma_{ys} + A(\bar{\epsilon}_p^n + \Delta\gamma - \epsilon_L)^m \quad (4.8.9)$$

which is solved for $\Delta\gamma$ using Newton Raphson iteration. The computed value of $\Delta\gamma$ is substituted back into the expression for S_{ij}^{n+1} , Equation (4.8.8).

The bulk response is assumed to be linear elastic. The pressure at the end of the step is calculated using the volumetric strain rate, d_{kk} , through the relation

$$p^{n+1} = p^n + Kd_{kk}\Delta t \quad (4.8.10)$$

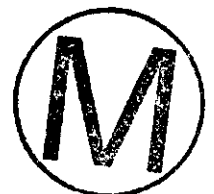
where K is the bulk modulus of the material, Δt is the time step size, and p^n is the pressure at the beginning of the step. The stress from the deviatoric and bulk responses are combined to give the final stress state.

The power law hardening material uses two internal state variables:

- RADIUS - current radius of the yield surface
- EQPS - equivalent plastic strain.

The PROP array for this material contains the following entries:

- PROP(1) - Young's modulus, E
- PROP(2) - Poisson's ratio, ν
- PROP(3) - Yield Stress, σ_{ys}
- PROP(4) - Hardening constant, A
- PROP(5) - Hardening exponent, m
- PROP(6) - Lüders strain, ϵ_L
- * PROP(7) - 2μ
- * PROP(8) - 3μ
- * PROP(9) - λ





4.9 Power Law Creep Material Model

The power law creep material model described here is commonly used to model the time-dependent behavior of metals, brazes, or solders at high homologous temperatures as well as the time-dependent behavior of geologic materials such as salt. The model is cast as a conventional power law secondary creep model of the form

$$\dot{\epsilon}_c = A \bar{\sigma}^m \exp\left(\frac{-Q}{R\Theta}\right) \quad (4.9.1)$$

where $\bar{\sigma}$ is the effective deviatoric stress, A and m are material constants, Θ is the absolute temperature, R is the universal gas constant ($1.987 \frac{\text{cal}}{\text{moleK}}$), and Q is the activation energy.

We choose to write the expression for the deviatoric stress at the end of the step as

$$S_{ij}^{n+1} = S_{ij}^n + \dot{S}_{ij}(S_{ij}^n) \Delta t \quad (4.9.2)$$

where we have used a forward Euler integration for the stress. We can write the stress rate at step n as

$$\dot{S}_{ij} = 2\mu(\dot{\epsilon}_{ij} - \dot{\epsilon}_{c,ij}) \quad (4.9.3)$$

where $\dot{\epsilon}_{c,ij}$ are the creep strain rate components. The creep strain rate components for von Mises flow are

$$\dot{\epsilon}_{c,ij} = \frac{3}{2} \dot{\bar{\epsilon}}_c \frac{S_{ij}}{\bar{\sigma}} \quad (4.9.4)$$

where $\dot{\bar{\epsilon}}_c$ is the effective or equivalent creep strain rate. Substituting into the expression for the stress rate gives

$$\dot{S}_{ij}^n = 2\mu \left(\dot{\epsilon}_{ij} - \frac{3}{2} A \exp\left(\frac{-Q}{R\Theta}\right) \bar{\sigma}^{m-1} S_{ij}^n \right) \quad (4.9.5)$$

where $\bar{\sigma}$ is evaluated at step n . The stress rate is computed and stored as a state variable for use during step $n+1$.

Numerical analysis of the forward Euler operator shows that the method is conditionally stable. It is possible to calculate an estimate of the critical time step for stability of the forward Euler operator based on the form of the flow potential and the elastic constants (Corneau, 1975). Following procedures outlined in Corneau (1975), the critical time step for stability is calculated to be

$$\Delta t_{st} < \frac{4(1+\nu)}{3EA \exp\left(\frac{-Q}{R\Theta}\right) m \bar{\sigma}^{m-1}} \quad (4.9.6)$$

where E and ν are Young's modulus and Poisson's ratio, respectively. Accuracy of the method is assured if the time steps are sufficiently small, but the stable time step does not guarantee an accurate solution. However, our experience with the method has shown that the solution obtained using Δt_{st} is indeed accurate. The standard power

law secondary creep model is requested in SANTOS by using the material name POWER LAW CREEP while the adaptive time-stepping version is requested by using the name ADAPTIVE PL CREEP.

The volumetric behavior of the material is assumed to be linearly elastic as shown below

$$p^{n+1} = p^n + K d_{kk} \Delta t \quad (4.9.7)$$

where K is the bulk modulus, d_{kk} is the volumetric strain rate, Δt is the time step size, and p^n is the pressure at the beginning of the step. The stress from the deviatoric and bulk responses is combined to give the final stress state for the material.

The power law creep material uses a single state variable:

EQCS - equivalent creep strain.

The PROP array for this material contains the following entries:

- PROP(1) - 2μ
- PROP(2) - K
- PROP(3) - A
- PROP(4) - m
- PROP(5) - $\frac{Q}{R\Theta}$ if isothermal or $\frac{Q}{R}$ if not.

4.10 Thermoelastic Material Model

This material model represents the behavior of an elastic material with temperature-dependent material constants. Both Young's modulus and Poisson's ratio are allowed to vary with temperature. The values of Young's modulus and Poisson's ratio at the beginning (step n) and end (step $n+1$) of the time step are stored as state variables. The relationship between the property value and temperature is specified using a FUNCTION definition.

We will choose to separate the stress and strain behavior into bulk and deviatoric response. The resulting equation for the elastic deviatoric stress response is

$$S_{ij}^{n+1} = 2\mu(\Theta^{n+1}) \epsilon_{ij}^{n+1} \quad (4.10.1)$$

where the shear modulus μ is a function of the temperature, Θ^{n+1} , at the end of the step. For our numerical implementation, we will cast the problem in an incremental form. The stress at the end of the step now becomes

$$S_{ij}^{n+1} = S_{ij}^n + \dot{S}_{ij}(S_{ij}^{n+1}) \Delta t \quad (4.10.2)$$





We choose to write the stress rate term, \dot{S}_{ij} , as

$$\dot{S}_{ij} = \left(2\mu(\Theta^{n+1}) \dot{\epsilon}_{ij} + 2\dot{\mu}(\Theta^{n+1}) \epsilon_{ij}^n \right) \quad (4.10.3)$$

with the expression for $\dot{\mu}(\Theta^{n+1})$ defined as

$$\dot{\mu}(\Theta^{n+1}) = \frac{\mu(\Theta^{n+1}) - \mu(\Theta^n)}{\Delta t} \quad (4.10.4)$$

This definition for the stress increment is neither a pure forward or backward Euler representation but a hybrid method where we choose to use the total strain at the beginning of the step along with a backward difference for

$\dot{\mu}(\Theta^{n+1})$. If we employ the fact that $\epsilon_{ij}^n = \frac{s_{ij}^n}{2\mu(\Theta^n)}$, we can write the final expression for the deviatoric stress as

$$S_{ij}^{n+1} = S_{ij}^n \left(\frac{\mu(\Theta^{n+1})}{\mu(\Theta^n)} \right) + 2\mu(\Theta^{n+1}) \dot{\epsilon}_{ij} \Delta t \quad (4.10.5)$$

The temperature-dependent elastic bulk response is computed in a similar fashion. The equation for the bulk response at step $n+1$ is

$$\sigma_{kk}^{n+1} = 3K(\Theta^{n+1}) \epsilon_{kk}^{n+1} \quad (4.10.6)$$

We can write the above equation in an incremental form that is more suitable for numerical implementation.

$$\sigma_{kk}^{n+1} = \sigma_{kk}^n \left(\frac{K(\Theta^{n+1})}{K(\Theta^n)} \right) + 3K(\Theta^{n+1}) \dot{\epsilon}_{kk} \Delta t \quad (4.10.7)$$

The stress from the deviatoric and bulk responses is combined to give the final stress state.

The thermoelastic material uses the following state variables:

- YM0 - Young's modulus at the beginning of the step
- YM1 - Young's modulus at the end of the step
- XNU0 - Poisson's ratio at the beginning of the step
- XNU1 - Poisson's ratio at the end of the step.

The PROP array for this material contains the following entries:

- PROP(1) - Young's modulus, E
- PROP(2) - Poisson's ratio, ν

- PROP(3) - Modulus function identification
- PROP(4) - Poisson's ratio function identification.

4.11 Thermoelastic-Plastic Power Law Hardening Material Model

This material model represents the behavior of an elastic-plastic power law hardening material with temperature-dependent material constants. Both Young's modulus and Poisson's ratio are allowed to vary with temperature along with the material yield stress. The values of Young's modulus, Poisson's ratio, and yield stress at the beginning and end of the time step are stored as state variables. The relationship between the material property value and temperature is specified using a FUNCTION definition.

We will separate the material behavior into deviatoric and bulk responses. If we consider only deviatoric behavior, the model has the following form during a plastic loading process

$$\bar{\sigma} = \sigma_{ys}(\Theta) + A \langle \bar{\epsilon}_p - \epsilon_L \rangle^m \quad (4.11.1)$$

where A and m are material constants, σ_{ys} is the temperature-dependent initial yield stress, $\bar{\epsilon}_p$ is the equivalent plastic strain, $\bar{\sigma}$ is the effective stress, and ϵ_L is the Lüders strain or yield plateau strain. The use of brackets in the above expression denotes the use of a Heaviside function. The function is zero until the arithmetic expression within the brackets becomes positive. The material constants for this model can be determined from measured stress versus strain data through simple curve-fitting procedures. By suitably choosing the material constants A and m, the form of the model can represent either elastic/perfectly plastic or linear hardening material behavior in addition to the power law hardening response. The temperature dependence is captured by allowing the initial yield stress and elastic constants to be a function of temperature.

The expression for the stress at the end of the step is

$$S_{ij}^{n+1} = S_{ij}^n + \dot{S}_{ij}(\dot{S}_{ij}^{n+1})\Delta t \quad (4.11.2)$$

where we have used a backward Euler integration for the stress. The stress rate at the end of the step, \dot{S}_{ij}^{n+1} , is defined as follows

$$\dot{S}_{ij} = 2\dot{\mu}(\Theta^{n+1})\left(\epsilon_{ij}^n - \epsilon_{p_{ij}}^n\right) + 2\mu(\Theta^{n+1})\left(\dot{\epsilon}_{ij} - \dot{\epsilon}_{p_{ij}}\right) \quad (4.11.3)$$

where $\epsilon_{p_{ij}}$ are the components of the plastic strain. We choose to use this expression for the stress rate because in the absence of plastic strain we recover the same expression for the stress as derived for the thermoelastic model. We define the difference expression for $\dot{\mu}(\Theta^{n+1})$ as

$$\dot{\mu}(\Theta^{n+1}) = \frac{\mu(\Theta^{n+1}) - \mu(\Theta^n)}{\Delta t} \quad (4.11.4)$$





For von Mises flow, we can write the above as

$$\dot{S}_{ij} = \left(\frac{\mu(\Theta^{n+1}) - \mu(\Theta^n)}{\Delta t} \right) \left(\frac{S_{ij}^n}{\mu(\Theta^n)} \right) + 2\mu(\Theta^{n+1})\dot{\epsilon}_{ij} - 2\mu(\Theta^{n+1}) \left(\frac{3\gamma}{2} \frac{S_{ij}^{n+1}}{\bar{\sigma}^{n+1}} \right) \quad (4.11.5)$$

where γ is a scalar quantity.

Substituting the above expression for \dot{S}_{ij}^{n+1} into the expression for S_{ij}^{n+1} results in

$$S_{ij}^{n+1} = S_{ij}^n \left(\frac{\mu(\Theta^{n+1})}{\mu(\Theta^n)} \right) + 2\mu(\Theta^{n+1})\dot{\epsilon}_{ij}\Delta t - 3\mu(\Theta^{n+1}) \frac{S_{ij}^{n+1}}{\bar{\sigma}^{n+1}} \Delta\gamma \quad (4.11.6)$$

where $\Delta\gamma = \gamma\Delta t$. The first two expressions on the right-hand-side of the equation define the trial stress S_{ij}^{tr} so that the final expression becomes

$$S_{ij}^{n+1} = S_{ij}^{tr} - \left(3\mu(\Theta^{n+1}) \frac{S_{ij}^{n+1}}{\bar{\sigma}^{n+1}} \Delta\gamma \right) \quad (4.11.7)$$

We make use of the following identity

$$\frac{S_{ij}^{n+1}}{\bar{\sigma}^{n+1}} = \frac{S_{ij}^{tr}}{\bar{\sigma}^{tr}} \quad (4.11.8)$$

to get the final expression for the stress at the end of the step

$$S_{ij}^{n+1} = S_{ij}^{tr} \left(1 - \frac{3\mu(\Theta^{n+1})\Delta\gamma}{\bar{\sigma}^{tr}} \right) \quad (4.11.9)$$

The plastic strain increment, $\Delta\gamma$, is the only unknown in the equation. To solve for the plastic strain increment, we must go back to our expression for the yield function. Combining the yield function with the expression for S_{ij}^{n+1} and making use of the identity, we get

$$\bar{\sigma}^{tr} - 3\mu(\Theta^{n+1})\Delta\gamma = \sigma_{ys}(\Theta^{n+1}) + A(\bar{\epsilon}_p^n + \Delta\gamma - \epsilon_L)^m \quad (4.11.10)$$

which is solved for $\Delta\gamma$ using Newton Raphson iteration. The computed value of $\Delta\gamma$ is substituted back into the expression for S_{ij}^{n+1} , Equation (4.11.9).

The bulk response is assumed to be linear elastic. The pressure at the end of the step is calculated using the volumetric strain, ϵ_{kk} , through the relation

$$\sigma_{kk}^{n+1} = 3K(\Theta^{n+1})\epsilon_{kk}^{n+1} \quad (4.11.11)$$

where $K(\Theta^{n+1})$ is the temperature-dependent bulk modulus at the end of the step. Following the procedure outlined for the thermoelastic material model, we can arrive at the final expression for the bulk response.

$$\sigma_{kk}^{n+1} = \sigma_{kk}^n \left(\frac{K(\Theta^{n+1})}{K(\Theta^n)} \right) + 3K(\Theta^{n+1})\dot{\epsilon}_{kk}\Delta t \quad (4.11.12)$$

The stress from the deviatoric and bulk responses is combined to give the final stress state.

The thermoelastic-plastic material uses the following state variables:

EQPS	- Equivalent plastic strain
YM0	- Young's modulus at the beginning of the step
YM1	- Young's modulus at the end of the step
XNU0	- Poisson's ratio at the beginning of the step
XNU1	- Poisson's ratio at the end of the step
YS0	- Yield stress at the beginning of the step
YS1	- Yield stress at the end of the step
RADIUS	- Radius of the yield surface.

The PROP array for this material contains the following entries:

PROP(1)	- Young's modulus, E
PROP(2)	- Poisson's ration, ν
PROP(3)	- Yield stress, σ_y
PROP(4)	- Modulus function identification
PROP(5)	- Pr function identification
PROP(6)	- Yield function identification
PROP(7)	- Hardening constant, A
PROP(8)	- Hardening exponent, m
PROP(9)	- Lüders strain, ϵ_L .

4.12 Multi-mechanism Deformation (M-D) Creep Model

A multi-mechanism deformation (M-D) model proposed by Munson and Dawson (1979, 1982, 1984) and extended by Munson et al. (1988) has been included in SANTOS to model the creep behavior of rock salt. This model, which is based on the deformation map for salt, describes the relationship between the steady-state creep rate, stress, and temperature in terms of three deformation mechanisms in salt. Two of these mechanisms are dislocation glide and dislocation climb. The effects of a third mechanism are also included in the M-D model. Although this mechanism has not been characterized in terms of microstructural processes, its effects are observed in creep



experiments. Transient workhardening and recovery responses are incorporated through a state variable function that modifies the steady-state creep rates.

In the M-D model, the equivalent creep strain rate at steady-state, $\dot{\epsilon}_s$, is assumed to be equal to the sum of three terms, each arising from one of the three mechanisms described above, i.e.,

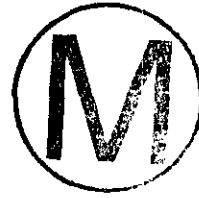
$$\dot{\epsilon}_s = \dot{\epsilon}_{s1} + \dot{\epsilon}_{s2} + \dot{\epsilon}_{s3} \quad (4.12.1)$$

The three equivalent strain rates appearing on the right-hand-side of the above equation are given by the following functions:

$$\dot{\epsilon}_{s1} = A_1 \exp\left(-\frac{Q_1}{R\Theta}\right) \left(\frac{\sigma_e}{\mu}\right)^{n_1} \quad (4.12.2)$$

$$\dot{\epsilon}_{s2} = A_2 \exp\left(-\frac{Q_2}{R\Theta}\right) \left(\frac{\sigma_e}{\mu}\right)^{n_2} \quad (4.12.3)$$

$$\dot{\epsilon}_{s3} = H(\sigma_e - \sigma_o) \left[B_1 \exp\left(-\frac{Q_1}{R\Theta}\right) + B_2 \exp\left(-\frac{Q_2}{R\Theta}\right) \right] \sinh\left(\frac{q(\sigma_e - \sigma_o)}{\mu}\right) \quad (4.12.4)$$



where the A_i 's, B_i 's and n_i 's are constants, the Q_i 's are activation energies, Θ is the absolute temperature, R is the universal gas constant, μ is the elastic shear modulus, σ_e is the equivalent stress, q is a constant, σ_o is the stress limit of the dislocation slip mechanism, and H is the Heaviside step function. In the above equation, $\dot{\epsilon}_{s1}$ represents the effects of the dislocation climb mechanism, $\dot{\epsilon}_{s2}$ represents the effects of the unidentified mechanism, and $\dot{\epsilon}_{s3}$ represents the effects of the glide mechanism. The relationship between σ_e and the components of the stress tensor under general loading conditions depends on the choice of the stress generalization and will be discussed later.

Transient creep is incorporated in the M-D model through the use of a scaling function F , which modifies the steady-state creep rate. The total equivalent creep rate $\dot{\epsilon}$ is given by:

$$\dot{\epsilon} = F(\sigma_e, \Theta, \zeta) \dot{\epsilon}_s \quad (4.12.5)$$

The arguments of the transient scaling function are equivalent stress, temperature, and an internal state variable, ζ . The evolution of ζ is described by a separate rate equation. Three branches of the function F can be identified: (1) a workhardening branch where F assumes a value greater than unity, (2) an equilibrium branch where F is equal to unity, and (3) a recovery branch where F is less than unity. The expression for F is

$$F = \exp\left(\left[1 - \frac{\zeta}{\epsilon_t^*}\right]^2 \Delta\right) \text{ for } \zeta < \epsilon_t^* \quad (4.12.6)$$

$$F = 1 \text{ for } \zeta = \epsilon_t^* \quad (4.12.7)$$

$$F = \exp\left(-\left[1 - \frac{\zeta}{\epsilon_t^*}\right]^2 \delta\right) \text{ for } \zeta > \epsilon_t^* \quad (4.12.8)$$

In the above equations, Δ and δ are referred to as the workhardening and recovery functions, respectively, while ϵ_t^* is referred to as the transient strain limit. The workhardening and recovery functions are assumed to be of the form

$$\Delta = \alpha_w + \beta_w \log\left(\frac{\sigma_e}{\mu}\right) \quad (4.12.9)$$

$$\delta = \alpha_r + \beta_r \log\left(\frac{\sigma_e}{\mu}\right) \quad (4.12.10)$$

The transient strain limit is a function of temperature and stress given by

$$\epsilon_t^* = K_0 \exp(c\Theta) \left(\frac{\sigma_e}{\mu}\right)^m \quad (4.12.11)$$

where K_0 and c are constants. Finally, the evolution equation for the internal variable ζ is

$$\dot{\zeta} = (F - 1)\dot{\epsilon}_s = \dot{\epsilon} - \dot{\epsilon}_s \quad (4.12.12)$$

To complete the generalization of the M-D constitutive model, an equivalent stress and flow rule for the creep strain rate must be defined. These two definitions provide the necessary linkage among the three-dimensional stress state, the creep strain rate, and the invariant creep relationships described earlier. According to Munson et al. (1988), the Tresca stress generalization provides the most appropriate definition of the equivalent stress for rock salt. With the Tresca stress generalization, the equivalent stress becomes

$$\sigma_e^I = 2\sqrt{J_2} \cos\psi = \sigma_1 - \sigma_3 \quad (4.12.13)$$

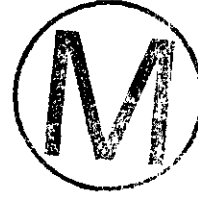
where ψ is the Lode angle defined by

$$\sin 3\psi = \frac{-3J_3\sqrt{3}}{2J_2^{3/2}}$$

In the two preceding equations, J_2 and J_3 are the second and third invariants of the deviatoric part of the stress tensor, and σ_1 and σ_3 are the maximum and minimum principal stresses, respectively. The flow is assumed to be associative so that the direction of $\dot{\bar{\epsilon}}$ is normal to the Tresca flow surface. Unfortunately, the normal is undefined as $\psi = \pm \frac{\pi}{6}$ where sharp corners exist in the Tresca flow surface. At these locations, the flow is assumed to be normal to the von Mises flow surface. The von Mises flow surface is characterized by a constant value of σ_e^{vM} where



$$\sigma_e^{vm} = \sqrt{3J_2} \quad (4.12.14)$$



Note that $\sigma_e^{vm} = \sigma_e^t$ for $\psi = \frac{\pi}{6}$.

The expression for the effective or equivalent creep strain rate, $\dot{\bar{\epsilon}}_{ij}^c$, for Tresca flow is

$$\dot{\bar{\epsilon}}_{ij}^c = \dot{\epsilon} \left[\frac{\cos 2\theta}{\cos 3\theta \sqrt{J_2}} S_{ij} + \frac{\sin \theta \sqrt{3}}{\cos 3\theta J_2} \left(S_{ip} S_{pj} - \frac{2J_2}{3} \delta_{ij} \right) \right] \quad (4.12.15)$$

where $\bar{\epsilon}$ can be replaced by $F\dot{\epsilon}_s$. The resulting expression for the stress rate, \dot{S}_{ij}^n , now becomes

$$\dot{S}_{ij}^n = 2\mu \left(\dot{\epsilon}_{ij} - F\dot{\epsilon}_s \left[\frac{\cos 2\theta}{\cos 3\theta \sqrt{J_2}} S_{ij}^n + \frac{\sin \theta \sqrt{3}}{\cos 3\theta J_2} \left(S_{ip}^n S_{pj}^n - \frac{2J_2}{3} \delta_{ij} \right) \right] \right) \quad (4.12.16)$$

which is highly nonlinear.

Integration of this equation and the evolutionary equation governing the rate of change of ζ requires the use of a numerical procedure. Studies of various numerical integration methods have revealed that simple forward Euler integration is as effective as any method. Following the methodology outlined previously for the Power Law Creep Model, the stress at step n+1 is simply

$$S_{ij}^{n+1} = S_{ij}^n + \dot{S}_{ij}^n \Delta t \quad (4.12.17)$$

and in a similar fashion

$$\zeta^{n+1} = \zeta^n + \dot{\zeta}^n \Delta t \quad (4.12.18)$$

The forward Euler operator is conditionally stable. The critical time step for stability can be determined using the method of Corneau (1975) based on the form of the flow potential and the elastic constants. This has been done for the M-D model. Two estimates for the critical time step are computed, and the minimum of the two is used for the calculation. These time step estimates are given by

$$\Delta t_{st1} \leq \frac{1}{\mu \left(\frac{\partial \dot{\bar{\epsilon}}^c}{\partial \tau_{max}} \right)} \quad (4.12.19)$$

and

$$\Delta t_{st2} \leq \frac{-\sqrt{3}}{\left(\frac{\partial \dot{\bar{\epsilon}}^c}{\partial \zeta} \right)} \quad (4.12.20)$$

where $\tau_{max} = \cos \theta \sqrt{J_2} = \frac{\bar{\sigma}}{2}$. The equivalent Tresca stress, $\bar{\sigma}$, is the value at the end of step n.

Accuracy of the method is assured if the time steps are sufficiently small, but using the stable time step cannot be guaranteed to always produce an accurate solution. However, comparison of results using this integration method with known solutions for complex two- and three-dimensional creep problems has shown the method to be very accurate when the stable time step is used.

For a typical application, the time increment, Δt_{st1} , is smallest when $\bar{\sigma}$ is largest, and as the effective stress decreases, such as when the problem approaches steady-state creep, the critical time step increases. In most instances, the user-specified time step, Δt , will be larger than the time step needed for stability, $\min(\Delta t_{st1}, \Delta t_{st2})$. Therefore, the solution time step is broken into subincrements for integrating the constitutive model with the size of each subincrement changing with the stress. The subincrementation procedure is discussed at the beginning of this chapter.

The transient creep part of the M-D model causes the stress to change rapidly, which causes the time step to be very small. The adaptive time step feature was developed to accommodate the small time step initially and allow it to grow as the solution proceeds toward steady state. Experience has shown that an initial time step size of 1.0×10^{-5} seconds works well with a tolerance of 0.01. The maximum time step size depends on the time scale of the problem and the degree of nonlinearity.

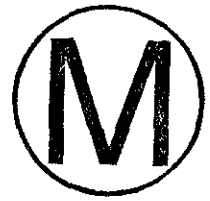
The M-D creep model uses the following state variables:

EQCS	- equivalent creep strain
ZETA	- current values of the evolutionary parameter
SDOT	- stress rate for the current time step
TRESCA	- equivalent stress computed using TRESCA criterion
ETSTAR	- transient strain limit.

The PROP array for this material contains the following entries:

PROP(1)	- 2μ
PROP(2)	- K
PROP(3)	- A1
PROP(4)	- $\frac{Q1}{R}$
PROP(5)	- n1
PROP(6)	- B1
PROP(7)	- A2
PROP(8)	- $\frac{Q2}{R}$
PROP(9)	- n2
PROP(10)	- B2
PROP(11)	- σ_0
PROP(12)	- q
PROP(13)	- m
PROP(14)	- K_0
PROP(15)	- $c\theta$





- PROP(16) - α_w
 PROP(17) - β_w
 PROP(18) - δ
 PROP(19) - RN3, exponent of workhardening and recovery term used to compute F
 PROP(20) - AMULT, scalar multiplier of time step needed for stability (default 0.98)

4.13 Volumetric Creep Model

The consolidation behavior of geomaterials and salt, in particular, is of interest to analysts because of the use of these materials as backfill and as a sealing material in waste disposal applications. The volumetric creep model implemented in SANTOS is based on the work of Sjaardema and Krieg (1987), who developed their model based on the hydrostatic consolidation tests of salt with added water by Holcomb and Shields (1987). Time-dependent behavior is included in both the volumetric and the deviatoric response. The form of the model is such that the mechanical response of the consolidated material becomes identical to that of the intact material as the density approaches that of the intact material. The elastic moduli were found from the tests to depend on the density, ρ , of the material through relationships of the form

$$K = K_0 \exp(K_1 \rho) \quad (4.13.1)$$

$$\mu = \mu_0 \exp(\mu_1 \rho) \quad (4.13.2)$$

where K_0 , K_1 , μ_0 , and μ_1 are material constants.

For the discussion of the volumetric creep model, it is appropriate to decompose the total strain rate into volumetric and deviatoric parts. Because intact salt creeps deviatorically when subjected to a deviatoric stress state, crushed salt should logically be expected to creep deviatorically. This expectation becomes more reasonable as the density increases because, in the limit, the crushed salt becomes intact salt. The deviatoric crushed salt creep model presented here is based on the power law secondary creep model, which has been used to describe the creep behavior of intact salt. This model is described in Section 4.9, Power Law Creep Material Model.

The development proceeds by envisioning that the porous crushed salt uniaxial sample is composed of cylinders of salt, each of which has the intact salt secondary creep behavior separated by areas of open space. The local stress acting on the salt cylinders is then stated in terms of the average stress on the porous sample. The cross-sectional area of the porous sample is expressed in terms of the net cross-sectional area of the salt cylinders. The final resulting continuum model for the rate of the deviatoric stress of crushed salt is then

$$\dot{S}_{ij}^n = 2\mu(\rho) \left(\dot{\epsilon}_{ij} - \frac{3}{2} A \left(\frac{\rho_\infty}{\rho} \right)^m \exp\left(\frac{-Q}{R\Theta}\right) \bar{\sigma}^{m-1} S_{ij}^n \right) \quad (4.13.3)$$

where the constants A , Q , m , and ρ_∞ refer to values for the intact material. The integration of the deviatoric part of the stress is performed using the forward Euler operator. The integration method is the same as used for the power law creep model, and the details of the integration may be found in Section 4.9, Power Law Creep Material Model.

The volumetric part of the model can be written as the sum of elastic and inelastic parts as shown below

$$d_{kk} = \frac{\dot{p}}{K(\rho)} + d_{kk}^c \quad (4.13.4)$$

where d_{kk} is the volumetric strain rate, $\dot{p} = \frac{\dot{\sigma}_{kk}}{3}$ is the rate of change of the pressure, d_{kk}^c is the volumetric creep strain rate, and $K(\rho)$ is the density-dependent bulk modulus. Laboratory consolidation tests on crushed salt have shown the volumetric creep strain rate to be fit well by an expression of the form

$$d_{kk}^c = \frac{1}{\rho} B_0 \left[e^{B_1 p} - 1 \right] e^{A p} \quad (4.13.5)$$

where B_0 , B_1 , and A are material constants obtained from the experiments. The density ρ is computed from the relationship

$$\rho = \rho_0 \exp \left(\int_{t_0}^t d_{kk} dt \right) \quad (4.13.6)$$

where ρ_0 is the density at time t_0 . Equation (4.13.4) is solved for \dot{p} and combined with the definition of the volumetric creep strain rate, Equation (4.13.5), to produce

$$\dot{p} = K(\rho) \left[d_{kk} - \frac{1}{\rho} B_0 \left(e^{B_1 p} - 1 \right) e^{A p} \right] \quad (4.13.7)$$

which is the expression to be integrated.

The expression for the pressure is integrated using the backward Euler operator. This operator is unconditionally stable for any time step size. The expression for the pressure at the end of the step is

$$p^{n+1} = p^n + \dot{p}^{n+1} \Delta t \quad (4.13.8)$$

which can be rewritten using the above equation as

$$p^{n+1} = p^n + \left(K(\rho^{n+1}) \left[d_{kk} - \frac{1}{\rho^{n+1}} B_0 \left(e^{B_1 p^{n+1}} - 1 \right) e^{A p^{n+1}} \right] \right) \Delta t \quad (4.13.9)$$

Let us define a trial pressure as $p^{tr} = p^n + K(\rho^{n+1}) d_{kk} \Delta t$, which lets us rewrite the above expression as

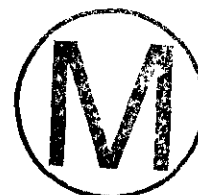
$$p^{n+1} = p^{tr} - K(\rho^{n+1}) \left(\frac{1}{\rho^{n+1}} B_0 \left(e^{B_1 p^{n+1}} - 1 \right) e^{A p^{n+1}} \right) \Delta t \quad (4.13.10)$$



We need to solve the above expression for the pressure, p^{n+1} , for which we have chosen to use a Newton Raphson scheme with a fixed number of iterations. Once we have the pressure at the end of the step, it is combined with the deviatoric stresses to produce a trial stress state for the material. The trial stresses are accepted as the final stresses if: (1) the mean stress is tensile; (2) the out-of-plane trial stress is compressive; or (3) the mean stress is compressive, and the out-of-plane trial stress is tensile but is less than 10% of the absolute value of the mean stress. If these conditions are not met, then the deviatoric stresses are scaled back so that the out-of-plane stress is equal to 10% of the absolute value of the mean stress.

The volumetric creep material model uses the following state variables:

- EQCS - equivalent creep strain
- DENSITY - current density of the consolidating material.



The PROP array for this material contains the following entries:

- PROP(1) - 2μ
- PROP(2) - K
- PROP(3) - A , creep constant
- PROP(4) - m stress exponent
- PROP(5) - $\frac{Q}{R\Theta}$ if isothermal or $\frac{Q}{R}$ if not
- PROP(6) - μ_1 , shear exponent
- PROP(7) - K_1 , bulk exponent
- PROP(8) - B_0
- PROP(9) - B_1
- PROP(10) - A_1
- PROP(11) - ρ_{intact} , intact density
- PROP(12) - ρ_0 , initial density.

4.14 Viscoelastic Material Model

The mechanical response of many plastics, rubbers, epoxies, glasses, and other polymeric compounds can be described quite well by a linear viscoelastic constitutive law. In the absence of any changes in temperature, the stress at time t in a linear material with memory depends only on the past strain history. This can be expressed in general terms as

$$S_{ij} = 2 \int_{-\infty}^t G(t - \tau) \dot{\epsilon}_{ij}(\tau) d\tau \tag{4.14.1}$$

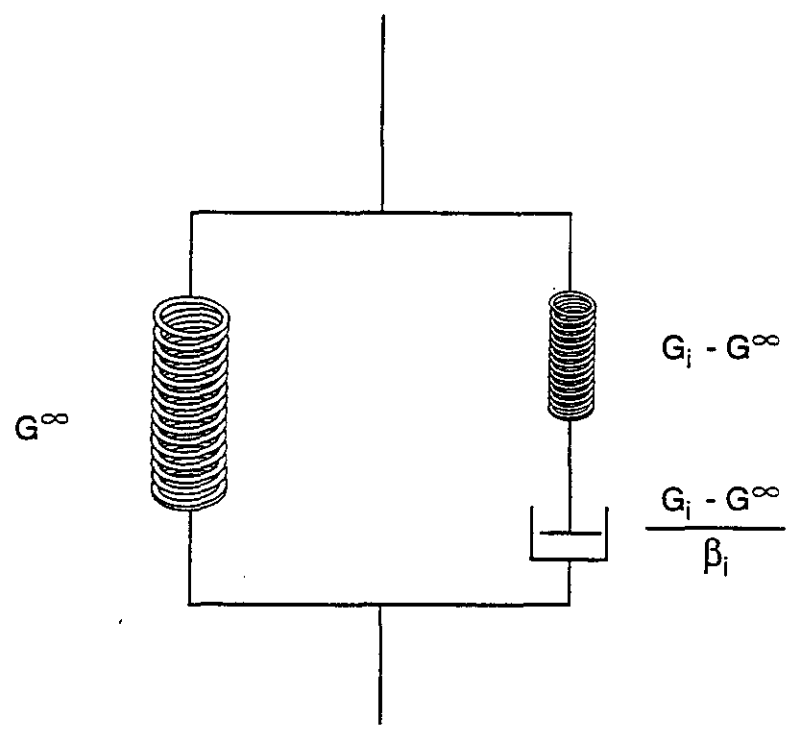
for the shear response and

$$\sigma_{kk} = 3 \int_{-\infty}^t K(t - \tau) \dot{\epsilon}_{kk}(\tau) d\tau \tag{4.14.2}$$

for the bulk response, where $G(t)$ and $K(t)$ are the shear and bulk relaxation moduli, respectively.

Unlike elastic constitutive equations in which the material moduli are constants, viscoelastic relations employ moduli that relax over some period of time. A specific form for the relaxation moduli is obtained by considering the mechanical analogy of the standard linear viscoelastic solid shown in Figure 4.14.1. The springs represent the elastic response and the dashpots represent the viscous response. By stringing together N such elements the relaxation moduli can be written as (Ferry, 1970)

$$G(t) = G^\infty + \sum_{\alpha=1}^{N_s} (G_\alpha - G^\infty) e^{-\beta_\alpha t} \tag{4.14.3}$$



TRI-6348-42-0

Figure 4.14.1 Mechanical analogy of the standard linear solid.

and

$$K(t) = K^\infty + \sum_{\alpha=1}^{N_b} (K_\alpha - K^\infty) e^{-\beta_\alpha^b(t)} \tag{4.14.4}$$

where the β 's are relaxation constants ($1/\beta =$ relaxation time) and G^∞ and K^∞ are the long-time moduli. Since the bulk and shear behaviors are assumed to be independent, N_b may be different from N_s and the same goes for β^b 's and the β^s 's. Ideally, an arbitrary number of elements could be used to gain the most accurate representation of the behavior of the material. However, because of computer storage considerations, modeling of the bulk response is limited to one term while the shear response is limited to a three-term representation. It should be noted that Equations (4.14.3) and (4.14.4) differ slightly from the usual representation in that the long-time modulus is subtracted from each relaxation modulus. This was done to simplify the data format, but caution should be used in determining material property data for the material model to ensure that it conforms to the form of Equations (4.14.3) and (4.14.4).

The constitutive law discussed above is based on the assumption that the entire body remains at a uniform temperature. The relaxation moduli and the material parameters necessary to evaluate them can be regarded as having been determined at a base-line temperature, Θ_0 . To evaluate the effects of temperature changes, first let us consider the modifications to the constitutive law if a uniform change in temperature is allowed. To do this, let $G(t, \Theta)$ be the shear relaxation modulus at the constant temperature, Θ . The remainder of the theory will be developed using the shear modulus as an example. The modifications to the bulk modulus are handled in the same manner and will not be repeated.

Using a change of variable, the shear modulus at the base-line temperature can be written as a function of $\log t$. We can now apply the hypothesis of temperature-time equivalence (Ferry, 1970; Leaderman, 1943; Ferry, 1950), which states that all response functions (e.g., relaxation moduli) are affected by the uniform temperature change only within a corresponding uniform shift of the logarithmic time scale. Materials exhibiting this kind of behavior have come to be termed "thermorheologically simple" materials (Schwarzl and Staverman, 1952) This leads to the following form for the relaxation moduli:

$$G(t, \Theta) = L[\log t + \Psi(\Theta)] \tag{4.14.5}$$

where $\Psi(\Theta)$ is the "shift function" and is usually written as

$$\Psi(\Theta) = \log \phi(\Theta) \tag{4.14.6}$$

where the "shift factor," $\phi(\Theta)$, conforms to

$$\phi(\Theta_0) = 1, \phi(\Theta) > 0, \frac{d}{d\Theta} \phi > 0 \tag{4.14.7}$$

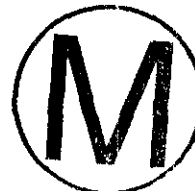
If we now define a "reduced time" by

$$\xi = t\phi(\Theta) \tag{4.14.8}$$



then

$$G(t, \Theta) = G(\xi) \quad (4.14.9)$$



This means that the entire family of response functions can be determined by one member $G(t) = G(t, \Theta_0)$, provided the shift factor is known. The shift factor is assumed to be a material property that can be determined experimentally. It should be noted that the temperature dependence of the responses in shear and in bulk could be governed by two different shift functions. However, this is ruled out by the assumption of a thermorheologically simple material because the relaxation modulus in tension displays the shift property only if the bulk and shear shift functions are identical (Muki and Sternberg, 1961).

An additional modification required to account for varying temperature is that the concept of reduced time has to be redefined. Morland and Lee (1960) have shown that if the reduced time is defined as

$$\xi(x, t) = \int_0^t \varphi[\Theta(x, \lambda)] d\lambda \quad (4.14.10)$$

then a generalized relaxation integral law can be derived from Equations (4.14.3) and (4.14.4). Assuming no deformation has taken place before time, $t = 0$, the constitutive model can be written in the following form:

$$\begin{aligned} \xi(x, t) &= \int_0^t \varphi[\Theta(x, \lambda)] d\lambda \\ \xi' &= \xi(x, \tau) \\ S_{ij}(x, t) &= 2 \int_0^t G(\xi - \xi') \dot{\epsilon}_{ij}(x, \tau) d\tau \\ \sigma_{kk}(x, t) &= 3 \int_0^t K(\xi - \xi') \dot{\epsilon}_{kk}(x, \tau) d\tau \\ G(\xi - \xi') &= G^\infty + \sum_{\alpha=1}^{N_s} (G_\alpha - G^\infty) e^{-\beta_\alpha^s (\xi - \xi')} \\ K(\xi - \xi') &= K^\infty + \sum_{\alpha=1}^{N_b} (K_\alpha - K^\infty) e^{-\beta_\alpha^b (\xi - \xi')} \end{aligned} \quad (4.14.11)$$

For problems where changes in temperature are important, the shift factor must be specified. For convenience, a specific form of the shift factor is incorporated into the material subroutine. An empirical equation which has been

shown to reflect accurately the behavior of many polymers near the glass transition temperature is used. This equation, known as the WLF equation (Ferry, 1970; Williams, 1955; Williams et al., 1955) is given by

$$\log \phi_{10}(\Theta) = \frac{C_1^0(\Theta - \Theta_0)}{C_2^0 + \Theta - \Theta_0} \quad (4.14.12)$$

where C_1^0 and C_2^0 are WLF constants which have been determined for many common polymers [37]. If a different shift factor is available for the material of interest, it can easily be incorporated into the subroutine in place of the WLF equation.

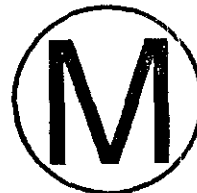
Integration of the shear and bulk equations is done in an identical manner. The equations could, in principle, be integrated directly. However, this would require additional computer storage because the integration for each time step is over all previous history. The storage requirements for this method would be prohibitive. A better method for determining the stresses at each time step is based on the development of a recursion relation so that the stress at time $n+1$ can be determined from historical quantities at time n and the current value of the strain rate. The development of this recursive method as implemented in SANTOS is described in Costin and Stone (1985). The deviatoric and the bulk stress components are combined to give the final stress state for the material.

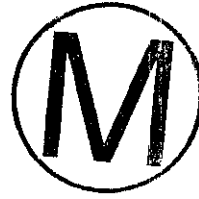
Historical information for each stress component is stored as a state variable. The viscoelastic material has the following state variables:

BLKDECAY	-	single term bulk pressure
DECAYX1	-	shear relaxation term 1 x-stress
DECAYY1	-	shear relaxation term 1 y-stress
DECAYZ1	-	shear relaxation term 1 z-stress
DECAYXY1	-	shear relaxation term 1 xy-stress
DECAYX2	-	shear relaxation term 2 x-stress
DECAYY2	-	shear relaxation term 2 y-stress
DECAYZ2	-	shear relaxation term 2 z-stress
DECAYXY2	-	shear relaxation term 2 xy-stress
DECAYX3	-	shear relaxation term 3 x-stress
DECAYY3	-	shear relaxation term 3 y-stress
DECAYZ3	-	shear relaxation term 3 z-stress
DECAYXY3	-	shear relaxation term 3 xy-stress.

The PROP array for this material contains the following entries:

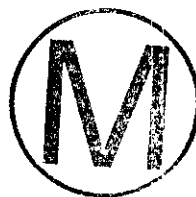
PROP(1)	-	Short Time Bulk Modulus, K
PROP(2)	-	Long Time Bulk Modulus, K^∞
PROP(3)	-	Bulk Relaxation Constant, β^k
PROP(4)	-	Long Time Shear Modulus, G^∞
PROP(5)	-	First Short Time Shear Modulus, G_1
PROP(6)	-	Second Short Time Shear Modulus, G_2





- PROP(7) - Third Short Time Shear Modulus, G_3
- PROP(8) - First Shear Relaxation Constant, β_1^s
- PROP(9) - Second Shear Relaxation Constant, β_2^s
- PROP(10) - Third Shear Relaxation Constant, β_3^s
- PROP(11) - First WLF constant, C_1
- PROP(12) - Second WLF constant, C_2
- PROP(13) - Reference Temperature for Material Properties, T_0 .

Intentionally Left Blank





5.0 CONTACT SURFACES

Many structures of interest are composed of two or more parts that are either in contact or may come into contact during service. After contact, these parts can also slide with respect to one another. In the field of computational mechanics, modeling contact and sliding behavior are done using contact surfaces, and there are several numerical approaches for modeling this behavior. One method utilizes a thin finite element with a special constitutive model to approximate gap and friction behavior (Goodman and Dubois, 1972). A second approach uses Lagrange multipliers to impose gap closure constraints and frictional stick-slip conditions (Hibbitt, Karlson & Sorenson, Inc., 1992). In the setting of the dynamic relaxation algorithm, SANTOS employs a sliding contact surface algorithm using a master-slave approach.

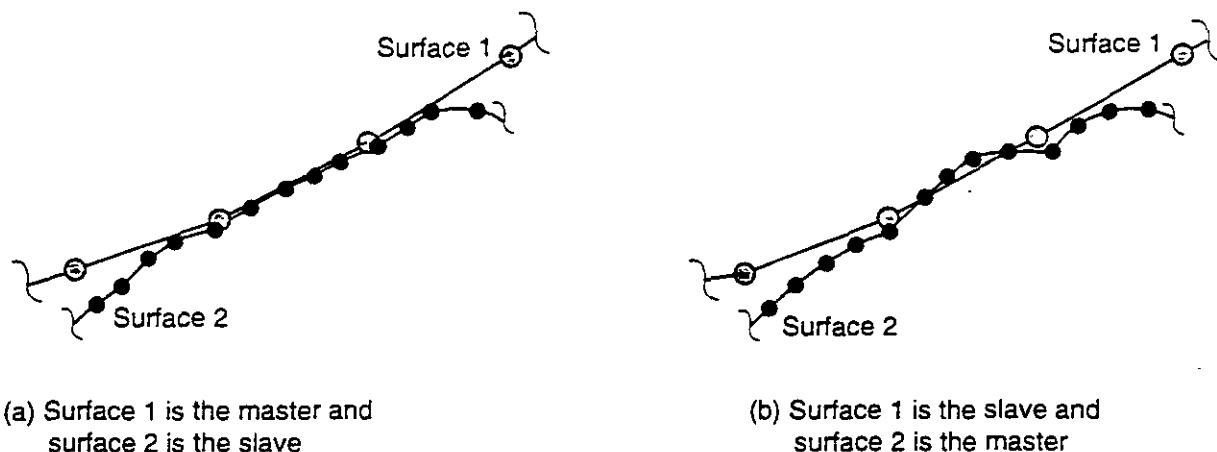
In the master-slave concept, the nodes on the designated slave surface are required by the algorithm to lie on the master surface. Any sliding or slip must occur along the master surface. In turn, nodal forces from the slave node are removed and applied to the master surface nodes. This transfer of forces maintains equilibrium at the interface. The tangential shear or friction force as well as the determination of slip or no slip is incorporated into this process involving the transfer of forces to the master surface. In SANTOS, the nodal forces are computed by the divergence of the stresses within an element. Therefore, nodal forces can be used in conjunction with a Mohr-Coulomb model for the contact surface friction. SANTOS currently supports two types of master-slave contact surface boundary conditions: (1) a deformable surface against a rigid plane, and (2) two distinct deformable surfaces against each other.

For a strict master-slave algorithm such as the one implemented in SANTOS, the user must specify which surface is the master surface and which surface is the slave. This choice can have a significant effect on the calculation and the efficiency of the solution. For example, the coarser mesh should be designated as the master surface when the two contacting materials are the same as shown in Figure 5.1a. If the master-slave surfaces are reversed as in Figure 5.1b, interpenetration that is not detected by the algorithm can result. The choice of master-slave roles is less clear when the materials of the contacting bodies are different. The user should typically select the stiffer of the two materials to be the master surface but be prepared to reverse the roles if convergence is slow or interpenetration is observed.

The contact surface algorithm is composed of two phases: (1) a location phase where the time, location, and amount of slave node penetration of the master surface is determined along with identification of the correct master surface segment and master surface nodes defining the segment, and (2) an application phase where the nodal force transfer from the slave node to the master surface nodes is performed along with a kinematic location of the slave node to the appropriate location on the master surface.

5.1 Location Phase

Contact location is accomplished by monitoring the displacements of the slave nodes throughout the calculation for possible penetration of a master surface. SANTOS uses an algorithm called neighborhood identification to pair those slave nodes and master surfaces where potential contact is likely. The neighborhood identification is usually the most time-consuming part of the location phase. Obviously, the most robust approach



TRI-6348-20-0

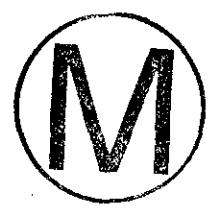
Figure 5.1. Schematic showing the effect of changing the master-slave designation between two surfaces.

would be to check every slave node against every master surface at every time step. This, however, is inefficient. The current strategy is to use a global search to determine which slave nodes are in close proximity to a master surface. The search process accumulates these potential interactions by constructing a local neighborhood around the master surface and globally searching for all slave nodes that fall within the neighborhood. The algorithm is based on a particle search technique, Heinstejn et al., 1993. It sorts the slave nodes by location and uses a binary search to construct a list of slave nodes in a master surface neighborhood. The search algorithm depends only on the number of slave nodes and not on the geometry of the problem. It takes advantage of the known positions of the slave nodes and master surfaces.

After gathering a list of potential interactions, a detailed contact check is done for each slave-node/master surface pair. This check determines: (1) which of the candidate master surfaces is in contact with the slave node, (2) the point of contact, (3) the amount of penetration, and (4) the direction the slave node should be pushed back. The contact check also tries to resolve pushback ambiguities that arise due to discretization of the master surface. A complete discussion of these ambiguities and their resolution can be found in Heinstejn et al., 1993.

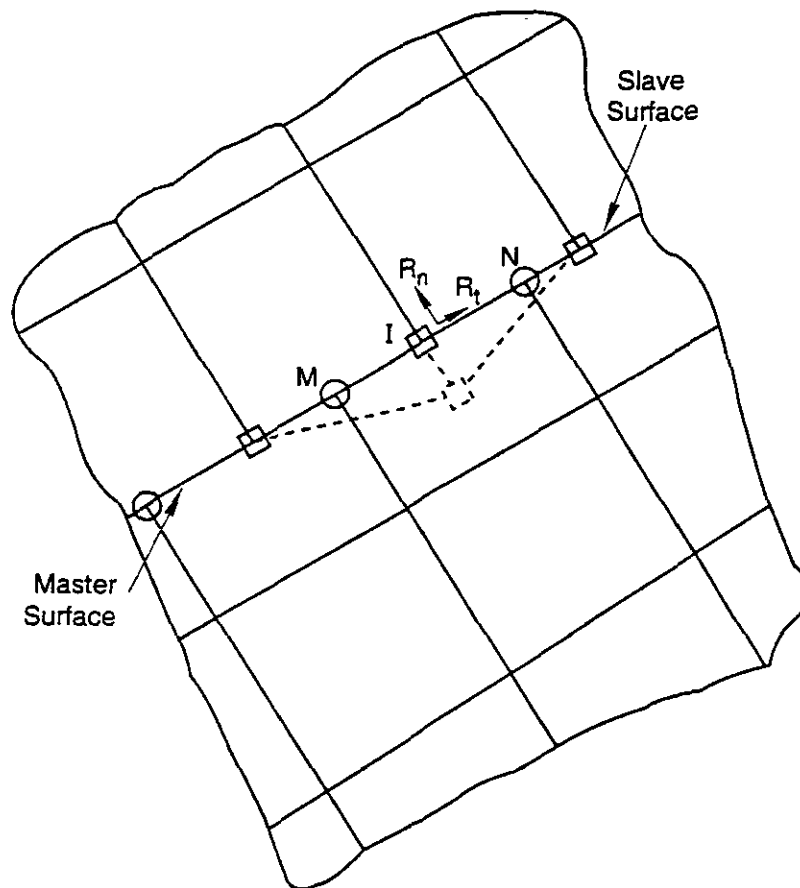
The benefits of reducing the time spent in the contact surface algorithms can be significant. For iterative solvers, such as dynamic relaxation, inaccuracies in the location phase lead to an increase in the number of iterations required for convergence. These inaccuracies arise mainly from incorrectly determining the location of contact as a slave node slides across another surface. For large finite element simulations with large numbers of slave nodes and master surfaces, as much as 50% of the total CPU time is spent in the location phase. Thus, the speed and efficiency of the contact detection algorithms are important.





5.2 Application Phase

The operation of the master-slave scheme can be demonstrated in the following example where slave node I lies between master nodes M and N, as shown in Figure 5.2.1. The location phase algorithm has already determined that node I has penetrated the master surface segment connecting nodes M and N. Because node I has penetrated the master surface, the normal force (R_n) and tangential force (R_t) at node I are determined. The coefficient of friction, μ , is used in conjunction with R_n to determine the threshold value for slip, μR_n . If R_t is less than μR_n , then no slip occurs and both the values of R_n and R_t are transferred to the master surface nodes using a weighting procedure based on the position of the slave node along the master segment.



TRI-6348-21-0

Figure 5.2.1. Schematic showing the penetration of the master surface by slave node I. Node I is kinematically restored to the master surface, and its nodal forces are transferred to the master surface nodes M and N.

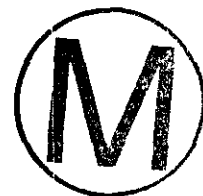
The enforcement of the contact constraint is done using nodal velocities rather than displacements. In addition, the constraint is not enforced in one iteration but over several iterations to improve the convergence of the nonlinear equilibrium iterations. The nodal velocity of slave node I is rotated into normal and tangential components. For the no-slip case, the tangential velocity of the slave node is assigned a new nodal velocity based on the tangential velocity of the corresponding point on the master surface. The normal velocity component of the slave node is given the normal velocity of the master surface modified by an incremental velocity based on the depth of penetration, δ , by the slave node. The incremental velocity is applied in a direction to move the slave node back towards the master surface. The resulting equation for the normal velocity component is computed as

$$v_n^s = v_n^m + 0.1 \frac{\delta}{\Delta t} \quad (5.2.1)$$

The pushback factor of 0.1 ensures that the slave node is not pushed back to the master surface in a single iteration. For the case when R_t is greater than μR_n , slip can occur. The tangential force R_t is reduced to its maximum allowable value of μR_n which results in a force imbalance and allows movement of the slave node along the master surface to a new equilibrium position. The slave node forces, R_n and R_t , are again transferred to the master nodes. The normal velocity of the slave node is modified exactly as in the no-slip case while the tangential velocity component is not modified at all.

The nodal mass associated with each contacting slave node is transferred to the appropriate master surface nodes using the weighting procedure used for transferring slave node forces. The transfer of mass is used by the solution algorithm during the calculation of the nodal accelerations, $a = \frac{F}{m}$. This transfer of mass, which is performed for each iteration, allows the master surface nodal accelerations to reflect the presence of the slave surface.

Incorporated within the contact surface model is the capability for two surfaces initially in contact to separate at a prescribed load level and for two distinct surfaces to contact and remain in contact during deformation. The user is allowed to specify the separation force level and to specify the separation tolerance with which both surfaces are assumed to be in contact. The default value of the separation force level is $1. \times 10^{40}$. The default value of the separation tolerance is .02 times the length of the master surface segment. Inclusion of friction does have the effect of increasing the number of iterations required for convergence in many cases.





6.0 LOADS AND BOUNDARY CONDITIONS

SANTOS contains several types of loads and boundary conditions. Displacements, pressures, concentrated forces, and body forces may be prescribed. In this section, we describe how these are implemented in the program.

6.1 Kinematic Boundary Conditions

The kinematic boundary conditions described below are all accomplished by altering the acceleration, velocities, and displacements of the nodal points. The application of these boundary conditions does not vectorize because they require a function look-up and a scatter of values. All of the kinematic boundary conditions are applied to nodal point sets.

6.1.1 No-Displacement Boundary Conditions

The no-displacement boundary conditions are accomplished by setting the appropriate component of the acceleration, velocity, and displacement of the node to zero. The imbalance force component for the node is accumulated with other no-displacement nodes to produce a total reaction force which is written as a global variable (RX and RY) at each load step. The imbalance force component for the node is then set to zero.

6.1.2 Prescribed Displacement Boundary Conditions

The prescribed displacement boundary conditions are accomplished by setting the displacement component of the node point to the required displacement value corresponding to the end of the step. The appropriate components of the acceleration and velocity of the nodal points are set to zero along with the imbalance force component.

6.1.3 Sloping Roller Boundary Conditions

This displacement boundary condition requires the nodal point set to displace along a line defined by the analyst. The analyst defines the line by providing the components of the surface outward normal. The acceleration and velocity of the node point are rotated into a coordinate system normal and tangential to the line. The normal acceleration and velocity components are set to zero, and the remaining tangential components are rotated back to the global coordinate system. The imbalance force associated with the node is also rotated into the normal and tangential coordinate system. The normal force component is set to zero, and the remaining tangential force is rotated back into the global coordinate system.

6.2 Traction Boundary Conditions and Distributed Loads

The boundary conditions described below apply external forces to selected nodes. The pressure boundary condition is associated with element side sets while the nodal force boundary condition applies to nodal point sets. Body forces (distributed loads) are applied to each node in proportion to the mass of the material that surrounds it.

6.2.1 Pressure

The set of consistent nodal point forces arising from pressures distributed over an element side is defined via the principle of virtual work by

$$\delta u_{iI} f_{iI} = \delta u_{iI} \int_s \phi_I (-p n_i) dA \quad (6.2.1)$$

where the range of the lower-case subscripts is 1 to 2 and the upper-case subscripts 1 to 4.

Since the virtual displacements are arbitrary, they may be eliminated to yield

$$f_{iI} = - \int_s \phi_I p n_i dA \quad (6.2.2)$$

The most general pressure distribution we allow is mapped from nodal point pressure values via the isoparametric shape functions. The resulting expression for the consistent nodal forces is

$$f_{iI} = - p_J \int_s \phi_I \phi_J n_J dA \quad (6.2.3)$$

For the four-node constant stress element used in PRONTO, ϕ_I is given by

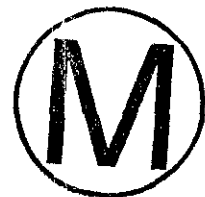
$$\phi_I = \frac{1}{2} \Sigma_I + \xi \Lambda_I, \quad -\frac{1}{2} \leq \xi \leq \frac{1}{2} \quad (6.2.4)$$

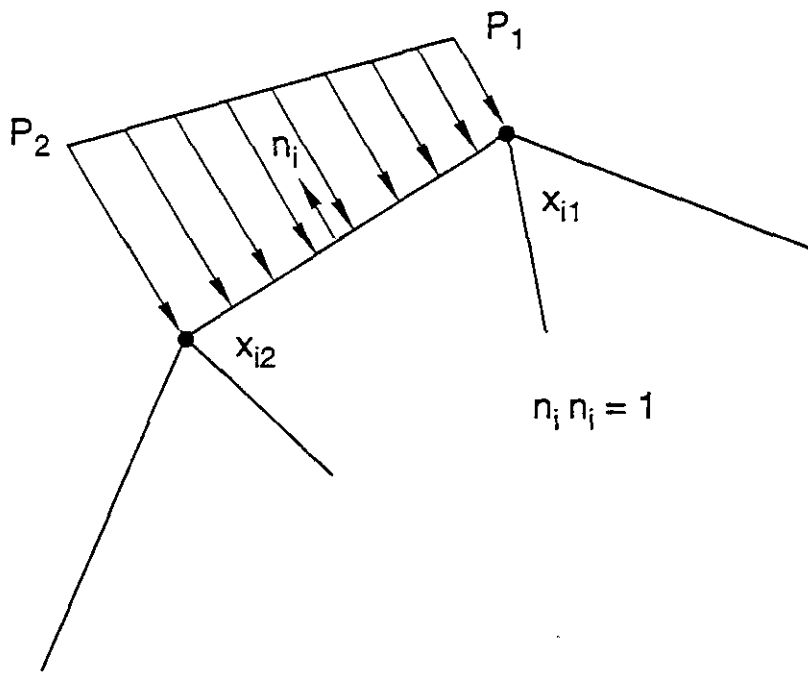
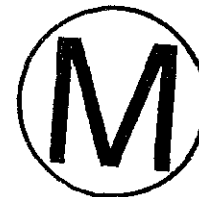
where

$$\Sigma_i = \begin{Bmatrix} 1 \\ 1 \end{Bmatrix} \quad \Lambda_I = \begin{Bmatrix} -1 \\ 1 \end{Bmatrix} \quad (6.2.5)$$

and $n_i n_i = 1$. For the geometry and pressure distribution shown in Figure 6.2.1, it can be shown that

$$x_i = x_{iI} \phi_I \quad (6.2.6)$$





TRI-6348-43-0

Figure 6.2.1. Definition of a pressure boundary condition along an element side.

and

$$n_i dA = e_{ij3} \frac{\partial x_i}{\partial \xi_j} d\xi = e_{ij3} x_{jK} \Lambda_K d\xi \quad (6.2.7)$$

Then the consistent nodal forces can be written as

$$f_{iI} = -p_j e_{ij3} x_{jK} \Lambda_K \int_{\frac{1}{2}}^{\frac{1}{2}} \phi_I \phi_J d\xi \quad (6.2.8)$$

Combining Equations (6.2.4), (6.2.5), and (6.2.8):

$$f_{iI} = -p_j e_{ij3} x_{jK} \Lambda_K \left[\frac{1}{4} \Sigma_I \Sigma_J + \frac{1}{12} \Lambda_I \Lambda_J \right] \quad (6.2.9)$$

The above expression is evaluated as

$$N_i = -e_{ij3} x_{jK} \Lambda_K = \begin{Bmatrix} y_1 - y_2 \\ x_2 - x_1 \end{Bmatrix} \quad (6.2.10)$$

and

$$f_{iI} = N_i \cdot \frac{1}{6} \begin{bmatrix} 2 & 1 \\ 1 & 2 \end{bmatrix} \cdot \begin{Bmatrix} p_1 \\ p_2 \end{Bmatrix} \quad (6.2.11)$$

The nodal values for the pressure are calculated using the user-supplied scale factor and time history function. The values are calculated for the beginning of the time step.

The application of the pressure boundary conditions is fully vectorized. Blocks of element sides are processed in vector blocks using the scratch element space. After the consistent nodal point forces are calculated for a block of element sides, they are accumulated into the global nodal force array.

6.2.2 Adaptive Pressure

The adaptive pressure boundary condition in SANTOS allows the analyst to model the behavior of gas-filled cavities that change internal pressure as the cavity deforms. The analyst defines the cavity using a side set identifier, and the volume of the cavity is computed every iteration based on the current deformed shape. The cavity volume is passed to SUBROUTINE FPRES, which is user supplied, where the gas pressure is computed. This gas pressure is then applied to the defined side set as a pressure boundary condition.

6.2.3 Nodal Forces

Nodal point external forces are applied to each point in the node set. The magnitude of the force is determined by the user-supplied scale factor and a time history function. The time history function is evaluated at the end of the load step. If the analysis type is axisymmetric, then the nodal forces are input as force per radian.

6.2.4 Gravity Forces, Body Forces, and Distributed Loads

Gravity and body forces are computed using the third integral in Equation (3.1.8). The same routines that compute the diagonal mass matrix are used to form the gravity load vector. The density, ρ , is the input density for the specific material and not the fictitious density computer for the stable time increment. The component direction accelerations are specified on the GRAVITY input card. In addition to the x- and y-direction accelerations, the code supports an angular acceleration. The magnitude of the acceleration is determined by the user-supplied scale factor and a time history function. The time history function is evaluated at the end of the load step.

The nodal values of the distributed loads are read from an externally written file, fort.38, in the following format:

```
READ(38) TIME, (DISTX(I), I=1,NNOD), (DISTY(I), I=1,NNOD)
```

at the desired time intervals. DISTX and DISTY are the nodal point distributed load components in the x and y directions, respectively. These nodal values are in units of force per unit volume. This force/volume is multiplied by the appropriate nodal volume to obtain the magnitude of the nodal loading. The nodal volume is computed using the



diagonal mass matrix routines with a density equal to one. An example of this type of loading is the body force generated by the presence of a magnetic field.

6.2.5 Thermal Forces

Nodal point temperatures for performing thermal/structural analyses are input into SANTOS in two ways. The first method is to read an externally written temperature file, fort.56, in the following format:

```
READ(56) TIME, (T(I), I = 1, NNOD)
```

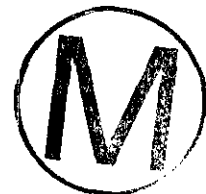
where the temperature, T, is read for each nodal point. SANTOS interpolates linearly between thermal time steps to obtain the thermal solution for the time requested by the structural analysis. On the THERMAL STRESS input card, the entry type is set to EXTERNAL to request this method.

The second method is best suited for problems where the structure is heated uniformly. The analyst can define the temperature history of the body using an input function, and SANTOS will interpolate the body temperature at the time requested by the structural analysis. On the THERMAL STRESS input card, the entry type is set to INTERNAL.

SANTOS requires the analyst to input, for each material, the curve of thermal strain versus temperature. This curve is defined using an input function. With the temperature of each element known, it is a simple process to interpolate the thermal strain for each element. If we difference the thermal strain computed at the beginning and at the end of the load/time step and divide by Δt , we obtain a thermal strain rate. SANTOS computes the total strain rate, using the velocity gradients, which can be decomposed into mechanical and thermal strain rate components. The thermal strain rate is subtracted from the total strain rate to obtain the mechanical strain rate, which is passed into the SANTOS constitutive models.



Intentionally Left Blank



7.0 REFERENCES

- Biffle, J.H., and M.L. Blanford. 1994. *JAC2D - A Two-Dimensional Finite Element Computer Program for the Nonlinear Quasi-Static Response of Solids with the Conjugate Gradient Method*. SAND93-1891. Albuquerque, NM: Sandia National Laboratories.
- Corneau, I. 1975. "Numerical Stability in Quasi-Static Elasto/Visco-Plasticity," *International Journal for Numerical Methods in Engineering*. Vol. 9, no. 1, 109-127.
- Costin, L.S., and C.M. Stone. 1985. *A Linear Viscoelastic Material Mode for SANCHO*. SAND85-1836. Albuquerque, NM: Sandia National Laboratories.
- Dienes, J.K. 1979. "On the Analysis of Rotation and Stress Rate in Deforming Bodies," *Acta Mechanica*. Vol. 32, 217-232.
- Ferry, J.D. 1950. "Mechanical Properties of Substances of High Molecular Weight. VI. Dispersion in Concentrated Polymer Solutions and its Dependence on Temperature and Concentration," *Journal of the American Chemical Society*. Vol. 72, 3746-3752.
- Ferry, J.D. 1970. *Viscoelastic Properties of Polymers*. 2nd ed. New York, NY: John Wiley & Sons, Inc.
- Flanagan, D.P., and T. Belytschko. 1981. "A Uniform Strain Hexahedron and Quadrilateral with Orthogonal Hourglass Control," *International Journal for Numerical Methods in Engineering*. Vol. 17, 679-706.
- Flanagan, D.P., and T. Belytschko. 1984. "Eigenvalues and Stable Time Steps for the Uniform Strain Hexahedron and Quadrilateral," *Transactions of the ASME, Journal of Applied Mechanics*. Vol. 51, no. 1, 35-40.
- Flanagan, D.P., and L.M. Taylor. 1987. "An Accurate Numerical Algorithm for Stress Integration with Finite Rotations," *Computer Methods in Applied Mechanics and Engineering*. Vol. 62, 305-320.
- Goodman, R.E., and J. Dubois. 1972. "Duplication of Dilatancy in Analysis of Jointed Rocks," *Journal of the Soil Mechanics and Foundations Division, Proceedings of the American Society of Civil Engineers*. Vol. 98, no. 4, 399-422.
- Goudreau, G.L., and J.O. Hallquist. 1982. "Recent Developments in Large-Scale Finite Element Lagrangian Hydrocode Technology," *Computer Methods in Applied Mechanics Engineering*. Vol. 33, no. 1-3, 725-757.
- Heinstein, M.W., S.W. Attaway, J.W. Swegle, and F.J. Mello. 1993. *A General-Purpose Contact Detection Algorithm for Nonlinear Structural Analysis Codes*. SAND92-2141. Albuquerque, NM: Sandia National Laboratories.
- Hibbitt, Karlson & Sorenson, Inc. 1992. *ABAQUS, Theory Manual, Version 5.2*.
- Holcomb, D.J., and M. Shields. 1987. *Hydrostatic Creep Consolidation of Crushed Salt with Added Water*. SAND87-1990. Albuquerque, NM: Sandia National Laboratories.
- Hughes, T.J.R. 1987. *The Finite Element Method: Linear Static and Dynamic Finite Element Analysis*. Englewood Cliffs, NJ: Prentice-Hall.



- Hughes, T.J.R., and J. Winget. 1980. "Finite Rotation Effects in Numerical Integration of Rate Constitutive Equations Arising in Large-Deformation Analysis," *International Journal for Numerical Methods in Engineering*. Vol. 15, no. 12, 1862-1867.
- Johnson, G.C., and D.J. Bammann. 1984. "A Discussion of Stress Rates in Finite Deformation Problems," *International Journal of Solids and Structures*. Vol. 20, no. 8, 725-737.
- Key, S.W., Z.E. Beisinger, and R.D. Krieg. 1978. *HONDO II - A Finite Element Computer Program for the Large Deformation Dynamics Response of Axisymmetric Solids*. SAND78-0422. Albuquerque, NM: Sandia National Laboratories.
- Krieg, R.D. 1978. *A Simple Constitutive Description for Cellular Concrete*. SC-DR-72-0883. Albuquerque, NM: Sandia National Laboratories.
- Krieg, R.D., and D.B. Krieg. 1977. "Accuracies of Numerical Solution Methods for the Elastic-Perfectly Plastic Model," *ASME Journal of Pressure Vessel Technology*. Vol. 99, 510-515.
- Leaderman, H. 1943. *Elastic and Creep Properties of Filamentous Materials and Other High Polymers*. Washington, DC: Textile Foundation, Inc.
- Morland, L.W., and E.H. Lee. 1960. "Stress Analysis for Linear Viscoelastic Materials with Temperature Variation," *Transactions of the Society of Rheology*. Vol. IV, 233-263.
- Muki, R., and E. Sternberg. 1961. "On Transient Thermal Stresses in Viscoelastic Materials with Temperature-Dependent Properties," *Journal of Applied Mechanics*. Vol. 28, Series E, no. 2, 193-207.
- Munson, D.E., and P.R. Dawson. 1979. *Constitutive Model for the Low Temperature Creep of Salt (with Application to WIPP)*. SAND79-1853. Albuquerque, NM: Sandia National Laboratories.
- Munson, D.E., and P.R. Dawson. 1982. *A Transient Creep Model for Salt During Stress Loading and Unloading*. SAND82-0962. Albuquerque, NM: Sandia National Laboratories.
- Munson, D.E., and P.R. Dawson. 1984. "Salt Constitutive Modeling Using Mechanism Maps," *The Mechanical Behavior of Salt. Proceedings of the First Conference, Pennsylvania State University, University Park, PA, November 9-11, 1981*. Eds. H.R. Hardy, Jr. and M. Langer. Rockport, MA: Karl Distributors. 717-737.
- Munson, D.E., A.F. Fossum, and P.E. Senseny. 1988. *Advances in Resolution of Discrepancies Between Predicted and Measured In Situ WIPP Room Closures*. SAND88-2948. Albuquerque, NM: Sandia National Laboratories.
- Neilsen, M.K., H.S. Morgan, and R.D. Krieg. 1987. *A Phenomenological Constitutive Model for Low Density Polyurethane Foams*. SAND86-2927. Albuquerque, NM: Sandia National Laboratories.
- Otter, J.R.H., A.C. Cassell, and R.E. Hobbs. 1966. "Dynamic Relaxation," *Proceedings of the Institution of Civil Engineers*. Paper No. 6986. Vol. 35, 633-656.
- Papadrakakis, M. 1981. "A Method for the Automatic Evaluation of the Dynamic Relaxation Parameters," *Computer Methods in Applied Mechanics and Engineering*. Vol. 25, 35-48.
- Red-Horse, J.R., W.C. Mills-Curran, and D.P. Flanagan. 1990. *SUPES Version 2.1 - A Software Utilities Package for the Engineering Sciences*. SAND90-0247. Albuquerque, NM: Sandia National Laboratories.
- Schreyer, H.L., R.F. Kulak, and J.M. Kramer. 1979. "Accurate Numerical Solutions for Elastic-Plastic Models," *ASME Journal of Pressure Vessel Technology*. Vol. 101, 226-234.



- Schwarzi, F., and A.J. Staverman. 1952. "Time-Temperature Dependence of Linear Viscoelastic Behavior," *Journal of Applied Physics*. Vol. 23, no. 8, 838-843.
- Sjaardema, G.D. 1993. *Overview of the Sandia National Laboratories Engineering Analysis Code Access System*. SAND92-2292. Albuquerque, NM: Sandia National Laboratories.
- Sjaardema, G.D., and R.D. Krieg. 1987. *A Constitutive Model for the Consolidation of WJPP Crushed Salt and Its Use in Analyses of Backfilled Shaft and Drift Configurations*. SAND87-1977. Albuquerque, NM: Sandia National Laboratories.
- Stone, C.M., R.D. Krieg, and Z.E. Beisinger. 1985. *SANCHO - A Finite Element Computer Program for the Quasistatic, Large Deformation, Inelastic Response of Two-Dimensional Solids*. SAND84-2618. Albuquerque, NM: Sandia National Laboratories.
- Stone, C.M., G.W. Wellman, and R.D. Krieg. 1990. *A Vectorized Elastic/Plastic Power Law Hardening Material Model Including Luders Strain*. SAND90-0153. Albuquerque, NM: Sandia National Laboratories.
- Taylor, L.M., and D.P. Flanagan. 1987. *PRONTO 2D - A Two-Dimensional Transient Solid Dynamics Program*. SAND86-0594. Albuquerque, NM: Sandia National Laboratories.
- Taylor, L.M., and D.P. Flanagan. 1988. *An External Code Interface for the PRONTO Family of Transient Solid Dynamics Programs*. SAND87-3003. Albuquerque, NM: Sandia National Laboratories.
- Truesdell, C.A. 1966. *The Elements of Continuum Mechanics*. New York, NY: Springer-Verlag.
- Underwood, P.G. 1983. "Dynamic Relaxation," *Computational Methods for Transient Analysis*. Eds. T. Belytschko and T.J.R. Hughes. New York, NY: Elsevier.
- Williams, M.L. 1955. "The Temperature Dependence of Mechanical and Electrical Relaxations in Polymers," *Journal of Physical Chemistry*. Vol. 59, 95-96.
- Williams, M.L., R.F. Landel, and J.D. Ferry. 1955. "The Temperature Dependence of Relaxation Mechanisms in Amorphous Polymers and Other Glass-forming Liquids." *Journal of the American Chemical Society*. Vol. 77, 3701-3707.





**APPENDIX A:
SANTOS Users Manual**

Intentionally Left Blank



SANTOS Users Manual

Listed below, in the order they appear in the text, are all the key words used in the SANTOS input.

1. TITLE
2. PLANE STRAIN
3. AXISYMMETRIC
4. STEP CONTROL
5. AUTOSTEP
6. OUTPUT TIME
7. PLOT TIME
8. PLOT NODAL
9. PLOT ELEMENT
10. PLOT STATE
11. TIME STEP SCALE
12. RESIDUAL TOLERANCE
13. MAXIMUM ITERATIONS
14. INTERMEDIATE PRINT
15. MAXIMUM TOLERANCE
16. GLOBAL CONVERGENCE
17. LOCAL CONVERGENCE
18. ELASTIC SOLUTION
19. PREDICTOR SCALE FACTOR
20. DISTRIBUTED LOADS
21. INITIAL STRESS
22. THERMAL STRESS
23. GRAVITY
24. MINIMUM DAMPING FACTOR
25. NO DAMPING
26. WRITE RESTART
27. READ RESTART
28. HOURGLASS STIFFENING
29. XBEGIN
30. XEND
31. EXIT
32. FUNCTION
33. NO DISPLACEMENT
34. PRESCRIBED DISPLACEMENT
35. SLOPING ROLLER
36. PRESCRIBED FORCE
37. PRESSURE
38. ADAPTIVE PRESSURE
39. CONTACT SURFACE
40. RIGID SURFACE
41. MATERIAL
42. MATERIAL POINT



43. DELEte MATerial

The input data to SANTOS is in a free field form using key words. The key words are intended to define a user friendly program language input. The input is order independent and can be entered in any order the user finds convenient. The words as typed below in UPPER CASE represent key-words in the list above. Most of the words can be abbreviated to the first few characters. In the list above the upper case characters indicate the shortest abbreviation allowed. The words typed in lower case below indicate variables for which the user should enter a value. An example data file is shown below.

The free field input allows the user to delineate entries by either a blank, a comma, or an equals sign. We find it useful to use blanks with commands (keywords), equal signs to separate keywords and/or lists, and commas for lists of values. The material data requires material cues and their associated values and equal signs are useful there. See the example input below.

A dollar sign indicates that whatever follows on the line of input is a comment and is ignored. An asterisk indicates that the line is to be continued on the next line.

1. TITLE

(enter a suitable title on the next line)

2. PLANE STRAIN

Indicates that a plane strain analysis is to be performed. If the analysis type keyword is omitted then a plane strain analysis is selected as default.

3. AXISYMMETRIC

Indicates that an axisymmetric analysis is to be performed.

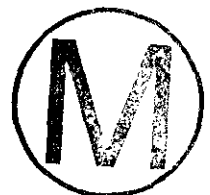
4. STEP CONTROL

n, t1
m, t2
...
...
END

n ... number of load steps in interval $0 < t < t1$
t1 ... end time for first load step interval
m ... number of load steps in interval $t1 < t < t2$
t2 ... end time for second load step interval

This command specifies the static load control parameters for the problem. The analysis is assumed to begin at $t=0$ and take *n* steps to time *t1*. The code then will take *m* load steps to time *t2*. This set of input is completed by an END card. Any number of step-time cards is allowed.

5. AUTO STEP, tol, dtmax, dtmin, dtinit



tol ... tolerance value used for controlling change of time step in material model
dtmax ... maximum value of time step allowed. Values of dt computed to be greater than dtmax will be set to dtmax.
dtmin ... minimum value of time step allowed. Computed time step cannot be smaller than this value. If the user does not wish the time step to shrink insert **NOREDUCE** in this field.
dtinit ... initial value of time step to be used in the calculation

This command can be used to automatically grow the solution time step for any time dependent material model that allows such a feature. The command specifies a solution tolerance change allowed over the step, along with allowable values of the time step (*dtmax*, *dtmin*, *dtinit*). The time step will grow and shrink according to satisfaction of *tol*. If the user does not wish to allow the time step to shrink, then insert the word **NOREDUCE** in place of *dtmin*.

6. OUTPUT TIME

n, *t1*
m, *t2*
 ...
 ...
END

n ... frequency of printed output in interval $0 < t < t1$
t1 ... end time for first output time control
m ... frequency of printed output in interval $t1 < t < t2$
t2 ... end time for second output time control

This command specifies how often the requested printed output is to be written to the output file. The required information is an integer number specifying how often, not the number of outputs, the printed information is to be written. For example, if *n* or *m* is 1 then the output file will be written every load increment. If *n* or *m* is 2 then the file will be written every 2 load increments. Currently, the times *t1* and *t2* must match the values specified on the STEP CONTROL card. An **END** card terminates this section of input.

7. PLOT TIME

n, *t1*
m, *t2*
 ...
 ...
END

n ... frequency of plotted output in interval $0 < t < t1$
t1 ... end time for first output time control
m ... frequency of plotted output in interval $t1 < t < t2$
t2 ... end time for second output time control

This command specifies how often the requested plotting output is to be written to the output file.

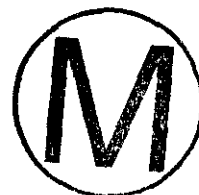


The required information is an integer number specifying how often, not the number of outputs, the plotting information is to be written. For example, if n or m is 1 then the output file will be written every load increment. If n or m is 2 then the file will be written every 2 load increments. Currently, the times t1 and t2 must match the values specified on the STEP CONTROL card. An END card terminates this section of input.

8. PLOT NODAL, nodal name 1, nodal name 2,

allowable nodal variable names:

- DISPLACEMENT - nodal displacements (DISPLX,DISPLY)
- RESIDUAL - nodal residuals (RESIDX, RESIDY) and a scalar value (RESID)
- MASS - nodal lumped masses (MASS)
- REACTION - nodal force reactions (FX, FY)



The default nodal variables written on the plotting data base are the displacements whether requested or not. The MASS specification results in having the lumped nodal masses written on the data base. The names in parenthesis indicate the alphanumeric name of the variables which are written on the plotting data base.

9. PLOT ELEMENT, element variable 1, element variable 2,

allowable element variable names:

- STRESS - stresses (SIGXX,SIGYY,SIGZZ,TAUXY)
- STRAIN - total strains (EPSXX,EPSTYY,EPSTZZ,EPSTXY)
- RATEDFM - deformation rates (DXX,DYY,DZZ,DXY)
- STRETCH - material stretches: V of F = V R (STRECHXX,STRECHYY,STRECHZZ,STRECHXY)
- ROTATION - material rotations: R of F = V R (COSTHETA,SINTHETA)
- DENSITY - current mass per unit volume (DENSITY)
- PRESSURE - pressures (PRESSURE)
- VONMISES - Von Mises equivalent stress (VONMISES)
- HG - hourglass resistance forces (HGX,HGY)
- EFFMOD - element effective modulus values used for the stable time step and mass scaling (EFFMOD)
- TEMPERATURE - element centroidal temperatures (TEMP)

The names in parenthesis indicate the alphanumeric name of the variables which are written on the plotting data base. The default element variables are the stresses.

10. PLOT STATE, state variable 1, state variable 2,

The user can ask for any of the internal state variables to be written on the plotting data base. Since all materials do not have the same internal state variables (some have none), a zero will be written on the data base for an element using a material model that does not have a state variable which is specified by the user. Hence, if the user asks for EQPS (equivalent plastic strain) and ALPHA11,ALPHA22,ALPHA33, and ALPHA12 (back stress components for kinematic hardening) and he has a model where half the mesh uses the ELASTIC material and half the mesh uses the ELASTIC PLASTIC material, much of the data written on the plotting data base will contain zeros. The table below gives all the internal state variables names for all the material models.

See the theory section for definitions of the variables if they are not obvious. The default state variables are none. **WARNING:** Indiscriminate use of this option can create extremely large plotting data bases.



allowable state variable names:

ELASTIC = (no internal state variables)
ELASTIC PLASTIC = EQPS ALPHA11 ALPHA22 ALPHA33 ALPHA12 RADIUS
POWER LAW CREEP = EQCS
LOW DEN FOAM = (no internal state variables)
SOIL N FOAMS = EVMAX EVFRAC EV NUM
EP POWER HARD = RADIUS EQPS
LINEAR VISCOELASTIC = BLKDECAY DECAYX1 DECAYY1 DECAYZ1 DECAYXY1
DECAYX2 DECAYY2 DECAYZ2 DECAYXY2 DECAYX3 DECAYY3 DECAYZ3
DECAYXY3
THERMO EP = EQPS YM0 YM1 XNU0 XNU1 YS0 YS1 RADIUS
THERMOELASTIC = YM0 YM1 XNU0 XNU1
VOLUMETRIC CREEP = EQCS DENSITY
M-D CREEP MODEL = EQCS ZETA SDOT TRESCA ETSTAR

11. TIME STEP SCALE, scft

scft ... scale factor to be applied to the internally calculated time step (default=1.0)

12. RESIDUAL TOLERANCE, value

value ... number, in percent, that is used to check for equilibrium and convergence of the solution. Default is 0.5.

13. MAXIMUM ITERATIONS, value

value ... number of iterations allowed for any solution step. Default is two times the number of nodes.

14. INTERMEDIATE PRINT, value

value ... frequency of intermediate print that provides information such as current equilibrium imbalance, number of steps, and applied load magnitudes.

15. MAXIMUM TOLERANCE, value

value ... when the maximum number of iterations is reached, if the convergence tolerance is less than *value* then the solution is assumed to be converged and the problem is advanced to the next solution step.

16. GLOBAL CONVERGENCE

This card specifies that a global convergence measure is to be used for determining satisfaction of equilibrium. This is the default method.

17. LOCAL CONVERGENCE, plocal

plocal ... threshold residual value to be used in computation of local convergence. Values of the nodal residual below this value will be replaced by *plocal* in the convergence check. The default is *plocal* =1.0.

This card specifies that a local convergence measure will be used for determining satisfaction of equilibrium. The convergence check is done on a node by node basis and convergence is assumed if each nodal residual is below the specified value on the **RESIDUAL TOLERANCE** card.

18. ELASTIC SOLUTION

This specifies that a load step is requested using only time independent material response for the step. This card should be used only with the time-dependent material models.

19. PREDICTOR SCALE FACTOR, function id

function id... function id controlling the definition of the predictor scale factor

This option specifies the function id which defines the multiplier to be used for predicting the displacements on the next load step. The multiplier is used on the incremental changes in displacement over the previous load increment. The multiplier can be useful for reducing the number of iterations required for a solution. The default value of the multiplier is 1.

20. DISTRIBUTED LOADS

This option specifies that an external file 38 is to be read for nodal values of a distributed force per unit volume. This force/volume is multiplied by the nodal volume to obtain the magnitude of the required loading. An example of this option is the body force generated by the presence of a magnetic field.

21. INITIAL STRESS, type, sig1, sig2, sig3, sig4

type ... specifies how the initial stress state will be specified. The choices are 'USER', or 'CONSTANT'. If 'USER' is selected then a user written subroutine must be supplied. If type is 'CONSTANT' then the values of sig1, sig2, sig3, and sig4 must be provided. The stresses will be assigned to each element in the model.

22. THERMAL STRESS, type, to, ithf, thforc

type ... identifies that a thermal stress analysis is to be performed. Default is no thermal stress analysis. If type is 'EXTERNAL' then an external file56 is required in the proper format for use by the code. If type is 'INTERNAL' then the following input parameters are needed.

to ... initial stress free temperature. Default is 0.

ithf ... function id controlling temperature time response

thforc ... thermal load norm for use in convergence tests. This parameter will be used as the applied load norm. The default is 0.

23. GRAVITY, igrvf, gravx, gravity, omega

igrvf ... function id controlling load time response

gravx ... specified acceleration in x-direction

gravity ... specified acceleration in y-direction





omega ... specified angular velocity

24. MINIMUM DAMPING FACTOR, *fac*

fac ... this option allows the user to define the minimum allowable damping factor used in the dynamic relaxation algorithm. The allowable values of damping range from zero to one. If a damping value is computed that is less than *fac*, then the value is set equal to *fac*. The default value is set to 0.2.

25. NO DAMPING, *iter*, *ndstep*

iter ... number of iterations with zero damping.

ndstep ... number of load steps with zero damping

This option is useful for problems with thin beam like behavior. The problem is allowed to deform without damping for a user specified number of iterations. This allows the problem to more quickly reach the fundamental deformation mode before damping begins. *Iter* should be selected as twice the number of elements meshed along the length direction. The normal damping algorithm can be initiated after performing *ndstep* load steps.

26. WRITE RESTART, *n*

n ... this option specifies that a SANTOS restart tape is to be written at a frequency of every *n* increments. This information is written to file 30.

27. READ RESTART, *n*

n ... this option specifies that a SANTOS restart tape is to be read at step *n* and a new analysis performed. Some internal checking is performed to insure that the restart tape is valid. The restart tape is assigned to file 32.

28. HOURGLASS STIFFENING, *hgstiff*, *hgvis*

hgstiff ... hourglass stiffening factor (default=.05 for plane strain and .01 for axisymmetric)

hgvis ... hourglass viscosity factor (default=.0 for plane strain and .03 for axisymmetric)

29. XBEGIN, *code name*

code name ... name of the external code to be coupled with SANTOS.

This option indicates that the following lines are input data for the external code

30. XEND

This option indicates an end to the external code input data

31. EXIT (required to terminate the input data)

32. FUNCTION, *function id*

function id ... any nonzero number you wish to identify with this function; after a FUNCTION statement you must enter a list of points defining your function:

x1, *f(x1)*

x2, *f(x2)*

...

...
xn, f(xn)
END

(The list is terminated by a line containing the word END as shown. Any other valid input cue will also work)

If the function represents a time history function to be used with one of the nodal boundary condition specifications (e.g. PRESCRIBED DISPLACEMENT) or with a PRESSURE boundary condition, if the value of time is not within the limits defined by x1 and xn, no boundary condition will be applied until the current value of time falls within the limits. This means that you can have a boundary condition turn on at a specific time and/or turn off at a specific time.

33. NO DISPLACEMENT, direction, node set flag

direction ... either X or Y

node set flag ... identifying number from the input data base which identifies the nodes you want to have no displacement (note: this is a nodal bc!)

34. PRESCRIBED DISPLACEMENT, dir, node set flag, function id, scale factor, a0, b0

dir ... either X, Y, RADIAL, TANGENT, or NORMAL

node set flag ... identifying number from the input data base which identifies the nodes you want to have this displacement (note: this is a nodal bc!)

function id ... identifying number of the function you want to use to specify the time dependence of the displacement

scale factor ... scale factor to be applied to the function (default=1.0)

a0,b0 ... not used (if direction = X or Y) center of cylinder of sphere (if direction = RADIAL or TANGENT) components of normal (if direction = NORMAL)

35. SLOPING ROLLER, node set flag, n1, n2

node set flag ... identifying number from the input data base which identifies the nodes that have this bc (note: this is a nodal bc!)

n1, n2 ... components of the surface outward normal

36. PRESCRIBED FORCE, direction, node set flag, function id, scale factor, a0, b0

direction ... either X, Y, RADIAL, TANGENT, or NORMAL

node set flag ... identifying number from the input data base which identifies the nodes you want to have this force (note: this is a nodal bc!)

function id ... identifying number of the function you want to use to prescribe the time dependence of the force

scale factor ... scale factor which will be applied to the function (default=1.0)

a0,b0 ... not used (if direction = X or Y) center of cylinder of sphere (if direction = RADIAL or TANGENT) components of normal (if direction = NORMAL)

37. PRESSURE, side set flag, function id, scale factor

side set flag ... identifying number from the input data base which identifies the sides you want to have this pressure (note: this is a side or element bc!)

function id ... identifying number of the function you want to use to prescribe the time depen-



dence of the pressure
scale factor ... scale factor which will be applied to the function (default=1.0)

38. ADAPTIVE PRESSURE, side set flag, x0, y0

side set flag ... identifying side set flag from the input data base which identifies the sides you want to have this pressure
x0,y0 ... coordinates of point used to determine cavity area

This option allows the user to define a pressure boundary condition which depends on the solution. The user can write a subroutine FPRES which can adaptively apply a pressure boundary condition based on various factors. An example of this option is the application of pressure due to compression of an ideal gas.

39. CONTACT SURFACE, side set flag 1, side set flag 2, mu,dis, tenrel

side set flag 1 ... identifying number from the input data base which identifies the master surface. (note: this is a side or element bc!)
side set flag 2 ... identifying number from the input data base which identifies the slave surface. (note: this is a side or element bc!)
mu ... coefficient of friction (default = 0.) if mu = FIXED then the surfaces are treated as fixed surfaces
dis ... fraction of element side length used to determine tolerance for proximity to master surface check (default is 1.e-8)
tenrel ... residual normal force acting on the slave node used to determine release conditions.(default = 1.e40)

40. RIGID SURFACE, slave flag, x0, y0, nx, ny, mu

slave flag ... identifying number from the input data base which identifies sides that are slaved to the rigid surface (note: this is a side or element bc!)
x0,y0 ... coordinates of a point on the rigid surface
nx,ny ... outward unit normal to the rigid surface
mu ... coefficient of friction (default = 0.) If mu = FIXED then the surface is assumed to be fixed to the rigid surface.

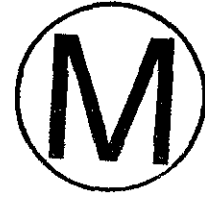
41. MATERIAL, material id flag, material name, density, func id, thermal strain scaling factor

material id ... material identification number from the input data base
material name ... valid material type name

The current material types allowed in SANTOS are:

ELASTIC
ELASTIC PLASTIC
POWER LAW CREEP
LOW DEN FOAM
SOIL N FOAMS
EP POWER HARD
LINEAR VISCOELASTIC
THERMO EP





THERMOELASTIC
VOLUMETRIC CREEP
M-D CREEP MODEL

density ... material density

func id ... function id to be used for specifying function number with proper thermal strain variation with temperature. This value needed for THERMAL STRESS problems.

thermal strain ... scaling factor multiplier for function values given from thermal strain function. The default value of this factor is 1.

The allowable material names and their required material cues are given below. The material data can be entered in any order separated by commas. An END statement is required to terminate the material data. The material constant associated with each material cue, as defined in Section 4, is given in parentheses.

1. ELASTIC (number of cues=2)

YOUNGS MODULUS (E)

POISSONS RATIO (ν)

2. ELASTIC PLASTIC (number of cues=5)

YOUNGS MODULUS (E)

POISSONS RATIO (ν)

YIELD STRESS (σ_{ys})

HARDENING MODULUS (H)

BETA (β)

3. POWER LAW CREEP (number of cues=5)

TWO MU (2μ)

BULK MODULUS (K)

CREEP CONSTANT (A)

STRESS EXPONENT (m)

THERMAL CONSTANT ($\frac{Q}{R\Theta}$ if isothermal or $\frac{Q}{R}$ if not)

4. LOW DEN FOAM (number of cues=7)

YOUNGS MODULUS (E)

A

B

C

NAIR (contribution of trapped air to foam response; 1 for yes, 0 for no contribution)

P0

PHI (ϕ)

5. SOIL N FOAMS (number of cues=7)

TWO MU (2μ)

BULK MODULUS (K)

A0

A1

A2

FUNCTION ID (function number of curve defining pressure-volume strain relationship)

PRESSURE CUTOFF (valid (negative) tensile fracture pressure)

6. EP POWER HARD (number of cues=6)

YOUNGS MODULUS (E)

POISSONS RATIO (ν)

YIELD STRESS (σ_{ys})

HARDENING CONSTANT (A)

HARDENING EXPONENT (m)

LUDERS STRAIN (ϵ_L)

7. LINEAR VISCOELASTICITY (number of cues =13)

BULK (K)

BULK INF (K^∞)

BULK RELAX (β^K)

SHEAR INF (G^∞)

SHEAR ONE (G_1)

SHEAR TWO (G_2)

SHEAR THREE (G_3)

RELAX ONE (β_1^s)

RELAX TWO (β_2^s)

RELAX THREE (β_3^s)

C1 (C_1^0)

C2 (C_2^0)

TEMP0 (reference temperature for the material properties)

8. THERMO EP (number of cues = 9)

YOUNGS MODULUS (E)

POISSONS RATIO (ν)

YIELD STRESS (σ_{ys})

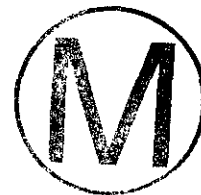
MODULUS FUNCTION (function defining Young's modulus variation with Θ)

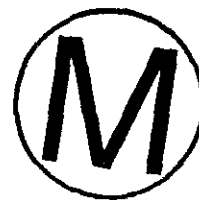
PR FUNCTION (function defining Poisson's ratio variation with Θ)

YIELD FUNCTION (function defining yield stress variation with Θ)

HARDENING CONSTANT (A)

HARDENING EXPONENT (m)





LUDERS STRAIN (ϵ_L)

9. THERMOELASTIC (number of cues = 4)

YOUNGS MODULUS (E)

POISSONS RATIO (ν)

MODULUS FUNCTION (function defining Young's modulus variation with Θ)

PR FUNCTION (function defining Poisson's ratio variation with Θ)

10. VOLUMETRIC CREEP (number of cues = 12)

TWO MU (2μ)

BULK MODULUS (K)

CREEP CONSTANT (A)

STRESS EXPONENT (m)

THERMAL CONSTANT ($\frac{Q}{R\Theta}$ if isothermal or $\frac{Q}{R}$ if not)

SHEAR EXPONENT (μ_1)

BULK EXPONENT (K_1)

B0

B1

A1

INTACT DENSITY (ρ_{intact})

INITIAL DENSITY (ρ_0)

11. M-D CREEP MODEL (number of cues = 20)

TWO MU (2μ)

BULK MODULUS (K)

A1

Q1/R

N1

B1

A2

Q2/R

N2

B2

SIG0 (σ_0)

QLC (q)

M (m)

K0

C ($c\Theta$)

ALPHA (α_w)

BETA (β_w)

DELTLC (δ)

RN3 (exponent of workhardening and recovery term used to compute F)
AMULT (scalar multiplier of time step needed for stability, default 0.98)

Examples for the ELASTIC PLASTIC material are given below to illustrate how the user might input the data in different forms. All three examples are identical as far as SANTOS is concerned.

Example 1:

```
MATERIAL, 1, ELASTIC PLASTIC, 1., 1, 5.E-6
HARDENING MODULUS = 30.E4
YOUNGS MODULUS = 30.E6
BETA = .5
POISSONS RATIO = .3
YIELD STRESS = 30.E3
END
```

Example 2:

```
MATERIAL, 1, ELASTIC PLASTIC, 1., 1, 5.E-6
YOUNGS MODULUS = 30.E6 POISSONS RATIO = .3 BETA = .5
YIELD STRESS = 30.E3 HARDENING MODULUS = 30.E4
END
```

Example 3:

```
MATERIAL, 1, ELASTIC PLASTIC, 1., 1, 5.E-6
YOUNGS MODULUS = 30.E6 POISSONS RATIO = .3 BETA = .5
YIELD STRESS = 30.E3 HARDENING MODULUS = 30.E4 END
```

42. MATERIAL POINT, x, y

x, y ... coordinates of a material point which will be monitored and printed at the output intervals,

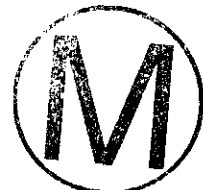
43. DELETE MATERIAL, material id, deletion time

material id ... material identification number

deletion time ... time at which all elements made up of this material should be deleted from the mesh.

Example Input File:

```
TITLE
EXAMPLE INPUT FILE
AXISYMMETRIC
STEP CONTROL
10 1.
END
OUTPUT TIME
2 1.
END
PLOT TIME
1 1.
END
NO DISPLACEMENT, X = 1
PRESCRIBED DISPLACEMENT, Y , 1, 1, .05
```





```
FUNCTION,1
0,0
1.,1.
END
MATERIAL,1,ELASTIC PLASTIC,1. $ 21-6-9 Stainless Steel
YOUNGS MODULUS=29.4+6 POISSONS RATIO=.3
YIELD STRESS=58.0E+3 HARDENING MODULUS=29.4E+4 BETA=1.
END
MATERIAL,2,ELASTIC,1. $ Tape Joint Filler (Steel)
YOUNGS MODULUS=29.4E+6 POISSONS RATIO=.3
END
MATERIAL,3,ELASTIC,1. $ Equivalent mass elements simulating remainder
YOUNGS MODULUS=30.E6 POISSONS RATIO=.3 END
RIGID SURFACE = 100,0.,0.,0.,0.,1.
CONTACT SURFACE = 101,102
CONTACT SURFACE = 103,104
CONTACT SURFACE = 105,106
CONTACT SURFACE = 107,108
EXIT
```



**APPENDIX B:
User Subroutines**



Intentionally Left Blank

User Subroutines

SANTOS allows the user to supply their own subroutines for defining an initial stress state (SUBROUTINE INITST) and an adaptive pressure routine (SUBROUTINE FPRES). The initial stress feature is particularly useful for geomechanics applications where an overburden stress is a function of depth. The adaptive pressure capability has been successfully used to define the pressure acting on the walls of a deforming cavity based on an assumption of ideal gas behavior.

The call to SUBROUTINE INITST has the following form:

```

SUBROUTINE INITST ( SIG, COORD, LINK, DATMAT, KONMAT, SCREL )
C
  INCLUDE 'params.blk'
  INCLUDE 'psize.blk'
  INCLUDE 'contrl.blk'
  INCLUDE 'bsize.blk'
  INCLUDE 'timer.blk'
C
  DIMENSION LINK(NELNS, NUMEL), KONMAT(10, NEMBLK),
  COORD(NNOD, NSPC), SIG(NSYMM, NUMEL), DATMAT(MCONS, *),
  SCREL(NEBLK, *)
  .
  .
  .
  RETURN
  END

```

where the calling arguments are defined as:

SIG - element stress array which must be returned with the required stress values

COORD - global nodal coordinate array

LINK - element connectivity array

DATMAT - material property array

KONMAT - material property integer array

SCREL - scratch element storage space

The arguments contained in the DIMENSION statement are located in the COMMON blocks which will be included during the program MAKE operation. If the MAKE utility is not used then the COMMON blocks will have to be explicitly included. This subroutine is called once prior to beginning the calculation by SUBROUTINE INIT. An example of a typical routine used for a geomechanics application is shown below. In this example, only material #1 is being initialized with respect to depth. Other materials in the problem are having their initial stresses set to zero.



```

SUBROUTINE INITST( SIG,COORD,LINK,DATMAT,KONMAT,SCREL )
C
C *****
C
C DESCRIPTION:
C THIS ROUTINE PROVIDES AN INITIAL STRESS STATE TO SANTOS
C
C FORMAL PARAMETERS:
C SIG REAL ELEMENT STRESS ARRAY WHICH MUST BE RETURNED
C WITH THE REQUIRED STRESS VALUES
C COORD REAL GLOBAL NODAL COORDINATE ARRAY
C LINK INTEGER CONNECTIVITY ARRAY
C DATMAT REAL MATERIAL PROPERTIES ARRAY
C KONMAT INTEGER MATERIAL PROPERTIES INTEGER ARRAY
C
C CALLED BY: INIT
C
C *****
C
C   INCLUDE 'params.blk'
C   INCLUDE 'psize.blk'
C   INCLUDE 'contrl.blk'
C   INCLUDE 'bsize.blk'
C   INCLUDE 'timer.blk'
C
C   DIMENSION LINK(NELNS,NUMEL),KONMAT(10,NEMBLK),
C   COORD(NNOD,NSPC),SIG(NSYMM,NUMEL),DATMAT(MCONS,*),
C   SCREL(NEBLK,*)
C
C   DO 1000 I = 1,NEMBLK
C       MATID = KONMAT(1,I)
C       MKIND = KONMAT(2,I)
C       ISTRT = KONMAT(3,I)
C       IEND = KONMAT(4,I)
C       IF( MATID .EQ. 1 )THEN
C           DO 500 J = ISTRT,IEND
C               II = LINK( 1,J )
C               JJ = LINK( 2,J )
C               KK = LINK( 3,J )
C               LL = LINK( 4,J )
C               ZAVG = 0.25 * ( COORD(II,2) + COORD(JJ,2) + COORD(KK,2) +
C               *           COORD(LL,2) )
C               STRESS = - 2.256E4 * ( 655. - ZAVG )
C               SIG(1,J) = STRESS
C               SIG(2,J) = STRESS
C               SIG(3,J) = STRESS
C               SIG(4,J) = 0.0
C           500 CONTINUE
C       ELSE
C           DO 600 J = ISTRT,IEND
C               SIG(1,J) = 0.0
C               SIG(2,J) = 0.0
C               SIG(3,J) = 0.0
C               SIG(4,J) = 0.0

```



```

        600      CONTINUE
              END IF
        1000 CONTINUE
              RETURN
              END

```

The call to SUBROUTINE FPRES has the following form:

```

SUBROUTINE FPRES ( VOLUME, TIME, PGAS )
.
.
.
RETURN
END

```

where the calling arguments are defined as:

VOLUME - computed volume of the cavity

TIME - current analysis time

PGAS - calculated gas pressure to be returned to calling program

This subroutine is called each iteration from SUBROUTINE EXLOAD. An example of a typical routine used for a geomechanics application is shown below. In this example, the volume coming into the subroutine corresponds to one-quarter of the total cavity volume due to the use of symmetry modeling conditions. The gas generation rate varies with time. The volume is multiplied by 4 to get the correct volume and the volume of solids is subtracted to get the free volume. The ideal gas law is then used to compute the internal cavity gas pressure.

```

SUBROUTINE FPRES( VOLUME, TIME, PGAS )
C ....
C .... THE PRESSURE IS COMPUTED ON THE BASIS OF THE IDEAL GAS LAW,
C .... PV = NRT. THE TOTAL NUMBER OF MOLES OF GAS, N (EN), PRESENT
C .... AT ANY TIME IS DETERMINED ON THE BASIS OF A CONSTANT RATE OF GAS
C .... GENERATION. R IS THE UNIVERSAL GAS CONSTANT AND THETA IS THE ROOM
C .... TEMPERATURE, 300 K. V IS THE CURRENT VOLUME OF THE ROOM. THE VOLUME
C .... MUST BE CORRECTED BY MULTIPLYING BY 2 OR 4 TO ACCOUNT FOR THE USE OF
C .... HALF OR QUARTER -SYMMETRY MODELS. THE VOLUME MUST ALSO BE MULTIPLIED
C .... BY A FACTOR TO ACCOUNT FOR 3D LENGTH.
C ....
C
R = 8.314
THETA = 300.
C
IF( TIME .LT. 1.7325E10 )THEN
PVALUE = 0.0
RATE = 4.32E-4
TSTAR = 0.0
ELSE IF( TIME .LT. 3.3075E10 )THEN

```



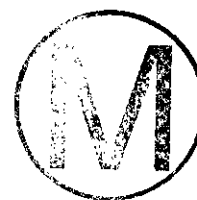
```
PVALUE = 7.48E6
RATE = 2.16E-4
TSTAR = 1.7325E10
ELSE
PVALUE = 1.0886e7
RATE = 0.0
TSTAR = 0.0
END IF
C
C .... CORRECT VOLUME AT THIS TIME TO GET VOLUME OF VOIDS
C
EN = PVALUE + RATE * ( TIME - TSTAR )
SCALE = 1.0
SYMFAC = 4.
XLENG = 91.44
C
C .... THIS MODIFICATION REMOVES THE BACKFILL FROM VSOLID
C
VSOLID = 1229.
VOLUME = SYMFAC * VOLUME * XLENG - VSOLID
IF( VOLUME .LE. 0.0 )VOLUME = 1.
C
PGAS = SCALE * EN * R * THETA / VOLUME
C
RETURN
END
```





APPENDIX C:
Printed Output Description

Intentionally Left Blank



Printed Output Description

The SANTOS printed output begins with an echo of the input data stream from input unit 5. This is followed by the PROBLEM DEFINITION section that lists the number of elements, nodal points, number of materials, analysis type, etc. that pertain to defining the problem to be solved. The information presented in this section also includes the solution algorithm parameters such as convergence tolerances, hourglass stiffness and viscosity values, and the effective modulus status. The amount of output written in this section depends on the analysis type and the options requested. An example of this output for a sample analysis is shown below.

P R O B L E M D E F I N I T I O N

NUMBER OF ELEMENTS	216
NUMBER OF NODES	247
NUMBER OF MATERIALS	1
NUMBER OF FUNCTIONS	1
NUMBER OF CONTACT SURFACES	0
NUMBER OF RIGID SURFACES	2
NUMBER OF MATERIAL POINTS MONITORED	0
ANALYSIS TYPE	AXISYMMETRIC
GLOBAL CONVERGENCE MEASURE	
RESIDUAL TOLERANCE	5.000E-01
MAXIMUM NUMBER OF ITERATIONS	3000
ITERATIONS FOR INTERMEDIATE PRINT	10
MAXIMUM RESIDUAL TOLERANCE	5.000E+00
PREDICTOR SCALE FACTOR FUNCTION	0
MINIMUM DAMPING FACTOR	2.000E-01
EFFECTIVE MODULUS STATUS	CONSTANT
SCALE FACTOR APPLIED TO TIME STEP	1.000E+00
STRAIN SOFTENING SCALE FACTOR	1.000E+00
HOURGLASS STIFFNESS FACTOR	1.000E-02
HOURGLASS VISCOSITY FACTOR	3.000E-02

Following the PROBLEM DEFINITION section are the definitions of the load steps, printed output frequency and the plotted output frequency. A sample output for these sections is shown below. LOAD STEP DEFINITIONS shows the number of steps taken between each defined time interval. The PRINTED OUTPUT FREQUENCY data echo shows the number of load steps between printed output dumps during the defined time interval. PLOTTED OUTPUT FREQUENCY echos the number of load steps between plot dumps during the defined time interval.



LOAD STEP DEFINITIONS

TIME	NO. OF STEPS	TIME
0.000E+00	100	1.000E+00

PRINTED OUTPUT FREQUENCY

TIME	STEPS BETWEEN PRINTS	TIME
0.000E+00	1	1.000E+00

PLOTTED OUTPUT FREQUENCY

TIME	STEPS BETWEEN PLOTS	TIME
0.000E+00	1	1.000E+00

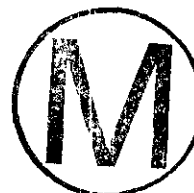
The next output grouping echos back the material type and material constants. Some additional constants which are computed by SANTOS within the constitutive model pre-processor are also printed.

MATERIAL DEFINITIONS

```

MATERIAL TYPE .....ELASTIC PLASTIC
MATERIAL ID ..... 1
DENSITY ..... 7.833E-06
MATERIAL PROPERTIES:
    YOUNGS MODULUS      = 2.000E+02
    POISSONS RATIO     = 3.000E-01
    YIELD STRESS       = 7.000E-01
    HARDENING MODULUS  = 3.000E-01
    BETA                = 1.000E+00
    
```

The next section of output echos back the processed input data regarding kinematic and traction boundary condition data. This data also includes function specifications and contact surface definitions. Distinction is made between NO DISPLACEMENT and PRESCRIBED DISPLACEMENT kinematic boundary conditions.





F U N C T I O N D E F I N I T I O N S

FUNCTION ID	1	NUMBER OF POINTS	2
N	S	F(S)	
1	0.000E+00	0.000E+00	
2	1.000E+00	1.000E+00	

N O D I S P L A C E M E N T B O U N D A R Y C O N D I T I O N S

NODE SET FLAG	DIRECTION
4	X

P R E S C R I B E D D I S P L A C E M E N T B O U N D A R Y C O N D I T I O N S

NODE SET FLAG	DIRECTION	FUNCTION ID	SCALE FACTOR	A0	B0
1	Y	1	9.000E+00	-	-

R I G I D S U R F A C E S

SURFACE NUMBER	SIDE SET FLAG	COEFFICIENT OF FRICTION	X0	Y0	NX	NY
1	300	FIXED	0.000E+00	1.500E+01	0.000E+00	-1.000E+00
2	200	FIXED	0.000E+00	1.500E+01	0.000E+00	-1.000E+00

The next grouping defines the quantities written to the plotting data base. The plotted output is grouped by whether the variable being written is a nodal, element, or global quantity. The global quantities, FX and FY, written to the data base refer to the sum of the applied loads in the x and y-directions, respectively. The quantities, RX and RY, refer to global reaction forces in the x and y-directions summed at nodes specified to have NO DISPLACEMENT boundary conditions applied. For axisymmetric analyses, the forces FX, FY, RX, and RY are output per radian. The nodal variables, RESIDX RESIDY RESID, refer to imbalance or residual forces acting at the nodes. The variables RESIDX and RESIDY refer to the x and y-component directions of the imbalance forces, respectively. The variable RESID is the scalar magnitude of the components. Material model state variables appear as element variables in the plotting data base.

VARIABLES ON PLOTTING DATA BASE

NODAL	ELEMENT	GLOBAL
-----	-----	-----
DISPLX	PRESSURE	FX
DISPLY	VONMISES	FY
RESIDX	EQPS	RX
RESIDY		RY
RESID		ITER

If the INTERMEDIATE PRINT option is in effect then the following output is obtained every n iterations. For this example, n is specified to be every 10 iterations. The values under the STEP column refer to the number of iterations taken relative to this load step. The column labeled TIME shows the problem time for which an equilibrium solution is being sought. The column labeled TIME STEP shows the stable time step internally computed within SANTOS which is being used to integrate the equations of motion. This number may change from one iteration to the next as the element is deformed. The column labeled DAMPING FACTOR provides the current adaptive dynamic relaxation damping parameter. The next two columns provide information regarding convergence of the load step. The APPLIED LOAD NORM refers to the L2 norm of the externally applied loads while the RESIDUAL LOAD NORM is the L2 norm of the imbalance forces at each node. The PERCENT IMBALANCE column is the result of dividing the RESIDUAL LOAD NORM by the APPLIED LOAD NORM which is the measure used to determine convergence of the iterative scheme. The column defined as TOTAL STEPS gives a running total of the number of iterations for the problem.

STEP	TIME	TIME STEP	DAMPING FACTOR	APPLIED LOAD NORM	RESIDUAL LOAD NORM	PERCENT IMBALANCE	TOTAL STEPS
10	1.000E-02	9.984E-03	7.105E-01	2.927E+01	1.047E+02	357.71	10
20	1.000E-02	9.991E-03	7.024E-01	2.395E+01	2.456E+01	102.55	20
30	1.000E-02	9.994E-03	5.261E-01	1.748E+01	7.866E+00	44.99	30
40	1.000E-02	9.996E-03	9.896E-01	1.600E+01	4.727E+00	29.55	40
50	1.000E-02	9.997E-03	9.574E-01	1.311E+01	2.591E+00	19.77	50
60	1.000E-02	9.998E-03	9.069E-01	1.259E+01	2.011E+00	15.97	60
70	1.000E-02	9.998E-03	9.428E-01	1.236E+01	1.604E+00	12.97	70
80	1.000E-02	9.999E-03	9.346E-01	1.200E+01	1.096E+00	9.13	80
90	1.000E-02	9.999E-03	8.438E-01	1.166E+01	7.562E-01	6.49	90

The final output section to be described is the printed output that results when the iterative solution reaches equilibrium as measured by the PERCENT IMBALANCE. The printed output provides descriptive information about the problem such as when the problem was run, version of the software, title of the problem and a summary of information about the convergence of the load step.



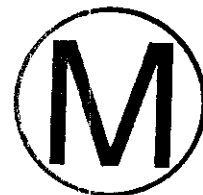


1 SANTOS, VERSION SANTOS 2.0 ,RUN ON 01/20/95 ,AT 16:15:25
UPSETTING OF A CYLINDRICAL BILLET

SUMMARY OF DATA AT STEP NUMBER 1, TIME = 1.000E-02
NUMBER OF ITERATIONS = 212, TOTAL NUMBER OF ITERATIONS = 212
FINAL CONVERGENCE TOLERANCE = 4.901E-01
SUM OF EXTERNAL FORCES IN X-DIRECTION = 0.000E+00
SUM OF EXTERNAL FORCES IN Y-DIRECTION = 0.000E+00
SUM OF REACTION FORCES IN X-DIRECTION = 0.000E+00
SUM OF REACTION FORCES IN Y-DIRECTION = -3.561E+01

**** PLOT TAPE WRITTEN AT TIME = 1.000E-02 STEP NUMBER 1 ****

Intentionally Left Blank





APPENDIX D:
Adding a New Constitutive Model to SANTOS

Intentionally Left Blank



Adding A New Constitutive Model to SANTOS

A material interface subroutine has been incorporated which allows the constitutive model developer to add a new material model with very little effort. The interface has been designed so that the developer does not need to understand the internal workings of SANTOS especially with respect to allocation and management of computer memory. If the developer follows the instructions in subroutine MATINT, then SANTOS will handle all memory allocation, material data reading, and material data printing. There are three steps that should be followed when adding a new model.

Step 1

Subroutine MATINT contains instructions using FORTRAN comment cards which outline the steps that should be followed to add a new material model. Most of the required changes involve adding or changing numbers in DATA and PARAMETER statements. Since we have no prior knowledge of what the material constants represent for a particular material, the code requires that a few lines of FORTRAN be added to compute the initial dilatational modulus ($\lambda + 2\mu$) and the initial shear modulus (2μ) for the material. The dilatational modulus and the shear modulus must be stored in the variables DATMOD and SHRMOD, respectively. At this same location in the code it is possible to calculate any combination of the input parameters that may be required in the constitutive subroutine (e.g. bulk modulus from Young's modulus and Poisson's ratio).

There is a restriction to twenty characters in the material name, material cues, and internal state variable names which are defined in subroutine MATINT. The names may have blanks which means that multiple word cues are allowed. The names must be defined such that each word in the name is unique to the first three characters. This means that material cues C1, C2, C3, etc., are legal; but CON1, CON2, CON3, etc., are not.

Step 2

This step is optional and is only required if the new material model contains internal state variables which must be initialized to some value other than zero (all internal state variables are initialized to zero by default). If state variables must be initialized, an ELSE IF statement must be added to subroutine SVINIT for this material. This statement should read:

```
ELSE IF( MKIND .EQ. (new material number) ) THEN
```

```
    initialize internal  
    state variables here
```

```
    .  
    .  
    .
```

This new material number corresponds to the position where the material resides in the list of



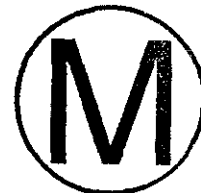
material names defined in subroutine MATINT. Generally, when adding a new material, the new material is the last one defined and its number will be the same as the number of materials defined in STEP 1. The application of this step should be obvious from inspecting the coding of the other material models. Please use comments to record changes to the code.

Step 3

In subroutine UPDSTR, the call to the new material model must be added. The material subroutine may have any appropriate name, but current convention has been to name the material subroutines MAT1, MAT2, MAT3, etc., where the number corresponds to the material number defined in Step 2. The call is included by adding an ELSE IF block to subroutine UPDSTR which should read:

```
ELSE IF( MKIND .EQ. (new material number) ) THEN  
    CALL new subroutine( ..... argument list .....
```

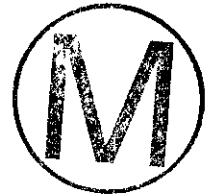
The application of this step should be obvious from inspecting the coding of the other material models. Please use comments to record changes to the code.





APPENDIX E:
Verification and Sample Problems

Intentionally Left Blank



Verification and Sample Problems

Sample problems are included to demonstrate code verification and to acquaint the user with the SANTOS program. The problems were selected to exercise and demonstrate many of the major features and options in the code.

Large Deflection Analysis of a Cantilever Beam

The large deformation of an elastic cantilever beam is included for comparison with the analytical solution as formulated by Holden (1972). The beam problem is challenging for the uniform strain quadrilateral elements and for the dynamic relaxation (DR) algorithm. The beam has a length-to-thickness ratio of 30. The beam material is assumed to be elastic with a Young's modulus of $1. \times 10^7$ psi and a Poisson's ratio equal to zero. Both gravity and normal pressure loading conditions are considered.

The first loading condition considered is the beam loaded with gravity, which keeps the direction of loading constant throughout the analysis. Following the notation and development of Holden, the equation for the slope of the beam is

$$\frac{d^2 \theta}{d\bar{s}^2} = -k\bar{s} \cos \theta, \quad (\text{EQ E-1})$$

where θ is the angle between the beam neutral axis and the x-axis; $\bar{s} = s/L$ is the normalized arc length along the beam neutral axis; $k = w \frac{L^3}{EI}$ is a nondimensional loading parameter; L is the length of the beam; w is the loading intensity (load per unit length); E is Young's modulus; and I is the beam's moment of inertia. This equation describes the finite deflection of uniform beams using the Euler-Bernoulli theory of bending subject to vertical (gravity) loading. Boundary conditions for the cantilevered beam are a specified zero rotation at the fixed end.

The normalized horizontal and vertical deflections of the free end of the beam are then given by

$$h/L = \int_0^1 \cos \theta d\bar{s} \quad (\text{EQ E-2})$$

and

$$\delta/L = \int_0^1 \sin \theta d\bar{s}, \quad (\text{EQ E-3})$$

respectively. Equation E-1 is solved using a Runge-Kutta procedure, the integrations for deflections are computed using adaptive quadrature, and the results are checked by comparison to



Holden's published solution. Figure E-1 shows a schematic of the beam geometry and boundary conditions. The beam has thirty elements along its length and four through the beam thickness. The nonlinear beam response is calculated with SANTOS (triangles and squares) and compared to Holden's published solution (solid line) in Figure E-2. The comparison for this case is excellent. The deformed shape of the beam corresponding to $k = 0.$, 6.5, and 20. is shown in Figure E-3.

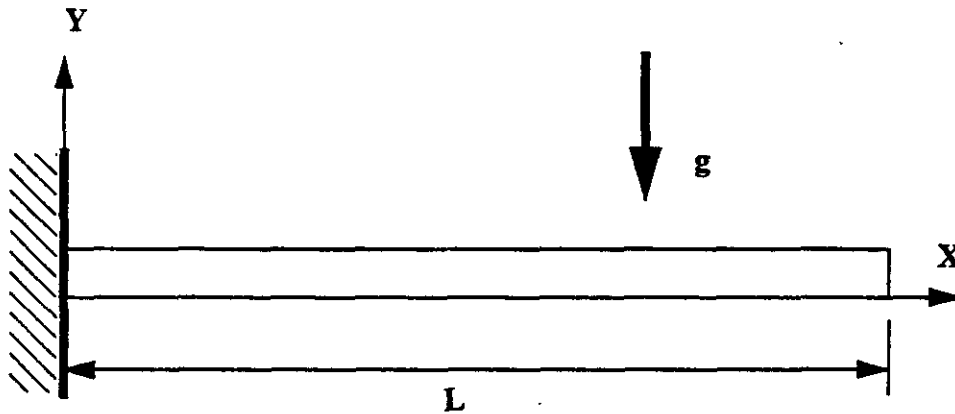


Figure E-1. Schematic of Cantilever Beam With Gravity Loading Showing the Geometry and Boundary Conditions

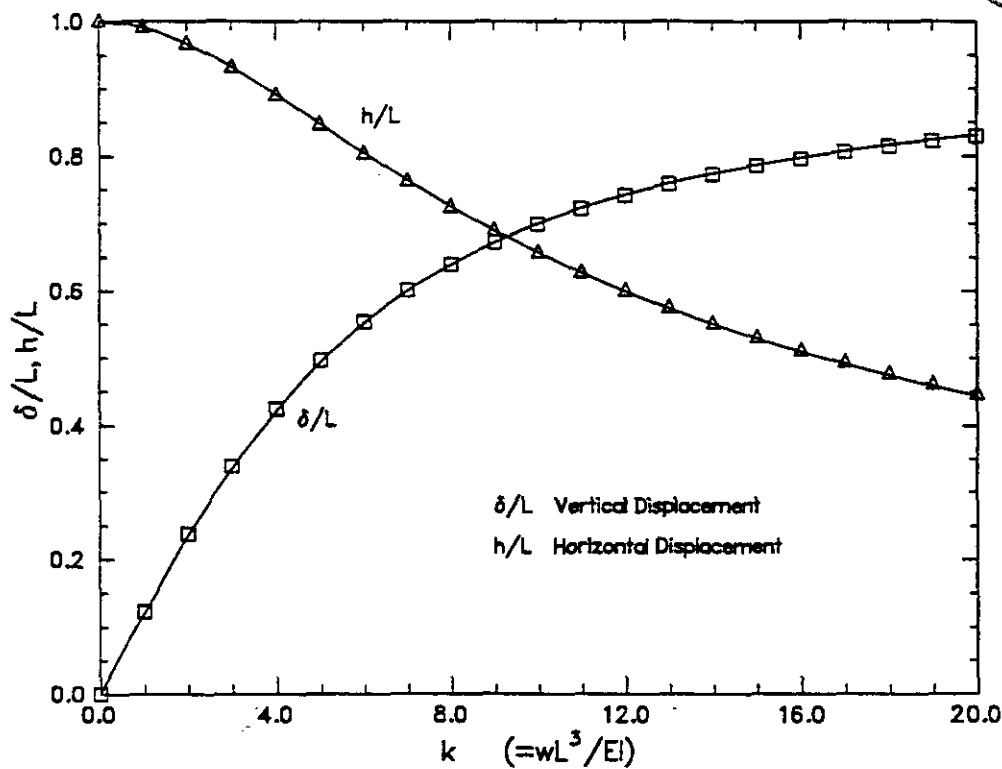


Figure E-2. Comparison of Analytic (solid line) and SANTOS (triangles and squares) Tip Displacements for the Beam With Gravity Loading.

To obtain a solution to the gravity loaded beam problem using DR, we must make use of the NO DAMPING option. This option turns off the damping for a specified number of iterations which allows the beam to take on a more correct deformed shape before damping begins. In addition, this option is invoked only for the first 50 load steps which corresponds to the tip of the beam reaching a deflection magnitude equal to the thickness of the beam. Some large imbalance forces are experienced with the early load steps but these quickly disappear as the beam deforms and the deformation mode changes from small-deformation bending behavior to large-deformation bending behavior. A total of 310 load steps were taken for the gravity loaded case with each load step averaging 733 iterations. The SANTOS input file for the gravity loaded beam problem is shown in Figure E-4.

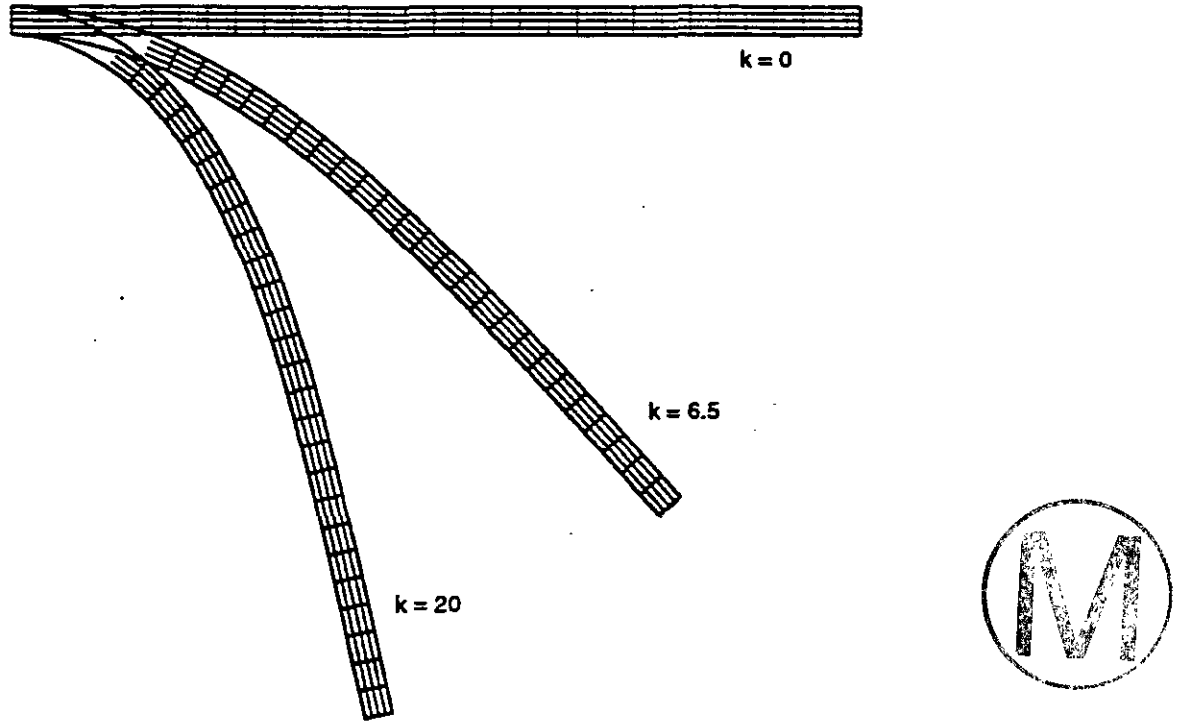


Figure E-3. Deformed Shape of the Beam Under Gravity Loading.
Deformed Shapes Correspond to k = 0.0, 6.5, and 20.

The second loading condition is pressure applied along the top of the beam so that the loads remains normal to the surface throughout deformation. The beam theory equation for this case is

$$\frac{d^2 \theta}{ds^2} = -k\bar{s}, \tag{EQ E-4}$$

with the same boundary conditions as before. For large load magnitudes, this configuration causes more severe bending of the beam as shown in Figure E-5. The analytic solution (solid line) is compared to the SANTOS solution (triangles and squares) in Figure E-6. For this load case the finite element model is stiffer than the Euler-Bernoulli beam theory predicts at the higher loads. This difference is probably due to the fact that when the beam starts bending back on itself, the

```

TITLE
  30 TO 1 BEAM WITH GRAVITY LOADS - SANTOS QA PROBLEM
RESIDUAL TOLERANCE, 0.5
MAXIMUM ITERATIONS, 3000
INTERMEDIATE PRINT, 100
MAXIMUM TOLERANCE, 1000
NO DAMPING, 100, 50
PLANE STRAIN
STEP CONTROL
  310 1.55
END
PLOT TIME
  10 1.55
END
OUTPUT TIME
  1 1.55
END
PLOT NODAL DISPLACEMENT
PLOT ELEMENT STRESS,VONMISES
NO DISPLACEMENT Y, 4
NO DISPLACEMENT X, 4
GRAVITY,1,0.,1.,0.
FUNCTION, 1 $ FUNCTION TO DEFINE GRAVITY LOADS
0. 0.
2. -2.
END
MATERIAL, 1, ELASTIC, 400.
YOUNGS MODULUS = 1.E7
POISSONS RATIO = 0.0
END
EXIT

```

Figure E-4. SANTOS Input File for the Gravity Loaded Beam Verification Problem.

radius of curvature is no longer large compared to the thickness of the beam. The SANTOS solution employed 1550 load steps with an average of 270 iterations per load step. The input file for this load case is shown in Figure E-7.

Elastic-Plastic Thick-Walled Hollow Sphere

The problem of a thick-walled hollow sphere loaded into the plastic range by an internal pressure serves as a good check of the elastic-plastic material model. The two cases analyzed are for an elastic-perfectly plastic sphere and an elastic-plastic sphere with linear strain hardening. The sphere analyzed has an internal radius of one and an outer radius of two. The internal pressure is increased from the start of initial yield at the inner surface and is increased until the sphere becomes fully plastic. The problem is analyzed using the axisymmetric option in SANTOS. In addition, symmetry boundary conditions are assumed so that only a quarter of the sphere is modeled as shown in Figure E-8. The mesh discretization uses 30 elements spaced uniformly in the radial direction and 20 elements spaced uniformly around the circumference for a total of 600 elements. The sphere material has a Young's modulus of 207. GPa and a Poisson's ratio of 0.3. The yield



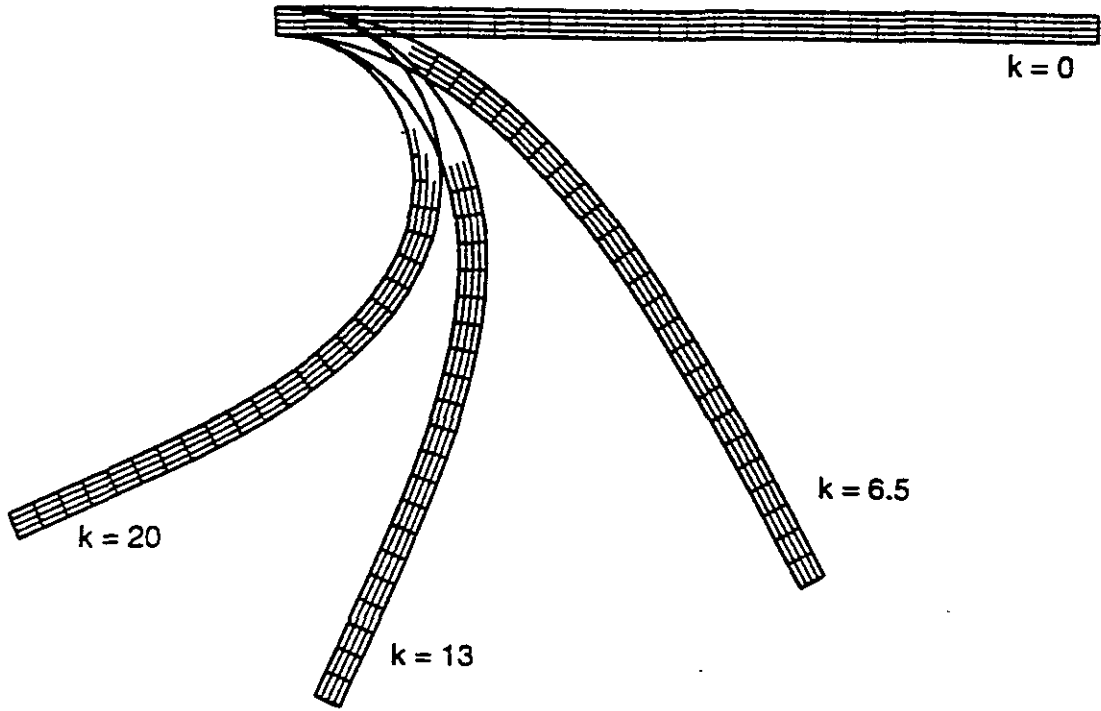


Figure E-5. Deformed Shape of the Beam With Applied Pressure Loading. Deformed Shapes Correspond to $k = 0.0, 6.5, 13.,$ and $20.$

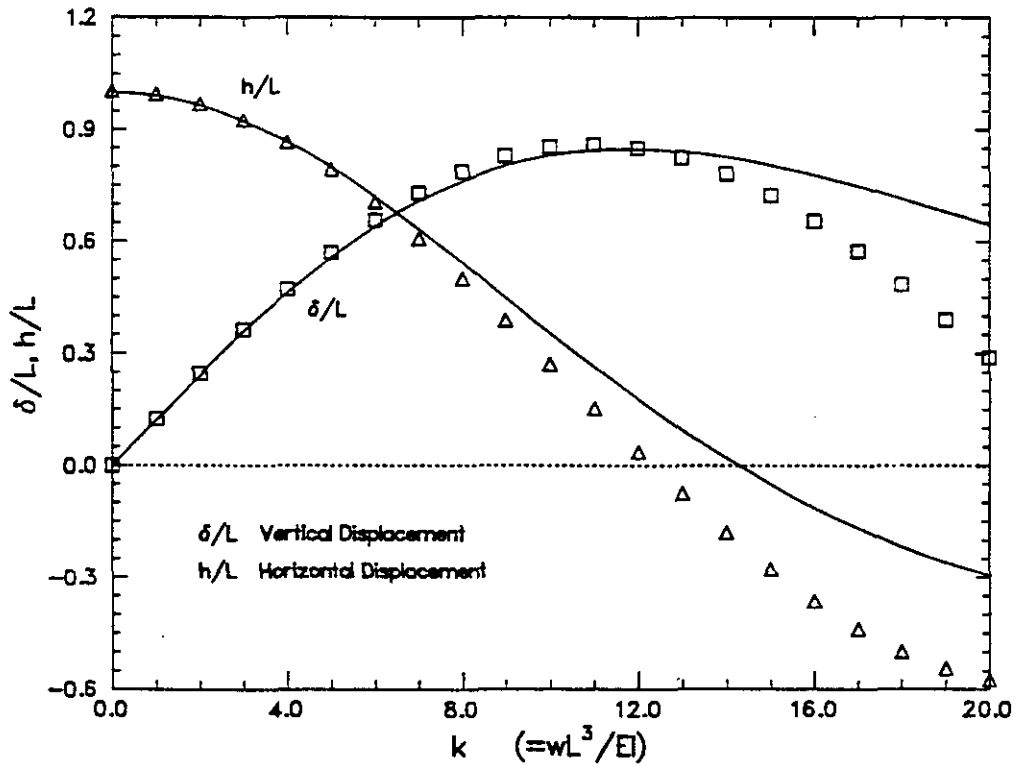


Figure E-6. Comparison of Analytic (solid line) and SANTOS (squares and triangles) Tip Displacements for the Beam With Applied Pressure Loading.



```

TITLE
  30 TO 1 BEAM WITH APPLIED PRESSURE
RESIDUAL TOLERANCE, 0.5
MAXIMUM ITERATIONS, 3000
INTERMEDIATE PRINT, 100
MAXIMUM TOLERANCE, 1000
NO DAMPING, 100, 50
PLANE STRAIN
STEP CONTROL
  1550 1.55
END
PLOT TIME
  10 1.55
END
OUTPUT TIME
  1 1.55
END
PLOT NODAL DISPLACEMENT
PLOT ELEMENT STRESS,VONMISES
NO DISPLACEMENT Y, 4
NO DISPLACEMENT X, 4
PRESSURE, 30, 1, 400.
FUNCTION, 1 $ FUNCTION TO DEFINE PRESCRIBED DISPLACEMENT
0. 0.
2. 2.
END
MATERIAL, 1, ELASTIC, 2167.
YOUNGS MODULUS = 1.E7
POISSONS RATIO = 0.0
END
EXIT

```

Figure E-7. SANTOS Input File for Pressure Loaded Beam Verification Problem.

stress is set to 10000. and the hardening modulus is 20.7 GPa for the linear strain hardening problem. The hardening modulus is set to zero for the elastic-perfectly plastic analysis.

The analytical solutions for these problems were derived by Mendelson (1968). For an internally pressurized sphere, the elastic/plastic interface expands radially outward from the inner surface of the sphere according to the following equations taken from Mendelson. The first relation is for the elastic perfectly-plastic material and defines the radius, c , of the elastic-plastic interface

$$P = 2 \ln \rho_c + \frac{2}{3} \left(1 - \frac{1}{\beta_c^3} \right) \quad (\text{EQ E-5})$$

and the second equation defines the elastic-plastic interface for the linear strain hardening material.

$$P = \frac{\frac{4m}{3}(1-\nu)\left(1 - \frac{1}{\beta^3}\right)\rho_c^3 + 2(1-m)\ln\rho_c + \frac{2}{3}(1-m)\left(1 - \frac{1}{\beta^3}\right)}{1 - m + 2m(1 - \nu)} \quad (\text{EQ E-6})$$

The non-dimensional variables used in Equations E-5 and E-6 are: $P = p/\sigma_y$ is the ratio of applied internal pressure to material yield stress, σ_y ; $\rho_c = c/a$ is the ratio of the elastic-plastic interface radius to the sphere's internal radius, a ; $\beta_c = b/c$ is the ratio of the sphere's outer radius, b , to the elastic-plastic interface radius; $\beta = b/a$ is the ratio of the sphere's outer to inner radii; m is the ratio of the hardening modulus to the Young's modulus; and ν is Poisson's ratio.

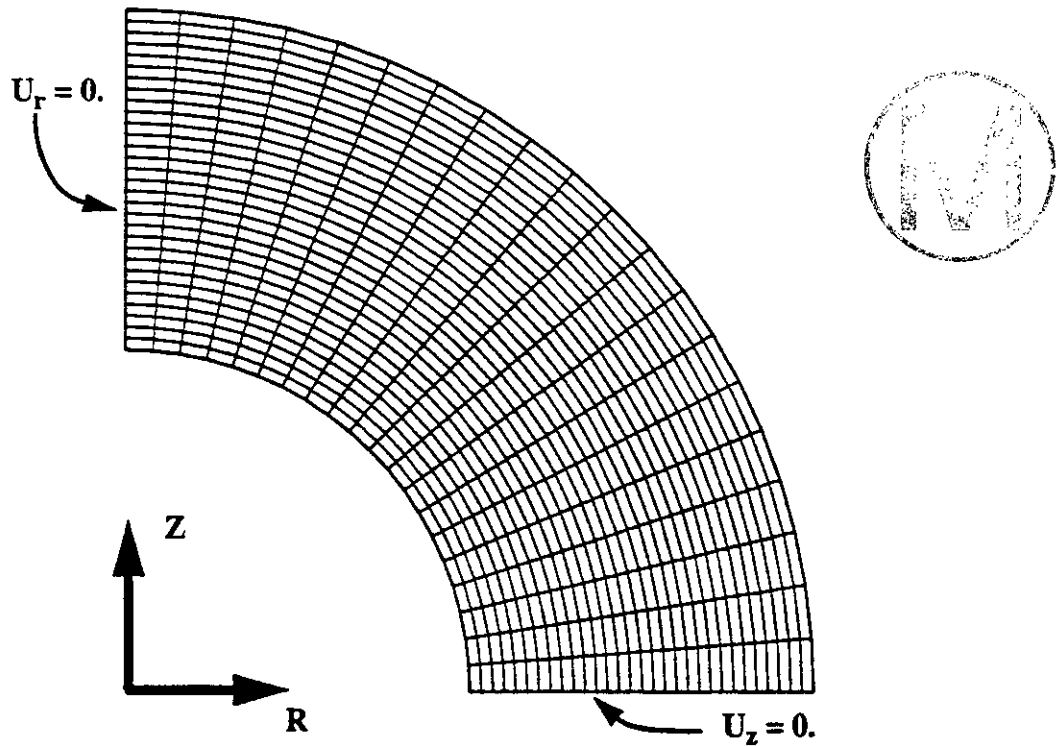


Figure E-8. Finite Element Mesh Discretization Used for the Thick-Walled Hollow Sphere Analyses.

In Figures E-9 and E-10, the non-dimensional effective stress is plotted as a function of radius for loadings starting from initial plastic yield at the sphere inner radius to full plastic yielding of the sphere. The analytical solutions are plotted as solid lines in the figures. As can be seen from the plots of normalized effective stress, the computed and analytical results match almost exactly. The only deviation between the solutions is seen in Figure E-9 for the case where the sphere should be fully plastic. The SANTOS solution does not predict a fully plastic sphere. The normalized effective stress for the element at the sphere outer surface does not yield although the pressure applied should induce full plastic yielding of the sphere. It appears that full plastic yielding results in an increase in the calculated outer radius by an amount to stop further yielding and obtain

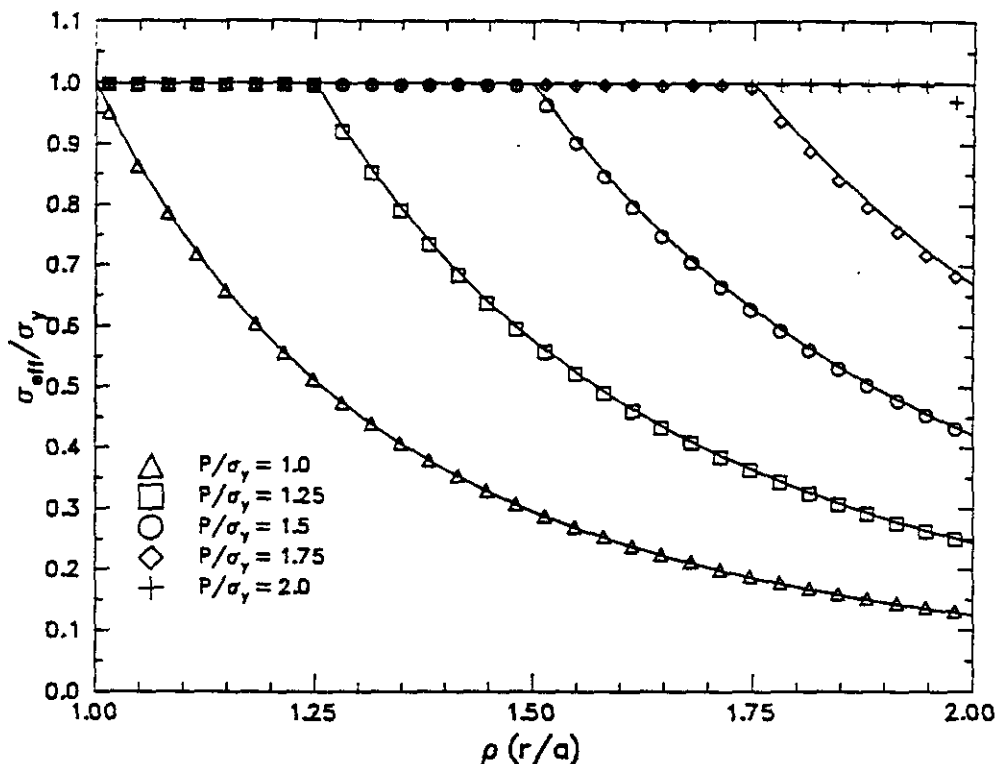


Figure E-9. Normalized Effective Stress Results for the Internally Pressurized Elastic-Perfectly Plastic Thick-Walled Hollow Sphere

equilibrium. In addition, if the sphere were to become fully plastic for an elastic-plastic material with no hardening, the solution would be difficult to converge since the material would be flowing in an unrestrained manner. The SANTOS input file for the internally pressurized elastic-plastic thick-walled hollow sphere is given in Figure E-11.

Upsetting of a Cylindrical Billet

This verification problem examines the behavior of a cylindrical metallic billet that has undergone a 60% upset by compression between two flat, rigid dies. The billet has as initial dimensions a length of 30 mm and a diameter of 20 mm. The axisymmetric option in SANTOS is used and only the top half of the billet is modeled since the middle surface of the billet can be viewed as a plane of symmetry. The time history of the die force is to be compared to computational results by other analysts (Taylor, 1981).

The die material is assumed to be elastic-plastic with linear strain hardening. The material properties are taken from Lippmann (1979). The billet has a Young's modulus of 200 Gpa and a Poisson's ratio of 0.3. The initial yield stress of the material is 700 Mpa with a hardening modulus of 300 Mpa. A uniform mesh containing 216 quadrilateral elements is used. The mesh discretization and boundary conditions used are shown in Figure E-12. The middle surface of the billet is given a prescribed vertical displacement which compresses the billet against the top rigid die. The rigid die is modeled using the RIGID SURFACE option in SANTOS. The die surface is assumed to be rough which results in a no slip condition between the billet and die. This behavior can be achieved by specifying the friction value as FIXED on the RIGID SURFACE option.



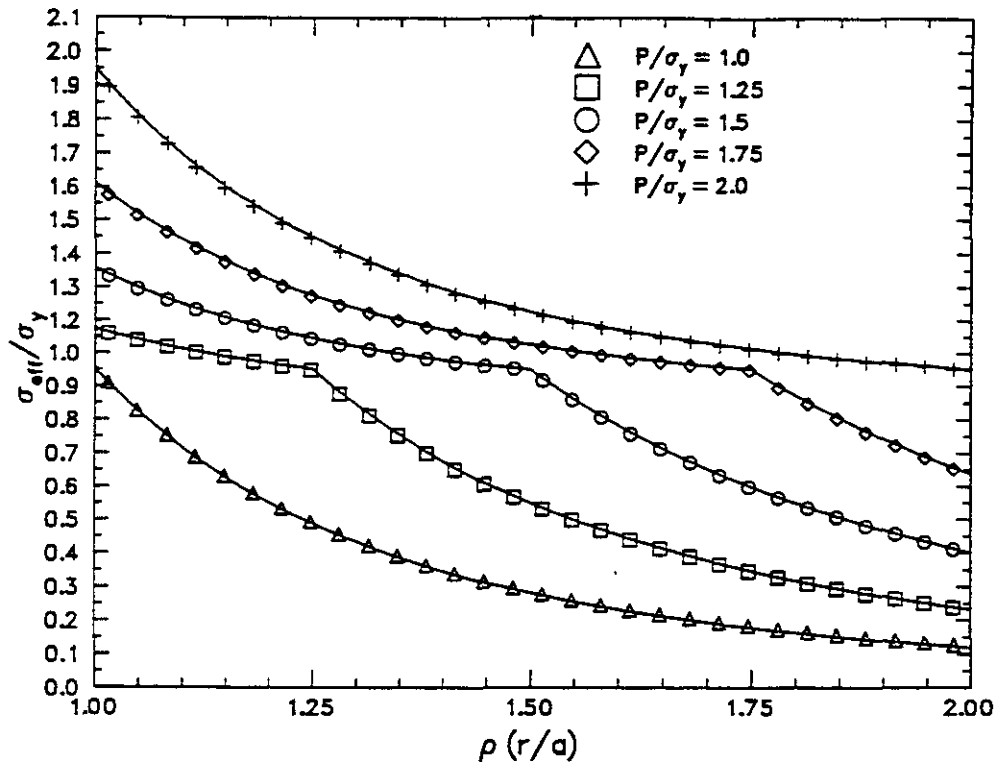


Figure E-10. Normalized Effective Stress Results for the Internally Pressurized Elastic-Plastic Thick-Walled Hollow Sphere With Linear Hardening.

During deformation it is expected that the external surface of the billet will fold and come into contact with the rigid die, which means that the definition of the side set associated with the rigid surface must include both elements along the top of the billet and elements along the external boundary. One hundred load steps were taken for this analysis.

Figure E-13 shows the deformed shape of the billet at several different times during the upset process. The folding of the billet's external surface is clearly seen as well as its contact with the rigid die. A close-up of the billet's final deformed shape at 60% upset is shown in Figure E-14. Figure E-15 shows a comparison of the upset force vs. die displacement with results taken from Taylor (1981). The agreement is seen to be excellent until the die displacement reaches 7.0 mm. At this value of displacement, the billet is folding and the first nodal point on the external surface is just coming into contact with the rigid surface. The slight difference in the upset force seen in the figure at die displacements greater than 7.0 mm is related to the contact occurring between the folding billet and the rigid surface. The SANTOS input file for the upsetting of the cylindrical billet is given in Figure E-16.

Closure of a Waste Disposal Room in a Salt Stratigraphy

Bedded salt is being considered as a storage medium for the long-term disposal of contact-handled transuranic wastes produced as a by-product of the defense activities of the United States. Salt was selected because of its propensity to creep under the action of deviatoric stresses. This creep deformation would eventually entomb the waste and isolate it from the biosphere. Under the



```
TITLE
  SANTOS QA PROBLEM - HOLLOW SPHERE - 10/26/94 - HARDENING M = 0.1
AXISYMMETRIC
MAXIMUM ITERATIONS 20000
RESIDUAL TOLERANCE .01
MATERIAL,1,ELASTIC PLASTIC,1.0
YOUNGS MODULUS 2.07E+11
POISSONS RATIO 0.3
YIELD STRESS 10000.
HARDENING MODULUS 2.07E+10
BETA 0.
END
FUNCTION,1
  0.      0.
  1.      5833.
  1.25    9756.5
  1.5     13003.2
  1.75    15798.4
  2.      18278.8
END
STEP CONTROL
  1,1.
  1,1.25
  1,1.50
  1,1.75
  1,2.0
END
PLOT TIME
  1,1.
  1,1.25
  1,1.50
  1,1.75
  1,2.0
END
OUTPUT TIME
  1,1.
  1,1.25
  1,1.50
  1,1.75
  1,2.0
END
NO DISPLACEMENT,X,1
NO DISPLACEMENT,Y,2
PRESSURE,3,1,1.
EXIT
```



Figure E-11. SANTOS Input File for the Internally Pressurized Elastic-Plastic Thick-Walled Hollow Sphere With Linear Hardening.

current plan, the wastes are to be stored in disposal rooms, which are part of a mined repository, 650 m underground. The disposal rooms are 10.06 m wide by 3.96 m high and 91.44 m in length. As part of the repository performance assessment activity, it was a requirement to determine the

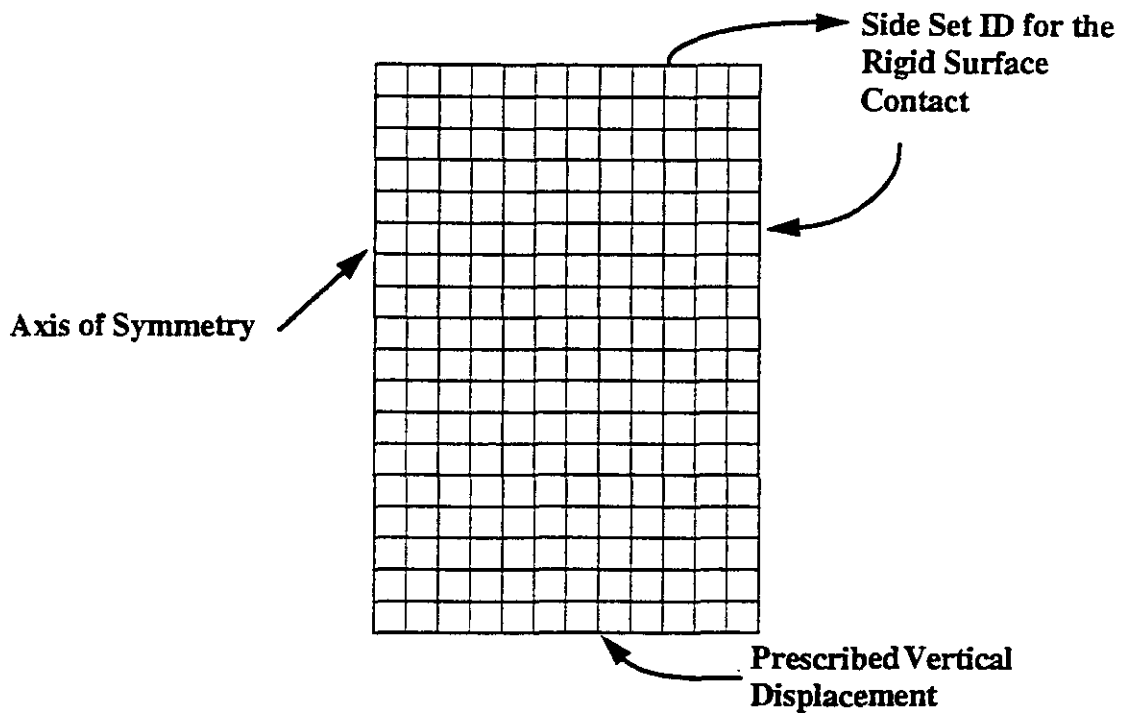


Figure E-12. Mesh Discretization and Boundary Conditions Used for the Analysis of the Upsetting of a Cylindrical Billet.

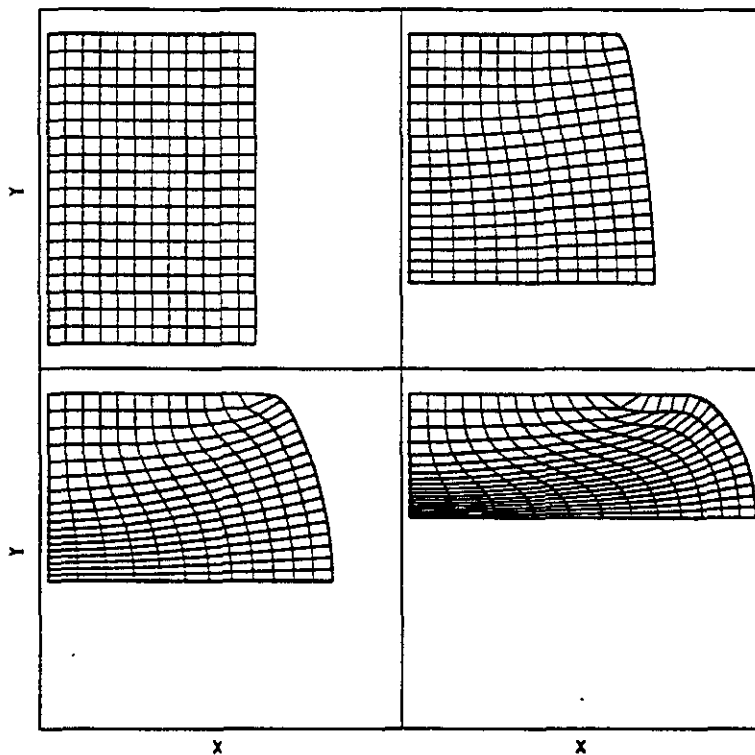


Figure E-13. Plots of the Deforming Billet at Various Times During the Upset. Plots Shown Correspond to Non-Dimensional Times of 0., 0.33, 0.667, and 1.0.



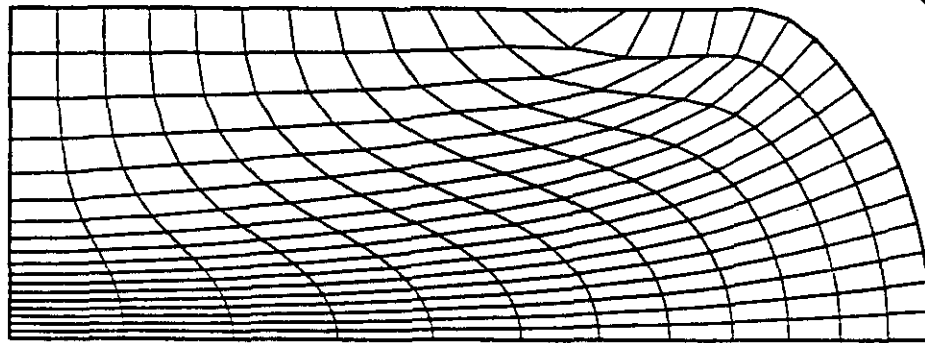
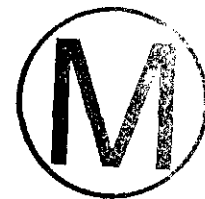


Figure E-14. Final Deformed Shape of the Billet After 60% Upset.

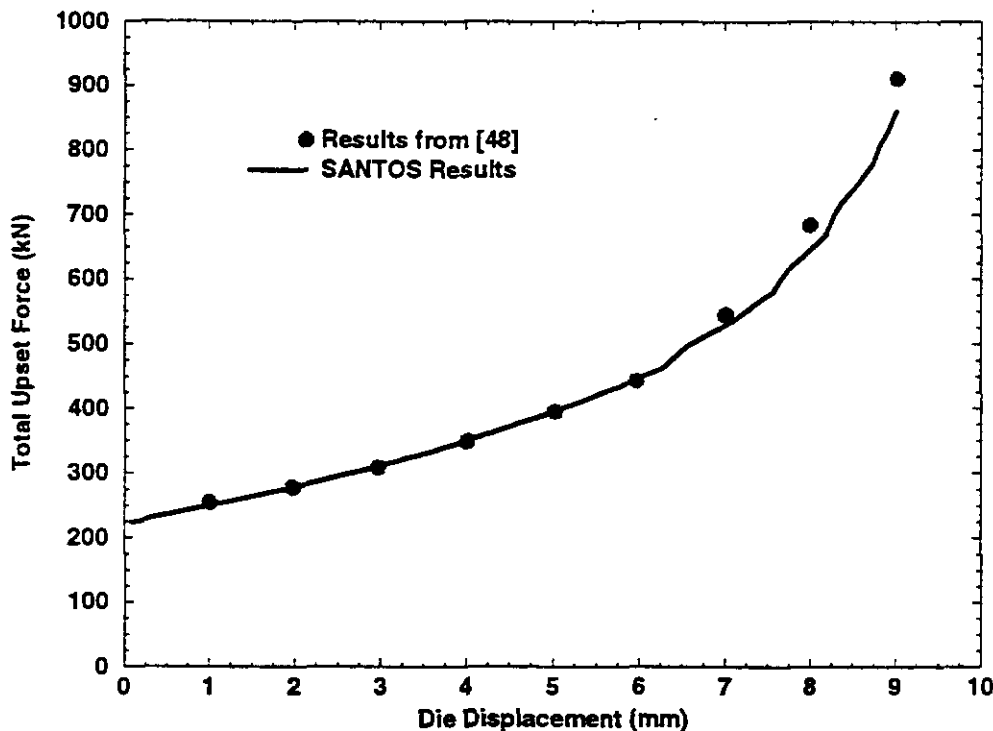


Figure E-15. Comparison of SANTOS Calculation With Numerical Results Taken From Taylor (1981) for the Upset of a Cylindrical Billet.

time required for the disposal room to creep closed. In answering this question, a model of a disposal room in an all salt stratigraphy was developed.

In the disposal room model, it is assumed that the disposal room is one of infinite number of parallel rooms located at the repository horizon. This assumption allows the use of vertical planes of symmetry at the room centerline and in the center of the pillar between rooms which results in the problem geometry shown with the discretized mesh in Figure E-17. The horizontal mesh dimension between symmetry planes is 20.27 m. The vertical mesh boundaries are located

```

TITLE
  UPSETTING OF A CYLINDRICAL BILLET
AXISYMMETRIC
STEP CONTROL
100,1
END
INTERMEDIATE PRINT= 10
MAXIMUM ITERATIONS = 3000
RESIDUAL TOLERANCE = 0.5
MAXIMUM TOLERANCE = 100.0
OUTPUT TIME
1,1
END
PLOT TIME
1,1
END
PLOT NODAL = DISPLACEMENT,REACTION,RESIDUAL
PLOT ELEMENT = VONMISES,PRESSURE
PLOT STATE = EQPS
NO DISPLACEMENT,X = 4
PRESCRIBED DISPLACEMENT,Y = 1,1,9.E-3
FUNCTION = 1
0,0
1,1
END
RIGID SURFACE = 500 , 0., 15.E-3, 0., -1., FIXED
MATERIAL,1,ELASTIC PLASTIC,7.833E-6
YOUNGS MODULUS = 200e9 , POISSONS RATIO = .3
YIELD STRESS = .7e9 , HARDENING MODULUS = .3e9 , BETA = 1
END
EXIT

```

Figure E-16. SANTOS Input File Used for Analyzing the Upsetting of a Cylindrical Billet.

approximately 50 m from the disposal room. The vertical extent of the problem is designed to remove the effect of the boundaries away from the disposal room. The problem has a traction representing the overburden load applied at the top boundary and the bottom boundary has a traction applied to equilibrate the overburden load plus the additional loads produced by applied gravity forces. An initial hydrostatic stress state is assumed to exist with the value of the stress set to the lithostatic stress. Vertical motion of the model is restrained at a location near the top surface as shown in Figure E-17. Contact surfaces are defined around the interior of the disposal room to accommodate contact that occurs during the large-deformation room closure. Contact pairings are defined between the roof-floor, pillar-roof, and pillar-floor. The coefficient of friction is assumed to be zero for this calculation.

The salt is modeled using the M-D creep model from the SANTOS material library. The M-D model is a combined transient-secondary creep constitutive model for rock salt. The model includes the effects of workhardening and recovery through a state variable function that modifies the steady-state creep rate. The Tresca stress generalization is used in the model for the effective stress definition. The M-D material constants for argillaceous salt are given in Table 1. The AUTO



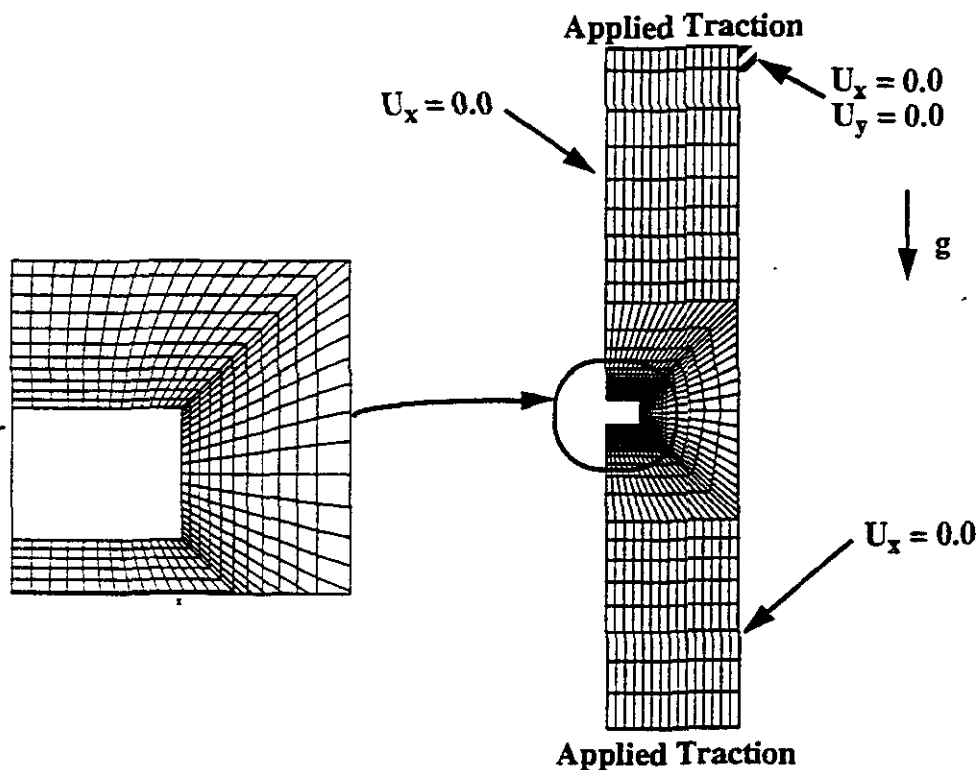


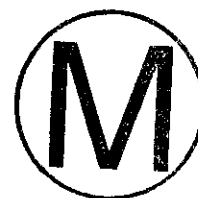
Figure E-17. Geometry, Boundary Conditions and Mesh Discretization for Analyzing the Closure of a Disposal Room in Salt.

STEP option is used with the M-D material model for this problem. The time step necessary for a stable and accurate solution for the M-D model is very small at the start of the analysis. The AUTO STEP option begins with a small initial time step, $1. \times 10^{-5}$ seconds, and allows it to grow to an analyst specified maximum of 2.592×10^6 seconds. Without invoking the AUTO STEP option, it is very time consuming to perform this analysis.

Figure E-18 shows the deformed shape of the disposal room at several different times from the initial undeformed state to final closure. The closure process is characterized by shortening of the pillar and an inward displacement of the disposal room roof and floor. Contact between the roof-pillar and floor-pillar occurs near the room corners. As contact occurs, the rate of room closure slows as the pillar begins to support the roof and floor. A close-up of the disposal room at closure is shown in Figure E-19. The contact of the disposal room interior surfaces is clearly shown in this figure. Figure E-20 shows the time history of room closure as measured by the sum of the displacements of the floor and roof centerline nodal points. When the sum of the displacements reaches 3.96 m then the floor and roof have come into contact and the disposal room is assumed to be closed. Closure is seen to occur at approximately 57 years. The SANTOS input file for analyzing the closure of a waste disposal room in salt is given in Figure E-21.

Table 1: M-D Argillaceous Salt Creep Properties

Parameters (units)	Parameter Value
G (MPa)	12,400
E (MPa)	31,000
ν	0.25
A_1 (/sec)	1.407E23
Q_1 (cal/mole)	25,000
n_1	5.5
B_1 (/sec)	8.998E6
A_2 (/sec)	1.314E13
Q_2 (cal/mole)	10,000
n_2	5.0
B_2 (/sec)	4.289E-2
σ_o (MPa)	20.57
q	5,335
M	3.0
K_o	2.470E6
c (/T)	9.198E-3
α	-14.96
β	-7.738
δ	0.58



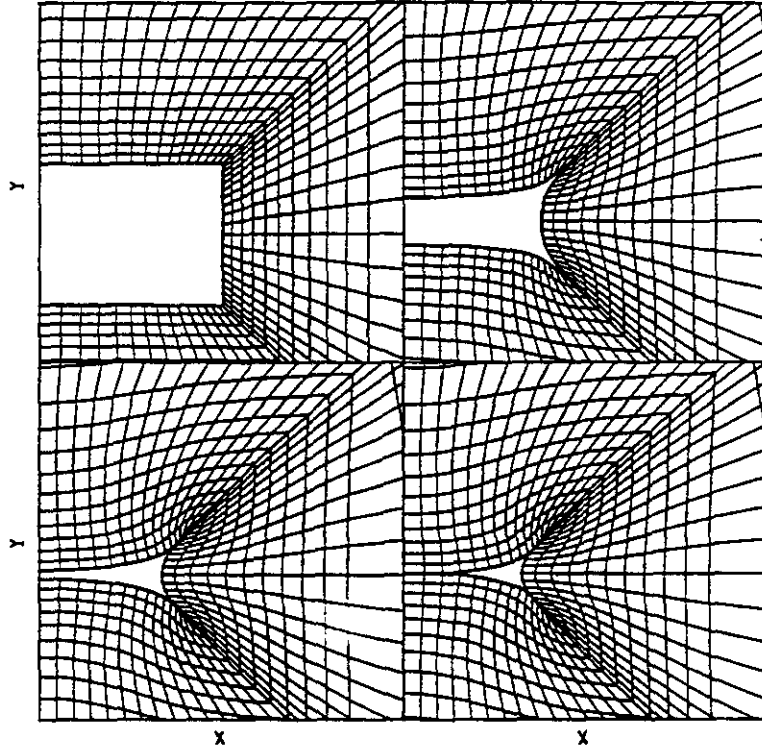


Figure E-18. Plots of the Deforming Disposal Room at Selected Times From Initial Excavation to Final Closure. Times 0., 25. 50., and 80 Years.

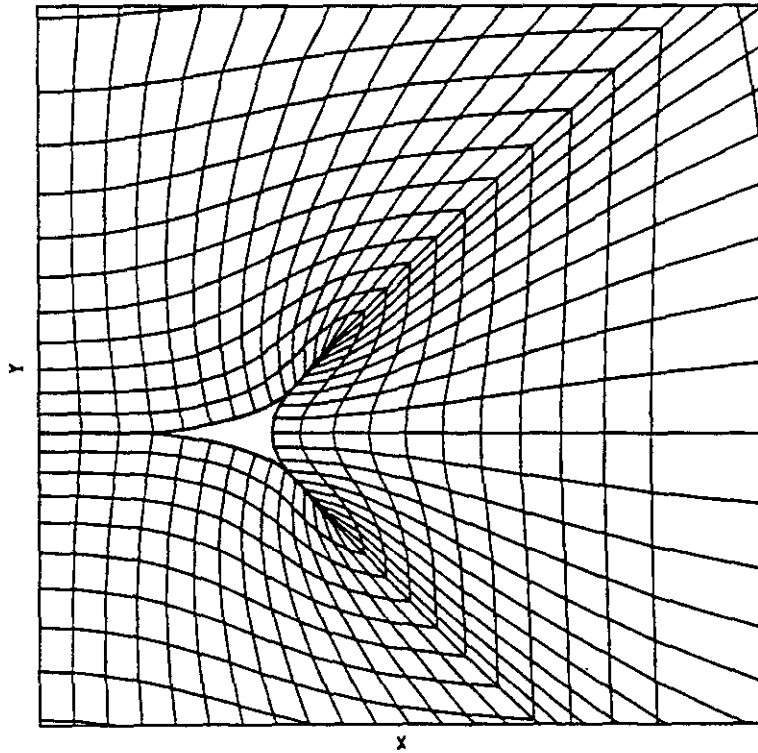


Figure E-19. Deformed Shape of the Disposal Room 100 Years After Excavation.



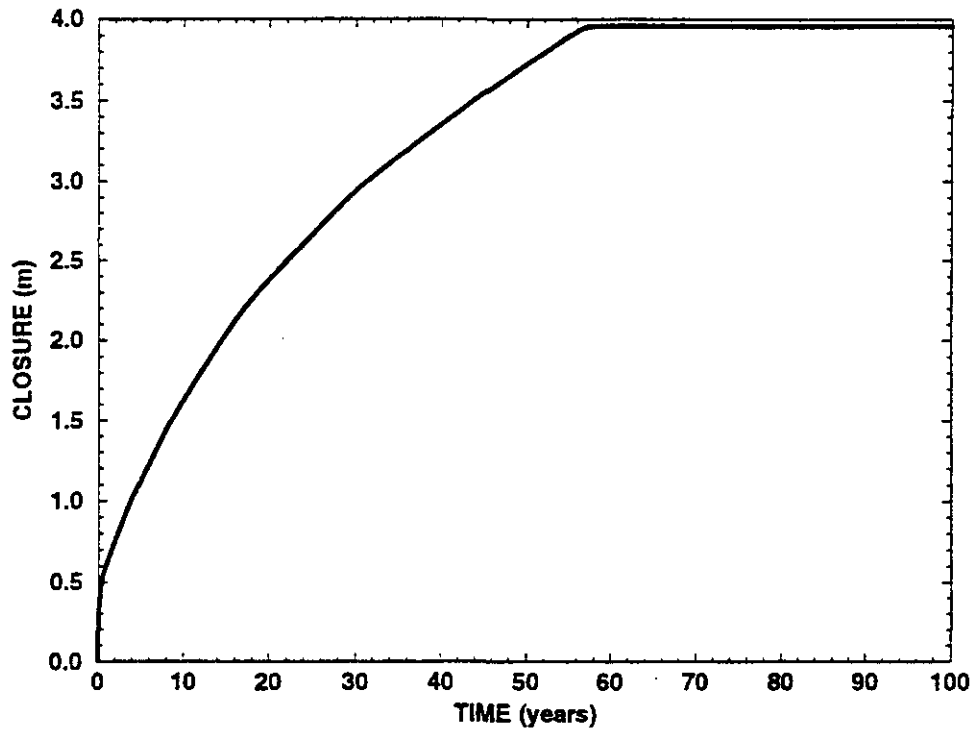


Figure E-20. Closure History of the Disposal Room Centerline. Contact of the Floor and Roof is Reached at Approximately 57 Years.

References

- Holden, J. T. 1972. "On the Finite Deflections of Thin Beams," *International Journal of Solids and Structures*. Vol 8, 1051-1055.
- Lippmann, H., ed. 1979. *Metal Forming Plasticity*. New York, NY: Springer Verlag.
- Mendelson, A. 1968. *Plasticity: Theory and Application*. New York, NY: The Macmillan Company. 138-156.
- Taylor, L. M. 1981. "A Finite Element Analysis for Large Deformation Metal Forming Problems Involving Contact and Friction." Ph.D. Dissertation. Austin, Tx: University of Texas at Austin.

```

TITLE
DISPOSAL ROOM CALCULATION TO CLOSURE ALL SALT - M-D CREEP MODEL
RESIDUAL TOLERANCE = 0.5
MAXIMUM ITERATIONS = 3000
INTERMEDIATE PRINT = 100
MAXIMUM TOLERANCE = 10.0
PLANE STRAIN
ELASTIC SOLUTION
INITIAL STRESS = USER
GRAVITY = 1 = 0. = -9.8066 = 0.
AUTO STEP .02 2.592E6 NOREDUCE 1.E-5
HOURLASS STIFFENING = .005
STEP CONTROL
4000 3.15E9
END
PLOT TIME
10 3.15E9
END
OUTPUT TIME
10 3.15E9
END
PLOT NODAL DISPLACEMENT, RESIDUAL
PLOT ELEMENT STRESS, VONMISES, EFFMOD
PLOT STATE EQCS
NO DISPLACEMENT X, 1
NO DISPLACEMENT X, 3
NO DISPLACEMENT Y, 3
FUNCTION, 1
0. 1.
10.E9 1.
END
PRESSURE, 4, 1, 13.57E6
PRESSURE, 2, 1, 15.96E6
CONTACT SURFACE, 200, 100, 0., 1.E-6, 1.E40
CONTACT SURFACE, 300, 200, 0., 1.E-6, 1.E40
CONTACT SURFACE, 100, 300, 0., 1.E-6, 1.E40
MATERIAL, 1, M-D CREEP MODEL, 2300. $ ARGILLACEOUS HALITE
TWO MU = 24.8E9
BULK MODULUS = 20.66E9
A1 = 1.407E23
Q1/R = 41.94
N1 = 5.5
B1 = 8.998E6
A2 = 1.314E13
Q2/R = 16.776
N2 = 5.0
B2 = 4.289E-2
SIG0 = 20.57E6
QLC = 5335.
M = 3.0
K0 = 2.47E6
C = 2.759
ALPHA = -14.96
BETA = -7.738
DELTLC = .58
RN3 = 2.
AMULT = .95
END
EXIT

```

Figure E-21. SANTOS Input File for Analyzing the Closure of a Waste Disposal Room in Salt.

